BNL-52351-2006

Laboratory Directed Research & Development Program Activities For FY 2006

Annual Report

BROOKHAVEN NATIONAL LABORATORY
BROOKHAVEN SCIENCE ASSOCIATES
UPTON, NEW YORK 11973-5000
UNDER CONTRACT NO. DE-AC02-98CH10886
UNITED STATES DEPARTMENT OF ENERGY

December 2006

Acknowledgments

The Laboratory Directed Research and Development (LDRD) Program is managed by Leonard Newman, who serves as the Scientific Director, and by Kevin Fox, Special Assistant to the Assistant Laboratory Director for Finance (ALDF). Preparation of the FY 2006 report was coordinated and edited by Leonard Newman and Kevin Fox, who wish to thank D.J. Greco and Maria Ohlsen for their assistance in organizing, typing, and proofing the document. A special thank you is also extended to the Production Services Group for their help in publishing. Of course, a very special acknowledgement is extended to all of the authors of the project annual reports and to their assistants.

Table of Contents

Table of Contents

Table of Contents

Table of Contents

Table of Contents

Introduction

Brookhaven National Laboratory (BNL) is a multidisciplinary laboratory that carries out basic and applied research in the physical, biomedical, and environmental sciences, and in selected energy technologies. It is managed by Brookhaven Science Associates, LLC, (BSA) under contract with the U. S. Department of Energy (DOE). BNL's total annual budget has averaged about $460 million. There are about 2,500 employees, and another 4,500 guest scientists and students who come each year to use the Laboratory's facilities and work with the staff.

The BNL Laboratory Directed Research and Development (LDRD) Program reports its status to the U.S. Department of Energy (DOE) annually in March, as required by DOE Order 413.2B, "Laboratory Directed Research and Development," April 19, 2006, and the Roles, Responsibilities, and Guidelines for Laboratory Directed Research and Development at the Department of Energy/National Nuclear Security Administration Laboratories dated June 13, 2006. In accordance this is our Annual Report in which we describe the Purpose, Approach, Technical Progress and Results, and Specific Accomplishments of all LDRD projects that received funding during Fiscal Year 2006.

BNL expended $11.1 million during Fiscal Year 2006 in support of 85 projects. The program has two categories, the annual competed LDRDs and Strategic LDRDs, which combine to meet the overall objective of the LDRD Program.

Proposals are solicited annually for review and approval concurrent with the next fiscal year, October 1. An LDRD Selection Committee, comprised of the Associate Laboratory Directors (ALDs) for the Scientific Directorates, an equal number of scientists recommended by the Science Council, plus the LDRD Scientific Director, and the Assistant Laboratory Director for Policy and Planning, review the proposals submitted in response to the solicitation. This competed LDRD category emphasizes innovative research concepts with limited management filtering to encourage the creativity of individual researchers. The competition is open to all BNL staff in programmatic, scientific, engineering, and technical support areas. Researchers submit their project proposals to the LDRD Scientific Director.

A portion of the LDRD budget is held for the Strategic LDRD (S-LDRD) category. These funds are used to establish and enhance initiatives that are consistent with Laboratory priorities. Projects in this category focus on innovative R&D activities that are likely to develop new programmatic areas within BNL's mission responsibilities and enhance the Laboratory's science and technology base. The Laboratory Director entertains requests or articulates the need for S-LDRD funds at any time. The Director selects two people to provide written reviews of the proposals.

These Projects are driven by special opportunities, including:

- Research project(s) in support of a Laboratory strategic hire,
- Evolution of Program Development activities into research and development activities,

- ALD proposal(s) to the Director to support unique research opportunities,
- Research project(s) in support of Laboratory strategic initiatives as defined and articulated by the Director.

The goals and objectives of BNL's LDRD Program can be inferred from the Program's stated purposes. These are to (1) encourage and support the development of new ideas and technology, (2) promote the early exploration and exploitation of creative and innovative concepts, and (3) develop new "fundable" R&D projects and programs. The emphasis is clearly articulated by BNL to be on supporting exploratory research "which could lead to new programs, projects, and directions" for the Laboratory. We explicitly indicate that research conducted under the LDRD Program should be highly innovative, and an element of high risk as to success is acceptable. In the solicitation for new proposals for Fiscal Year 2006 we especially requested innovative new projects in support of RHIC and the Light Source and any of the Strategic Initiatives listed at the LDRD web site. These included support for NSLS-II, RHIC evolving to a quantum chromo dynamics (QCD) lab, nanoscience, translational neuroimaging, genomes to life, computational sciences, nonproliferation and national security, energy sciences, and environmental sciences.

As one of the premier scientific laboratories of the DOE, BNL must continuously foster groundbreaking scientific research. At Brookhaven National Laboratory one such method is through its LDRD Program. This discretionary research and development tool is critical in maintaining the scientific excellence and long-term vitality of the Laboratory. Additionally, it is a means to stimulate the scientific community and foster new science and technology ideas, which becomes a major factor in achieving and maintaining staff excellence and a means to address national needs within the overall mission of the DOE and BNL.

LABORATORY DIRECTED RESEARCH AND DEVELOPMENT

2006 PROJECT PROGRAM SUMMARIES

Hydrogen Atom Transfer from Carbon to Metal — Relevance of a Novel Reaction to Catalyzed Hydrocarbon Conversions

Morris Bullock *03-104*

PURPOSE:

The purpose of this project is to investigate the feasibility of a new method for cleavage of the carbon-hydrogen (C-H) bonds in hydrocarbons through hydrogen (H) atom transfer reactions from a carbon to a metal. We seek to carry out fundamental kinetic and mechanistic studies to investigate this novel chemical reaction that is relevant to homogeneously catalyzed hydrocarbon conversions.

APPROACH:

A fundamental understanding of reaction mechanisms is required for the rational design of new homogeneous catalysts. Both kinetic and thermodynamic issues are important in assessing the viability of new proposed steps that might be used in catalytic cycles. We seek an improved understanding of the reactivity of metal complexes that catalyze organic reactions. Synthetic, kinetic and mechanistic studies on organometallic complexes are performed towards this goal.

Selective conversion of hydrocarbons to functionalized organic compounds presents a formidable scientific and practical challenge and is a major goal of organometallic chemistry and homogeneous catalysis. We are examining a novel reaction in which cleavage of a C-H bond proceeds by hydrogen atom transfer from a hydrocarbon to a photochemically generated metal-centered radical.

Post doc Jie Zhang carried out synthesis and characterization of the metal complexes used in this study along with photochemical studies using continuous irradiation. Experiments using laser flash photolysis and transient infrared spectroscopy measurements were carried out in collaboration with Etsuko Fujita and David Grills. Kuo-Wei Huang, a Goldhaber Fellow at BNL, carried out computations to determine energetics of the reactions and bond strengths of the bonds being cleaved or formed in the reactions.

TECHNICAL PROGRESS AND RESULTS:

Laser flash photolysis (355 nm) of a solution of $[Cp(CO)_2Os]_2$ leads to an instantaneous bleaching of the ν(CO) IR bands of the dimer and appearance of new bands assigned to the osmium-centered radical $Cp(CO)_2Os\bullet$. These experiments were carried out by time-resolved infrared (TRIR) spectroscopy using a step-scan FTIR spectrometer. The kinetics of the metal-to-carbon hydrogen atom transfer (shown below) were determined to be first-order in osmium radical and first-order in 1,4-cyclohexadiene.

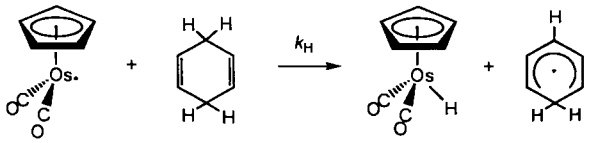

The second-order rate constant for the hydrogen atom transfer was determined to be $k_H = (2.1 \pm 0.2) \times 10^6\ M^{-1}\ s^{-1}$ at 23°C. Experiments using deuterated cyclohexadiene are consistent with a large kinetic deuterium isotope effect, but the precise value of k_H/k_D has not been determined yet from the data.

While these experiments show that transient IR measurements can be used to determine rate constants for carbon-to-metal hydrogen atom transfers, we sought to prepare more soluble osmium dimers that might provide better sensitivity in the kinetics measurements owing to higher solubility. A new synthetic route was developed for $[Cp^*(CO)_2Os]_2$ ($Cp^* = \eta^5$-C_5Me_5) through reaction of $[Cp^*(CO)_2OsH$ with 2,2'-azo-bis-isobutyrylnitrile. A single crystal x-ray diffraction study of this complex shows that that the solid state structure of $[Cp^*(CO)_2Os]_2$ has two bridging CO ligands, in contrast to $[Cp(CO)_2Os]_2$, which has only terminal CO ligands. Infared spectroscopic data also indicate bridging CO ligands for this complex in solution.

Much higher solubility was obtained by substituting four hydrogens on each Cp ring by isopropyl groups. Reaction of tetra-isopropylcyclopentadiene with $[(CO)_3OsI]_2$ provides $(^iPr_4C_5H)(CO)_2OsI$, which can be converted to $(^iPr_4C_5H)(CO)_2OsH$ through reduction with NaK followed by treatment with EtOH. Reaction of $(^iPr_4C_5H)(CO)_2OsH$ with 2,2'-azo-bis-isobutyrylnitrile gives $[(^iPr_4C_5H)(CO)_2Os]_2$, which is much more soluble than $[Cp^*(CO)_2Os]_2$.

Density functional theory (DFT) calculations on these Os-Os dimers reveal the energetics of different geometrical isomers. The *anti*- and *gauche* isomers of $[Cp(CO)_2Os]_2$, with terminal CO ligands, are significantly more stable than the *trans*- and *cis* isomers with bridging CO ligands, while the stability the *anti*-isomer of $[Cp^*(CO)_2Os]_2$ is similar to that of its *trans*-isomer. Computations on the energetics of the isomers with a $[C_5(CF_3)_5]$ ligand suggest that the difference observed for Cp and Cp* complexes is mainly due to electronic rather than steric effects of the Cp groups.

Photolysis of an osmium dimer with tris(pyrazolyl)borate ligands, $[Tp(CO)_2Os]_2$, results in carbon-to-metal hydrogen atom transfers from even stronger C-H bonds. Photolysis ($\lambda > 300$ nm) in THF results in carbon-to-osmium hydrogen atom transfer, and this reaction can be used synthetically as a route to $Tp(CO)_2OsH$ (68% isolated yield). The osmium deuteride, $Tp(CO)_2OsD$, results from photolysis of $[Tp(CO)_2Os]_2$ in toluene-d_8. The C-H bond dissociation energies of THF (92 kcal/mol) and toluene (90 kcal/mol) show that this method can be used to cleave C-H bonds that are much stronger than those of 1,4-cyclohexadiene.

Photolysis of the ruthenium dimer $[Cp^*(CO)_2Ru]_2$ in THF-d_8 in the presence of 1,4-cyclohexadiene produced $Cp^*(CO)_2RuH$ and benzene, indicates that a carbon-to-metal hydrogen atom transfer does not require the formation of an unusually strong M-H bond. The reactions of $[Cp^*(CO)_2Ru]_2$ and $[Tp(CO)_2Os]_2$ all involve carbon-to-metal hydrogen atom transfers that are thermodynamically unfavorable. We cannot rule out the possibility that more complex mechanisms are involved compared to the $[Cp(CO)_2Os]_2$ reaction.

SPECIFIC ACCOMPLISHMENTS:

Publications:

"Efficient Synthesis of the Os-Os Dimers $[Cp(CO)_2Os]_2$, $[Cp^*(CO)_2Os]_2$, and $[(^iPr_4C_5H)(CO)_2Os]_2$ and Computational Studies on the Relative Stabilities of Their Geometrical Isomers," Zhang, J.; Huang, K.-W.; Szalda, D. J.; Bullock, R. M. *Organometallics*, **2006**, *25*, 2209-2215.

Carbon-to-Metal Hydrogen Atom Transfer: Direct Observation Using Time-Resolved Infrared Spectroscopy, Zhang, J.; Grills, D. C.; Huang, K.-W.; Fujita, E.; Bullock, R. M. *Journal of the American Chemical Society,*

2005, *127*, 15684-15685. http://dx.doi.org/10.1021/ja0555724

Presentations:

Ionic hydrogenations using proton and hydride transfer reactions of metal hydrides, and hydrogen atom transfers of osmium complexes, Bullock, R. M.; Dioumaev, V. K.; Kimmich, B. F. M.; Zhang, J. 229th National American Chemical Society Meeting, San Diego, CA, March 13-17, 2005. (Invited talk at a symposium, given by Morris Bullock)

Carbon-to-metal hydrogen atom transfers in the formation of metal hydrides, Zhang, J.; Grills, D. C.; Huang, K.-W.; Fujita, E.; Bullock, R. M. Pacifichem 2005 conference (Honolulu, HI, Dec. 15-20, 2005, Invited talk to be given by Morris Bullock at a symposium on metal hydrides and dihydrogen complexes)

"Nanosecond time-resolved step-scan FTIR spectroscopy: A powerful tool for investigating photocatalytic processes," Grills, D. C.; Bullock, R. M.; Fujita, E.; Huang, K.-W.; Muckerman, J. T.; and Zhang, J. at The 3rd International Conference on Advanced Vibrational Spectroscopy (ICAVS-3), Delavan, WI, Aug 14-19 2005. (poster presented by David Grills)

LDRD FUNDING:

FY 2003 (April – September)	$20,000
FY 2004	$56,480
FY 2005	$58,039
FY 2006 (October – March)	$32,516

Femtosecond Photoinitiated Nanoparticle Surface Chemistry

Nicholas Camillone III *04-011*

PURPOSE:

The goal of this project is to bring together the ultra-fast and the ultra-small to understand the physics behind the unique chemistry of nanostructured materials. In this pursuit we have developed capabilities to probe with femtosecond time resolution the chemical dynamics of molecules adsorbed on supported nanoparticles. This involves ultrafast laser-based techniques for initiating and following chemical transformations in real time in ultra-high vacuum (UHV), an undertaking that has brought new capabilities and expertise to BNL.

APPROACH:

About ten years ago a new class of surface chemistry, involving excitation driven by femtosecond light pulses, was demonstrated[1] and has recently begun to be exploited to study reaction dynamics on planar surfaces.[2] However, little has been done to explore these phenomena on nanoscale materials,[3,4] where size-dependent properties are expected to impact the surface chemical dynamics.[5] In particular, on supported metal nanoparticles, spatial confinement of electrons, size-dependent electronic structure[6] and changes in electron-phonon coupling[7] are expected to significantly affect hot electron lifetimes in small nanoparticles. Furthermore, enhancements in photoelectron yield from nanoparticles have been indicated.[8] These effects are expected to impact the dynamics of adsorbates on nanoparticles. We aim to explore these dynamics as the size of the nanoparticles is varied through the regime spanning the non-metal to metal transition.

Our experiments employ the two-pulse correlation (2PC) technique[2,9] wherein, the 800 nm photoexcitation pulse is split into two pulses separated in time by a variable delay and directed to impinge upon the target. The photoinduced desorption yield is measured by a quadrupole mass spectrometer (QMS). In part because the relaxation times of the electronic and lattice temperatures differ by an order of magnitude, the 2PC desorption yield correlation width depends upon the desorption mechanism. This enables distinctions to be drawn among possible reaction mechanisms[2] and allows for quantification of their timescales.

Such time-resolved measurements on nanoparticles require a high energy (~ 1 mJ) source of ~ 100 fs laser pulses, a UHV environment, a well-characterized substrate surface, manipulation and introduction of the pulses into the UHV, an ion counting scheme to detect photodesorbed species, and the capability to grow nanoparticles in UHV.

COLLABORATORS:

Development of this project, and design, assembly and operation of the experiment has depended heavily on the efforts of postdoctoral research associate Paul Szymanski (Chemistry) and has involved the collaboration of Alexander Harris (Chemistry) and James Misewich (Materials Science). In addition, components crucial to the effort have been supplied through collaboration with Michael White (Chemistry BNL and SUNY Stony Brook).

TECHNICAL PROGRESS AND RESULTS:

During FY 2006 several important milestones have been reached:

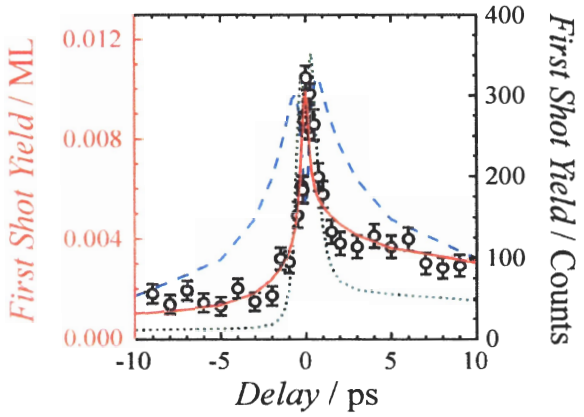

Figure 1. 2PC measurements of photoinduced desorption of O_2 from Pd(111) with "best" fits for three numerical models: two models with a T_{el} -independent friction (dashed and dotted lines) and one model with a T_{el} -dependent friction (solid line).

• Femtosecond photoinduced desorption of O_2 from Pd(111): detailed 2PC and fluence-dependence measurements were performed as a function of initial O_2 surface coverage.

• Femtosecond photoinduced desorption of CO from Pd(111): detailed 2PC and fluence-dependence measurements were performed as a function of initial surface temperature.

• Computer software for performing simulations of femtosecond-pulse photodesorption has been completed. Simulations are based on the two-temperature model[10] (2TM) and incorporate a phenomenological frictional coupling of the substrate electronic and vibrational degrees of freedom to the adsorbate.[11]

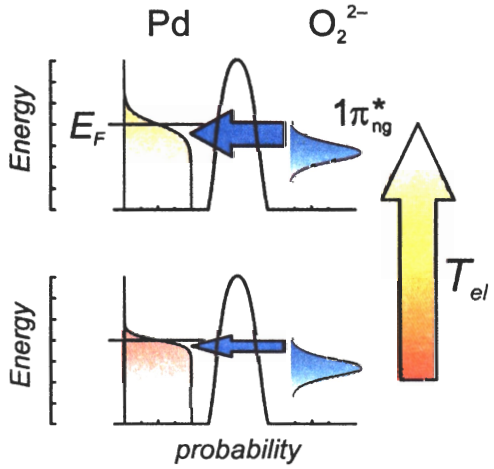

Figure 2. A schematic illustration of how the strength of electron-mediated molecule–surface coupling increases with increasing electronic temperature within the DIMET hole-capture model

As a result of our investigations, we have reached three significant scientific conclusions.

First, we find that the strength of electron-mediated molecule–surface coupling ("electronic friction") depends on electronic temperature (T_{el}). This conclusion derives from the failure of T_{el}-independent friction to explain the observed 2PC response. Only by incorporating T_{el}-dependent friction does the 2TM successfully model the observation (See Fig. 1). This result is consistent with the hole-capture DIMET (desorption induced by multiple electron transitions) mechanism believed to be responsible for desorption of O_2 from Pd,[12] as illustrated in Fig. 2.

Second, the strength of the molecule–surface coupling for O_2/Pd(111) appears to depend on binding site and to be correlated with molecule–surface binding strength. This conclusion follows from analysis of the observed increase in the photodesorption yield

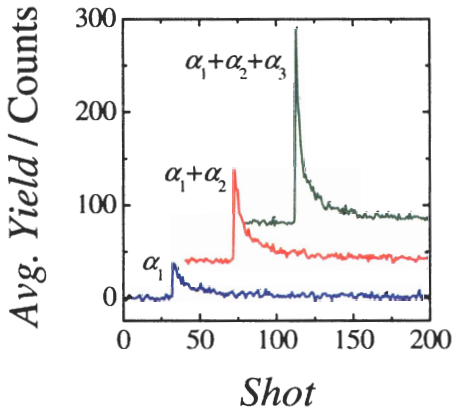

Figure 3. O_2 photodesorption yield at a fluence of ~ 7 mJ/cm^2 for three coverages. The increase in yield is more than expected based on the increase in coverage, but less than expected based on the 2TM, simple energetic arguments and the observed coverage independence of the 2PC response.

with increasing coverage. Population of increasingly less tightly-bound surface sites (termed α_1, α_2 and α_3) was found to result in an increase in photodesorption probability (Fig. 3) somewhat less than would be expected based on energetic arguments alone. This fact, in conjunction with 2TM modeling of the observed coverage independence of the 2PC data indicated that the efficiency of energy transfer from the surface to the molecule decreases as the strength of the molecule–surface bond decreases.

Third, we have begun to collect new evidence in support of the current understanding of ultrafast photodesorption. This model involves separating the excitation step, assigned to interaction with a non-equilibrium electron distribution, from the actual desorption step, assigned to a process that is identical to thermally-activated surmounting of an energetic barrier to desorption. A significant component of our understanding derives from our temperature-dependent measurements of the desorption dynamics of CO from Pd(111). These dynamics are only consistent with the 2TM when the exit channel is described by an activation barrier (E_a) equal to that measured by temperature-programmed desorption experiments. Thus a reasonable case can be built in support of the pseudo-thermal description for desorption induced by ultrafast laser pulses.

Reaching the above-described technical milestones and scientific conclusions has involved the development of expertise and instrumentation necessary to conduct state-of-the-art time-resolved photoinduced desorption investigations. Our original goal of exploring the size-dependence of the desorption dynamics of molecular adsorbates from nanometer scale metal particles is yet to be achieved. In these experiments our interest is to investigate the possibility that surface chemical dynamics can be "tuned" by variation of the size of the metal substrate material at the nanoscale. This size regime is of interest because the reactivity of such particles for the catalytic oxidation of CO shows a marked peak for particles ~ 3 nm in diameter, and this peak in reactivity coincides with the non-metal to metal transition.[13,14] Our aim is to measure the desorption dynamics of CO from nanoparticle assemblies as a function of nanoparticle size, to begin to probe the chemical dynamics behind the marked size-dependence of the reactivity of this model catalytic system.

Continued development of the central themes of this work will be supported by funding under the Surface Chemical Dynamics component of the DOE BES-supported Chemical Physics Program in the BNL Chemistry Department. Related work will be supported by a new effort funded as part of the DOE BES Chemical Imaging initiative.

This project did not involve animal vertebrates and/or human subjects.

SPECIFIC ACCOMPLISHMENTS:

Presentations:

- *"Femtosecond Photoinitiated Nanoparticle Surface Chemistry,"* N. Camillone III, oral presentation at the *Mid-Year Review of LDRD Projects* (BNL, May 3, 2004).

- *"Femtosecond Photoinitiated Nanoparticle Surface Chemistry,"* N. Camillone III, oral presentation at the *Mid-Year Review of LDRD Projects* (BNL, April 13, 2005).

- *"Femtosecond Photoinitiated Nanoparticle Surface Chemistry,"* N. Camillone III, oral presentation at the *Mid-Year Review of LDRD Projects* (BNL, July 12, 2006).

- *"Adsorption-state-dependent subpicosecond surface chemical dynamics,"* P.

Szymanski, A. Harris, M. White, J. Misewich, N. Camillone III, invited presentation (St. John's University, April 27, 2006).

REFERENCES:

1. J.A. Misewich, T.F. Heinz, D.M. Newns, *Phys. Rev. Lett.*, **68**, 3737 (1992).
2. M. Bonn, S. Funk, C. Hess, D.N. Denzler, C. Stampfl, M. Scheffler, M. Wolf, G. Ertl, *Science*, **285**, 1042 (1999).
3. A. Wille, R. Buchwald, K. Al-Shamery, *Appl. Phys. A*, **78**, 205 (2004).
4. S. Kwiet, D.E. Starr, A. Grujic, M. Wolf, A. Hotzel, *Appl. Phys. B*, **80**, 115 (2005).
5. A. Wille, K. Al-Shamery, *Surf. Sci.*, **528**, 230 (2003).
6. M. Valden, X. Lai, D.W. Goodman, *Science*, **281**, 1647 (1998).
7. T. Valla, M. Kralj, A. Šiber, M. Milun, P. Pervan, P.D. Johnson, D.P. Woodruff, *J. Phys.: Condens. Matter*, **12**, L477 (2000).
8. P.V. Kamat, M. Flumiani, G.V. Hartland, *J. Phys. Chem. B*, **102**, 3123 (1998).
9. J.A. Misewich, A. Kalamarides, T.F. Heinz, U. Höfer, M.M.T. Loy, *J. Chem. Phys.*, **100**, 736 (1993).
10. S.I. Anisimov, B.L. Kapeliovich, T.L. Perel'man, *Sov. Phys. JETP*, **39**, 375 (1974).
11. S. Funk, M. Bonn, D.N. Denzler, C. Hess, M. Wolf, G. Ertl, *J. Chem. Phys.*, **112**, 9888 (2000).
12. J.A. Misewich, S. Nakabayashi, P. Weigand, M. Wolf, T.F. Heinz, *Surf. Sci.*, **363**, 204 (1996).
13. S.B. DiCenzo, S.D. Berry, J. E.H. Hartford, *Phys. Rev. B*, **38**, 8465 (1988).
14. C. Binns, *Surf. Sci. Rep.*, **44**, 1 (2001).

LDRD FUNDING:

FY 2004	$ 79,532
FY 2005	$121,071
FY 2006	$ 54,737

Chirped Pulse Amplification at the DUV-FEL

Li Hua Yu *04-013*

PURPOSE:

We propose to investigate the Chirped Pulse Amplification (CPA) by free-electron laser at the Deep Ultraviolet-Free-Electron Laser (DUV-FEL) facility. In a seeded FEL when the seed laser is chirped and the electron bunch is also chirped accordingly, the output radiation is also amplified and chirped. When the chirped output is compressed by an appropriate optical system, the output can have a very short pulse with very high peak power.

APPROACH:

Our approach is to use the HGHG process to carry out CPA at the DUVFEL. The High Gain Harmonic Generation (HGHG) approach utilizes a laser-seeded FEL to produce amplified, longitudinally coherent, Fourier-transform-limited output at a harmonic of the seed laser. Since the output wavelength is reduced by the harmonic number but with the same percentage of chirp as the seed, the pulse length is also reduced by the harmonic number when compared with the bandwidth limited seed pulse length. This makes it possible to achieve ultra-short pulse length with high peak power. With the existing laser technology of 6% bandwidth (most updated techniques allow for 9% bandwidth), with the possible energy chirped chirp range of 3% at the DUVFEL. Our calculation showed that it is possible to achieve 7 fs with 6 GW peak power at 266 nm. Recently we have carried out the HGHG experiment at 266 nm using the Near Infra-Red Scalable Undulator System (NISUS) undulator at the DUV-FEL. The results agree with the theory very well. Short-pulse amplification is also an important part of the cascaded HGHG experiment to achieve x-ray FEL. Here, we plan a first CPA experiment to confirm this principle, with the ultimate goal of providing an intense, highly coherent ultra-short pulse source of hard x-rays.

TECHNICAL PROGRESS AND RESULTS:

Since we have achieved stable HGHG output at 266 nm using 800 nm seed, we started to chirp the seed and the electron beam energy within the electron bunches. By varying the energy chirp we change the matching between the seed and the electron bunch, and in the mean time measure the bandwidth. The results showed a maximum bandwidth at a certain chirp rate of the electron bunch, and the bandwidth is 1.5 nm, quite close to the theoretically expected maximum bandwidth achievable, i.e. 1.8 nm. This gave us confidence for the desired CPA.

We then proceeded to install the Spectral Interferometry for Direct Electric-Field Reconstruction (SPIDER) to measure the phase distortion of the HGHG output. We were able to carry out the SPIDER measurement on the HGHG output, and start to vary the chirp and change the bandwidth. The results showed the output is chirped agreeing with theory, and hence should be able to be compressed.

- After the shut-down for energy upgrade at the Source Development Laboratory we started to repeat what had been previously achieved. Evidence showed that the photo-cathode laser pulse length is shorter than what is optimized for the operation, causing a larger space charge effect and degraded the performance. We overcome this difficulty by carrying out the CPA experiment at 800 nm direct

seeding and used Frequency-Resolved Optical Gating (FROG) to measure the pulse length after compression. The result showed that HGHG FEL can be used to carry out chirped pulse amplification into shorter wavelength regions; and when saturated, it is possible to use the nonlinearity to generate pulses larger than the seed bandwidth, and a shorter final pulse.

SPECIFIC ACCOMPLISHMENTS:

Publications

- T.Shaftan, Z. Huang, A. Doyuran, L. Carr, W.S. Graves, C. Limborg, H.Loos, J. Rose, B. Sheehy, Z. Wu, L.H. Yu, "Experiments with electron beam modulation at the DUVFEL accelerator," Volume 528, Issues 1-2 , 1 August 2004, Pages 397-401

- J. Rose, B. Podobedov, J. Murphy, T. Shaftan, B. Sheehy, X.J. Wang, L.H Yu, "A SCRF Linac as a FEL Driver and Storage Ring injector," PAC2003

- T. Shaftan, L.H.Yu, "HGHG with Variable Wavelngth," BNL-72034-2004-JA

- Adnan Doyuran, Louis DiMauro, William Graves[§], Richard Heese, Erik D. Johnson, Sam Krinsky, Henrik Loos, James B. Murphy, George Rakowsky, James Rose, Timur Shaftan, Brian Sheehy, Yuzhen Shen, John Skaritka, Xijie Wang, Zilu Wu, and Li Hua Yu, "Experimental study of a high-gain harmonic-generation free-electron laser in the ultraviolet," Phys. Rev. ST Accel. Beams 7, 050701 (2004)

- Adnan Doyuran, Louis DiMauro, Richard Heese, Erik D. Johnson, Sam Krinsky, Henrik Loos,, James B. Murphy, George Rakowsky, James Rose, Timur Shaftan, Brian Sheehy, Yuzhen Shen, John Skaritka, Xijie Wang, Zilu Wu, Li Hua Yu, "Preliminary Chirped Pulse Amplification of HGHG-FEL at DUV-FEL Facility in BNL," NIM, A,Volume 528, Issues 1-2, Pages 467-470 (2004)

- L.H.Yu, "R&D experiments at BNL to address the associated issues in the Cascading HGHG scheme," Proceedings of International FEL Conference, 2004, Trieste, Italy

- Z. Wu, H. Loos, Y. Shen, B. Sheehy, E. D. Johnson, S. Krinsky, J. B. Murphy, T. Shaftan, , X.-J. Wang, L. H. Yu, "Spectral Phase Modulation and chirped pulse amplification in High Gain Harmonic Generation," Proceedings of International FEL Conference, 2004, Trieste, Italy

- Timur Shaftan and Li Hua Yu, Phys. Rev. E 71, 046501 (2005), "High-gain harmonic generation free-electron laser with variable wavelength"

- L.H. Yu, T. Shaftan, D. Liu, T. Tsang, J. Rose, X.J. Wang, T. Watanabe. "Chirped pulse amplification experiment at 800nm," Proceedings of FEL2006

LDRD FUNDING:

FY 2004	$ 78,404
FY 2005	$119,331
FY 2006	$ 54,633

Overcoming Coherent Instabilities at Medium-Energy Storage Rings

Jiunn-Ming Wang *04-025*

PURPOSE:

A charged particle beam can be unstable due to its interaction with the electromagnetic fields generated by oscillating beams in different components distributed around the storage ring. To estimate the effect of these fields on the beam dynamics, many light sources throughout the world e.g. APS, ESRF, SOLEIL, PETRA, DIAMOND and CLS have made efforts to calculate the threshold and initial growth rate of potential instabilities. The average current and current per bunch can be limited due to generated fields in major components such as RF cavities, mini-gap undulators, scrapers and tapered transitions. The purpose of this LDRD is to carry out research aimed at advancing our ability to calculate the impedance of medium energy storage rings and thus provide a more reliable basis on which to predict current limiting phenomena.

APPROACH:

1. Verify 3D GdfidL code with already evaluated data.
2. Investigate the electrodynamic properties for several components.
3. Carry out short-range and long-range wakefield analysis.
4. Study effect of ferrite on wakepotential in SCRF cavities.
5. Carry out Rsh, Rsh/Q and Q analysis for longitudinal and transverse modes of SCRF cavity.

The collaborators of this work include Alexei Blednykh, Samuel Krinsky, Boris Podobedov, James Murphy, James Rose and Stephen Kramer.

TECHNICAL PROGRESS AND RESULTS:

a) For acceleration of the electron beam in the 3-GeV NSLS-II storage ring, three Superconducting RF cavities are planned to be installed. In addition to three 500MHz main RF cavities, three passive 1500MHz harmonic cavities will be located in the ring. The cavity has a complex geometry. A special fluted beam pipe is applied for HOM coupling. For HOM damping two ferrite liners are located in the beam pipe on both sides of the each cavity. Damping of HOM allows for the avoidance of coupled bunch instabilities. We have studied the ferrite effect on short-range and long- range wake potentials. The shape of the short-range wake potential does not change due to one or two ferrite rings. FFT of the long-range wake potential allows one to evaluate resonance impedance parameters. Parameters of the first eight HOMs were taken into account for the estimation of growth rates. For three installed RF cavities the longitudinal coupled bunch growth rates were found to be below the damping rate.

b) Results of GdfidL calculations for a pill-box cavity with ferrite material inside were compared with measurement results of Harald Hahn, C-AD, BNL. S-parameters were calculated using a simple pill-box cavity of 12.4 cm diameter with lined ferrite of 5 mm thick inside the cavity. These studies show that GdfidL can reproduce measurement results and the code can be used for computations of more complex geometries with damping materials.

c) GdfidL also shows a good agreement with analytical results for the empty pill-box cavity. K. Bane and A. Novokhatski have derived the analytical expressions for the loss and kick factors for the diffraction regime. GdfidL calculations were shown to agree with their results.

d) Both Superconducting Undulators (SCU) and Cryo Permanent Magnet Undulators (CPMU) are planned to be installed in the future NSLS-II storage ring. Vacuum chamber for the Superconducting undulator (SCU) has two tapered transitions. Fields arise due to a change in cross section of an elliptical pipe. CPMU is a more complex geometry. Two permanent magnets are located inside a rectangular vacuum chamber. Its geometry looks like a cavity. Investigation of the electrodynamic parameters of CPMU shows that the driving charge can excite some strong resonant modes in the structure in the frequency range above 200 MHz. The lowest resonant frequency depends on the gap between two magnet arrays. All modes in the structure were identified and classified. Existence of the resonant mode at low frequencies can contribute to the couple bunch instabilities. This type of instability needs additional research. It can be done experimentally using the X25 MGU in the X-Ray ring of the NSLS storage ring.

e) The tapered elliptic vacuum chamber for superconducting MGU has a smaller contribution (by a factor of ~2) to the transverse impedance than CPMU.

f) For some components of the future NSLS-II storage ring we have carried out a series of analytical verifications of the received numerical code calculated data. For example, analytical results for the coaxial waveguide with a rectangular slot (using the theoretical Bethe-hole predictions, the theoretical study of the A. Fedotov, L. Gluckstern, S. Kurennoy and G. Stupakov) has been shown to be in agreement with the GdfidL calculations.

g) A preliminary impedance budget for an example of a medium energy storage ring including the most important components has been determined. All data are entered into a table. This table will be useful as a starting point for analyses of instabilities that may limit the current in future medium energy storage rings.

SPECIFIC ACCOMPLISHMENTS:

Publication:
A. Blednykh and S. Krinsky, "Preliminary impedance budget for NSLS-II," submitted to PAC2007.

Proceedings:
A. Blednykh, S. Krinsky, B. Podobedov, and J.M. Wang, "Transverse impedance of small-gap undulators for NSLS-II," Proc. EPAC06, Edinburgh, UK, June 26-30, 2006, p2970.

A. Blednykh, "Calculation of the budget impedance for the NSLS-II" NSLS, October 27, 2005

A. Blednykh, "Preliminary Impedance Budget for the NSLS-II," NSLS, December 9, 2005.

Report:
A. Blednykh, "Trapped modes in tapered vacuum chambers for a mini-gap undulator magnet," BNL-75839-2006-IR, 2006.

LDRD FUNDING:

FY 2004	$ 91,415
FY 2005	$128,858
FY 2006	$ 53,795

Layered Cobaltates with High Thermoelectric Power

Qiang Li *04-033*

PURPOSE:

We carried out a systematic study of the fundamental thermoelectric and related material properties of layered cobaltates necessary for potential practical utilization. Through coordinated research on synthesis and characterization, we will be able to understand the mechanism controlling the thermoelectric properties, as well as gaining the ability to tune various materials parameters in order to optimize their thermoelectric performance. The proposed research can lead to the discovery of new phenomena in strongly correlated electron systems, novel functionality, and many practical applications.

APPROACH:

Cobaltates (A_xCoO_y) are transition-metal misfit layered oxides that feature self-assembled alternatively-stacked blocks with incoherent layer boundaries, producing highly anisotropic properties along their crystallographic directions. Recently, it was discovered that some cobaltates have a thermoelectric performance challenging that of conventional thermoelectric materials. Through the coordinated studies of the electronic structure and thermoelectric properties, we are able to establish a new direction for bulk thermoelectric research that is using the electron correlation as a tuning parameter to enhance the thermoelectric power factor of oxides. We also explore the role of self-assembly in the growth of cobaltate thin films by focusing our study at the properties and structure of $Ca_3Co_4O_9$ single crystals, and thin films grown on various single crystalline, polycrystalline, and amorphous substrates. A coordinated transmission electron microscope and thermoelectric property characterization is performed to understand the growth mechanism and the correlation between the structures and thermoelectric properties.

TECHNICAL PROGRESS AND RESULTS:

Post-doctoral research associate (Y. Hu) was hired and a graduate student (Q. Jie) from the State University of New York at Stony Brook was supported to participate in this project.

Specifically:

1) We set up the three-zone furnace and successfully grew Na_xCoO_2 and $Ca_3Co_4O_9$ single crystals, which were characterized and used for electron correlation studies in collaboration with the photoemission and IR optical spectroscopy groups of BNL

2) A new high temperature thermoelectric and transport characterization system was built. It became the main instrument for evaluating the thermoelectric properties up to 1000K.

3) Thin films of $Ca_3Co_4O_9$ have been successfully grown on various substrates, including single crystalline $SrTiO_3$, $LaAlO_3$, Si, and Al_2O_3, polycrystalline Al_2O_3, and glass, using pulsed laser deposition, in collaboration with Dr. W. Si

4) High resolution transmission electron microscopy was used to characterize the microstructures of $Ca_3Co_4O_9$ films, in collaboration with Drs. E, Sutter and R. Klie of Center for Functional Nanomaterials.

5) High-quality c-axis oriented $Ca_3Co_4O_9$ thin films were grown directly on Si (100) and Si (111) wafers by pulsed laser deposition without pre-chemical treatment of the substrate surface. Cross-sectional

transmission electron microscopy shows excellent crystallinity of the $Ca_3Co_4O_9$ films. The Seebeck coefficient and resistivity of the $Ca_3Co_4O_9$ thin films on Si (100) substrate are 126 μV/K and 4.3 micro-Ohm.cm respectively at room temperature, comparable to the single crystal samples. This advance demonstrated the possibility of integrating the cobaltate based high thermoelectric materials with the current state-of-the-art silicon technology for thermoelectricity-on-a-chip application, such as thermochemistry-on-a-chip, bio-thermoelectric chip, and active cooling for microelectronic processors.

6) *c*-axis oriented $Ca_3Co_4O_9$ thin films have been grown directly on a glass (fused silica) substrate by pulsed laser deposition. Detailed microstructure analysis showed stacking faults abundant throughout the films. However, the Seebeck coefficient (~ 130 μV/K) and resistivity (~ 4.3 mΩ•cm) of these films on glass substrates at room temperature were found comparable to the single crystal samples. The presence of these structural defects could reduce thermal conductivity, and thus enhance the overall performance of cobaltate films to be potentially used in the thermoelectric devices.

7) A new direction for thermoelectric research is proposed that is using the electron correlation as a tuning factor to enhance the thermoelectric power.

SPECIFIC ACCOMPLISHMENTS:

Publications:

1) "*In situ* growth of *c*-axis oriented $Ca_3Co_4O_9$ thin films on Si (100)" Y. Hu, et al, Appl. Phys. Lett. **86** 082103 (Feb. 2005),
2) "Thermoelectric properties and microstructure of c-axis oriented $Ca_3Co_4O_9$ thin films on glass substrates" Y. F. Hu, et al, Appl. Phys. Lett. **87** 171921 (Oct. 2005)
3) "Microstructure of $Ca_3Co_4O_9$ Single Crystals and Thin Films" Y. F. Hu, E. Sutter, W. D. Si, and Qiang Li, Mater. Res. Soc. Symp. Proc. Vol. 886, 0886-F01-08.1 (2006)
4) "On the Thermoelectric Properties of Layered Cobaltates," Qiang Li, Mater. Res. Soc. Symp. Proc. Vol. 886, 0886-F01-05.1 (2006)

Presentations:

Invited "Layered Cobaltates with High Thermoelectric Power" Q. Li (presenter), 6th Pacific Rim Conference on Ceramic and Glass Technology, Maui, Hawaii September 11-16, 2005

Invited "Layered Cobaltates with High Thermoelectric Power" Q. Li (presenter), Materials Research Society 2005 Fall meeting, Boston MA, Nov. 28-Dec. 2, 2005

Invited "New Direction in Thermoelectric Research" Q. Li (presenter), the 5th Joint Meeting of the Chinese Physicists Worldwide and International Conference on Frontier Physics, June 27-30, 2006

"Layered Cobaltates with High Thermoelectric Power" Q. Li (presenter), Y. Hu, W. Si, and E. Sutter, The Direct Energy Conversion Program Review and Workshop, organized by DARPA and ONR, December 13-15, 2004 at Coronado, CA

"Transport and Thermoelectric Properties of $Ca_3Co_4O_9$ Thin Films" Y. Hu (presenter), W. Si, E. Sutter, Q. Li, APS march meeting, Los Angeles, CA, March 21-25 2005

"Thermoelectric Properties and Microstructure of c-axis Oriented

$Ca_3Co_4O_9$ Thin Films" Y. Hu (presenter), W. Si, E. Sutter, Q. Li, Materials Research Society 2005 Fall meeting, Boston MA, Nov. 28-Dec. 2, 2005

"Pulsed Laser Deposition of Thermoelectric Cobaltate Thin Films" W. Si (presenter), Y. Hu, and Q. Li, Materials Research Society 2005 Fall meeting, Boston MA, Nov. 28-Dec. 2, 2005

"Thermoelectric and Structural Properties of the $Ba_2Ho(Cu_{3-x}Co_x)O_{7-z}$ Solid Solution" W. Wong (presenter), Y. Hu, Q. Li, et al, in Materials Research Society, Boston MA, Nov. 28-Dec. 2, 2005

"Thermoelectric Properties and Microstructure of c-axis Oriented $Ca_3Co_4O_9$ Thin Films" Y. Hu (presenter), W. Si, E. Sutter, Q. Li, 2005 ICT (International thermoelectirc conference) Clemson, SC, June 2005

One patent application "Cobalt Oxide Thermoelectric Compositions and Uses Thereof" Y. Hu, Q. Li, and W. Si

A full proposal was encouraged and submitted for funding (~1M$/year) from the DOE BES office using the high performance thermoelectric materials to harvest solar energy.

LDRD FUNDING:

FY 2004	$ 61,780
FY 2005	$103,160
FY 2006	$ 25,616

Complex Thin Films and Nanomaterial Properties

Jim Misewich *04-038*

PURPOSE:

The purpose of this LDRD is to develop state-of-the-art tools for high sensitivity probing of nanomaterials and thin films. The ultimate limit we seek is a capability to probe multiple properties of a single nanowire. The properties we wish to measure include transport properties as well as optical properties such as Rayleigh, Raman, electroluminescence and photo-conductivity spectroscopies. It is highly desirable to integrate these capabilities with other capabilities at Brookhaven for the structural characterization of the same individual nanomaterial sample.

APPROACH:

Our approach starts with the nano-lithographic capability at the CFN to fabricate test structures with the nanometer scale dimensions necessary for contacting ultra-small structures. This is combined with dispersion techniques to enable the fabrication of a single nanowire in a specially designed test structure with electrical contacts. With these samples we will use high sensitive electronics to measure the transport properties, and optical techniques including emission spectroscopy, nonlinear spectroscopy, laser spectroscopy and broadband spectroscopy at the NSLS to get a complete picture of the optical properties. Finally, we will determine the physical structure of the same single nanowires.

TECHNICAL PROGRESS AND RESULTS:

Previously we established our ability to fabricate the test structures, to disperse single nanowires in our test structures, to measure the transport properties of these test structures, and to do optical studies on individual nanowires. This includes photo-conductivity on single nanowires as well as electroluminescence from single nanowires. We have now been able to extend these studies to include Rayleigh spectroscopy characterization and for the first time to connect these capabilities with the ability to measure the physical structure of the *same* single nanowires. This has been done via collaboration with the advanced electron microscopy group at Brookhaven. In FY07, we will further extend these capabilities by designing experiments to measure the broadband IR optical properties of single nanowires at NSLS.

SPECIFIC ACCOMPLISHMENTS:

Publications:

1. Sfeir, M.Y., et al., Optical spectroscopy of individual single-walled carbon nanotubes of defined chiral structure. Science, 2006. 312(5773): p. 554-556.
2. Hemraj-Benny, T., et al., Near-edge X-ray absorption fine structure spectroscopy as a tool for investigating nanomaterials. Small, 2006. 2(1): p. 26-35.
3. Upton, M.H., et al., Effect of number of walls on plasmon behavior in carbon nanotubes. submitted to Phys. Rev. Lett., 2006.
4. Panessa-Warren, B.J., et al., Biological cellular response to carbon nanoparticle toxicity. Journal Of Physics-Condensed Matter, 2006. 18(33): p. S2185-S2201.

Our work has led to an FWP on nanomaterial synthesis and characterization from the Division of Materials Science and Engineering of DOE Basic Energy Sciences.

LDRD FUNDING:

FY 2005	$190,532
FY 2006	$370,772
FY 2007 (budgeted)	$195,000

Lattice QCD relevant for RHIC and AGS

Péter Petreczky *04-041*

PURPOSE:

The purpose of this LDRD project was to identify and in the long run solve lattice Quantum Chromodynamics (QCD) problems relevant for the physics program at RHIC and AGS, especially those related to the Quark Gluon Plasma (QGP) created at RHIC. One of the main motivations for the project was the creation of the Center for Lattice Gauge Theory at BNL with a 10Tflop QCD on chip (QCDOC) supercomputer, as well as, the availability of the 10Tflop QCDOC machine at RIKEN-BNL Research Center.

APPROACH:

The central questions for the RHIC heavy ion program are related to the creation of new states of strongly interacting matter and investigation of its properties. Lattice QCD can contribute to answering these questions by first principles calculations of the relevant quantities, for example, critical temperature and the associated energy density for QGP formation and quarkonium yield from a QGP.

To address the problem of the critical temperature and energy density finite temperature, we have carried out lattice calculations with an improved staggered fermion action, called *p4fat3*. It turns out that this lattice fermion action is suitable to study QCD thermodynamics even on relatively coarse lattices.

To gain insight on the fate of different quarkonium states in hot and dense strongly interacting matter, the corresponding meson spectral functions have been calculated in quenched lattice QCD (where the effect of dynamical quarks is neglected) and spectral functions have been extracted using the *Maximal Entropy Method* based on a new algorithm.

The following problems were addressed in FY05:

- Quenched lattice QCD calculations of charmonia and bottomonia spectral on anisotropic lattices (P. Petreczky, K. Petrov)

- Study of the transition at finite temperature with improved staggered fermion formulation in three flavor QCD (P. Petreczky, K. Petrov, C. Schmidt, T. Umeda)

TECHNICAL PROGRESS AND RESULTS:

Detailed calculations of charmonium and bottomonium correlators and spectral functions at several lattices spacings have been done. Numerical calculations have been performed on QCDOC supercomputer. The use of different lattice spacings allowed us to estimate the importance of the cutoff effects in quarkonium correlators at finite temperature. We have tested and used a newly developed implementation of the *Maximum Entropy Method.* The new algorithm does not rely on the singular value decomposition and have been proven to be more stable numerically than the standard algorithm (the so-called Bryan algorithm) which has been previously used in the literature. Therefore, we could calculate reliably the spectral functions at zero temperature, where the results obtained from the *Maximum Entropy Method* can be compared with the results obtained from it and thus establish the reliability of the method. We have identified the main structures in the quarkonium spectral functions: ground state, excited states and the continuum. We have established that S-wave quarkonium spectral functions do not show any temperature dependence within the estimated errors till temperatures as high as $1.5T_c$, with T_c being the transition temperature. The P-wave

spectral functions, on the other hand, show significant changes right above the transition temperature. We have identified the transport contribution to the lattice correlators in the vector channel for the first time, and give an estimate of the averaged thermal velocity of the heavy quark in Quark Gluon Plasma.

We have investigated the finite temperature transition in three flavor QCD using improved staggered action, the *p4fat3* action. Calculations have been performed on the QCDOC supercomputer using the *Hybrid Molecular Dynamics* algorithm. This algorithm has finite step-size errors. Therefore, we also crosschecked our results using the recently developed *Rational Hybrid Monte Carlo* algorithm, which has no step-size errors. The parameters of this new algorithm have been optimized to suit the finite temperature calculations with *p4fat3* fermion action. We have found that the finite step-size errors in our calculations are significantly smaller than the statistical errors. We have calculated the transition temperature at two lattice spacings and several quark masses, which enabled us to extrapolate to the continuum and chiral limit.

The value of the transition temperature in units of the Sommer scale, r_0, turns out to be $r_0 T_c = 0.429(8)$. This value of the transition temperature is only by 5% smaller than the transition temperature in 2+1 flavor theory.

SPECIFIC ACCOMPLISHMENTS:

Publications:

A. Jakovác, P. Petreczky, K. Petrov and A. Velytsky, *"Quarkonium correlators and spectral functions at zero and finite temperature,"* BNL-NT 06/44, submitted to Physical Review D

Presentations:

P. Petreczky, *QCD Spectral functions at finite Temperature Modeling the QCD Equation of State at RHIC*, Edward Teller Education Center, LLNL, February 9-10, 2006

P. Petreczky, *Lattice QCD at finite temperature,* 22nd Winter Workshop on Nuclear Dynamics, March 11-19, 2006, La Jolla, CA, nucl-th/0606013, to be published in Heavy Ion Physics

P. Petreczky, *Heavy quark diffusion and lattice correlators,* Finite Density QCD, March 21-25, 2006, ECT* Trento, Italy

P. Petreczky, *Quarkonium correlators and spectral functions (invited talk),* Strangeness in Quark Matter 2006, March 26-31, Los Angeles, CA, hep-ph/0606053, to be published in J. Phys. G

P. Petreczky, *Lattice simulations of strongly interacting matter under extreme condition* (invited talk), 2006 APS April Meeting, April 22–25, 2006, Dallas, Texas

T. Umeda, *QCD thermodynamics with* $N_f = 3$ *and* $2+1$ *near the continuum limit at realistic quark masses,* 2006 APS April Meeting, April 22–25, 2006, Dallas, Texas

P. Petreczky, *Heavy quark potentials and spectral functions,* The Physics of High Baryon Density, May 29 – June 2, 2006, ECT* Trento, Italy

LDRD FUNDING:

FY 2004	$ 69,272
FY 2005	$109,751
FY 2006	$ 48,156

Very Long Baseline Neutrino Oscillations

Milind V. Diwan *04-043*

PURPOSE:

We previously conducted extensive studies of the physics capabilities of a very long baseline neutrino oscillation experiment based at BNL. We now have a good understanding of how well such a facility will perform for the following goals: precise determination of the oscillation parameters Δm^2_{32} and $\sin^2(2\theta_{23})$ in ν_μ disappearance mode, detection of $\nu_\mu \rightarrow \nu e$ appearance, sensitivity to $\sin^2(2\theta_{13})$, measurement of Δm^2_{21} and $\sin^2(2\theta_{12})$ in appearance mode (independent on the value of θ_{13}), verification of matter enhancement and determination of the sign of Δm^2_{32}, determination the CP-violation parameter δ_{CP} in the neutrino sector, and confirmation of CP violation by dedicated anti-ν running.

DOE and NSF have issued a charge to the Neutrino Scientific Assessment Group (NUSAG) dated on March 3, 2006 to "address the American Physical Society's recommendation for a next-generation neutrino beam and detector configurations." To that end, NuSAG has initiated the US Long Baseline Neutrino Experiment Study, which is lead jointly by BNL and Fermi National Lab (FNAL). The co-leaders of the study's Advisory Committee are Milind V. Diwan from BNL and Gina Rameika from FNAL. As a result of the NuSAG charge, in FY 2006 we have expanded the scope of our study to encompass assessing the feasibility of long baseline neutrino experiments using beams from both the BNL AGS accelerator and the Fermi Lab Main Injector accelerator. We have compared the physics sensitivity of long baseline neutrino experiments using a neutrino beam from Fermi Lab or BNL in conjunction with the proposed NSF Deep Underground Science and Engineering (DUSEL) facility located at the Homestake Mine in South Dakota or the Henderson Mine in Colorado.

Our goal is to produce a detailed report on the technical feasibility and physics sensitivities of several US options for the next generation of long baseline neutrino experiments in collaboration with FNAL and University groups to be presented to the NuSAG in FY 2007. The BNL Physics Advisory Committee (PAC) has recommended that completion of this study be given the highest priority.

APPROACH:

Future neutrino oscillation experiments must be much more ambitious to precisely measure the parameters and, for the first time, observe violation of CP symmetry in the lepton sector. We recently studied the feasibility of a neutrino beam produced by an upgraded AGS sent over 2500 km to a massive underground detector. We concluded that such an experiment could indeed achieve the above goal.

The continuation of our LDRD study has two main approaches: 1) The determination of the spectrum and intensity of neutrinos from the FNAL Main Injector accelerator and comparison with our previous studies of the BNL AGS based neutrino beam. In addition, we continue to refine the BNL AGS beam targeting design: The beam-related work is in collaboration with Bill Weng, Harold Kirk, and others in the BNL Collider Accelerator Department (CAD) as well as collaborators at FNAL. It includes simulations of various geometries for producing the neutrino beam. 2) Optimizing the overall experimental sensitivity using the different neutrino beam designs, detector

technologies, and baselines. This work is carried out by both theoretical analysis (with help from Bill Marciano) and parametric simulations that attempt to approximate the detector response and estimate the physics sensitivities. The parametric simulations and sensitivity calculations are carried out in collaboration with University partners and BNL summer undergraduate interns.

TECHNICAL PROGRESS AND RESULTS:

For the beam simulation results, we have succeeded in implementing the target and horn system designs used for the BNL proposal E889 into the NuMI (Neutrinos at the Main Injector) beam simulation framework. The NuMI simulation framework has been verified with data from the MINOS experiment at FNAL. We have compared this new simulation with the previous simulations of the AGS neutrino beam and found them to be in reasonable agreement. We have varied many simulation parameters, including the beam targeting design, the proton beam energy, and the beamline geometry and have estimated the neutrino interaction rates and have identified several beam design options for on-axis and off-axis beams that could meet the physics sensitivity requirements. These results are being included in the report on the US Long Baseline Neutrino Experiment Study.

We have carried out many physics sensitivity estimates using the new FNAL and AGS beam configurations, experimental baselines and detector technologies. This work was carried out in collaboration with Dr. Patrick Huber of the University of Wisconsin and several other University research partners.

SPECIFIC ACCOMPLISHMENTS:

The formation of the US Long Baseline Neutrino Experiment Study group in response to the NuSAG was chaired by Sally Dawson (BNL) and Hugh Montgomery (FNAL). The study group is now in the process of preparing its report for the NuSAG under BNL leadership.

Publications:

"Precision Physics with a Wide Band Super Neutrino Beam." V. Barger, M. Dierckxsens, M. Diwan, P. Huber, C. Lewis, D. Marfatia, B. Viren. Phys. Rev. D 74 (2006) 0703004.

Proccedings:

"Physics of a Long and Very Long Baseline Neutrino Program," Milind V. Diwan, The April 2006 meeting of the American Physical Society, April 22-25, 2006, Dallas, TX.

Proposals:

Proposal to use the Homestake Mine in South Dakota as the site for the Deep Underground Science and Engineering Laboratory and conceptual design. NSF-05-506. PI: Kevin Lesko from LBNL. (Milind Diwan is part of the group that prepared this proposal for the National Science Foundation.)

BNL proposal to conduct Detector R&D for a future US Neutrino Physics Program. The proposal was divided in tasks with separate P.I.s. (M. Diwan (physics), B. Viren (detector simulation), C. Yanagisawa (background analysis), M. Dierckxsens (physics), M.Bishai (photosensors), R. Tayloe (Fine grained liquid scintillator), R.S. Raghavan (Liquid scintillator detector development), B. Fleming (liquid argon potential for physics). The proposal was submitted to DOE-OHEP in December, 2005.

LDRD FUNDING:

FY 2004	$ 71,099
FY 2005	$106,166
FY 2006	$ 46,012

Advanced ^{3}He Detectors for the Spallation Neutron Source

Graham C. Smith *04-046*
Bo Yu

PURPOSE:

The Spallation Neutron Source (SNS) at Oak Ridge National Laboratory is the nation's premier neutron user facility, having begun operations earlier this year. Most of the beam-lines will require detector upgrades as the beam intensity increases, over the next few years, in order to exploit fully the capabilities of the new facility. The technical goal of this LDRD project is to investigate an innovative readout method for ^{3}He-based neutron detectors that possesses extremely high rate capability and accurate position determination in two-dimensions, and with large solid-angle coverage. This development targets all types of neutron scattering techniques, particularly small angle neutron scattering (SANS), and also magnetism and liquids reflectometry.

APPROACH:

Several SNS instruments foresee rate requirements of $10^8 s^{-1}$ over areas ranging up to 1m × 1m. There is no detector technology at present that can provide this capability. A promising new technical approach is a detector operating in ionization mode, or unity gain, with discrete pixels, or pads, read-out in parallel. The challenges of this method include a high density of readout pads, and inclusion of much of the microelectronics inside the detector gas volume. This would represent a radical, new methodology for neutron user facilities.

Collaborators are G. DeGeronimo and N. Schaknowski (BNL).

TECHNICAL PROGRESS AND RESULTS:

Using an ionization chamber with depth of 40 mm, and anode pads on a 5 mm pitch, in a geometry shown in Figure 1, it has been

Figure 1. Anode pad arrangement for charge sharing measurements (part of a larger array using the same geometry). Center to center spacing is 5 mm.

shown in this project that adequate charge sharing of the electrons created after neutron conversion in ^{3}He can be achieved. Sample waveforms are shown in Figure 2, for a

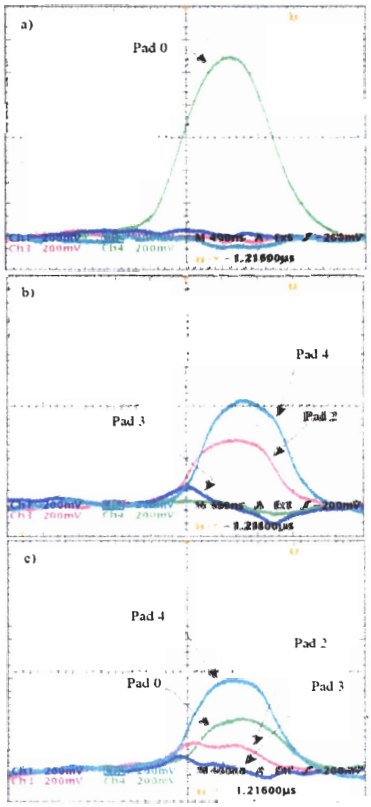

Figure 2. Waveforms from four adjacent pads for three neutron conversion events. (a) All charge collected by pad #0. (b) Charge shared between pad #4 and pad #2. (c) Charge shared between pad #0, pad #2 and pad #4.

mixture of 3 atm. ^{3}He and 1 atm. of propane. The ^{3}He provides very high efficiency conversion for neutrons from 2 - 10Å, while the propane acts to limit the range of the proton and triton created after neutron conversion. Simulations of the charge collection with this geometry are shown in Figure 3, for a conversion that occurs directly above pad #0, and in which all the

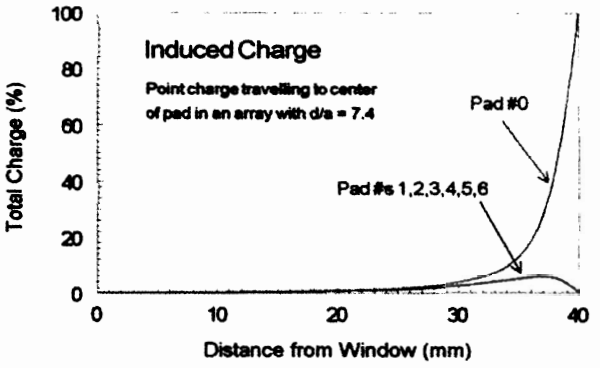

Figure 3. Simulation of charge induced on central seven pads for point charge originating at window, directly above and drifting to the center of pad #0.

charge is collected by that pad. It can be seen that the adjacent pads, though receiving a net charge of zero, experience a small induction of charge during the electron cloud's drift, and this effect is reflected in the waveforms of pad #3 in Figure 2 (b) and (c). This most important observation provides one of the keys to successful implementation of the technique - the lower level discriminator in the pad amplifiers must be high enough to exclude the induction signals, but also low enough to accept events where one third of the charge may be shared on a single pad. Since the overall charge is about 25k electrons, and the typical preamp noise is less than 1000 electrons FWHM with the low capacitance of the pad, this compromise setting of the lower threshold can successfully be achieved.

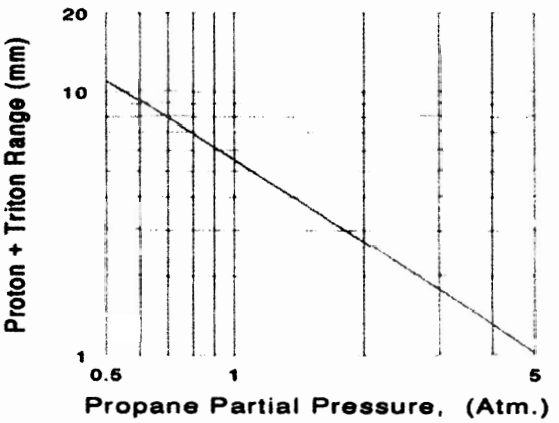

Figure 4. Calculation of combined proton/triton range as a function of propane pressure.

The test device has pad spacing of 5mm, and with charge sharing occurring between at most three pads, the spatial resolution achievable is about 2.5 mm. This new technique can be adapted for other position resolution requirements by tailoring the proton/triton range to different lengths, according to the propane pressure. Figure 4 shows calculations that have been performed, illustrating that at 1 atm. (as used here), the combined range is about 5 mm. Thus, a resolution of 1mm, for example, could be achieved with a propane pressure of about 2.5 atm. with a corresponding increase in the pad density.

SPECIFIC ACCOMPLISHMENTS:

Publication

Two-dimensional, ^{3}He Neutron Detectors with Pad Readout for High Rates. Schaknowski, N.A.; Smith, G.C.; Yu, B.; and J. Doumas. IEEE Trans. Nucl. Sci. In press.

LDRD FUNDING:

FY 2004	$ 72,953
FY 2005	$109,650
FY 2006	$ 50,173

Genetic NanoTags

James F. Hainfeld *04-055*

PURPOSE:

Genomics and proteomics have advanced to where it is of interest to identify and characterize cellular complexes or "machines." In order to isolate these complexes from cells for study, genetically engineered tags have been developed to bind the desired proteins to columns for purification. Unfortunately, most larger complexes do not crystallize for x-ray studies, so these are then studied by electron microscopy (EM). A difficulty exists in identifying component proteins (which protein is where?), and orienting smaller complexes, necessary for 3-D image reconstruction and solving the structure.

We propose to use the tags commonly genetically engineered into recombinant proteins for the purpose of biochemical purification to construct complementary gold labels that will bind to these tags. This could break the 500 kDa barrier for cryo-EM by identifying subunits and enabling their orientation and analysis. Currently, complexes <500 kDa are not generally solvable by cryo-EM since at the low dose required, distinctive features are not perceived, and the alignment with other molecules, necessary to solve the 3-D structure, is not possible. The work we propose should make it possible for cryo-EM to solve <500 kDa protein complexes at 10 Å resolution, which would be a significant advance for biology.

Four genetically engineered sequences investigated: these will be programmed into and expressed in target proteins. Gold nanoparticles will be designed that will bind to these four sequences: 1) Ni-NTA-gold binding to 6x-His tags, 2) negatively charged gold to 6x Arg tags, 3) monomaleimido gold linked to cysteine, and 4) gold targeted to a gold-binding sequence.

This work will be applied to three important molecular machine complexes required for life: Ku70/Ku80/DNA-PK complex, human chromatin remodeling complex ACF, and the human ligase IV/Xrcc4 complex, all being currently worked on in the Biology department. Cryo-EM single particle data will be collected in ice and reconstructions done.

This work is cogent to the DOE Genomes to Life (GTL) Initiative. The first goal of GTL is: "Identify and characterize the molecular machines of life." NIH is investing heavily in imaging (with their new National Institute for Biomedical Imaging and Bioengineering, NIBIB) with support for cryo-EM. Preliminary results from this LDRD would provide convincing evidence for follow-on funding. It would also help establish BNL as a unique cryo-EM center of excellence, especially since label development is deemed highly necessary for the field. We are in a unique position to answer this need, having established both nanoparticle labeling expertise and genetic production of tagged protein complexes.

APPROACH:

Three genetically engineered sequences investigated: these will be programmed into and expressed in target proteins. Gold nanoparticles will be designed that will bind to four sequences: 1) Ni-NTA-gold binding to 6x-His tags, 2) negatively charged gold to 6x Arg tags, 3) maleimido gold to link to cysteine residues, and 4) gold targeted to a gold-binding sequence.

TECHNICAL PROGRESS AND RESULTS:

Protein production and genetic engineering: several proteins in the complexes that we are to study have now been expressed in insect cells using the bacculovirus method. This includes Ku70, Ku80, Xrcc4, ISWI, and the ACF chromatin remodeling complex. These have been engineered with the 6x-Histidine tag and for a control, without the His tag, by substituting the Flag tag. Purification of these proteins has been completed, and various columns and buffer conditions were explored to maximize yield and maintain protein integrity. Under many conditions, the proteins aggregate or do not purify well. The conditions for Ku70/Ku80, ISWI, ACF1 and the complete ACF complex have now been worked out to reasonable satisfaction. ISWI has been expressed now with a GST tag.

Additional genetic tags have now been designed and have been produced: the Arg tag, Cysteine tag, calmodulin binding domain (CBD) tag, and gold-binding sequence tag. These were added to Chrac17, a component of the ACF complex, and expressed in bacteria.

The gold-binding sequence (GBS) tag was a significant advance. A phage display system was used to identify peptide sequences that bind strongly to gold nanoparticles. After increasing rounds of more stringent conditions, phage were isolated and grown that contained the binding sequence. The sequence was then identified by DNA sequencing. Another approach was to bind gold clusters to a "sticky" protein, fibrinogen, then digest it with trypsin (several enzymes were tested) and purify the gold-peptide conjugate. After releasing the gold by mercaptoethanol treatment, the peptide was determined by mass spectrometry. These two approaches to find the gold-binding sequence were combined and yielded several consensus sequences. The top four candidates were programmed into a plasmid to express Chrac17 with this sequence at its N-terminus. The tagged Chrac17 was then incubated with gold and purified by size exclusion gel chromatography. As a control, Chrac17 was incubated with the gold nanoparticles without the GBS tag. Results showed that one of the sequences had very specific binding with virtually no binding to the control. Another showed binding, but had some binding to the control. Electron microscopy is underway to document the specific binding morphologically.

Gold particle synthesis: 1.8 and 3-6 nm gold particles with the nitrilotriacetic acid functional ligand were synthesized. These were then charged with nickel. Binding to Ku70, Ku80, and ISWI was evaluated both by blots and column chromatography. Labeling with the gold targeted to the His tag was compared to gold binding to the same proteins without the His tags. A significant problem to overcome is that we found some binding of the gold particles to proteins without the His tag, even though there was more binding to those with the His tag. Methods to eliminate this "non-specific" binding were addressed, and include: high salt to reduce electrostatic binding, and use of detergents to reduce hydrophobic interactions. We found that high salt (0.3-0.5 M NaCl) was effective in reducing background by blocking charge interactions. We also found pre-reaction of the protein with N-ethylmaleimide also reduced background by blocking free thios that can interact with gold nanoparticles. Finally, a 10-20 molar excess of nickel ions was particularly useful in eliminating background binding. Changing the metal from nickel to copper, mercury, cobalt,

zirconium, and gadolinium was explored to give different binding affinities. Larger gold nanoparticles (3-6 nm) were synthesized and functionalized since they are more visible by electron microscopy. Positive results of specific binding to His-tagged proteins were obtained.

A significant result was the formation of various protein superstructures that we could control by adjusting the size of the gold nanoparticles, their surface functionality, and the placement of the genetic tags. With Adenovirus 12 (Ad12) knob proteins, we were able to form spherical, virus-like structures with the gold nanoparticle as the core. With the 20S proteasomes, we were able to form large, micron sized 2-D planar arrays. This advance should facilitate EM structural analysis of small proteins and protein complexes.

Electron microscopy and image analysis: Individual proteins, Ku70/80, ISWI, ACF1 and the ACF complex were prepared for negative stain EM. Various stains were investigated. The ACF complex visualization was successful and about 12,000 particles were obtained and processed to find the 3-D structure of this important protein which has never been solved. This is the first structural determination of this important chromatin remodeling complex.

SPECIFIC ACCOMPLISHMENTS:

Publication:

Rational design of protein suprastructures using functionalized nanoparticles: From discrete monomer to ordered network. Hu, M.; Qian, L.; Brinas, R.P.; Lymar, E. S.; and Hainfeld, J. F. Nano Letters (submitted).

LDRD FUNDING:

FY 2004	$ 12,933
FY 2005	$114,424
FY 2006	$135,077

The Use of Singular Point Genome Sequence Tags to Analyze Community Composition and Metabolic Potential

Daniel van der Lelie *04-060*

PURPOSE:

This project aims at developing a high throughput approach to compare closely related microbial strains and to analyze microbial communities and their metabolic potential. The proposed technique is a unique spin-off of the Genome Sequence Tag (GST) technology that was recently developed and patented by BNL.

APPROACH:

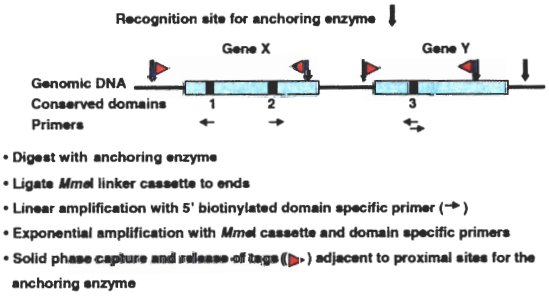

Figure 1: Schematic representation of the SP-GST approach on a conserved gene domain. Only one conserved region per gene of interest is required to generate genome signature tags. Tags (▶) can, depending on the orientation of the primer, be generated from the anchoring enzyme site located upstream or downstream of the primer annealing site. Different steps involved in generating tags are indicated in the figure. Numbers (1-3) indicate three different conserved regions located in genes X and Y.

To overcome the major limitation of the GST technology, namely the large number of tags, we used the 16S rRNA gene to develop the singular point GST technology, as it is ideal for the following reasons:

- 16S rRNA gene present in all prokaryotes.
- 16S rRNA copy number will define number of distinct GSTs per species.
- Database available with >100,000 16S rRNA gene entries.
- Tag frequencies will reflect community composition.
- Each tag will allow direct coupling with a 16S rRNA gene for species identification.

The principle of the SP-GST protocol we developed is presented in Figure 1. In addition to the 16S rRNA gene, it can be employed for any gene as long as one conserved domain is available. As anchoring enzyme we determined *Csp*6I as our best choice.

In addition, we are applying other 16S rDNA based approaches to analyze the composition of microbial communities found in association with trembling aspen.

TECHNICAL PROGRESS AND RESULTS:

16S rRNA based SP-GST tags of pure strains. To investigate whether 16S SP-GST tags generated would allow us to discriminate between closely related strains of *Bacillus cereus* and *Bacillus anthracis*. As the rDNA operons of the *B. anthracis* species are nearly identical, none of the 59 chosen anchoring enzymes yielded internal or upstream SP-GST tags from 16S rDNA that distinguished between the *B. anthracis* strains Ames, Ames 0581 and Sterne. Internal 16S SP-GST tags and SARST tags also failed to discriminate between *B. cereus* and *B. anthracis* on the species level. However, *Csp*6I-based identifier tags generated upstream of the 16S rDNA clearly do distinguish between *B. cereus* and *B. anthracis* species, as well as between

different *B. cereus* strains. Therefore, when comparing closely related members of the genus *Bacillus*, *Csp*6I SP-GST tags generated upstream of the 16S rDNA have better specificity than internal 16S SP-GST and SARST tags.

rDNA based libraries for microbial community analysis. To better understand the implications that elevated atmospheric CO2 has on microbial communities, we provide the first detailed analysis profiling changes in specific groups of microbes to specific soil processes. Classification of 6996 complete ribosomal DNA sequences from soil beneath trembling aspen provides an unprecedented, detailed and deep branching profile of changes in its complex microbial community composition induced by elevated atmospheric carbon dioxide (CO_2) (560ppm). Total bacterial and eukaryotic abundance does not change; however, an increase in heterotrophic decomposers and ectomycorrhizal fungi is observed. Nitrate reducers and ammonium oxidizing archaea significantly decreased under elevated CO_2. These changes in soil biota are evidence for altered interactions between trembling aspen and the microorganisms in its surrounding soil. This supports higher turn-over rates of biomass and availability of essential elements for increased plant growth under elevated CO_2.

These changes in the trembling aspen microbial community composition further support previously reported increases in fine root biomass turn-over rates, sustaining the availability and translocation of essential nutrients required for increased plant growth under elevated CO_2. This is further supported by Hu, et al., who noted that elevated CO_2 alters the interaction between plants and microbes in favor of plant N utilization, thus prolonging the observed increase in plant biomass production under elevated CO_2.

Our results show that microbial communities appear to be altered by elevated atmospheric CO_2 and that these changes can have implications for ecosystem function, especially via effects on the cycling of essential elements. Future investigations should shed more light on how elevated atmospheric CO_2 affects the diversity of life, the complexity and functioning of microbial communities in soil, the cycling of essential elements, and may further facilitate the prediction of such environmental impacts providing the key for their future correction.

SP-GST is a high throughput sequencing based method that only requires the presence of one conserved domain in the gene of interest. This makes SP-GST complementary to well established microarray methods for the analysis of microbial communities and their specific functions. The SP-GST concept on the 16S rRNA gene was part of a previously reported patent application entitled "Genome Signature Tags."

We performed the largest study of the microbial communities in the rhizosphere to date and confirmed the important role of Archaea in soil processes.

SPECIFIC ACCOMPLISHMENTS:

Publications:

Factors influencing the composition of bacterial communities found at abandoned copper-tailings dumps. De la Iglesia, R.; Castro, D.; Ginocchio, R.; van der Lelie, D.; and González, B. J. Appl. Microbiol. 100, 537-544 (2006).

Column experiments to assess the effects of electron donors on the efficiency of *in situ* precipitation of Zn, Cd, Co and Ni in contaminated groundwater applying the biological sulfate removal technology. Geets, J.; Vanbroekhoven, K.; Borremans, B.; Vangronsveld, J.; Diels, L.; and van der Lelie, D. Environ. Sci. & Pollut. Res. 13, 362-387 (2006).

DsrB gene-based DGGE for community and diversity surveys of sulfate-reducing bacteria. Geets, J.; Borremans, B.; Diels, L.; Springael, D.; Vangronsveld, J.; van der Lelie, D.; and Vanbroekhoven, K. J. Microbiol. Methods 66(2), 194-205 (2006).

Use of single-point genome signature tags as a universal tagging method for microbial genome surveys. van der Lelie, D.; Lesaulnier, C.; McCorkle, S.; Geets, J.; Taghavi, S.; and Dunn, J. Appl. Environ. Microbiol. 72(3), 2092-2101 (2006).

Elevated CO_2 affects soil microbial diversity associated with trembling aspen. Lesaulnier, C.; Papamichail, D.; McCorkle, S.; Ollivier, B.; Skiena, S.; Taghavi, S.; Zak, D.; and van der Lelie, D. PloS Biol. (in preparation).

LDRD FUNDING:

FY 2004	$121,236
FY 2005	$185,509
FY 2006	$ 77,544

3-D Electronic Wave Functions from EM Images

Joseph S. Wall *04-061*
Y. Zhu

PURPOSE:

Presently available detectors in the Scanning Transmission Electron Microscope (STEM) record only a small fraction of the available information. We have designed a new detector to record over 1000 signals simultaneously, instead of the present 3. We are using image simulation to understand how to combine these signals in order to determine atom locations and charge distribution in the specimen. The TEAM Project (Transmission Electron Aberration-corrected Microscope) is a major DOE/BES effort to improve the resolution of both conventional and STEM instruments. Development of better detectors is an important aspect of that project and our efforts, if successful, should enhance BNL's position to obtain the second TEAM Instrument (the first is already committed to Lawrence Berkeley National Lab).

APPROACH:

STEM makes an image by scanning a finely focused probe over a thin specimen while recording the number of electrons deflected as a result of striking atoms in the object. The scan is a TV-type raster and all signals are stored and displayed digitally. The 3 signals recorded currently give a quantitative map of the mass distribution and this is the basis of our BNL STEM user facility with over 50 active projects.

The three signals presently used are obtained by integration over annular regions of the detector plane using scintillators and photomultipliers to give quantum detection efficiency. Large-angle and small-angle scattering detectors give dark-field images proportional to the mass of atoms in the path of the beam. These signals are useful for quantitative microscopy and imaging of atom columns in thin specimens. As valuable as this information is, it is only a small fraction of what could be used.

The new approach supported by this LDRD is to utilize the additional information present in the detector plane, which is now lost by averaging. The actual intensity distribution consists of three components: 1) a convergent beam electron diffraction (CBED) pattern outside the disc of the transmitted beam giving information about the 3-D spatial arrangement of atoms within the probe, 2) an in-line hologram within the disc of the transmitted beam and 3) lateral displacement of the central beam disc due to electric or magnetic fields within the area probed by the beam.

We have adapted image-simulation software to study: 1) information available, 2) detector properties needed to record it, 3) methods to extract specimen information and 4) results to be expected on scientifically interesting specimens. The software uses the multi-slice method to accurately simulate propagation of an electron wave through a specimen containing up to 10^7 atoms, as well as the wave optics of image formation. This allows simulated imaging of all atoms in a 25 nm cube. Objects can be any known structure and can be placed on an amorphous or crystalline support and embedded in an amorphous or crystalline matrix.

In a previous LDRD we designed a high-resistivity Si detector with 32x32 elements, high detection efficiency and high speed, suitable for STEM use. The first device, fabricated in the Instrumentation Division had a serious defect. The second try was not perfect, but appears adequate to demonstrate the utility of the approach. Testing on STEM revealed problems with the electronics, which are being corrected by the Instrumentation Division. This prototype will play a key role in future application of the TEAM instruments

and strengthen BNL's case for hosting the second TEAM instrument.

To test our approach, we have selected two specimens of interest to the NanoScience community and available at BNL: 1.4 nm diameter gold particles (catalysts) and nanotubes.

TECHNICAL PROGRESS AND RESULTS:

We recruited a post doc, Xiaodong Tao. His tasks were to critique previous work in this area, work on reconstruction algorithms and aid in data analysis. Unfortunately, he left to take a permanent position elsewhere in July '05 and Steve Volkov, an Assistant Scientist in Y. Zhu's group, took his place, but with some loss of continuity.

The high-risk component is the attempt to retrieve asymmetric electronic charge distributions as well as atomic coordinates for ordered and "amorphous" objects. The intermediate goal is to retrieve the exit wave amplitude and phase, from which the atomic arrangement can be deduced.

Thus far we improved the simulation program and generated simulated data for gold particles and nanotubes. This data is free of practical limitations (such as vibration, finite dose, radiation damage, etc.) and is being used to test reconstruction algorithms.

All of the ideas regarding the "oversampling problem" have been summarized to solve the reconstruction problem for "in-line" holography for STEM and how the complex potential (projection) of any object could be retrieved from collecting and analyzing a series of CBED patterns have been summarized.

Volkov refined these ideas and developed new algorithms for "Position-Sensitive Diffractive Imaging in STEM by an Automated Chaining Diffraction Algorithm." We expect to continue after the expiration of the LDRD to test the version 2 STEM CBED detector in STEM3 in Biology and produce real data for comparison to the simulations. We will investigate the effect of charged atoms and asymmetrical charge distributions in simulation and reality. We will define the extent to which we can extract 3-D atomic positions and charge distributions from data acquired with the STEM CBED detector and the increase in value of the data relative to that available with the standard integrating annular detector.

SPECIFIC ACCOMPLISHMENTS:

Publication:

"Position-Sensitive Diffractive Imaging in STEM by an Automated Chaining Diffraction Algorithm," V. V. Volkov, J. Wall and Y. Zhu Submitted to Ultramicroscopy

Proceedings:

MSA Conference, Chicago, Jul.30 - Aug. 3, 2006, *"Simulation of Coherent Scattering in the STEM,"* J S Wall (platform)

"Exit Wave Function Retrieval from Diffraction Patterns with Variable SAED Aperture," V. Volkov, J. S. Wall, Y. Zhu (platform)

Award:

J. Wall, Microscopy Society of America, Scientist of the Year, 2006- Biology

LDRD FUNDING:

FY 2004	$ 98,945
FY 2005	$149,814
FY 2006	$ 67,144

Functional MRI Studies in Rats Using Implanted Brain Electrodes

Andrew N. Gifford *04-062*

PURPOSE:

The overall goal has been to determine the feasibility of using the animal MRI to identify regions of the brain that become activated by direct stimulation of the brain via an implanted electrode. These experiments are performed on anesthetized rats. Using the implanted electrode it is possible to activate very localized areas or specific fiber tracts in the brain to determine their effects on other regions of the brain to which they are connected. Having developed this new approach to functional brain mapping, we have used it to address specific issues that remain unresolved in the neurobiology field. For example, a question we have investigated is to determine the effect of neuronal activity in the striatum on functional activity in the substantia nigra, a brain region that receives direct neuronal input from this area.

The implications of this project in terms of the BNL institutional strategy are the development of a new and relatively powerful approach to using the animal MRI (and PET) instrumentation at BNL to perform functional brain imaging experiments in rodent models.

APPROACH:

The previous fMRI (functional Magnetic Resonance Imaging) studies performed in rats and mice have mostly involved mapping the changes in fMRI signals in the sensory cortex of the brain produced by sensory stimulation, such as pain signals or olfactory signals, in the anesthetized animal. Although these studies have been valuable in examining the fMRI response in the sensory cortex, they have been of little value in examining neuronal activity outside of this region. In our approach we have used an electrode implanted in the brain of the animal to provide direct and selective focal activation of regions outside of this one area. Our studies in this project focused on electrical stimulation in the striatum and motor cortex, since the anatomical connections of these regions to other brain areas is well documented and of significant clinical importance. Also, together with the MRI studies, we used ^{18}F-fluorodeoxyglucose (FDG) and ex vivo autoradiography to verify activation of the brain tissue by electrical stimulation via the implanted electrode.

The electrode development and surgeries were performed by Dr. Jasbeer Dhawan (senior research associate). Dr. Congwu Du and her student assisted us with setting up the MRI imaging.

TECHNICAL PROGRESS AND RESULTS:

Activation patterns from stimulation in the thalamus. We conducted several studies in which the stimulating electrode was placed in the thalamus of the rat. The stimulation was then switched on while simultaneously collecting images with the animal in the MRI scanner. Images were acquired over the frontal cortex area that corresponds to the expected region of activation from stimulation of this area. Analysis of the data from these rats indicated a pronounced fMRI activation in the frontal cortex on the side of the stimulation. This activation was in exactly the expected area from the known anatomical connections between the thalamus and the frontal cortex. These experiments thus effectively confirmed that fMRI neural activation could be

demonstrated by direct electrical stimulation of brain pathways, which was the primary goal of our project.

Activation patterns from stimulation in the striatum. Following the success of our thalamic stimulation experiments, we conducted a number of exploratory studies in which the stimulating electrodes were placed in the striatum, a component of the basal ganglia in the brain. Stimulation of this area is of interest since unlike the thalamic-cortical pathway, the pathways leading out of the striatum are inhibitory rather than excitatory. As we had hypothesized, stimulation of the striatum failed to produce a significant fMRI activation within the striatum itself, confirming our prediction that activation of inhibitory pathways in the brain would not produce an fMRI signal. However, in several of the rats we examined we saw robust fMRI activation in the thalamic region. This was interesting since this region is not directly connected to the striatum and suggests a disinhibition of nigral-thalamic neurons by the striatal stimulation.

SPECIFIC ACCOMPLISHMENTS:

Presentations: Mapping functional neural pathways in the rat brain using intracranial electrical stimulation. Dhawan, J.; Kanderappa, S.; and Gifford, A.N. Society for Neuroscience 35th Annual Meeting. Washington DC, Nov 12-16, 2005.

Future funding: Two NIH proposals employing the preliminary data collected in this LDRD have been submitted and are currently under review.

NIH-NBIB (Gifford; Benveniste as co-P.I.)
R01 (proposed dates: 04/07 - 03/10; $750,000 total direct)
Functional neuroimaging studies in the rat basal ganglia

NIH-NINDS (Gifford)
R01 (proposed dates: 08/07 - 07/11; $950,000 total direct)
Functional and pharmacological mapping of deep brain stimulation in rats

LDRD FUNDING:

FY 2004	$ 78,466
FY 2005	$119,912
FY 2006	$ 56,135

Optimizing Functional Neuroimaging Techniques to Study Brain Function in Health and Disease States

Rita Z. Goldstein *04-063*

PURPOSE:

The optimal study of functioning human brain circuits would reveal both the location and progression of the neural activities underlying mental processes. We combine simultaneously the high spatial resolution of functional magnetic resonance imaging (fMRI) with the high temporal resolution of event-related potential (ERP) brainwave analyses. This project brings a highly innovative technique to BNL for development as a high-resolution spatiotemporal functional neuroimaging for the assessment of cognitive-behavioral (e.g., sustained attention, working memory, inhibitory control) and emotional (e.g., salience/reward attribution) brain functions in addiction and other medical science research.

APPROACH:

A combination of the complementary fMRI and ERP techniques is a very attractive aim in neuroscience, and a number of research groups have taken up the challenge.

Goldman et al. (UCLA Brain Mapping Center) developed a method for acquiring simultaneous electroencephalography (EEG) and fMRI by combining analog preprocessing and digital post-processing to strongly suppress common artifacts. Their group implemented a functional scan protocol that yields windows of artifact-free EEG between short gradient and radio frequency bursts during functional scanning.

Bonmassar et al. (NMR Center at Massachusetts General Hospital). They recorded sensory ERPs using interleaved EEG and fMRI techniques. Their group demonstrated the feasibility of recording even small exogenous ERP components.

Kruggel et al. (Max-Planck Institute of Cognitive Neuroscience) has conducted combined ERP–fMRI experiments under cognitive stimulation using a 3 T MR scanner. Their group has studied later endogenous processes including Gestalt perception and target processing.

Other groups in the United Kingdom (Lemieux et al., Welcome Department of Cognitive Neurology; Allen et al., National Hospital for Neurology and Neurosurgery) reported on the basic science and clinical utility of the EEG/fMRI combination for localization of the generators of interictal epileptiform discharges.

Our laboratory has developed a response inhibition paradigm for examining reward processing and motivation in both fMRI and ERP environments. We have recorded control subjects as they performed the task during separate fMRI and ERP sessions. Amplitudes of the cognitive P300 ERP component were significantly larger in monetarily motivating conditions, and corresponded with subjective ratings of interest and excitement about the task. During fMRI in controls and cocaine addicts the task produced a distinct pattern of activation in the orbitofrontal cortex of cocaine addicts that mirrored subjective reports showing deficits in reward processing. We expected to find similar reward processing deficits in cocaine addicts under our ERP paradigm, as reflected by P300 amplitude and self-report measures.

TECHNICAL PROGRESS AND RESULTS:

During 2004 the hardware and software components required to acquire and analyze human cognitive ERPs were identified and acquired. After consideration of several state-of-the-art alternatives, a leading commercial ERP system was selected. Modifications of the existing research protocol to incorporate ERP testing were completed and approved by the BNL IRB.

In 2005 Tom Maloney was hired to develop the ERP laboratory. Dr. Maloney rehabilitated the BNL lab space and installed the NeuroScan ERP system for independent use outside the fMRI environment. Dr. Lisa Cottone ported the established fMRI paradigm for assessment of the sensitivity to monetary reward for use in eliciting cognitive ERPs. The development of novel cognitive tasks for use during simultaneous fMRI/ERP recordings was initiated, and produced 3 new tasks: the drug Stroop, threat Stroop, and the punishment Stroop. ERP data was collected for 16 cocaine-addicted subjects and 5 healthy controls.

We have now collected data from an additional 9 cocaine-addicted, and an additional 15 healthy control subjects (for a total of 45 subjects) using the monetary reward task. We have also been been joined by Muhammad Parvaz, a Ph.D. student from the SBU Biomedical Engineering program, who is working on the development and implementation of methods for the coregistration and analyses of the fMRI and ERP data. Data of the first 18 cocaine and 18 control subjects have been analyzed.

We have also collaborated with Giorgio Bonmassar at MGH, and pending final system modifications, we plan to purchase Dr. Bonmassar's unique system. Specifically, we are interested in taking advantage of the open SW source written mostly in high-level language (Labview) and the open HW schematics by customizing the system to our internal needs. We expect that the 128 channel MRI-compatible EEG system now in development will enable us to obtain supremely high resolution EEG recordings. The system employs a novel 128 Channel InkCap that allows safer EEG/MRI recordings at the very highest spatio-temporal resolution. We believe this system and its future derivatives will lead in the cognitive neuroscience market, as other currently available systems have not proven sufficiently reliable for our research purposes.

This integration of the EEG data with anatomical and functional MR images is essential for advancing our cognitive neuroscience studies by including highly accurate sampling of the scalp recorded electric field. Specifically, the EEG/fMRI multimodality will enable us to perform experiments where the number of stimuli is limited, and where consequently it is impossible to repeat the same experiment with the same subject using the two modalities separately. Studies of the effect of sleep deprivation or pharmacological intervention (e.g., methylphenidate) on long-term priming or learning are a prime example. Furthermore, scanner noise in the MRI environment (mostly during EPI) can influence the timing and amplitude of ERPs making the separate measurements incongruent.

This project involves human subjects.

SPECIFIC ACCOMPLISHMENTS:

PI received Woman of the Year in Science, Brookhaven Town Award.

PUBLICATIONS:

Goldstein, R.Z.; Leskovjan, A.C.; Hoff, A.L.; Hitzemann, R.; Bashan, F.; Khalsa, S.S.; Wang, G.-J.; Fowler, J.S.; and Volkow, N.D. (2004). Severity of neuropsychological impairment in drug addiction: association with metabolism in the brain reward circuit. Neuropsychologia, 42, 1447-1458. **The 5th most ***heavily downloaded articles from the journal, 7/05***.

Goldstein, R.Z.; Alia-Klein, N.; Leskovjan, A.C.; Fowler, J.S.; Wang, G.-J.; Gur, R.C.; Hitzemann, R.; and Volkow, N.D. (2005). Anger and depression in cocaine addiction: association with the orbitofrontal cortex. Psychiatry Res: Neuroimaging, 138, 13-22.

Volkow, N.D.; Wang, G.-J.; Begleiter, H.; Porjesz, B.; Fowler, J.S.; Telang, F.; Ma, Y.; Wong, C.; Logan, J.; Goldstein, R.Z.; Thanos, P.K.; and Alexoff, D. (2006). High Dopamine D2 Receptors in Unaffected Members of Alcoholic Families: Possible Protective Factors. Archives of General Psychiatry, 63, 999-1008.

Goldstein, R.Z.; Cottone, L.A.; Jia, Z.; Maloney, T.; Volkow, N.D.; and Squires, N.K. (2006). The effect of graded monetary reward on cognitive event-related potentials and behavior in young healthy adults. International Journal of Psychophysiology, 62, 272-279.

Goldstein, R.Z.; Tomasi, D.; Alia-Klein, N.; Cottone, L.A.; Zhang, L.; Telang, F.; and Volkow, N.D. (2006). Subjective sensitivity to monetary gradients is associated with frontolimbic activation to reward in cocaine abusers. Drug and Alcohol Dependence, in press.

Goldstein, R.Z.; Alia-Klein, N.; Tomasi, D.; Zhang, L.; Cottone, L.A.; Maloney, T.; Telang, F.; Caparelli, E.C.; Chang, L.; Ernst, T.; Samaras, D.; Squires, N.K.; and Volkow, N.D. (2007). Decreased prefrontal cortical sensitivity to monetary reward is associated with impaired motivation and self-control in cocaine addiction. American Journal of Psychiatry, 164, 1-9.

Alia-Klein, N.; O'Rourke, T.; Goldstein, R.Z.; and Malaspina, D. (2007). Insight into illness and adherence to psychotropic medications predict violence severity in a forensic sample. Aggressive Behavior, in press.

Fowler, J.S.; Alia-Klein, N.; Kriplani, A.; Logan, J.; Williams, B.; Zhu, W.; Craig, I.W.; Telang, F.; Goldstein, R.Z.; Volkow, N.D.; Alexoff, D.; Vaska, P.; and Wang, G.-J. Brain MAO A Activity and MAO A Genotype in Healthy Male Subjects. Biol Psychiatry, in press.

PROCEEDINGS:

Zhang, L.; Samaras, D.; Volkow, N.D.; and Goldstein, R.Z. (2005). Machine Learning for Clinical Diagnosis from Functional Magnetic Resonance Imaging (#169). In IEEE Proc. of Computer Vision and Pattern Recognition,I:1211-1217.

Zhang, L.; Samaras, D.; Tomasi, D.; Alia-Klein, N.; Cottone, L.A.; Leskovjan, L.C.; Volkow, N.D.; and Goldstein, R.Z. (2005). Exploiting Temporal Information in Functional Magnetic Resonance Imaging Brain Data. In Proc Medical Image Computing and Computer Assisted Intervention, pp. 679-687.

Zhang, L.; Samaras, D.; Alia-Klein, N.; Volkow, N.D.; Goldstein, R.Z. Modeling Neuronal Interactivity using Dynamic Bayesian Networks. Neural Information Processing Systems, accepted.

LDRD FUNDING:

FY 2004	$100,684
FY 2005	$144,278
FY 2006	$ 69,277

Technological Development of a Fluorescence Probe for Optical Detection of Brain Functional Activation *in vivo*

Congwu Du 04-066
H. Benveniste

PURPOSE:

The objective of this project is to develop an optical probe that concurrently tracks blood volume, tissue oxygenation and intracellular calcium changes in the rodent brain *in vivo*. The new optical probe will provide new modalities for future brain functional studies by measuring calcium transients from the brain surface, and will complement other strategic and planned 'Life and Physical Science interface' initiatives in drug addiction and developmental research at BNL.

APPROACH:

A prototype optical device was developed, in which we integrated the multi-functional measurements into a single system. This catheter-based 'optical diffusion and fluorescence probe' (ODF probe) is able to capture changes in blood volume, tissue oxygenation and intracellular calcium concurrently from the surface of a living organ, such as the cortex of the brain. In FY 2005, the sensitivity of the system was examined using a transient cerebral ischemia model. Our experimental results demonstrated the capability of the newly developed optical and fluorescent technology.

One of the research goals in FY 2006 was to further examine the ODF probe's capabilities as a new research tool for pharmacological and pathophysiological applications in a living brain, which was a challenge because the drug-induced hemodynamic changes in the brain are much more subtle and quantitatively smaller than those observed in the diseased brain (e.g. ischemia, stroke or seizures). In other words the signal sensitivity of the ODF probe was tested. Another goal was to initiate the correlative analysis between MRI and optical measurements to further demonstrate the instrumental feasibility.

TECHNICAL PROGRESS AND RESULTS:

Effects of an acute cocaine challenge on optical measurement in cocaine-naïve rats: Figure 1 summarizes the mean changes in blood volume (CBV), cerebral oxygenation (S_tO_2) and intracellular calcium ($[Ca^{2+}]_i$) in response to 1mg/kg cocaine in drug-naïve rats using two different anesthetic regimens including isoflurane and α-chloralose. The data presented in Figure 1 demonstrates two important findings: 1) the cerebral blood volume and tissue oxygenation response to cocaine is dependent on the anesthetic used

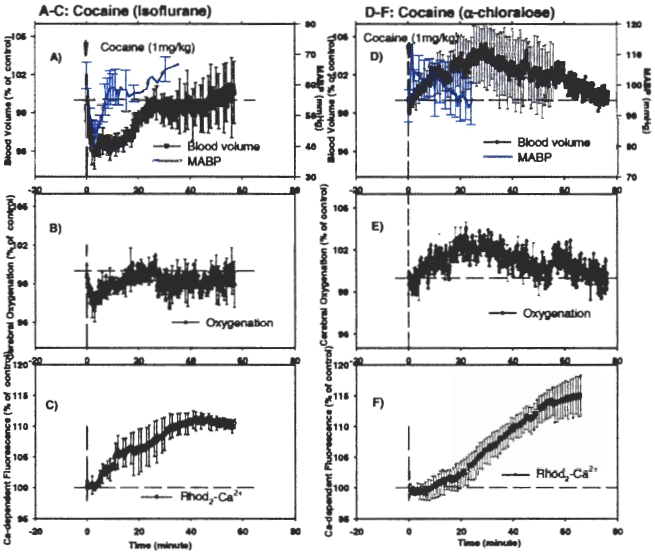

Figure 1: Cerebral responses to intravenous cocaine measured from the cortical surface of rats anesthetized with isoflurane- (Group 1, A-C, n=6) and α-chloralose (Group 2, D-F, n=4). A & D show the changes in cerebral blood volume, and B & E are the changes in tissue oxygenation, and C & F are the intracellular calcium changes induced by intravenous cocaine (1mg/kg). The overlaid solid-lines (blue) in A & D indicate the concurrent changes in mean arterial blood pressure (MABP); The vertical line signifies the time of the cocaine injection.

i.e., the CBV and tissue oxygenation signal decrease in the isoflurane-anesthetized rats (Fig.1A, B) and increase in the α-chloralose anesthetized rats (Fig. 1D, E); and 2) for both anesthetics cocaine induces a significant $[Ca^{2+}]_I$ increase as shown inFig.1C and Fig.1F. These data supported our original hypothesis that cocaine's toxic effects are not just the result of its cerebrovescular effects but also a consequence of its ability to increase $[Ca^{2+}]_i$. The finding of anesthesia-dependent CBV and S_tO_2 responses is shedding light on the current scientific literature reporting conflicting hemodynamic responses to cocaine when using functional magnetic resonance imaging to investigate the brain's effects of systemic cocaine. Our data demonstrating cocaine-induced increases in CBV and S_tO_2 in α-chloralose-anesthetized rats are in agreement with the finding of a positive BOLD response in fMRI studies using α-chloralose anesthetized rats following a systemic cocaine challenge.

MRI studies with cocaine administration has been initiated to examine the ODF probes role in pharmacological and patho-physiological applications. Diffusion-weighted MRI images were acquired, and the effect of cocaine on the apparent diffusion coefficient (ADC) of rat brains was calculated to characterize the possibility of tissue ischemia induced by cocaine. The experimental results complement the findings from our ODF probe.

Milestones for FY2006 were 1) Testing sensitivity of detecting drug-induced brain activations by measuring the changes in blood volume, oxygenation and intracellular calcium in the living animal; 2) Experimentally analyzing the difference of functional responses in the brain under various anesthetic conditions; 3) Initiating the diffusion-weighted MRI to analyze the correlation of MRI with optical measurements.

SPECIFIC ACCOMPLISHMENTS:

Publications:

1. Du, C.; Yu, M.; Volkow, N.D.; Koretsky, A. P.; Fowler, J.S.; and Benveniste, H. "Cocaine increases intracellular concentration of calcium in brain independent of its cerebrovascular effects." *J. of Neuroscience*, (in press, 2006).

Abstracts and Presentations:

1. Du, C.; Luo, Z.C.; Yu, M.; and Benveniste, H. "Optical approach to detect vascular functional changes induced by cocaine in living rat brain," *Proceeding of Biomedical Optics conference, Optical Society of America (OSA)*, TUI 5, 2006.
2. Du, C.; Wolf, A.; Perez, Y.; Pan, Y.T.; and Benveniste, H. "Microscopic Fluorescence Studies on Brain Intracellular Ca^{2+} Responses to Ischemia with and without Ca^{2+}- Channel Blockade," *Proceeding of Biomedical Optics conference, Optical Society of America (OSA)*, TUI 62, 2006.
3. Luo, Z.C.; Dhawan, J.; Benveniste, H.; Yu, M.; Gifford, A.; and Du, C. "Local cerebral blood flow responses to direct stimulation in somatosensory cortex: Laser doppler flowmetric and autoradiographic analysis," *Proceeding of Biomedical Optics conference, Optical Society of America (OSA)*, ME 17, 2006.
4. Du, C.; Ma, Y.; Forester, B.; Yu, M.; and Benveniste, H. "The effect of cocaine on the rat brain apparent diffusion coefficient, cerebral blood volume and mean arterial blood pressure," *Proceeding of 14th International Society for Magnetic Resonance in Medicine,* p3275, (2006).

Grant Proposal Pending:

NIH-K25 "*Optical and fMRI Studies of Cocaine in the Rat Brain,*" 12/01/06-11/30/11, 743,000 (direct cost).

LDRD FUNDING:

FY 2004	$ 27,032
FY 2005	$132,570
FY 2006	$121,180

Nuclear Control Room Unfiltered Air In-Leakage by Atmospheric Tracer Depletion (ATD)

Russell N. Dietz *04-069*

PURPOSE:

Nuclear plants with a licensing based, in part, on low control room (CR) unfiltered air in-leakage (UI) rates (<50 cfm), needed to use a tracer approach that directly measured this value; the standard tracer approach, which determines this value by difference, often results in an unacceptably large uncertainty. The goal was to use the Atmospheric Tracer Depeletion (ATD) approach at actual low in-leakage nuclear plants as the method for generating results mandated by the Nuclear Regulatory Commission (NRC). New programs, supported at BNL by specific nuclear plants for generating these NRC-required results, were a measure of the success of this project; results were reported to the NRC. There is a further mandate that such UI determinations be repeated on a tri-annual basis; once applied to a particular plant, repeat testing could be conducted less expensively by utility personnel employing ATD with BNL only performing the state-of-the-art analyses.

APPROACH:

Background. The mathematical hypothesis of this project was that the efficient removal of the ambient background concentration of certain perfluorocarbon tracers (PFTs) by the charcoal filters in a nuclear plant's dual control room emergency ventilation systems (CREVS) provides the means for the direct determination of UI. At steady state (SS), CR concentrations equal to those out of the charcoal implies no UI; a slight increase in the CR concentration means a slight amount of UI. The CR concentration relative to that in normal ambient air, times the rate of charcoal-filtered air, provides the UI quantification. This ATD approach had not been previously applied. The exploratory issues pertained to an assessment of the likely performance of installed charcoal systems for the nearly 100% removal of certain PFTs and the development of the sampling and analysis strategies for the successful quantification of the expected few one thousandths of the normal 5 to 10 parts per quadrillion ambient concentrations – a significant extension of the PFT technology.

Scope. **1)** Testing of commercial-grade nuclear charcoals for nearly 100% removal of PFT was needed with ASTM-type test cells & sampling apparatus. **2)** Nuclear plant charcoal filtration system tracer tent testing was to be compared to ATD testing. **3)** Accelerated depletion of PFT backgrounds in a large-volume nuclear facility required testing commercial portable charcoal-filtration units. **4)** The resulting low concentrations ($\sim 10^{-3}$ of ambient) required efficient high sampling rate systems. **5)** Such low-level analyses required enhancements to the gas chromatograph (GC) system. **6)** Unique ventilation designs at certain nuclear plants required revised flow modeling. **7)** ATD needed testing at commercial nuclear plants.

Methods. Standard laboratory procedures were used to conduct this research – with the exception of the state-of-the-art GC system and the use of nuclear control room facilities for conducting final demonstrations of ATD.

TECHNICAL PROGRESS AND RESULTS:

Early results included: **1)** Charcoal testing showed PFT removal efficiencies adequate for ATD – 99.90 to 99.94%. **2)** Four installed charcoal systems at an actual nuclear plant, tested for UI by ATD, perfectly tracked the traditional results. **3)** As expected, ATD testing in nuclear plants was expedited with 1000-cfm portable charcoal systems – rapidly depleting ambient PFT concentrations. **4)** Four types of low- to high-rate (50- to 500-mL/min) adsorbent sampling tube systems showed good efficiency **5)** Analyses of actual nuclear plant samples showed quantification difficulties with critical PFT peaks; GC enhancements

improved results. **6)** Flow modeling allowed the successful implementation of sampling strategies. **7)** The first ATD testing, where the utility is relying solely on this technique, was conducted at two nuclear plants.

FY 2005 results. The modeling and interpretation of the ATD results demonstrated the ability to determine UI in the complex case of a CR inside a control building (CB) – both with their own charcoal-filtration systems; conventional tracer testing was not applicable. Last year, the excellent replication of different samplers used in the 4 elevations of Plant-1 CB was presented; the following was the steady-state results for Plant-2 CB:

Steady State (SS) Conc. (cts/L) vs Elevation

Elevation	Train A	Train B
2073'	400 ± 30	703 ± 39
2032'	429 ± 23	831 ± 6
2016'	772 ± 69	1316 ±77
2000'	770 ± 31	1423 ±108
CB Avg:	601 ± 38	1093 ± 58

Surrogate ambient PFT conc of 7700 cts/L ≡ 10.2 ppq
(surrogate PFT is the average of 3 PFTs)

In FY06, it was concluded that the lower concentration on El 2073 & 2032 was due to out-leakage of the still lower concentration in the CR (see table below) on El 2046; same was observed at Plant 1. The precision of these low levels (750 cts/L ≡ 1.0 ppq) was excellent. At steady state, measured levels were significantly lower – especially in the CR and out of the charcoal systems (EVSs):

Surrogate PFT Conc (cts/L) at Two Plants

	Plant 1		Plant 2	
	Train A	Train B	Train A	Train B
CR	21 ± 1	74 ± 4	36 ± 3	17 ± 4
EVS	2 ± 1	46 ± 5	<1	<1
(net)	19 ± 1	28 ± 7	36 ± 3	17 ± 4
CB	<500	160 ±25	601 ±38	1093 ±58
EVS	1 ± 1	49 ± 7	10 ± 2	21 ± 3
(net)	<500	111 ±26	591 ±38	1072 ±58

Plant 1 CB Train-A test did not achieve steady state

The net CR and CB concentrations were used in the developed models to compute UI rates as shown in the next table. The plants, built as identical units but located in two different states, had the same CR rates but somewhat different CB rates. For both, UI met licensing specifications in the CRs (~10 cfm or less) and was much lower in the CBs than required (<300 cfm).

Unfiltered In-Leakage (UI) Rates (cfm)

	Plant 1		Plant 2	
	Train A	Train B	Train A	Train B
CR	6.9 ± 0.4	10.5 ± 2.6	10.1 ± 0.9	4.7 ± 1.1
CB	<63	14.2 ± 3.0	69.0 ± 3.4	109 ± 4

Plant 1 CB Train-A test did not achieve steady state

FY 2006 results. The modeling was revisited to include the out-leakage from the CR into the CB between the two uppermost elevations. The CB results now changed to a range:

Unfiltered In-Leakage (UI) Rates (cfm)

	Plant 1		Plant 2	
	Train A	Train B	Train A	Train B
CR	6.9 ± 0.4	10.5 ± 2.6	10.1 ± 0.9	4.7 ± 1.1
CB	<63 to 87	14 to 19	69 to 97	109 to 166
OA	903	969	833	674

OA was filtered outside-air rates (cfm) into CB.

Notice that higher OA rates into the CB (i.e., higher pressurization of the CB) gave lower UI rates. A presentation of these final results was given to the nuclear utility industry on January 19, 2006.

LDRD FUNDING:

FY 2004	$59,463
FY 2005	$88,764
FY 2006	$41,167

Perfluorocarbon Tracer Sampling, Tagging and Monitoring Techniques for use at the Urban Atmospheric Observatory

John Heiser *04-073*

PURPOSE:

As part of the Department of Homeland Security (DHS) initiatives, the Urban Dispersion Program (UDP) was designed to enhance emergency response capabilities in the event of airborne releases of harmful contaminants. An essential component of UDP is conducting field studies in NYC to provide data for improving and validating atmospheric models to simulate contaminant dispersal.

Perfluorocarbon tracers (PFTs) are uniquely qualified to provide the data necessary for model verification. PFTs can be used to safely simulate the behavior of contaminants under actual conditions within urban environments where it is particularly difficult to accurately predict fate and transport. This project is developing the crucial engineering hardware and methodology required to fully exploit the capabilities of PFTs to study transport of airborne contaminants in the deep urban canyons of NYC.

APPROACH:

The BNL Tracer Technology Group has done pioneering work in the development and practical use of PFTs. This expertise is being used to develop the equipment, methods and protocols for PFT sampling and tagging in the deep urban canyon. BNL was able to design, develop and deploy sampling and release equipment and methodologies in conjunction with UDP NYC field studies.

TECHNICAL PROGRESS AND RESULTS:

In the spring of 2005, the initial UDP field study (MSG05) was conducted in Midtown Manhattan. Six PFTs were released from five locations (for QA/QC, two at one location). Two 30-minute releases occurred each day, separated by 1½ hours of no release to allow the tracer to clear out prior to the next release. Dispersion of the tracers was determined by collecting air samples at various locations within a 400m radius. During this first study, the activities focused on vertical sampling protocol and personal dose monitoring.

The vertical extent and transport time of the tracer plume was measured by placing air samplers on surrounding buildings at various heights. To achieve a better time resolution at several of these sites, two samplers were co-located, with one sampler collecting 30-minute samples and the second collecting 5-minute samples. Results proved tracer transport occurred rapidly with significant levels seen in as little as 12 minutes.

Individual dose assessment studies were carried out by the EPA. Samples were collected using personal air samplers carried by 12 EPA volunteers. Each person had a fixed location or predetermined path to travel during the tracer release. BNL modified PAS-500 personal air samplers to accept a capillary absorption tube sampler and added a restrictor to the sampler to obtain a more consistent flow rate. Results of this sampling are being analyzed by the EPA.

During the summer of 2005, a second, larger UDP tracer study (MID05) was conducted in NYC, between Times Square and Central

Park, and bounded by 10th and 3rd Avenues. As in the first study, the Brookhaven Atmospheric Tracer Sampler (BATS) served as the primary air sampling device. Current BATS are over 25 years old and prone to failure. While the lids, containing the collection tubes are still "state-of-the-art", the operational bases are long past their prime and offer little versatility or convenience.

We developed a prototype of a new BATS base. The new unit included a new pumping system with variable, mass-flow controlled air flow, data logging, simplified programming using a web-based interface, greater program versatility such as variable sampling intervals and variable flow rates and now the unit can be addressed via cable or through wireless communication. The Personal Digital Assistant (PDA) was replaced with a single rugged chip.

As part of the MID05 study we were able to build and deploy three of the new BATS bases (Figure 1). The new BATS prototype performed flawlessly and represents a major improvement over the existing bases and has fully addressed quality assurance concerns of the older units.

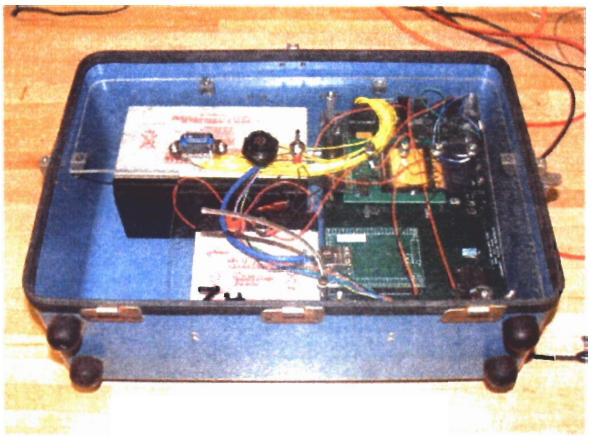

Figure 1. New Brookhaven Atmospheric Tracer Sampler base.

The MID05 study also required tracer release quantities considerably higher than those used in MSG05 which precluded cylinder releases. A new release system was developed (Figure 2). The system is battery operated, low power and portable and is based on a commercially available syringe pump. A prototype unit was built and tested. Release rates up to 15 g/min were achieved, which was much higher than required for the 4 sq km study area used in the MID05 tests.

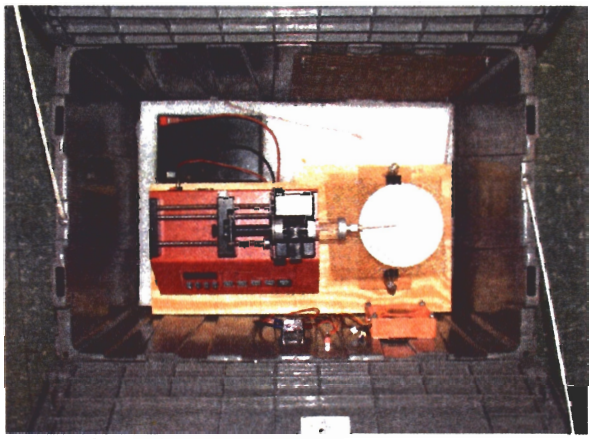

Figure 2. Syringe pump based portable Tracer Release System

For the MID05 study six units were built (using DHS funding) and deployed. The units preformed flawlessly, gave accurate, reproducible releases and were very well received by the UDP program manager and science community involved in the study.

In FY06, we developed a mass-flow controlled personal air sampler (PAS) to improve on the commercial PAS units used in MSG05 and MID05. The original samplers have quite a bit of variability in the flow rate which introduces uncertainty in the concentration measurements. The new units use mass flow measurement to control the flow rate and log the flow rate start and stop times. In addition, we continued to improve the programming for the BATS.

SPECIFIC ACCOMPLISHMENTS:

Presentations:

Plans for the Madison Square Garden 2004 (MSG04) Tracer Experiment in Manhattan, S. Hanna, M. Reynolds, J. Heiser, and R. Bornstein, Fifth Conference on Urban Environment, American Meteorological Society, Vancouver, BC, Canada, August 2004.

Reports:

T. Watson, J. Heiser, P. Kalb, R. Dietz, R. Wilke, and R. Wieser, The New York City Urban Dispersion Program March 2005 Field Study: Tracer Methods and Results, Brookhaven National Laboratory, Formal Report, July 2005.

LDRD FUNDING:

FY 2004	$65,530
FY 2005	$98,809
FY 2006	$45,056

Development of an Aerosol Mobility Size Spectrometer and an Aerosol Hygroscopicity Spectrometer

Jian Wang *04-079*

PURPOSE:

The technical objective of this project is to develop two novel instruments. The first instrument, referred to as the Aerosol Mobility Size Spectrometer (AMSS), will be capable of measuring aerosol size distributions for the entire diameter range of 15 nm to 1000 nm within ~1 second. AMSS offers a factor of 50 improvement in time resolution over current state-of-the-art research instruments. The second proposed system, referred to as the Aerosol Hygroscopicity and Volatility Spectrometer (AHVS), will be capable of measuring size-resolved aerosol hygroscopicity and volatility over the diameter range 15 nm to 600 nm within ~2 minutes. Both instruments will significantly improve our ability to characterize atmospheric aerosol properties and to study the evolution of aerosols (e.g. size distribution, hygroscopicity, and chemical compositions) as they are transported downwind of their sources.

APPROACH:

The current incomplete understanding of atmospheric aerosol properties and their controlling processes necessitates further intensive field projects involving aircraft-based measurements. As a result of the slow measurement speed of current techniques, accurate measurements of aerosols with high spatial variation, such as aerosols in the vicinity of clouds or inside a pollution plume, are not possible onboard research

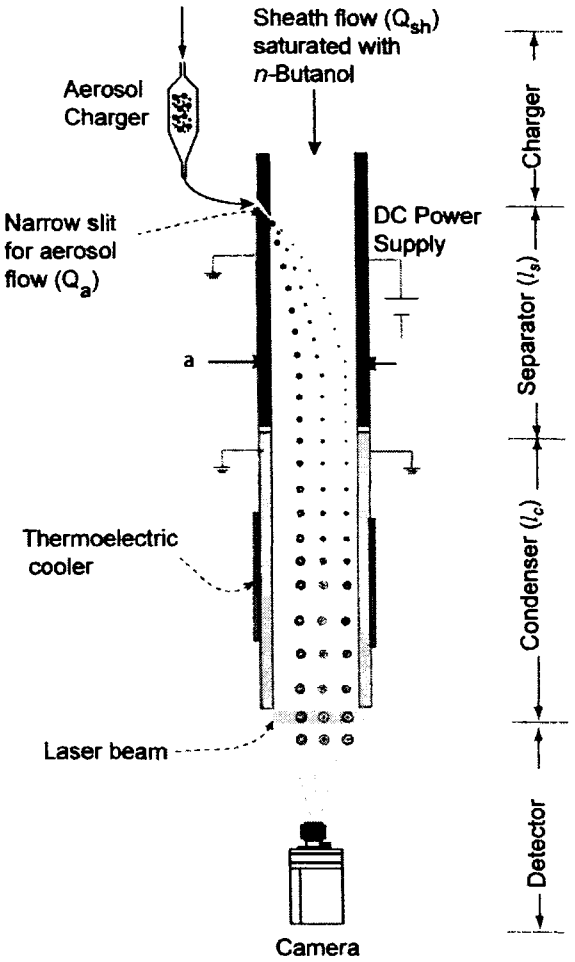

Figure 1. Schematic of the Aerosol Mobility Size Spectrometer (AMSS).

aircraft. The proposed AMSS addresses the issue of measurement speed by measuring charged particles of different sizes simultaneously. Figure 1 shows the schematic of the proposed AMSS, which consists of four major sections. Aerosol samples are first charged in a bipolar aerosol charger. The charged aerosol particles then enter a separator through a narrow slit. Particle-free sheath flow saturated with n-butanol is introduced into the separator from its top as shown in Figure 1. A constant electric field perpendicular to the flow direction is established inside the separator by applying a high voltage to one side of the chamber and grounding the other side.

Under the influence of this electric field, the charged particles are separated into different flow streams/locations according to their mobilities (sizes). The separated particles then enter a subsequent condenser. As no electrical field is applied in the condenser, the positions of the particles in the direction of electric field remain unchanged after particles exit the separator. Inside the condenser, the cooling of the flow generates a high supersaturation of butanol that activates particles as small as 5 nm in diameter. After aerosol particles grow into supermicron droplets, they are detected by an imaging system. A laser beam is collimated into a sheet of light, which illuminates the particles as they cross. The images of particles are recorded by a high speed CCD camera. Recorded particle images provide both the size dependent position and the concentration of particles, which are then used to derive aerosol size distributions.

Dr. Pramod Kulkarni and Dr. Peter Takacs participated in this project.

TECHNICAL PROGRESS AND RESULTS:

A prototype AMSS based on the theoretical analyses and simulations was constructed. The performance of the prototype AMSS, including the sizing accuracy, counting efficiency, and mobility resolution have been characterized in detail. In our characterization experiments, we used a differential mobility analyzer (DMA) to generate monodisperse aerosols of desired sizes, which were then simultaneously measured by the prototype AMSS and a commercial Condensation Particle Counter (CPC, TSI Inc., model 3760). Figure 2(a) shows that the particle sizes measured by the AMSS agree well with the DMA classified sizes over a wide size range, which indicates the AMSS is capable of measuring particle

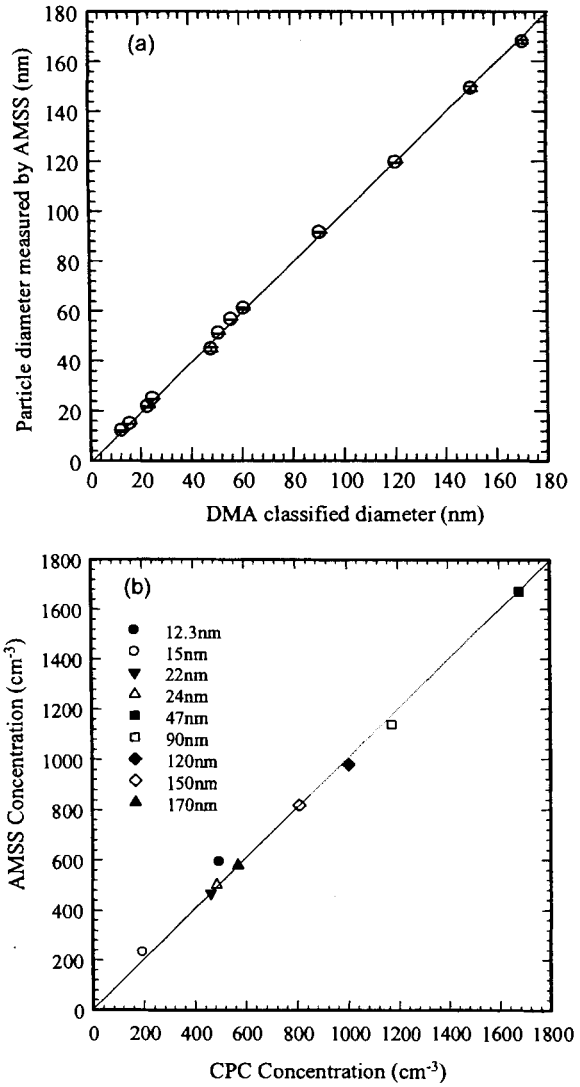

Figure 2. (a) Comparison of the particle diameters measured by AMSS to the DMA classified diameters. (b) Comparison of the particle concentrations measured by the AMSS to those measured by a CPC.

size with high accuracy. Figure 2(b) compares the simultaneous measurements of the particle concentrations by the AMSS and the CPC. When the particle diameter was greater than 15 nm, close agreement was found between the two measured concentrations, which suggest the AMSS has a counting efficiency of nearly 100% for particles larger than 15 nm. For particles smaller than 15 nm, the particle concentrations measured by the AMSS were higher than those measured by the CPC, indicating even higher counting efficiencies

of the AMSS for small particles. The characterization results showed that the prototype AMSS is capable of measuring aerosol size distributions with high speed, sizing accuracy, and counting statistics.

SPECIFIC ACCOMPLISHMENTS:

Publications:

Kulkarni, P. and J. Wang, 2006. "A New Fast Mobility Spectrometer for Real-Time Measurement of Aerosol Size Distribution: I. Concept and Theory," *Journal of Aerosol Science,* 37(10), pp1303-1325.

Kulkarni, P. and J. Wang, 2006. "A New Fast Mobility Spectrometer for Real-Time Measurement of Aerosol Size Distribution: II. Design, Calibration, and Performance Characterization," *Journal of Aerosol Science,* 37(10), pp 1326-1325

Presentations:

Kulkarni, P. and J. Wang. "A New Aerosol Mobility Size Spectrometer: Design, Calibration, and Performance Evaluation," *Annual Conference of American Association of Aerosol Research*, Austin, Oct. 2005.

LDRD FUNDING:

FY 2004	$65,589
FY 2005	$99,415
FY 2006	$53,471

Exploration of Thermal Diffusion Processes in CdZnTe for Improved Nuclear Radiation Detectors

Aleksey Bolotnikov *04-086*

PURPOSE:

The goal of the project is to achieve the high detection efficiency and high spectral resolution of virtual Frisch-grid CdZnTe (CZT) detectors by extending the high uniformity response over the entire volume of the bar-shaped CZT crystals.

APPROACH:

We propose to employ a PIN junction structure for CZT devices (similar structures were developed for Ge and Si detectors) to achieve full depletion of the active volume of the semiconductor detectors (virtual Frisch-ring detectors in this case) with minimum leakage current. This provides uniform response of CZT detectors and ensures their high performance.

Two approaches to produce PIN junctions are to be investigated: (1) by making the Schottky barrier contacts, and (2) by thermal diffusion of p-type dopants at high temperatures >500 C. The later approach leads to the formation of PN junctions near the contacts, which is equivalent to the first approach, but it provides a more reliable and controllable way of fabrication of blocking contacts on the CZT surface.

TECHNICAL PROGRESS AND RESULTS:

During FY 2004-2005, we investigated the first approach by showing improvement in spectroscopic properties of PIN junction CZT detectors. We fabricated several CZT crystals configured as Frisch-ring detectors. We developed the pulse shape analyses technique and x-ray mapping system to study the lateral and depth uniformity of the charge collection efficiency inside the Frisch-ring detectors. We developed the process of making high-quality Schottky contacts and surface passivation for the Frisch-ring detectors. With long (>10 mm) CZT devices achieved the energy resolution of less than 0.8% at 662 keV. The possibility to thermally diffuse p-type dopants at > 500 C was also investigated. It is known, that unlike Si and Ge, detector-grade CZT could not withstand high temperatures. We found experimentally that CZT material already irreversibly loses its semi insulating property above ~140 C (HPB material) and above ~200 C (MB material).

During FY 2006, we developed a new design for virtual Frisch-grid-type detectors. We investigated the factors limiting energy resolution of thick, >10 mm, CZT detectors with an emphasis on the role of Te inclusions and the possibility of using a high-temperature post-growth annealing process.

SPECIFIC ACCOMPLISHMENTS:

Continuation of this project is supported by U.S. Department of Energy, Office of Nonproliferation Research and Engineering, NA-22.

Publications

A. E. Bolotnikov, G. C. Camarda, G. W. Wright, R. B. James, "Factors limiting the performance of CdZnTe detectors" Nuclear Science, IEEE Trans. Nucl. Sci., NS 52, pp. 589-598, 2005.

A. E. Bolotnikov, G. S. Camarda, G. A. Carini, M. Fiederle, L. Li, D. S. McGregor,

W. McNeil, G. W. Wright, R. B. James, R.B., "Performance Characteristics of Frisch-Ring CdZnTe Detectors", IEEE Transactions on Nuclear Science, Vol. 53 (2), pp. 607-614, 2006.

A. E. Bolotnikov, M. Black, G. S. Camarda, G. A. Carini, Y. Cui, K. T. Kohman, L. Li, M. B. Salomon, and R. B. James, "The effect of Te precipitates on characteristics of CdZnTe detectors", Proceedings of SPIE Hard X-Ray and Gamma-Ray Detector Physics and Penetrating Radiation Systems VIII, edited by L. A. Franks, A. Burger, R. B. James, H. Bradford Barber, F. Patrick Doty, and Hands Roehrig (SPIE, Bellingham, WA, 2006), Vol. 6319, 631903-1.

G. S. Camarda, A. E. Bolotnikov, G. A. Carini, Y. Cui, K. T. Kohman, L. Li, and R. B. James, "High spatial resolution imaging of Te Precipitates in CZT material", (SPIE, Bellingham, WA, 2006), Vol. 6319, 63190Z-1.

LDRD FUNDING:

FY 2004	$ 86,077
FY 2005	$131,041
FY 2006	$ 60,502

An Integrated Approach of High Power Target Concept Validation for Accelerator Driven Systems

Nicholas Simos *04-088*

PURPOSE:

The success of a number of proposed high power accelerators is strongly linked to the ability of a few, non-conventional materials and composites to withstand high levels of irradiation damage combined with severe shock from intercepting energetic protons. The objective of this project is to explore, through a systematic and detailed experimental effort, the feasibility of a number of innovative new materials as accelerator production targets. Specifically, assessment of the irradiation effects on key physical and mechanical properties, which make these materials attractive in the first place, is sought through controlled irradiation exposure and post-irradiation tests.

Proof of irradiation and shock resilience of these novel materials will form the basis for:

- Accelerator initiatives such as the Muon Collider, the Neutrino Superbeam, the Next Linear Collider, etc.
- NASA's search for multifunctional materials performing shielding and structural functions while maintaining properties under irradiation exposure.
- Special industrial applications of these materials, including material surface treatment (irradiation effects on nano-film deposition, and plating).

APPROACH:

The challenge, common to all high power accelerator initiatives, is the feasibility and availability of materials that can meet the ever-increasing demand of power and energy deposition on targets. Recent irradiation damage studies showed that special materials exhibiting superb behavior in the non-irradiated state lose their distinct properties very rapidly with radiation. Results of these studies, combined with the requirements of recent accelerator initiatives (i.e. BNL Neutrino Superbeam), prompted the idea of focusing attention on a narrow material matrix and answering questions regarding the serious implications a material choice might have when used as an accelerator target as it experiences irradiation damage and severe shock.

To reach the goal, materials need be selected based on a figure of merit which combines the material Z value with properties like conductivity, coefficient of thermal expansion, fracture toughness, etc. Specimens appropriate for the experiment, the available apparatus, and the facility constraints are to be designed and fabricated then irradiated with the 200 MeV protons in order to induce damage or trigger changes in the physical properties of materials. Specimens are to be allowed to "cool-down" and then transferred to the BNL Hot Cell facility for activation measurements and post irradiation testing. Through a series of tests the irradiation effects on (a) mechanical properties such as loss of ductility, failure load and stress-strain relationship, (b) coefficient of thermal expansion and conductivity, and (c) degradation of the special surface treatment of aluminum was assessed.

Collaborators contributing in this effort are Dr. Harold Kirk (BNL), Dr. Hans Ludewig (BNL), Dr. Peter Thieberger (BNL), Dr. Leonard Mausner (BNL), Prof. Kirk McDonald (Princeton U.), Dr. John Sheppard (SLAC) and Dr. Kojii Yoshimura (KEK, Japan).

TECHNICAL PROGRESS AND RESULTS:

The research activity supported in part by LDRD funds has focused on the response to irradiation of several new alloys, carbon-based fiber-reinforced composites, various graphite grades and other materials of interest that can play a role in high power accelerators. While the primary objective was to assess materials that can withstand irradiation and beam-induced shock and potentially be used as production targets in the new, multi-MW power accelerator initiatives, materials were also assessed for their ability to collimate TeV-level proton beams (such as the LHC beam collimation system) or to function as magnetic horns in the future long baseline neutrino experiments. The research conducted in different phases that consisted of proton-radiation exposure at the BNL BLIP and subsequent post-irradiation characterization and analysis resulted in significant findings:
Self-healing (damage reversal) capabilities of some super-alloys through thermal annealing
Self-healing of carbon composites but also their inability to resist high radiation doses (as compared to graphite)
The ability of some materials to resist embrittlement and maintain ductility
The severe loss of ductility in some otherwise very promising super alloys (such as the gum metal)

SPECIFIC ACCOMPLISHMENTS:

Publications:

Irradiation Damage Studies of High-Power Accelerators, N. Simos, et al., Journal of Nuclear Materials (submitted for publication) 2006

Experimental Studies of Targets and Collimators for High-Intensity Beams, N. Simos, et al., High-Intensity High Britness beams (accepted for publication), 2006

Solid Target Studies for Muon Colliders and Neutrino Beams, **N. Simos**, H. Kirk, H. Ludewig, et al., Nuclear Physics B, 155, pp. 288-290, 2006

Material Irradiation Damage Studies for High Power Accelerators, **N. Simos**, et al., Proceedings of EPAC, Paper No. TUPLS133, 2006

A Free Jet Hg Target Operating in a High Magnetic Field Intersecting a High Power Proton Beam, V.B. Graves, P.T. Spampinato, **N. Simos**, et al., Nucl. Instr. Meth., A562, pp 928-931, 2006

Material Studies for Pulsed, High Intensity Proton Beam Targets, **N. Simos**, H. Kirk, P. Thieberger, et al., Nuclear Physics B (Proc. Suppl.), Volume 149, p. 259-261, 2005

Post-Irradiation Properties of Candidate Materials for High Power Targets, H. Kirk, H. Ludewig, **N. Simos**, et al., Proceedings of PAC05, Paper ID: 1703-ROAD003, May 2005

A Free Hg Jet System for Use in a High-Power target Experiment, P. Spampinato, T. Gabriel, **N. Simos**, et al., Proceedings of PAC05, Paper ID: 1206-FPAE073, May 2005

Target and Horn Cooling for the Very Long Baseline Neutrino Experiment, S. Bellavia, S. Kahn, H. Kirk, **N. Simos**, et al., Proceedings of PAC05, Paper ID: 1419-RPPE031, May 2005

Electro-migration Issues in High Current Horn, Wu Zhang, **N. Simos**, et al., Proceedings of PAC05, Paper ID: 1969-RPPT066, May 2005

A High Power Target Experiment, H. Kirk, S. Kahn, **N. Simos**, et al., Proceedings of PAC05, Paper ID: 1698-RPPT067, May 2005

Proceedings:

"High Power Target R&D," Plenary Talk at the Neutrino Factory 2006 Conference, UC Irvine, August 206

"Collimation of High Energy Proton Beams Experience & Material R&D," Institute of High Energy Physics, Beijing, China, September 2006

Presentation at the Neutrino Beam Instrumentation (NBI2006) Workshop, CERN, Switzerland, Sept. 2006

Target Material Studies – Status, Muon Collider Collaboration Meeting, LBNL, February 2005

"Material R&D Studies," Particle Physics Department, Rutherford-Appleton Laboratory, UK. Colloquia, October 2005

"Material Irradiation Studies for LHC Collimators – Phase I & II, LHC Accelerator Research Program Collaboration Meeting, Port Jefferson, NY, April 2005

POST-IRRADIATION PROPERTIES OF CANDIDATE MATERIALS FOR HIGH POWER TARGETS, Poster Presentation, PAC 2005, ORNL, TN, May 2005

BNL Target Studies for 2-4 MW Proton Driver, Neutrino Beam Instrumentation 2005 Conference, Fermi National Laboratory, June 2005

Irradiation Studies for High-Intensity Proton Beam Targets, Neutrino Beam Instrumentation 2005 Conference, Fermi National Laboratory, June 2005

US Solid Target Program - Neutrino Factory/Neutrino Super Beam. NuFact 2005 Conference, Frascati, Italy, July 2005

The LARP Collimation Program – Task 4 Summary, US LHC Accelerator Research Program Review, N. Simos and N. Mokhov, Fermi National Laboratory, September 2005.

PLUS numerous LHC, Muon Collider and Neutrino Superbeam presentations at scheduled collaboration meetings.

Reports:

Target System for a Long Baseline Neutrino Beam," (publication under BNL number in process), N. Simos, et al., BNL Report, DRAFT (in review), September 2006

US Participation in the T2K Long-baseline Neutrino Oscillation Experiment, Report to NuSAG, June 2005

LDRD FUNDING:

FY 2004	$ 82,747
FY 2005	$121,361
FY 2006	$ 53,954

Hydrogen Storage Using Complex Metal Hydrides for Fuel Cell Vehicles

James Wegrzyn *04-104*

PURPOSE:

The purpose of the study is to build upon the expertise and unique capabilities at BNL in the development of a practical hydrogen storage system for fuel cell vehicles. The goal is to enhance our fundamental understanding of both the kinetics and thermodynamic properties of complex metal hydrides and their mixtures. This knowledge can then be used as a foundation to respond to both the President's and Brookhaven's Hydrogen Initiatives.

APPROACH:

The renewed interest in the "concept of a hydrogen economy" provides the motivation for this study. The approach is to synthesize and test novel hydrogen storage materials. Materials of interest have been aluminum hydride, alkali hydrides and alanates. The role titanium plays as a catalyst has also been investigated.

TECHNICAL PROGRESS AND RESULTS:

Technical progress was realized for this past year in three areas: 1) the kinetic properties of aluminum hydride, 2) the thermodynamic properties of various complex metal hydrides, and 3) the functionality of the titanium catalyst.

The potential of using aluminum hydride as a hydrogen storage medium has been explored, in which accelerated desorption rates have been measured by the addition of small levels of alkali metal hydrides. DOE's 2010 gravimetric and volumetric system targets can be met, but off board regeneration of spent Al back to AlH_3 still needs to be addressed.

The thermodynamic properties of various complex metal hydrides have been investigated. The alanates (Na_2LiAlH_6, $KAlH_4$, K_3AlH_6, K_2NaAlH_6, etc.) were synthesized by mechanical alloying and the enthalpy and entropy of decomposition was determined by measuring pressure-composition isotherms. Preliminary results demonstrate that the equilibrium pressures can be changed substantially by partial substitution of the alkali metal. A better understanding of the thermodynamic effects of alkali-metal substitutions may lead to the development of new classes of high-capacity alanates with thermodynamic properties that are more favorable for PEM fuel cell applications.

At the NSLS, Ti *K*-edge x-ray absorption near-edge spectroscopy was used to determine the Ti valence and coordination in Ti-activated sodium alanate. These results demonstrated that the formal titanium valence is zero in doped sodium alanate and nearly invariant during H_2 cycling. A qualitative comparison of the edge fine structure suggests that the Ti is present on the surface in the form of amorphous $TiAl_3$.

SPECIFIC ACCOMPLISHMENTS:

Proceedings:

1) Hydrogen storage: Alanates. Graetz, J., J. Reilly, J. Johnson, A. Y. Ignatov, and T. A. Tyson, Battelle Fuel Cell Strategy Meeting, Salt Lake City, UT, 2004.

2) X-ray absorption study of Ti-doped sodium aluminum hydride. Graetz, J., A. Y. Ignatov, T. A. Tyson, J. Reilly, and J. Johnson,

Materials Research Society Fall Meeting, Boston, MA, Nov. 29-Dec.3, 2004.

3) Hydrogen driven metallurgical reactions (HDMR) to produce reactive, nano-scale and nano-composite materials. Reilly, J.,J. Johnson, J. Graetz, R. Klie, G. Sandrock, and J. Wegrzyn, Materials Research Society Fall Meeting, Boston, MA, Nov. 29-Dec. 3, 2004.

4) New Reversible Complex Hydride Storage Systems. Graetz, J. and J. Reilly, Materials Research Society Fall Meeting, San Francisco, CA, Mar. 28-Apr. 1, 2005.

5) Metal Hydrides, Materials R&D, Heat Transfer & Engineering. Reilly, J. (invited panelist) IPHE International Conference on

Follow on funding:

We have partnered with Sandia National Laboratory and were selected for funding under DOE's EERE Grand Challenge Hydrogen Storage Program. FY 05 funding awaits appropriation by Congress. We are assisting in the preparation of the proposal "Reversible Atomic Migration in Complex Metal Hydrogen Storage Materials" in response to DOE Basic Energy Sciences Lab Call 04-20.

Invention disclosure:

BNL No. 0423-Metallurgically Stimulated Aluminum Hydride

LDRD FUNDING

FY 2004	$ 70,265
FY 2005	$108,592
FY 2006	$ 36,891

Full Power Test of the Amplifier for the Optical Stochastic Cooling using JLAB FEL

Vitaly Yakimenko *05-003*

PURPOSE:

Optical stochastic cooling for the Relativistic Heavy Ion Collider (RHIC) based on optical parametric amplification was proposed by M. Babzien et al., Phys. Rev. ST Accel. Beams v.7, 012801, (2004). According to this proposal a CdGeAs2 nonlinear crystal is used as an active medium for the optical parametric amplifier because of an extremely large nonlinear coefficient, wide transparency range, and possibility to be phase matched over the required spectral range. We present experimental results of the parametric amplifier gain and coherency for the conditions applicable to optical stochastic cooling for RHIC.

We intend to develop and test an optical amplifier that would be suitable for the optical stochastic cooling (OSC) at RHIC. Our calculations demonstrate that OSC operated at a 12 micron wavelength can effectively improve RHIC performance. OSC can successfully replace microwave stochastic cooling (SC) that is currently proposed for RHIC and experiments planned for the near future. OSC has the potential to affect the whole beam contrary to SC, which only deals with a small portion of the beam. OSC is complimentary to electron cooling (EC), which is another RHIC cooling project. EC is more effective for the particles with small amplitudes, while OSC works faster at large amplitudes. Thus the addition of OSC to EC would dramatically reduce the requirements of the electron current in the EC project.

APPROACH:

Using an optical parametric amplifier (OPA) pumped by the second harmonic of the Accelerator Test Facility high power pulsed CO2 laser, we intend to characterize the amplification of a CW CO2 laser at 9 microns. Demonstration of successful amplification using this OPA will allow us to extrapolate the performance expected under the conditions required for OSC of RHIC. A pair of pulsed amplified CO2 oscillators is required to characterize phase conservation of the amplified signal.

TECHNICAL PROGRESS AND RESULTS:

The main goals of the present work are:

-measuring gain in the required spectral range

-experimentally verify that the signal maintains coherent properties after amplification

-definition of the angle requirements for CGA OPA alignment

The maximum gain of 9.2 times obtained in the experiment is close to the initial design requirement (~10). The gain decreased by ~28-35% with the wavelength increase from 11.1 to 11.4 μm. This is probably related to deterioration of the phase-matching conditions.

The interference pattern was measured to confirm preservation of the coherence in the central portion of the beam. Smearing of the phase information at the edges was verified in simulations and is attributed to the Gaussian intensity profile of the pump laser. This would lead to the less efficient utilization of the laser power in OSC. The phase distortion can be corrected with the shaping of the pump laser.

Angular alignment requirements are well understood and simulations are improved to reflect experimental results.

SPECIFIC ACCOMPLISHMENTS:

Proceedings:

M. Babzien, et al. Investigation of Optical Parametric Amplifier for Optical Stochastic Cooling. Proceedings of AAC 2006, AIP.

Igor Pavlishin, "Investigation of Optical Parametric Amplifier for Optical Stochastic Cooling," presentation at advanced accelerator concepts workshop, Lake Geneva, 2006

Vitaly Yakimenko, "Optical Stochastic Cooling for RHIC," MIT, December 18, 2005

Marcus Babzien, "OSC Requirements for 2 Micron OPA," MIT, December 18, 2005

V. Yakimenko, "Optical Stochastic Cooling: Electron Ring (demonstration) – RHIC (luminosity with gold and protons) – LHC (lead and protons)," LARP meeting, Port Jefferson, 2006

Proposal to NP DOE is under review to test OSC at MIT or VUV NSLS.

LDRD FUNDING:

FY 2005	$112,488
FY 2006	$160,571

Photon Coupling to an Electromagnetic Field Gradient

Carol Y. Scarlett *05-005*

PURPOSE:

This experiment is designed to search for anomalous coupling between a photon and an electromagnetic field. For the field strengths achievable with a RHIC dipole, Quantum Electro Dynamics (QED) predicts a coupling which induces an ellipticity change of order 10^{-12} rads. However, a previous experiment conducted at BNL has observed an effect of order 10^{-8} rads. In this experiment, we use a RHIC Quad in two configurations, with and without a mirror cavity, designed to both reproduce E949's results and to determine if the interaction was due to the strength of the field or its gradient. If such a large effect were due to an EM gradient, it may explain excess 'gravitational lensing' of galaxies believed to contain Dark Matter (DM). This would shed new light on the phenomena of DM in the universe. Follow up experiments could then introduce stronger field gradients to measure the coupling as a function of $\nabla \cdot B$. Alternatively, if the effect is due to the presence of axions, scaling with the field strength, we would be in a unique position to see their effects on propagating photons.

APPROACH:

We have expanded on the approach taken in E949's search for axions. Our goal is two fold: search for a deeper connection between photon interactions in a gravitational and magnetic field gradient and confirmation/ruling out of the previous observations of E949. This experiment was inspired by both DM research and the signal observed in E949.

Our experimental scope covers a field gradient of ~ 99T/m, over 5000 times what was achieved with a dipole magnet, and a magnetic field strength of ~ 1T. Introduction of a mirror cavity will increase the length through the field to 10-100 km, giving us comparable field strength parameters to E949 – with a gradient in excess of 10^7 of that seen in the previous experiment.

Thus far, data collection has been conducted using only a 'single-pass' through the field. For a second year of running, we are preparing to build a mirror cavity to increase transits through the field to ~ 10^5-10^6 to achieve the running conditions of E949. This cavity will also allow us to simultaneously probe a larger field gradient than used in similar experiments.

TECHNICAL PROGRESS AND RESULTS:

The most significant accomplishment for this funding year is the collection of data with the inclusion of shunt information. We have collected ~ 20000 minutes of data thus far. The first 10000 minutes were taken with various shunt configurations – some of which were designed to determine if we could observe movement due to magnetic fields near the leads.

As with all experimental setups, we also completed calibrations of our photo-receivers, conducted systematic studies of the change in laser energy output with changes in temperature, and studied the frequencies of floor vibrations with the magnet current on. These measurements have allowed us to understand the systematics of our detector.

A Fast Fourier Transform analysis program has been tailored to read in and analyze our data. The program was developed concurrently with the actual data taking and has already been used to analyze much of the existing data. The data has been packaged carefully in terms of running conditions and made available to the other collaborators (Yannis Semertzidis, Don Lazarus and Mike Sivertz) on line.

To date we continue to have evidence for a peak at the frequency at which the magnet was ramped. This evidence has appeared in several different runs. We will continue our analysis and include a background study, a shunt measurement, to verify that the effect is coming from within the cavity. A short note is being prepared at this time on all results.

SPECIFIC ACCOMPLISHMENTS:

Seminar at RPI (Rensselaer Polytech Institution), Troy, NY 12180, "Axion Search at BNL", C. Scarlett (presenter), Y. Sermertizidis, D. Lazarus, R. Burns, M. Sivertz

Poster presentation at AMPS (Alliance for Minority Participation), Philadelphia, PA, "Axion Search at BNL", C. Scarlett (presenter), Y. Sermertizidis, D. Lazarus, R. Burns, M. Sivertz

LDRD FUNDING:

FY 2005	$105,693
FY 2006	$175,406

Heavy Ion Physics with the ATLAS Detector

Helio Takai *05-006*

PURPOSE:

The ATLAS detector now under construction will be one of the two major experiments at CERN's Large Hadron Collider. This accelerator is designed for proton-proton collisions but will also collide heavy ions such as Lead (Pb) to study Quantum Chromodynamics (QCD) at temperatures never before achieved. At these temperatures it is expected that quarks and gluons approach asymptotic freedom, and it will be a unique opportunity to study QCD in the laboratory. RHIC has shown a range of interesting science and provides a strong motivation to study nucleus-nucleus collisions at the Large Hadron Collider (LHC). ATLAS with its large coverage and excellent calorimeter coverage will allow us to study how partons interact in the hot matter, via jets.

APPROACH:

The success of the RHIC program indicates that at higher partonic matter temperatures interesting phenomena is expected. To prepare for the initial round of experiments it is important to simulate its behavior to the high particle multiplicity environment of nucleus-nucleus collisions.

TECHNICAL PROGRESS AND RESULTS:

Dr. Arthur Moraes, a new hire, has contributed to this project. His contribution has been essential to create the ATLAS heavy ion physics group in BNL and also to start new initiatives within the ATLAS experiment. Since his arrival, we fully migrated to the ATLAS software framework and all simulations are done using full detailed detector information. This is a giant leap forward when compared to previous results with partial simulations. We have also started to use Grid Computing for simulations to take advantage of the vast network of computers within the US-ATLAS collaboration. The ATLAS heavy ion group has also initiated a program to study minimum bias proton-protonp collisions at the LHC. This group is co-led by Dr. Arthur Moraes and the studies will provide invaluable information for the most basic of the collisions for the heavy ion physics. This new initiative will also allow for the ATLAS heavy ion group to be fully integrated with the experiment.

SPECIFIC ACCOMPLISHMENTS:

Publication:

Prediction for minimum bias and the underlying event at LHC energies, A. Moraes, C. Buttar, and I. Dawson. SN-ATL-2006-057, CERN Document (ATLAS Scientific Note - Public) August 2006. To be published in The European Physics Journal Direct

Presentations:

- **Jet studies in preparation for ATLAS: from pp to heavy ion collisions** presented by A. Moraes (on behalf of the ATLAS collaboration) - American Physical Society - Dallas, TX - 22nd - 25th April 2006.

- **SUSY searches at the LHC** presented by A. Moraes (on behalf of the ATLAS Collaboration) at the International School on High Energy Physics (Session C) - LISHEP2006 - Rio de Janeiro / Itacuruca ; 2nd - 7th April 2006. *(Invited)*

- **Heavy Ion Physics with the ATLAS detector** presented by H. Takai (on behalf of the ATLAS Collaboration) at the Hard Probes Workshop - Asilomar, California. June 9th -16th 2006.

- **Minimum bias and underlying event studies at ATLAS** presented by A. Moraes at the University of Florida - High Energy Physics Seminars - Spring 2006 - Gainesville, Fl; 21st March 2006. *(Invited)*

Reports:

- **Underlying Event Tunes for the LHC**, A. Moraes. In: Tevatron-for-LHC Report of the QCD Working Group. Contributed to the Workshop "TeV4LHC". FERMILAB-CONF-06-359. (October 2006).

- **Preparing for measurements of dijet azimuthal decorrelation at ATLAS**, A. Moraes, C. Buttar, D. Clements and I. Skillicorn. ATL-PHYS-PUB-2006-013, CERN Document (ATLAS Note - Public) April 2006.

- **Tuning models for minimum bias and the underlying event**, A. Moraes and C. Buttar. In: 'Physics at Tev Colliders 2005' QCD, EW and Higgs Working Group: Summary Report. Contributed to the Workshop "Physics at TeV Colliders," Les Houches, France, 2nd - 20th May 2005. e-Print Archive: hep-ph/0604120, (April 13, 2006).

LDRD FUNDING:

FY 2005	$ 5,623
FY 2006	$124,143
FY 2007 (budgeted)	$104,000

Superconducting Lead Photoinjector Development

John Smedley *05-017*

PURPOSE:

The aim of this project is to investigate the photoemission properties of lead with the goal of improving the capabilities of superconducting (SC) photoinjectors. SC photoinjectors represent an important emerging class of electron sources, with the potential to deliver high average current and high peak current simultaneously. Before this investigation began, the choice of cathode for these injectors was limited to two options. The niobium wall of the injector could be used, but the low quantum efficiency (QE) of niobium limited the maximum current. Alternately, a radio-frequency (RF) choke joint could be used to introduce a non-SC cathode. While this technique allows a high-QE cathode to be used, the choke negatively impacts the RF properties of the cavity, and greatly increases the devices complexity. This project has introduced the concept of a hybrid lead-niobium injector, combining the superior SC and RF properties of a niobium cavity with the higher QE of a SC lead cathode. Since all of the materials in this design are superconductors, a choke joint is not necessary, making the device simpler to manufacture.

APPROACH:

This project can be broken into three distinct challenges that must be addressed. The first is to establish methods by which lead can be deposited onto a niobium substrate. This work has been done in collaboration with R. Lefferts and A. Lipski (Stony Brook University) and J. Langner and P. Strzyżewski (INS-Świerk, Poland).

The second is the measurement of the QE and surface properties of the various surfaces prepared in part one. This work has been performed in the BNL instrumentation division. Existing systems for the measurement of the photoemission properties of metals have been significantly upgraded as part of this project, enabling the material QE to be measured over a broad range of incident wavelengths.

The third portion of this project is the construction and test of a SCRF cavity with a lead cathode. Peter Kneisel has graciously agreed to allow this measurement to be performed using a cryostat at Jefferson Lab (Jlab), after the BNL cryostat intended for this project was taken off-line in January 2006. Existing infrastructure at Jlab has been used to perform the RF measurements on a cavity with a lead cathode. Preparations have been made to enable laser operation and photoemission measurements at Jlab as a part of this project.

TECHNICAL PROGRESS AND RESULTS:

The first and second phases of the project outlined above were completed in FY 2005. Four methods of depositing lead onto niobium were established (electroplating, vacuum deposition, arc deposition and sputtering). All of these coatings are thermally stable, and all can provide QE significantly superior to that of niobium. Two of the coating methods (electroplating and arc deposition) have surface finish qualities that appear to be consistent with operation inside a SC photoinjector. A procedure for laser-cleaning has been established for each of the lead samples to maximize the QE without damaging the cathode surface. The QE was measured at cryogenic temperatures, and found to be comparable to the room temperature values if the vacuum level is below 10 nTorr.

The third stage of the project – construction and measurement of a prototype hybrid injector – is well underway. A niobium cavity has been designed and constructed by Jacek Sekutowicz at Deutsches Elektronen-Synchrotron (DESY) and coated via arc deposition (Figure 1). A second cavity at Jlab is also available for this project. This cavity has a removable niobium plug in the cathode region that can be replaced with lead coated plugs. Plugs have been prepared via electroplating and arc-deposition.

The results of P. Kneisel's RF tests of the arc-deposited plug are shown in figure 2, along with results for the niobium plug. At low field, the Q value of the cavity is unchanged by the presence of lead. At high fields, the Q drops for the lead plug, however, the Q remains greater than 10^9 even for peak electric fields in excess of 35 MV/m. Preparations have been made for QE measurements in the cryostat at Jlab. The objective of this final test is to prove that the QE measured at laboratory conditions can be reproduced in a functioning superconducting injector, and that the laser used to extract electrons from the cavity wall will not cause the cavity to quench.

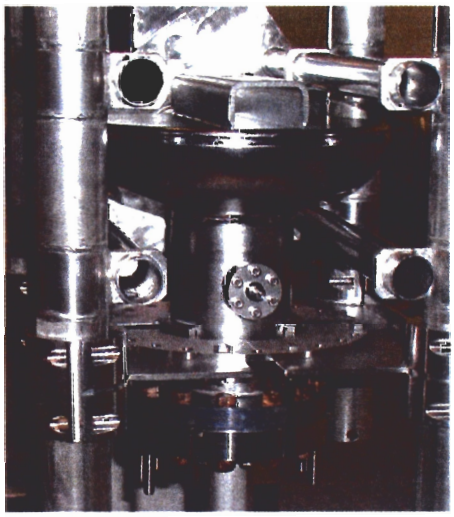

Figure 1: Niobium cavity

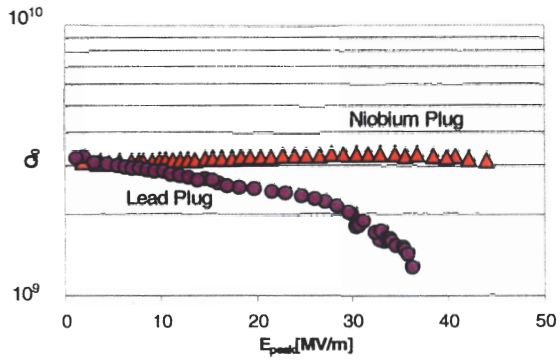

Figure 2: RF test of cavity with lead and niobium plugs

SPECIFIC ACCOMPLISHMENTS:

Presentations:

John Smedley; Photocathode Theory; Workshop on High Quantum Efficiency Photocathodes, Milan, Italy, October 3-7, 2006.

P. Strzyzewski, J. Langner, M. J. Sadowski, J. Witkowski, J. Sekutowicz, T. Rao, J. Smedley, P. Kneisel, L. Cultrera, G. Gatti, F. Tazzioli; Deposition of Pure Lead Photo-Cathodes by Means of UHV Cathodic Arc; Workshop on Thin Films and new ideas for pushing the limits of RF superconductivity; Legnaro National Laboratories, INFN (Padua) Italy, October 9-12, 2006.

LDRD FUNDING:

FY 2005	$117,500
FY 2006	$156,480

Controlled Formation of Nanostructured RuO_2 Catalysts

Peter Sutter *05-020*
J. Hrbek

PURPOSE:

Ruthenium dioxide (RuO_2) on Ru(0001), a low-temperature oxidation catalyst with exceptional activity, has recently become a model system for studying the perceived "pressure gap" in catalysis. A RuO_2 surface oxide, generated dynamically in strongly oxidizing environments (e.g., in O_2 at high pressure), was identified as the catalytically active phase while Ru metal, clean or with chemisorbed oxygen, is inactive. Catalytic reactions on RuO_2(110) have been studied for the past few years, yet the spontaneous generation of the active catalyst itself via surface oxidation of Ru metal remains poorly understood. *In-situ* microscopy of the Ru(0001) surface during oxidation, as pursued under this LDRD project, has the potential of identifying the atomistic mechanisms of surface oxidation, thus answering long-standing questions on the nature of transition metal oxidation reactions, and providing a basis for tailoring the nanoscale morphology and reactivity of the RuO_2 catalyst.

APPROACH:

Previous studies of Ru(0001) oxidation were entirely based on spatially averaging techniques, such as photoelectron spectroscopy or thermal desorption spectroscopy. These techniques are unable to capture the nanoscale dynamics involved in the initial nucleation and growth of a surface oxide. We used low-energy electron microscopy (LEEM), capable of real-time observations of surfaces with sub-10 nm resolution during exposure of the metal surface to oxygen. This approach provides quantitative data on nucleation, growth, and coalescence of individual nanoscale RuO_2 nuclei from which the microscopic mechanism of the oxidation reaction and its kinetics can be derived.

TECHNICAL PROGRESS AND RESULTS:

The oxidation of Ru(0001) was studied using nitrogen dioxide (NO_2) as a source of atomic oxygen. Having established general trends in the RuO_2 morphology, the structure of the oxide, and the overall activation energy of the oxidation reaction in FY 2005, the research performed in FY 2006 focused on understanding the microscopic pathway of the initial Ru(0001) surface oxidation.

Several reports in the literature have established that Ru metal can absorb large amounts (several equivalent monolayers, ML) of oxygen into sub-surface sites, prior to the nucleation of a surface oxide with well-defined structure and stoichiometry.

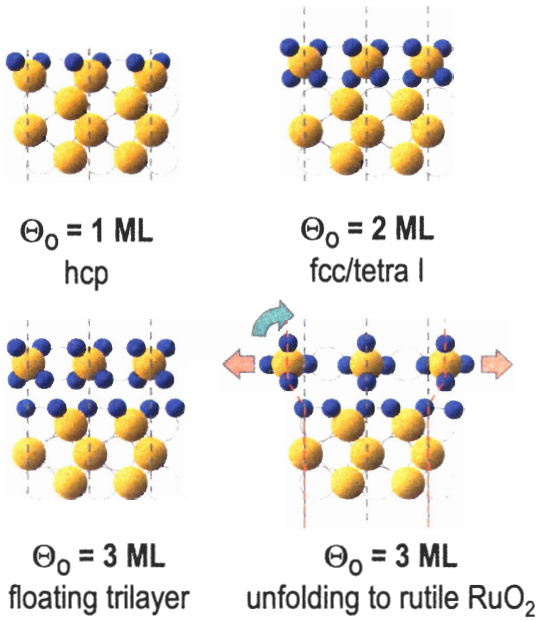

Figure 1 – Predicted oxidation pathway at the Ru(0001) surface, as a function of oxygen coverage (Θ_O). Ru: ● ; O: ●●. Based on K. Reuter et al., Chem. Phys. Lett. **353**, 311 (2002).

Specific stages of sub-surface oxygen loading have been predicted theoretically as precursors to RuO_2 (fig. 1).

In an effort to verify the predicted oxidation pathway, we pursued several avenues: (i) establish that oxygen is indeed the species limiting the rate of oxide growth at the nanoscale; (ii) spectroscopically identify the different phases involving sub-surface oxygen, and image their evolution during the oxidation reaction; and (iii) correlate the observed growth process of individual RuO_2 nuclei with the microscopic theoretical predictions. Point (ii) required a major upgrade of our LEEM microscope, involving its transfer to the National Synchrotron Light Source, where it now forms the core of a new contributing user end station for spectroscopic photoelectron microscopy (PEEM).

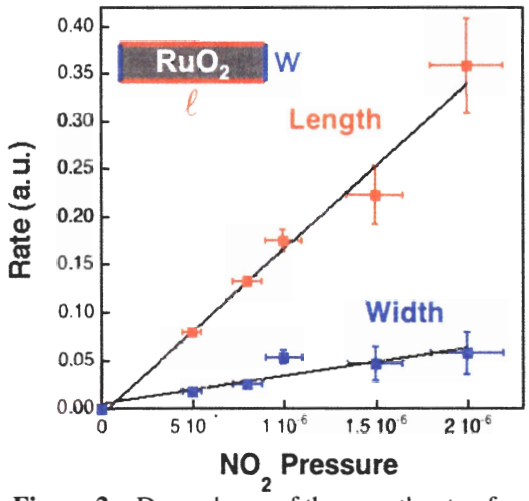

Figure 2 – Dependence of the growth rate of individual surface RuO_2 nuclei on oxygen supply (NO_2 pressure). Inset: sketch of the anisotropic shape of the RuO_2 nuclei.

Measurements of the growth rate of individual RuO_2 nuclei were performed as a function of NO_2 pressure (fig. 2). The growth rates in both length and width are strictly proportional to the supply of atomic oxygen over the entire available NO_2 pressure range, indicating that the microscopic oxidation process is limited by oxygen supply. Although obvious at first glance, this result is highly significant. It suggests that the displacement of metal atoms to accommodate the volume expansion of the surface oxide is not a limiting factor. And it points to a simple dependence of the rate of formation of all sub-surface oxygen precursors and of the surface RuO_2 on the oxygen chemical potential.

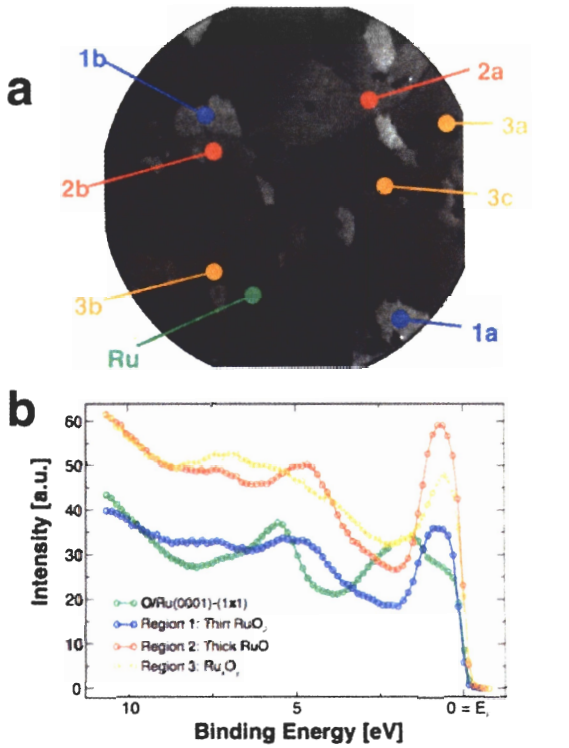

Figure 3 – Spectroscopic identification of oxygen-rich surface phases: **a)** LEEM image of the Ru (0001) surface after high-temperature oxidation (field of view: 20 μm). **b)** Local valence photoelectron spectra from different surface phases: ○: Ru(0001)-**O(1x1)**; ○: Floating trilayer; ○: thin RuO_2; ○: **thick** RuO_2.

We have developed spectroscopic imaging techniques to identify and distinguish the key near-surface structures at different local oxygen coverage: Ru(0001)-O(1x1) [Θ = 1 ML], the *fcc/tetra* structure [Θ = 2 ML], the *floating trilayer* structure [Θ = 3 ML], and the stoichiometric rutile RuO_2. By extracting local photoemission spectra from

synchrotron PEEM images and comparing the measured valence band density of states with theoretical predictions, the different near-surface structures could be identified unambiguously (fig. 3). In addition, we used spectroscopic imaging to demonstrate, that contrary to expectations, RuO_2 begins to grow in thickness significantly before full surface coverage is achieved.

With the different oxygen-rich surface phases identified by spectroscopic imaging, LEEM movies were used to observe how these phases follow each other in the overall oxidation process (fig. 4). Fig. 4 (a – c) show the spatially non-uniform loading of oxygen to generate the *fcc/tetra* structure in going from Θ_O = 1 ML to 2 ML. Bright

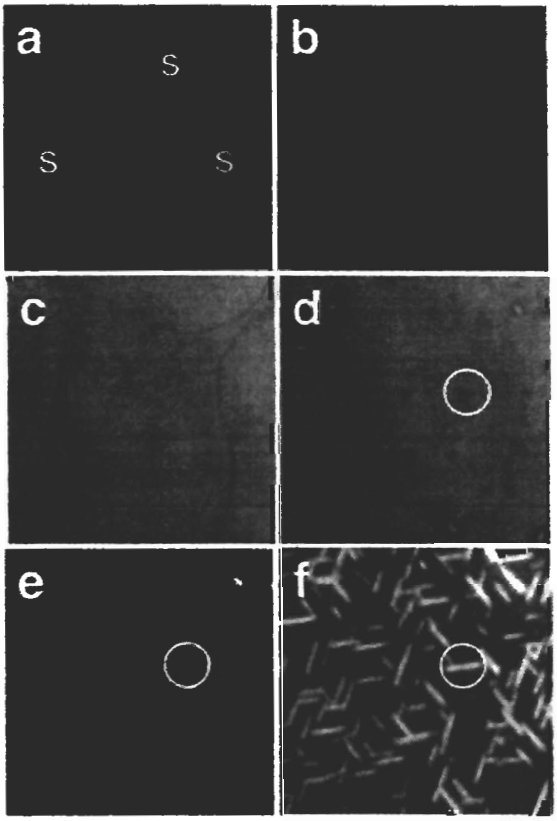

Figure 4 – Sequence of LEEM images at increasing exposure to NO_2 (T = 750 K, FOV 5 μm): **a)** 100 L; **b)** 300 L; **c)** 400 L; **d)** 600 L; **e)** 700 L; and **f)** 1500 L NO_2. S: atomic surface steps on the Ru(0001) substrate. O: same object in panels d – f.

contrast, indicative of sub-surface oxygen, is observed first at atomic steps (fig. 4 b, 'S'), and then spreads across the terraces, which eventually turn uniformly bright. With additional oxygen loading, first dark islands appear (fig. 4 d), whose contrast has been identified as that of the *floating trilayer* phase with local oxygen coverage Θ_O = 3 ML. Immediately after the nucleation of patches of *floating trilayer*, their center converts into rutile RuO_2 structure (fig. 4 d, e). These initial nuclei of RuO_2 surface oxide then grow into highly anisotropic, elongated islands, whose boundary remains surrounded by a band of *floating trilayer*. Hence, our experiments clearly identify sub-surface oxygen loading in a local *floating trilayer* structure as the immediate precursor to the RuO_2 surface oxide.

In summary, combining real-time and spectroscopic imaging under this LDRD project, we have solved the long-standing problem of identifying the complete microscopic pathway of surface oxidation of Ru(0001), an important model catalyst system. The LDRD project has opened up new avenues for studying surface reactions by in-situ microscopy, which we will seek to expand in the future.

This LDRD project played a major role in developing core research areas at BNL by contributing to three funded proposals to DOE-BES. It has further helped define the 'Nanocatalysis' science theme at BNL's Center for Functional Nanomaterials. A new spectro-microscopy end station at the National Synchrotron Light Source was established with partial support from this LDRD.

SPECIFIC ACCOMPLISHMENTS:

Project Review

Presentation at the Scientific Advisory Committee meeting of the BNL Center for Functional Nanomaterials, November 2005.

Publications

Q. Wu and J. Hrbek, "Coadsorption of Oxygen, Gold, and Carbon Monoxide on Ru(0001) and CO_2 Formation: A Thermal Desorption Study," *Surf. Sci.* **588**, 117 (2005).

J. I. Flege, E. Vescovo, G. Nintzel, L. H. Lewis, S. Hulbert, and P. Sutter, "A New Soft X-ray Photoemission Microscopy Beamline at the National Synchrotron Light Source," *Nucl. Inst. Meth.* B, accepted.

P. Sutter, J. I. Flege, and J. Hrbek, "Formation of an Oxidation Catalyst: Microscopic Mechanism of Ru(0001) Surface Oxidation," submitted.

Presentations

"In-Situ Microscopy of the Oxidation of Ru(0001)," P. Sutter, J. I. Flege, J. Hrbek, and R. Q. Hwang, 2006 Spring Meeting of the European Materials Research Society, Symposium J, Nice (France), May 29 – June 2, 2006. (Invited)

"Low-Energy Electron Imaging of the Nanoscale Movement at Surfaces," P. Sutter, 4th Annual BNL/Columbia Research Symposium in Chemistry and Nanoscale Materials Science, Columbia University, New York (NY), July 6, 2006. (Invited)

"Spatially and Chemically Resolved Imaging of Nanostructures," P. Sutter and J. I. Flege, 19th International Conference on the Application of Accelerators in Research and Industry, Forth Worth (TX), August 20 - 25, 2006. (Invited)

"Real-time in situ Microscopy and Spectroscopy of the Oxidation of Ru(0001)," J. Hrbek, P. Sutter, J. I. Flege, Q. Wu, and R. Q. Hwang, 232nd ACS National Meeting, San Francisco (CA), September 10 – 14 (2006). (Invited)

"In-situ Low-energy Electron Microscopy of Transition Metal Surface Oxidation," P. Sutter, J. I. Flege, and J. Hrbek, Gordon Research Conference on "Chemical Reactions at Surfaces," Ventura (CA), February 11-16, 2007. (Invited)

"In-Situ Microscopy of the Oxidation of Ru(0001)," P. Sutter, J. Hrbek, R. Q. Hwang, 2005 MRS Fall Meeting, Symp. U: Stability of Thin Films and Nanostructures, Boston (MA), Dec. 2005.

Low-Energy Electron Microscopy and X-Ray Photoemission Microscopy of the Oxidation of Ru(0001), P. Sutter, J. I. Flege, and J. Hrbek, European Conference on Surface Science, Paris (France), September 2006.

LDRD FUNDING:

FY 2005	$117,502
FY 2006	$148,357

Hydrogen Storage in Complex Metal Hydrides

Peter Sutter (T. Vogt) *05-021*
J. Muckerman
J. Reilly
J. Wegrzyn
D. Welch
L. Cooley

PURPOSE:

Hydrogen storage has been identified as a key bottleneck on the way to a hydrogen-based economy. Complex metal hydrides have the potential to become the material of choice for large-scale hydrogen storage if a compound with sufficiently high hydrogen density is found that easily incorporates and releases H_2 near ambient conditions. The hydrogenation reaction, which transforms spent material back into a hydrogen-rich storage compound, is particularly problematic as it proceeds for most materials only under extreme environmental conditions, e.g., at high H_2 pressures. The recent discovery that the decomposition of a particular hydride, sodium alanate ($NaAlH_4$), to NaH, Al, and H_2 can be made reversible at moderate temperatures and pressures by adding small amounts of Ti has demonstrated *doping* as a possible solution of this problem. Recent evidence obtained in part under this project suggests that active Ti-dopants in $NaAlH_4$ occupy near-surface sites. Yet, their role in the different elementary steps of the hydrogenation reaction remains largely unknown.

APPROACH:

Under this LDRD project, combined experimental and theoretical research is performed to assemble key data underpinning hydrogen storage in $NaAlH_4$, in particular to understand the role of transition metal (Ti) dopants and alkali substitutions in making this process reversible. The general approach is to *apply the multifaceted capabilities of an interdisciplinary research team* to the complex problem of hydrogen storage, a strategy for which a large laboratory such as BNL provides an ideal environment. Our experimental approach uses both *real-world bulk materials* and *well-defined model systems* to obtain relevant quantitative results that are readily accessible to theory and modeling. Specific groups of experiments include: (i) Advanced materials synthesis and characterization to study intrinsic properties of bulk materials; And (ii) Atomistic studies on carefully designed model systems to map the sites occupied by dopants, such as Ti, and to determine the effect of these additives on the kinetics of hydrogen uptake and release.

TECHNICAL PROGRESS AND RESULTS:

(i) Experiments on bulk hydrogen storage materials

Solid-state chemistry techniques were used to synthesize novel mixed alkali alanates of the form $M_xM'_{1-x}AlH_y$ (M, M' = Li, Na, K,...), and to investigate the possibility of continuously tuning their hydrogenation thermodynamics (reaction enthalpy) by cation substitution. In FY 2006, two new alanates were synthesized: K_2LiAlH_6 and K_2NaAlH_6. Both compounds reversibly absorb/desorb hydrogen without the need for a catalyst. Structural analysis using synchrotron x-ray diffraction showed that the smaller ion (M') in these compounds invariably occupies octahedral sites, while the larger ion (M) is located in 12-fold coordinated sites. The preferred occupation of specific sites by M and M' ions, i.e., the lack of a random alloy phase, implies that the projected approach of continuously

tuning the reaction enthalpy by cation substitution is generally *not feasible*.

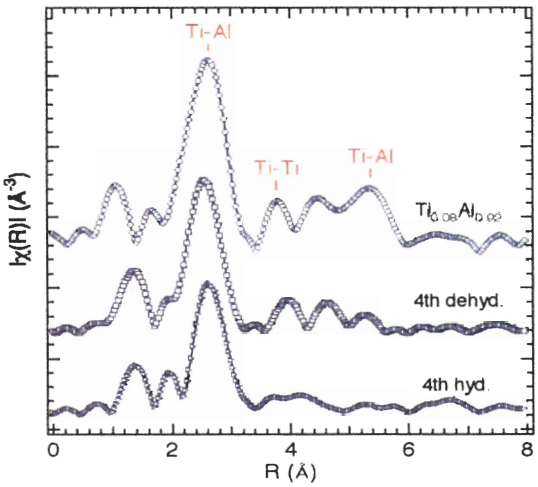

Figure 1 – Synchrotron XAS showing nearly zero-valent Ti, primarily in an Al matrix in spent sodium alanate.

In other work on bulk materials, aiming to shed light on the local environment of Ti dopants in $NaAlH_4$, x-ray absorption spectroscopy (XAS) was used to measure the local atomic environment of Ti in the decomposition products of sodium alanate. Our results clearly demonstrate that Ti resides primarily in a metallic Al matrix, is in a zero-valent state, coordinated by 10 Al atoms at ~2.8 Å. The reduced coordination by 10 Al atoms instead of the expected 12, and the lack of order beyond the first Al shell suggests that the Ti exists in dispersed clusters at or near the Al surface.

(ii) Experiments on single crystal model systems: Ti/Al(111)

Given the XAS evidence for prevalent near-surface Ti in the H_2-depleted material, our experiments on model systems focused on Ti on Al single crystal surfaces, and its possible effects in the reaction to hydrogen-rich $NaAlH_4$:

$$NaH + Al + 3/2\ H_2 \rightarrow 1/3\ Na_3AlH_6 + 2/3\ Al + H_2 \rightarrow NaAlH_4$$

A key step of this reaction is the adsorption of H_2 from the gas phase and dissociation to atomic-H, a process hindered by large energy barriers on Al surfaces, but possible when catalyzed by specific Ti-Al surface complexes (as predicted by our previous theoretical calculations). To evaluate if such catalytically active complexes indeed form spontaneously, we used scanning tunneling microscopy (STM) to map with atomic resolution the population of Ti atoms generated by evaporation onto Al(111) surfaces. Our observations showed that Ti can be kinetically stabilized at the Al surface in the form of a disordered Ti-Al surface alloy, whereas theory predicts that Ti should occupy only sub-surface sites in equilibrium.

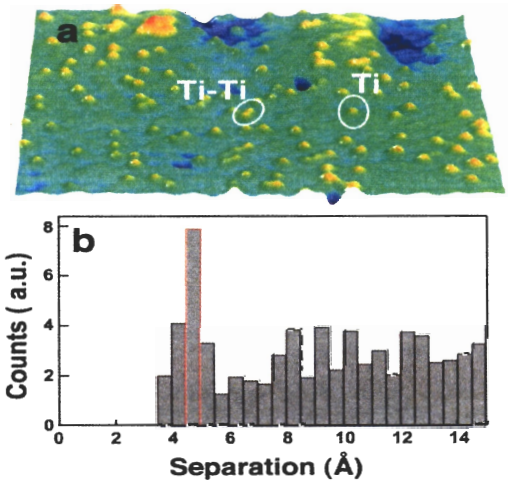

Figure 2 – a) STM micrograph (190 Å x 110 Å) of 0.05 ML Ti/Al(111), showing individual Ti atoms and Ti-Ti pairs. **b)** Histogram of Ti-Ti separations, showing the complete suppression of nearest neighbor pairs (separation: 2.86 Å), and increased large population of second-nearest neighbor pairs (separation: 4.9 Å).

Evaluating the short-range order in the Ti-Al alloy at low Ti coverage (< 0.05 monolayers), we find that the population of Ti-Ti pairs in nearest neighbor sites falls significantly below that expected for a random alloy. The most closely spaced Ti-Ti pairs observed are those in second-nearest neighbor sites, whose configuration fulfills the theoretically predicted requirements for catalyzing efficient dissociation of H_2. The suppression of nearest neighbor Ti pairs,

likely by a combination of elastic strain and preference for Ti-Al bonding, effectively boosts the population of *likely catalytically active* second-nearest neighbor Ti pairs, in particular at higher Ti coverage.

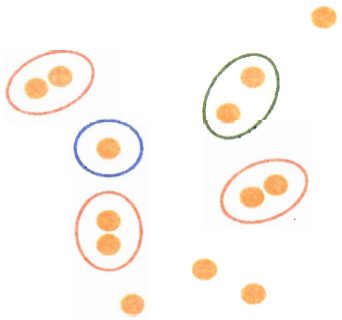

Figure 3 – Top view model of the Al(111) surface showing several configurations of substitutional surface Ti: individual Ti atoms (○); nearest neighbor Ti-Ti pairs (○); catalytically active second-nearest neighbor pairs (○).

As soon as Ti-catalyzed dissociation of H_2 produces a steady supply of atomic-H, the H atoms will likely react with surface Al to form mobile AlH_x. We have used STM to begin studying the atomic-scale mechanism by which this process occurs. Highly mobile atomic hydrogen appears to diffuse to atomic surface steps on Al(111), which are 'etched' preferentially while Al terraces remain unaffected. Concurrent with the removal of step atoms, STM shows the formation of ad-AlH, as well as of AlH_4 (alane).

Our microscopy experiments have provided an atomic-level understanding of elementary steps in the hydrogenation reaction of a complex metal hydride hydrogen storage material. Further reaction steps, such as the diffusion of AlH_4 and Al in the presence of Ti to react with NaH, will be investigated in follow-up research to this LDRD funded by a DOE-BES 'Hydrogen-Fuel Initiative' (HFI) grant.

SPECIFIC ACCOMPLISHMENTS:

"Atomistic transport mechanisms in reversible complex metal hydrides," PIs: P. Sutter, J. Muckerman, and Y. Chabal, Agency: DOE-BES (Hydrogen Fuel Initiative), *Funded* for the period 7/01/2005 – 6/30/2008, annual funding: $ 700,000

Ewald Wicke Award to Jason Graetz (Collaborator): This award is presented at the International Metal Hydride Symposium (every two years) to a young scientist for work in physical chemistry of metal hydrides, 2006.

Publications

E. Muller, C. Ciobanu, and P. Sutter, "Short-range order of dilute Ti-Al/Al(111) surface alloys: implications for dissociative chemisorption of H_2," *Phys. Rev.* B, submitted (2006).

J. Graetz, S. Chaudhuri, Y. Lee, T. Vogt and J.J. Reilly, "Pressure-induced structural and electronic changes in α-AlH_3," *Phys. Rev.* B, accepted (2006).

S. Chaudhuri, J. Graetz A. Ignatov, J. J. Reilly and J. T. Muckerman, "Understanding the role of Ti in reversible hydrogen storage as sodium alanate: A combined experimental and first-principles theoretical approach" *J. Amer. Chem. Soc.* **128** 11404 (2006).

J. Graetz, Y. Lee, J. J. Reilly, S. Park and T. Vogt, "Structure and thermodynamics of the mixed alkali alanates," *Phys. Rev.* B, **71** 184115 (2005).

Presentations

"Atomic and Molecular Hydrogen Interaction with Ti-Doped Al (100): Hydrogen Dissociation and Surface Alane Formation," E. Muller, P. Sutter, P. Zahl, S.

Chaudhuri, J. Muckerman, American Physical Society March Meeting, Baltimore, MD, March 2006.

"Interaction of Atomic and Molecular Hydrogen with Ti-Doped Al(100): Hydrogen Dissociation and Formation of Surface Alanes," P. Sutter, E. Muller, P. Zahl, S. Chaudhuri, and J. Muckerman, 2006 Spring Meeting of the Materials Research Society, San Francisco (CA), April 17 – 21, 2006.

"Atomistic Transport Mechanisms in Reversible Complex Metal Hydrides," P. Sutter, J. Muckerman, Y. Chabal, J. Graetz, J. Reilly, J. Wegrzyn, and E. Sutter, DOE Hydrogen Merit Review Meeting, Arlington (VA), May 16 – 19, 2006.

"Reversible Hydrogen Storage in Ti-Doped Sodium Alanate: Hydrogen Dissociation and Mass Transport Mechanisms," P. Sutter, E. Muller, P. Zahl and E. Sutter, European Materials Research Society Meeting, Symp. M: Materials, Devices and Prospects for Sustainable Energies, Nice (France), June 2006.

"Hydrogen Chemisorption on Ti-Doped Al(111): Implications on Reversible Hydrogen Storage in Complex Metal Hydrides," P. Sutter, E. Muller, E. Sutter, P. Zahl, S. Chaudhuri, and J. Muckerman, European Conference on Surface Science, Paris (France), September 2006.

"Atomistic Transport Mechanisms in Reversible Complex Metal Hydrides," P. Sutter, J. Muckerman, and Y. Chabal, DOE Division of Materials Science and Engineering Workshop on "Atomic-Scale Processes at Surfaces and Interfaces," Warrenton (VA), October 29, 2006.

"Kinetics and Thermodynamics of the Aluminum Hydride Polymorphs," *International Symposium on Metal-Hydrogen Systems*, Maui, HI, 2006.

"Bonding and Local Atomic Structure of Ti in Complex Metal Hydrides," *Spring Meeting of the Materials Research Society*, San Francisco, CA, 2006.

"New Reversible Complex Metal Hydrides," *March Meeting of American Physical Society*, Los Angeles, CA 2006.

Reports

A.Y. Ignatov, J. Graetz, S. Chaudhuri, T.T. Salguero, J.J. Vajo, M.S. Meyer, F.E. Pinkerton, and T. A. Tyson, "Spatial Configurations Of Ti- and Ni- Species Catalyzing Complex Metal Hydrides: An X-ray Absorption Studies And First-Principles DFT and MD Calculations," *XAFS13 Proc.* (2006)

LDRD FUNDING:

FY 2005	$123,301
FY 2006	$167,271

Behavior of Water on Chemically Modified Semiconductor Surfaces: Toward Photochemical Hydrogen Production

Etsuko Fujita *05-028*
J. Rodriguez
J. T. Muckerman

PURPOSE:

Photochemical water splitting to hydrogen, a renewable and non-polluting fuel, and oxygen using energy from solar radiation is extremely important for a sustainable source of energy. Hydrogen and oxygen have been successfully produced by UV irradiation of aqueous suspensions of various semi-conductor catalysts including TiO_2 (and transition metal-loaded TiO_2) and $SrTiO_3$, but a detailed mechanism of the conversion at the active catalytic center remains unclear. Recently nitrogen and carbon doped materials, $TiO_{2-x}N_x$, and $TiO_{2-x}C_x$, have been synthesized and used as photocatalysts that utilize visible light (> 420 nm). We are carrying out coordinated experimental and theoretical studies on the electronic properties of N-doped rutile, TiO_2(110), with an emphasis on attaining a fundamental understanding of the first elementary step in the water oxidation processes.

APPROACH:

The key issues associated with the doped semiconductors are their controlled synthesis, and characterization of band gaps, electronic properties, stability, and reactivity with water in ultrahigh vacuum (UHV). We prepare N-doped films of TiO_2 by modifying single-crystal semiconductor surfaces, characterize them by surface/materials science techniques under UHV conditions, and elucidate the electronic and proximal structures at the atomic level through both experiment and theory.

TECHNICAL PROGRESS AND RESULTS:

The nitrogen doped samples were prepared by N_2^+ ion implantation with a 3 keV ion acceleration energy under a 1×10^{-6} torr of N_2 back pressure using a conventional ion gun. For comparison, Ar^+ bombarded TiO_2(110) surfaces were prepared following the same procedure but replacing N_2^+ ions by Ar^+ ions. After these ion treatments, the sample was kept in ultrahigh vacuum (UHV) at 900K for 2 hours.

Figure 1 shows Ti 2p core level spectra for stoichiometric, N-implanted, and Ar^+ sputtered TiO_2(110). The Ti 2p spectrum of N-implanted TiO_2 was almost identical to that of Ar^+ sputtered TiO_2, and shows the formation of Ti^{3+} and a partially reduced Ti species with an oxidation state in between +4 and +3. The valence region of the N-doped

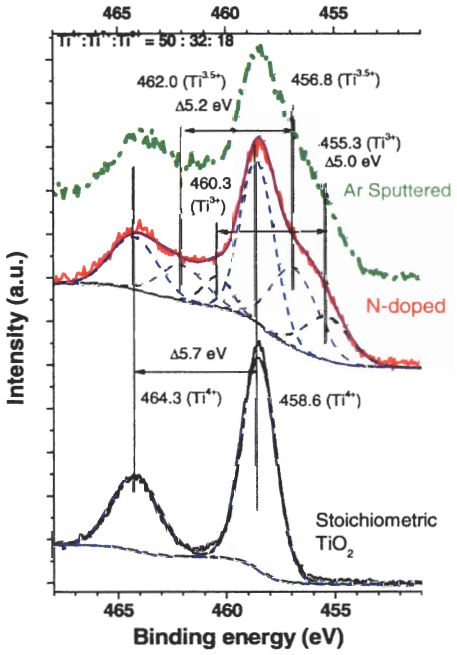

Figure 1. Ti 2p core level spectra for stoichiometric, N-implanted and Ar^+ spattered rutile TiO_2(110)

$TiO_2(110)$ systems exhibits a broad peak for Ti^{3+} near the Fermi level and N-induced features above the O 2p valence band that shift the edge up by ~ 0.5 eV. The magnitude of this shift is consistent with the "red shift" observed in the ultraviolet spectrum of N-doped TiO_2.

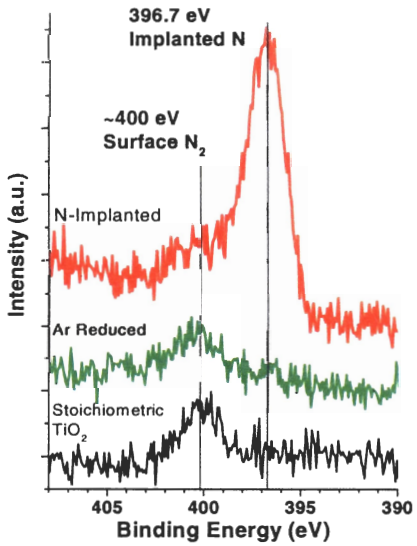

Figure 2. N 1s core level spectra for stoichiometric, Ar^+ spattered and N-implanted rutile $TiO_2(110)$

Figure 2 displays N 1s spectra. A peak centered at ~400 eV observed on stoichiometeric TiO_2 is assigned to a very minor amount of molecular nitrogen bonded to surface defects. The peak centered at 396.7 eV is observed only in the nitrogen implanted sample and is attributed to incorporated nitrogen species. Its binding energy (BE) is close to the reported BE of TiN, and this accordance suggests that the implanted nitrogen and titanium make bonds with each other.

The doping *via* N_2^+ ion bombardment leads to the implantation of N atoms that coexist with O vacancies in $TiO_{2-x}N_y(110)$. The maximum concentration of N implantation is ~5 %. The photoemission results point to a strong interaction between N impurities and oxygen vacancies.

The theoretical results also show the existence of attractive interactions between the dopant and O vacancies. First, the presence of N embedded in the surface layer reduces the formation energy of O vacancies. And second, the existence of O vacancies stabilizes the N impurities with respect to $N_2(g)$ formation. When oxygen vacancies and N impurities are together there is an electron transfer from the higher energy 3d band of Ti^{3+} to the lower energy 2p band of the N^{2-} impurities. Furthermore, the stabilization of the reduced Ti state can also add an important property to the TiO_2 surface for the evolution of hydrogen. Prior to the photo-induced hydrogen/oxygen formation ($2H^+ + 2e \rightarrow H_2$; $4OH^- + 4h \rightarrow 2H_2O + O_2$), the water splitting reaction ($H_2O \rightarrow H^+ + OH^-$) must take place on the surface, however, this reaction hardly takes place without a surface defect site (Ti^{3+} state). Therefore, not only the "red-shift" in the valence band but also the stabilization with oxygen vacancies in N-doped TiO_2 can be playing important roles in the hydrogen/oxygen synthesis reaction on this photocatalytic system.

SPECIFIC ACCOMPLISHMENTS:

Publication:

"N-doping of $TiO_2(110)$: Photoemission and Density Functional Studies," A. Nambu, J. Graciani, J.A. Rodriguez, Q. Wu, E. Fujita and J. Fernandez-Sanz, *J. Chem. Phys.* **2006**, *125*, 094706.

Presentation:

"Toward Photochemical Water Oxidation with Band-Gap-Narrowed Semiconductors and Polypyridylruthenium Complexes as Catalysts" was presented at the ACS Southwest Regional Meeting, Houston, TX, Oct. 19-21, 2006 by Etsuko Fujita. (invited)

LDRD FUNDING:

FY 2005	$ 89,092
FY 2006	$159,760
FY 2007 (budgeted)	$ 40,000

Assembling of Biological and Hybrid Complexes on Surfaces

Oleg Gang *05-030*
P. Freimuth

PURPOSE:

Versatile biological functions and highly specific interaction of viral proteins makes them an attractive component for functional self-assembled systems. Functionalized nanoparticles can specifically interact with cell receptors, and can be potentially used for the directed assembly of biological and inorganic objects, targeted drug delivery, and labeling. In the first stage of our research program we have investigated the functionalization of silica surfaces and nanoparticles with the receptor-binding protein of adenovirus, through the use of physical adsorption. In the second stage we developed strategy to use a highly symmetric adenovirus protein mutated to facilitate nanoparticle assembly. In the proof-of-concept system we demonstrated the feasibility of the approach using symmetric proteins as multidentate cross-linkers for nanoparticle assembly and organization. The developed approaches are explored for potential application in controllable nanoparticle clustering and targeted delivery.

APPROACH:

An adenovirus serotype 2 (Ad_2) protein, whose polypeptides form a highly durable trimer, has been genetically mutated to express free thiol functionalization in a three-fold symmetric design. The assembly process has been found to be highly tailorable depending upon protein/ nanoparticle assembly ratios, as well as position of the thiol groups at the adenovirus interface. The assembly systems have been characterized using UV-visible spectrophotometry and Dynamic Light Scattering, and morphology has been characterized via Transmission Electron Microscopy and Small-Angle X-ray Scattering.

TECHNICAL PROGRESS AND RESULTS:

The **Ad_2** protein is an ideal candidate to function as a multidentate mediator of nanoparticle assembly, due to its temperature stability, its pH durability, and its unique three-fold symmetry, which consists of a trimer of three polypeptide monomers. The **Ad_2** protein has been genetically altered and expressed to contain a series of three-fold symmetric thiol groups, which act as multidentate cross-linkers for gold nanoparticle assembly. In **1-Ad_2**, each molecule contains three free thiol groups extending from each monomer of the trimer **Ad_2** template. This position for the thiol expression was selected to maximize its extension from the **Ad_2** interface at an outer position. For protein **2-Ad_2**, an identical **Ad_2** template was modified so that the thiol groups were contained near the center apex of one side of the trimer, which should facilitate the multidentate attachment of the **2-Ad_2** to a single nanoparticle, limiting cross-linking and assembly. A similar design was chosen for **3-Ad_2**. We utilized Cit-capped **Au** due to the known weak electrostatic coordination of the citrate molecules to the gold interface, which facilitates exchangeable cross-linking with free thiol ligands. To study the self-assembly process between **1-Ad_2** and **Au**, we utilized UV-visible spectrophotometry, which probes the surface plasmon resonance band, which is associated with **Au** and assembled **Au** nanostructures. The particle details of structure and assembly were probed using Dynamic Light Scattering, TEM and Small-Angle X-ray Scattering.

We found that the **1-Ad$_2$** mutant is able to act as a cross-linking agent for nanoparticle assembly. Considering its size ~4 nm, approximately spherical shape, and a location of 3 thiol group it is possible for one **1-Ad$_2$** to cross-link three **Au**. In contrast, in the case of **2-Ad$_2$**, because of the location of the ~SH near the apex of symmetry, cross-linking is limited, and particle decoration by **2-Ad$_2$** is observed.

SPECIFIC ACCOMPLISHMENTS:

None

LDRD FUNDING:

FY 2005	$139,859
FY 2006	$188,818

Ultra High Resolution Photoelectron Spectrometer

Peter D. Johnson *05-033*

PURPOSE:

This project is aimed at the development of a new ultra high resolution (≤ 100 meV) photoelectron spectrometer for use with lasers or any other photon source having a high rep rate. Examples of the latter might be a Ti-Sapphire laser or the VUV FEL now being built at Jefferson Lab. The latter works at the same rep rate as the new Ti-Sapphire laser that has been purchased. The design involves the use of novel time of flight (TOF) techniques that may ultimately find use in other TOF spectroscopies.

APPROACH:

In 1999, the BNL group introduced a new methodology into the long established photoemission technique, namely the momentum distribution curve (MDC) measurement. Here one measures the intensity of photoemitted electrons as a function of momentum at constant energy as opposed to the intensity as a function of energy at constant momentum. A measurement at constant energy is equivalent to a measurement at constant time. Hence, the new methodology points to the possible advantage of time of flight (TOF) spectrometers.

A completely new type of TOF spectrometer has, therefore, been designed and is now in the fabrication phase. The design of the spectrometer includes a parabolic mirror that reflects the electrons into a velocity selecting filter that is the electronic equivalent of the velocity selecting chopper used in neutron scattering beamlines at neutron sources.

Several new experimental capabilities have been developed in order to test and ultimately use the spectrometer. We have demonstrated the ability to generate UV light via the fourth harmonic of a Ti-Sapphire laser. We have established a means of transporting the latter through to the UHV chamber.

TECHNICAL PROGRESS AND RESULTS:

Last year we reported that we had used sum frequency to obtain the third harmonic of a Ti-Sapphire laser. Since then we have determined that the easiest way to get to the fourth harmonic is simply to double the second harmonic. This has been successfully achieved and we have obtained 6 eV. Plans to obtain a crystal from Beijing that will allow the production of 7 eV photons are currently on hold because "approval is required from high levels in Beijing". However, we can work with the existing configuration for now.

Construction of the new spectrometer is proceeding at a reasonable pace. We have determined that the parabolic mirrors can be produced in the central shops at BNL. Indeed one has been machined out of aluminum. The current challenge is to determine the appropriate material that will allow a good mirror finish to be polished on the surface. This is currently being investigated.

SPECIFIC ACCOMPLISHMENTS:

None

LDRD FUNDING:

FY 2005	$67,053
FY 2006	$81,592

Metal-Metal Oxide Electrocatalysts for Oxygen Reduction

Miomir Vukmirovic *05-038*

PURPOSE:

The goal of this study is to explore platinum monolayers deposited on several metal oxides as electrocatalysts for the oxygen reduction reaction (ORR). The objectives of the study are: i) enhancing ORR kinetics, ii) preventing Pt dissolution, and iii) reducing Pt content in ORR electrocatalysts. The success of this work could ameliorate three major corresponding problems of existing fuel cell technology. Since there are no such studies of Pt deposited on well-defined single crystal metal oxide surfaces, a knowledge gained in this study can provide the basis for further work with far-reaching consequences for this potentially important area of electrocatalysis.

APPROACH:

Fuel cells are expected to become one of the major sources of clean energy in the not-too-distant future. Despite definitive advances in recent years, existing fuel-cell technology still has several drawbacks. The inadequate efficiency of energy conversion and the high Pt content of electrocatalysts are connected to the electrocatalytic ORR. Even on the best Pt-based ORR catalysts, the kinetics of ORR is rather slow. Slow ORR kinetics significantly decreases fuel cell efficiency, because for practical current densities of which the potential of oxygen cathodes is 0.3 to 0.4 V below the reversible thermodynamic value of 1.23V. For the same reason, practical current densities require a large number of reaction sites, i.e. a large Pt content in oxygen cathodes. A related major problem is dissolution of platinum nanoparticles at open circuit potentials of oxygen cathodes. This process has to be drastically reduced to achieve long-term fuel cell performance stability.

To meet the above objectives, the following investigations were carried out: i) synthesis and characterization of oxide substrates, ii) deposition and characterization of Pt monolayers on oxide surfaces, and iii) determining the electrocatalytic activity and stability of Pt monolayers.

Oxide surfaces were synthesized by electrochemical and chemical methods. Electrochemical deposition of Pt monolayers was used, including programmed potential pulses that first generate a high density of nuclei and then grow the nuclei to the desired particle size.

In situ electrochemical scanning tunneling microscopy (ECSTM) was used to determine the shape and size of Pt islands and clusters. The electronic properties of Pt deposits were studied by *in situ* X-ray absorption near edge spectroscopies (XANES). Kinetics of the ORR on single crystal samples was determined by potentiostatic methods. A thin film rotating disk electrode, which allows a realistic test of the catalytic properties needed for an actual fuel cell, was used for high surface area samples.

The study was done in collaboration with R. Adzic and K. Sasaki.

TECHNICAL PROGRESS AND RESULTS:

It was found that Pt-OH inhibits the ORR kinetics. Therefore, to enhance the kinetics, the Pt-OH coverage should be decreased. This can be achieved by replacing some of

the Pt atoms with metal atoms, M, that are oxidized at lower potentials than Pt. In that way, higher OH or O coverage on M than on Pt in the Pt-M mixed monolayer would increase lateral repulsion between the OH adsorbed on Pt and the OH or O adsorbed on a neighboring surface metal atom, M. As a consequence, an increased activity for the ORR should be observed. This hypothesis was verified by the enhanced ORR activity for $(Re_{0.2}Pt_{0.8})_{ML}$ mixed monolayer deposited on Pd(111) compared to Pt(111). The enhancement was observed also with the nanoparticle electrocatalyst (Fig. 1.). The voltammetry and an *in situ* XANES experiments showed that Pt-OH coverage on Pt-Re was considerably decreased compared to pure Pt.

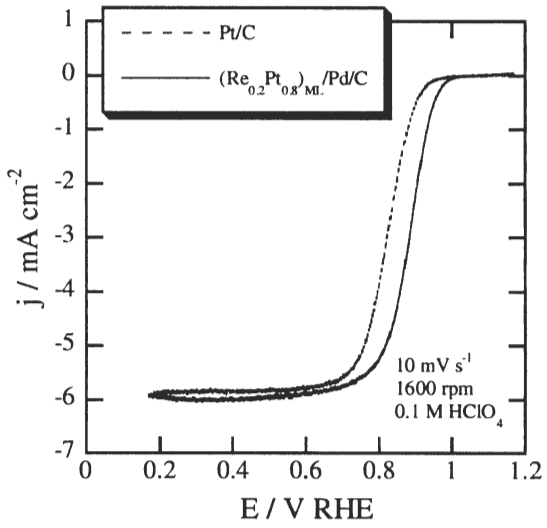

Figure 1. Polarization curves for $(Re_{0.2}Pt_{0.8})_{ML}$/Pd/C and Pt/C, containing 3.8 μg Pt cm^{-2} and 12.2 μg Pt cm^{-2} respectively.

Pt was electrochemically deposited from 1 mM K_2PtCl_4 on electrochemically grown RuO_2. Electrochemically grown RuO_2 was obtained by oxidizing Ru(0001). The ECSTM reveals that Ru(0001) surface is covered with RuO_2 islands. Their size and population could be controlled by the potential. Also, ECSTM revealed that Pt deposits exclusively on RuO_2, not on the surrounding OH-covered Ru surface. The half-wave potential of the ORR on Pt/RuO_2 is 60 mV less positive than that on Pt(111) suggesting high activity of this surface.

The electrodeposition of Pt on RuO_2(110) was studied by programmed potential pulses or potential sweeps from several Pt complexes in acid solutions. The RuO_2(110) single-crystal surface was obtained by gas-phase oxidation of Ru(0001) using our newly developed induction heating setup. The electro-deposition process is characterized by a large crystallization overpotential, random surface coverage and three-dimensional growth from a Pt adlayer. A mismatch between the RuO_2(110) and Pt lattices is the likely origin of that overpotential. The nucleation is instantaneous, as verified by potential step experiments. The process starts with depositing 0.25 mL of Pt, with Pt atoms arranged in c(2x2) array (Fig.2), which is followed by Pt island growth, similarly as in the Stranski-Krastanov mode.

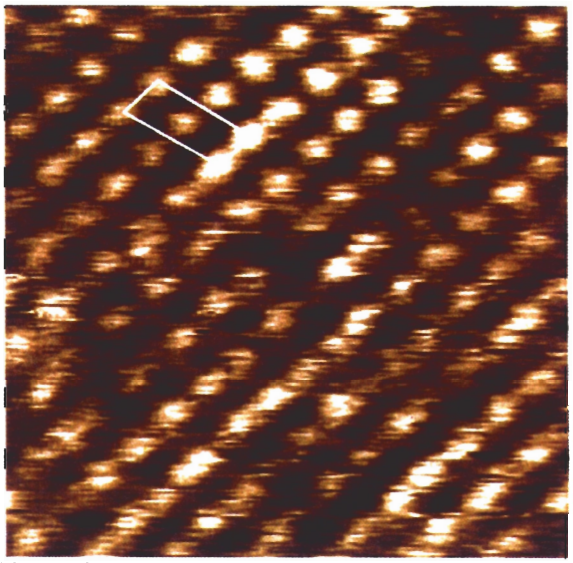

Figure 2. ECSTM image of 0.25 ML of Pt with Pt atoms arranged in c(2x2) array. Frame size 3.9 x 3.9 nm.

Density functional theory calculations were used to help in elucidating atomically resolved ECSTM images of initial stages of Pt deposition. A Pt monolayer on $RuO_2(110)$ has a moderate catalytic activity for the oxygen reduction reaction, in agreement with a large calculated down-shift of the *d-band* center.

Synthesis and evaluation of new electrocatalysts comprising monolayer-level Pt on niobium oxide nanoparticles (NbO_2) for ORR were also carried out. The average diameter of the niobium oxide nanoparticles was *ca* 11 nm determined by TEM and XRD. Preliminary electrochemical tests using the rotating disk electrode technique indicated that the $Pt/NbO_2/C$ electrocatalyst (5 μg cm^{-2} Pt) showed more than 5 times higher Pt mass activity for the ORR compared with that of a commercial Pt/C electrocatalyst (Fig. 3.). The half-wave potential for the ORR on the $Pt/NbO_2/C$ electrocatalyst was 40 mV higher than that for the commercial Pt/C electrocatalyst. This is a new promising system for practical applications.

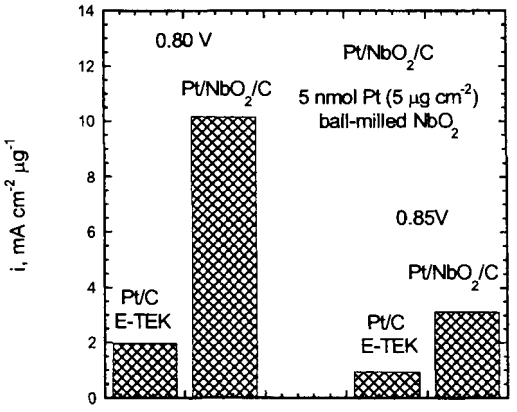

Figure 3. Pt mass activities for $Pt/NbO_2/C$ and commercial Pt/C electrocatalysts for the ORR in 0.1 M $HClO_4$. Data obtained by K. Sasaki.

SPECIFIC ACCOMPLISHMENTS:

1. One patent application submitted for H&B Docket No. 369-215, BNL No. BSA 05-12, Request No. 2118: Electrocatalyst for Oxygen Reduction with Reduced Platinum Oxidation and Dissolution Rates.

2. Expected funding from GM, certain DuPont ($85,000 for one year) for Synthesis and Characterization of Low Platinum Content Electrocatalysis for Methanol Oxidation.

Publications

Mixed-metal Pt Monolayer Electrocatalysts with Enhanced Activity for O_2 Reduction J. Zhang, M. B. Vukmirovic, K. Sasaki, A. U. Nilekar, M. Mavrikakis, and R. R. Adzic, J. Am. Chem. Soc., **127** (2005) 12480.

Presentations

Mixed-metal Pt Monolayer Electrocatalysts with Enhanced Activity for O_2 Reduction, Adzic R., Zhang J., Vukmirovic M., Nilekar A., and Mavrikakis M. presented on the 207th Meeting of The Electrochemical Society in Quebec City, Canada, May 2005.

Electrodeposition of Pt on a $RuO_2(110)$ single-crystal surface, M. B. Vukmirovic, P. Liu, J. T. Muckerman, and R. R. Adzic, presented on the 34th Northeast Regional Meeting of the American Chemical Society, Binghamton, NY, October 2006.

Electrodeposition of Pt and Au on single crystal metal oxide surfaces, M. B. Vukmirovic, P. Liu, J. T. Muckerman, and R. R. Adzic, presented on the 210th Meeting of The Electrochemical Society in Cancun, Mexico, October-November, 2006.

LDRD FUNDING:

FY 2005	$ 99,510
FY 2006	$137,025

Multifunctional Nanomaterials for Biology

Stanislaus S. Wong *05-041*

PURPOSE:

Synthesize nanomaterials with simultaneous biological and physical function for application in life sciences. As a starting point explore the use of carbon nanotubes as a platform for integrating biological specificity with physical function such as fluorescence or conductivity. Seek to put Brookhaven in a position of leadership in *highly-specific* biochemical detection.

Will allow to probe biological systems in ways that are not readily accessible using other methods. Although this project has a high risk since no laboratory has yet demonstrated nanotube based biosensing with high biochemical specificity, the proposed team combines broad interdisciplinary expertise in nanomaterial synthesis and functionalization, biology, nanoelectronics, photonics, and micro-fluidics. These projects will advance the application of physical methodologies to biological sciences.

APPROACH:

In the present work, we have investigated the biocompatibility and feasibility of a ligand-receptor protein system bound to oxidized single walled carbon nanotubes (SWNTs), via a diimide linkage. The proteins of interest in our study include an adenovirus protein, Ad12 Knob, and its complementary human 'coxsackievirus and adenovirus receptor', i.e. CAR. Adenoviruses are one of many subclasses of viruses that can cause infection, such as the common cold as well as mild ailments associated with the upper respiratory and gastrointestinal tracts. Unlike viruses such as HIV, Ebola, and poliovirus, adenoviruses do not use envelope proteins or capsid domains to infect cells. Rather, infection is initiated by the formation of a high affinity complex between the Knob trimer and its complementary adenovirus CAR receptor, present in the human cell. Upon CAR binding, the Knob coated virus replicates within the nuclei of the cells causing infections. Adenoviruses are currently leading candidates as vectors in gene therapy.

The purpose of the present work is two-fold. The first one has been to demonstrate that the binding of Knob and CAR to the SWNT surface occurs through a diimide linkage. The second purpose has been to investigate the biological activity and specificity of bound proteins onto carbon nanotubes.

TECHNICAL PROGRESS AND RESULTS:

Obtained an Atomic Force Microscope (AFM) height image of AO-SWNTs spun coated onto a freshly cleaved mica substrate. The carbon nanotubes appear to form small bundles with an average height of 12.45 ± 1.5 nm. The dehydrated CAR proteins were found to cluster as small aggregates. Nevertheless, we observed individual CAR molecules, measuring 3.66 ± 0.48 nm in diameter. The small size discrepancy with respect to the actual size of the CAR molecules, expected at 1.5-2 nm, can be attributed to an AFM tip broadening effect. We also obtained an AFM height image of carbon nanotube-protein constructs. We noted a high density of protein, densely decorating the nanotube surface. The height of these constructs was found to be 19.12 ± 2.39 nm, thereby confirming the presence of a thin layer of protein on the nanotubes within experimental error and tip convolution effects. This result was important because it implied that the biological activity of proteins subsequently measured was associated with species directly bound to the nanotubes as opposed to protein aggregates stuck together. By analogy, SWNT-Knob constructs, analyzed by AFM, measured 24.11 ± 4.10 nm on average, in height. Heights of Knob proteins on the mica

substrate were noted to be 5-7 nm, suggestive of the presence of a thin layer of Knob on the nanotube surface. It should be noted that 35-40 measurements were taken for each sample, to determine average heights and standard deviations.

After confirming the formation of our protein-SWNT constructs, we studied the interaction of these aggregates with both complementary and non-complementary-labeled proteins with our SWNT- protein conjugates, enabling us to test the activity and specificity of the bound, attached proteins. All optical and fluorescence images of the labeled proteins were recorded using a fluorescence microscope.

The biological activity of bound Ad 12 Knob was investigated by targeting rhodamine labeled anti-Knob antibodies to the AO-SWNT-Knob constructs. These antibodies were purified by using an affinity column of immobilized Ad 12 Knob, and hence targeted only Knob proteins folded in specifically active conformations. Non-specific binding of rhodamine-labeled anti-Ad 12 Knob protein attached to carbon nanotubes was prevented by using 4% milk as a blocking agent. The presence of fluorescent carbon nanotubes confirms that Ad 12 Knob bound to SWNTs indeed retains its biological activity. As control experiments, labeled anti-Knob antibodies were targeted to SWNTs in the absence of protein, both in the presence and absence of milk blocking. We observed sample fluorescence in the absence of milk blocking, indicating the presence of binding of labeled antibodies onto the SWNTs. Conversely, there was little or no fluorescence observed for SWNTs that had been blocked with milk, suggesting the efficacy of milk as a blocking agent. Hence, we demonstrated that labeled anti- knob antibodies could specifically target bound Knob proteins on the nanotubes.

By analogy, to investigate the biological activity and specificity of bound CAR, we used fluorescently labeled Knob, which shows high specific binding to CAR. In a separate experiment, attachment of YieF, an unrelated 22.4 kDa protein isolated from *E. coli* bacteria, was used as a control experiment. Whereas Ad12 Knob is specific to CAR, YieF is nonspecific to CAR. Hence, the presence of bound CAR proteins will show specificity to Knob proteins. SWNT-CAR constructs were blocked by 0.4 % milk to avoid any non-specific binding of the labeled proteins to the nanotubes. We demonstrated that the sample fluoresces, indicating the presence of binding of Knob to bound CAR proteins. On the other hand, the samples did not fluoresce at all when the labeled Ad 12 knob was replaced by labeled YieF. This observation satisfied three purposes: (1) this experiment gave additional evidence that CAR is bound to the carbon nanotubes; (2) the bound CAR is biologically active; and (3) the CAR functionalized nanotubes are specific to the presence of Ad 12 knob. Thus, this idea can be used as the basis of a biological sensor for the determination of the presence of Ad 12 Knob viral protein.

We are currently finalizing conductance measurements on these systems as well.

Goal for FY 2007

We will use proteins involved in mercury resistance as a model system. Many of these proteins are also found as part of other heavy metal resistance systems, such as lead resistance, which will allow us to extrapolate our results to the construction of new sensors with different metal specificity. The different proteins will be integrated in a nanotube matrix to obtain a functional biosensor.

SPECIFIC ACCOMPLISHMENTS:

None

LDRD FUNDING:

FY 2005	$128,192
FY 2006	$145,480
FY 2007 (budgeted)	$ 25,000

Polariton-enhanced FRET for Device-integration of Plasma Membranes from Rhodobacter Sphaeroides

Chi-Chang Kao *05-042*

PURPOSE:

The purpose of this project was to investigate the influence of surface plasmon polaritons on the fluorescence resonance energy transfer (FRET) between chromophores on metal surfaces. The suspicion is that the nonlocality of surface plasmons will enhance FRET over large distances, which could become a means to exploit this phenomenon in a device. It was our intention to investigate plasma membranes from the photosynthetic bacteria rhodobacter Sphaeroides, as well as free fluorescent dyes, deposited on metal surfaces.

APPROACH:

FRET occurs between donor acceptor pairs, i.e. pairs of molecules in which the absorption energy of one (the acceptor) is matched to the emission energy of the other (the donor). If they are sufficiently close together (< 100 Å) energy can be transferred nonradiatively from donor to acceptor. The way FRET is measured experimentally is to excite the donor and look for fluorescence from the acceptor.

Our strategy for this project was to first build a fluorescence spectroscopy setup consisting of a solid state dye laser and fiber emission spectrometer. The plan was to deposit dyes and membranes proteins on metal surfaces by suspending them in volatile solvents (e.g. methanol, acetone) at controlled concentrations and depositing them on the surfaces with a micropipette. The intention was to also experiment with self-assembly techniques for the membrane proteins. We would then measure the efficiency of FRET in these samples as a function of density, morphology etc., to see if FRET might occur, for example, over a larger distance than in solution.

The plasma membranes were to be grown in the lab of James Shapleigh in the Microbiology Department at Cornell University.

TECHNICAL PROGRESS AND RESULTS:

First, we constructed the complete fluorescence setup for FRET measurements. It consists of a Spectra Physics air-cooled Ar ion laser, Ocean Optics USB2000 fluorescence spectrometer, focusing optics, and a sample stage. Fluorescence is coupled into the spectrometer with an optical fiber. This project requires very clean, evaporated films of Au and Ag. After some initial attempts to procure an evaporator we eventually purchased pre-evaporated Ag, Au and Al microscope slides from EMF Corporation.

For simplicity we chose to begin measurements with dyes rather than bacterial membranes. We chose to use Fluorescein 1300 ("F", the donor) and Tetramethylrhodamine 668 ("T", the acceptor) because the absorption band of F1300 is matched to the 488 nm line from the Ar laser and the absorption band of T668 is matched to the emission band of F1300. These were purchased from Molecular Probes. We had also already obtained purified plasma membranes of rhodobacter Sphaeroides from the Shapleigh lab.

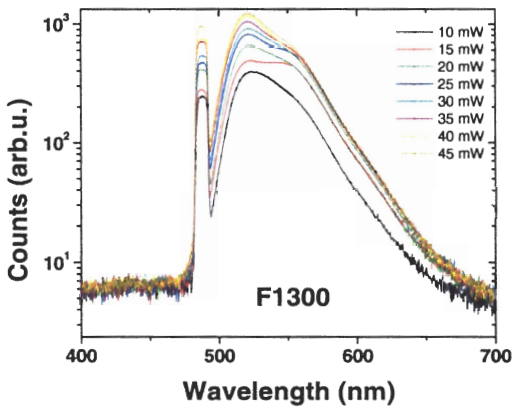

Figure 1: Emission spectrum of fluorescein F1300 excited by laser light of variable power at 488 nm.

Fluorescence measurements from dye F1300 dissolved in methanol on a clean glass substrate were made for different laser powers and are displayed in Figure 1. The sharp peak is due to elastic scattering at the laser excitation wavelength. The broad shoulder at longer wavelengths is the fluorescent dye emission spectrum. The fluorescence spectrum maximum intensity is plotted in Figure 2. The linear dependence shows that molecular photobleaching does not take place in this case and the molecules remained optically active at the highest laser powers tested.

We did measurements of dyes deposited on Ag and Au surfaces. T and F were deposited on substrates using the solvent technique described. The fluorescence we observed was transient, decreasing rapidly as the solvent evaporated and the dye molecules approached the metal surface. The fluorescence from the dyes was being quenched by increased contact with the metal surface. Adding pure solvent resulted in reappearance of the fluorescence signal showing that the decrease in fluorescence was not due to dye molecules evaporating together with the solvent. Preventing this required placing an optically inactive buffer layer between the metal film and the dyes, which can also enhance the interaction with surface plasmons by placing the dyes in the peak of the plasmon evanescent field. Therefore, we spin coated the Ag substrates with PMMA, which is insulating, optically inactive and whose thickness could easily be controlled. Adding a 6 μm thick polycarbonate foil on top of the liquid film also reduced the evaporation rate and increased the fluorescence decay time.

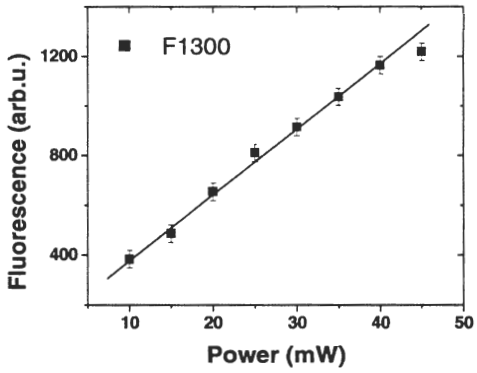

Figure 2: Dependence of the intensity of the fluorescence emission spectrum on incident laser power. The linear relationship shows that photobleaching does not occur.

Using PMMA had an accidental benefit. In addition to acting as a spacer layer, it can also provide a means to pattern the surfaces, which would allow control the geometry of dyes on the surface. This would also eventually help explore device-relevant geometries.

LDRD FUNDING:

FY 2005	$ 79,321
FY 2006	$103,218

Intense THz Source and Application to Magnetization Dynamics

G. Lawrence Carr *05-044*
D. A. Arena

PURPOSE:

Coherent THz pulses (CTPs) are typically half, single, or few cycle electromagnetic pulses with duration on the order of 1 picosecond. Though pulses with energy up to 1 μJ have been produced in laser-based systems, the electric and magnetic field intensities are insufficient for changing the polarization state in a ferroelectric or ferromagnetic material. It is now recognized that the coherent THz from relativistic electrons can be orders of magnitude larger, opening the door to studying materials in the "high field regime" (E-field greater than 10^5 V/cm). In this LDRD project we are developing an innovative coherent THz source based on relativistic electrons from the Source Development Lab (SDL) linac of the National Synchrotron Light Source. In preliminary work, we observed extremely intense and ultrashort THz pulses from this linac source. This project intends to fully characterize the source, and then initiate a set of measurements where the intense THz pulses are used to induce dynamical processes in magnetic thin films. Other measurements being planned or considered include ultra-fast current transients in superconductors and non-linear optical effects in polar crystals (e.g., ferroelectrics) or carbon nanotubes.

APPROACH:

The SDL linac-based produces ultra-short (~350 fs) electron bunches having energies up to 300 MeV and with charge approaching 1 nC (about $3x10^9$ electrons). These electron bunches are used to produce coherent THz pulses in the form of "transition radiation" by directing the electron bunches onto an aluminum metal mirror. Since the electron bunches are significantly less than 1 ps in duration, they emit coherently to frequencies of about 2 THz. The energy per pulse can be 100 μJ, about a factor of 100X higher than what is achieved using photoconductive switch sources. When focused to a small spot, the electric field is expected to peak near values of 1 MV/cm, with a correspondingly strong magnetic field of $B = E/c \sim 3kG$. Thus, the SDL THz pulse could be used to investigate strong-field properties of materials on ultra-fast time scales. We envision using the transient magnetic field for the practical study of magnetization dynamics, which is a primary theme for this project.

The initial phase of the scientific plan is to develop the optical apparatus and more fully characterize the THz source. This involves designing and constructing THz collection and focusing optics and incorporating a facility to co-propagate an ultra-short laser pulse that will be used for electro-optic sampling of the THz fields.

Once the THz fields are well-characterized, experiments involving a type of magnetic "imprinting" will be conducted. In these measurements, magnetic thin films are exposed to the THz pulses, which should result in a re-orientation of the magnetic domain pattern. The resulting domain pattern can be imaged *ex-situ* and the results compared to images of the domain pattern of unexposed samples.

TECHNICAL PROGRESS & RESULTS:

This second year of the LDRD project was devoted to characterizing the coherent THz pulses using the Pockels (electro-optic) effect along with a synchronized laser. Our requirement is to have a detailed measure of

the THz waveform at or near a focus. The magnetization dynamics study requires a half-cycle pulse (the 2nd half of a full-cycle pulse would simply undo the effect of the 1st half). This requires efficient collection and transport of low frequency Fourier components and moving outside of the Rayleigh range for the focus. Since there is significant jitter between the sampling laser and THz pulses, we pursued a single-shot technique where the sampling laser pulses are chirped. The technique involves collecting and focusing the coherent THz onto a ZnTe crystal and co-propagating a polarized, chirped laser pulse. The THz E-field induces a birefringence in the ZnTe,

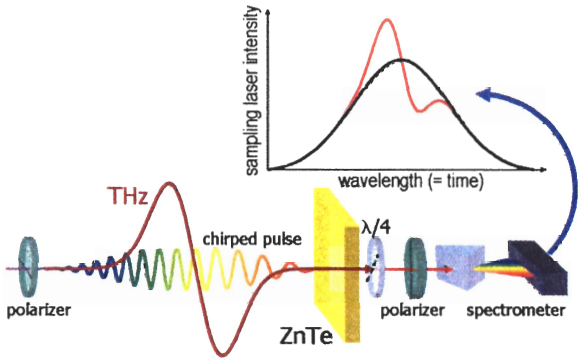

Figure 1. Single-shot EO sampling of coherent THz pulses using a chirped laser and spectrometer.

which in turn modifies the polarization of the laser pulse. Spectral analysis of the modified laser pulse should be directly related to the instantaneous electric field of the THz. A schematic of that setup is shown in Fig. 1. The instrumentation for this method was installed in FY05 with most of the measurements conducted in FY06. We discovered anomalies in the results that were traced to the very strong THz E-field, which led to a novel non-linear optical phenomena; cross phase modulation due to the time-dependent Pockels effect. From this result we discovered that THz pulses can spectrally control and even shape ultrafast laser pulses.

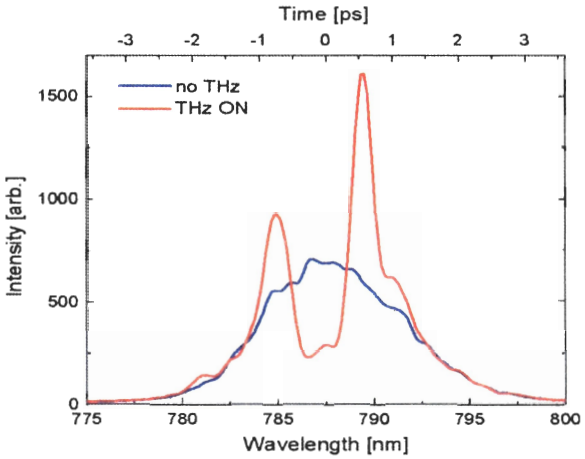

Figure 2. Single-shot EO sampling of a THz pulse, showing the anomalously large signal at λ=790nm.

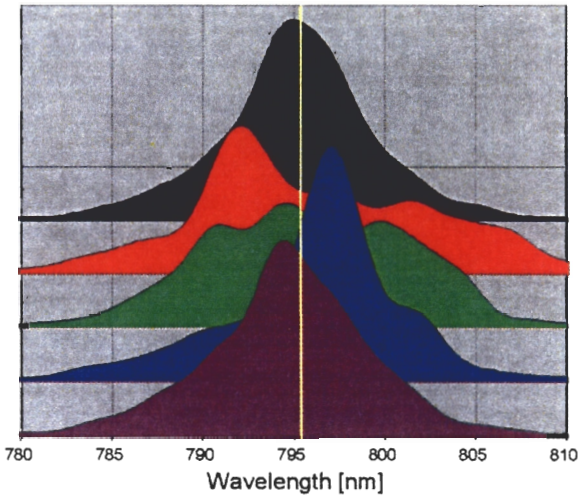

Figure 3. Spectral shifting and chirping of an ultrafast laser pulse by THz-induced cross phase modulation.

SPECIFIC ACCOMPLISHMENTS:

"Magneto-dynamics with an Accelerator-Based THz Source" (INVITED) G.L. Carr, H. Zhang, H. Tashiro, D. Reitze, D.B. Tanner, L. Mihaly, R.P.S.M. Lobo, R.J. Smith, H. Loos, B. Sheehy, D. Arena, C-C Kao, J. Murphy, D. Liu, T. Watanabe, and X-J Wang, Presented at the Nat'l High Magnetic Field Lab - FEL Workshop, October 2005, Gainesville, FL

"The Time-dependent EO Effect in ZnTe and Implications for THz Detection" (INVITED) D. Arena, Y. Shen, T. Watanabe, D. Liu, J.B. Murphy, X.-J. Wang, R. Smith,

L. Miller and C.-C. Kao, Presented at the SURA THz Applications Symposium, June 06, Washington, DC

"Materials Science Studies using Incoherent and Coherent THz radiation at the NSLS" (INVITED), G.L. Carr, R.P.S.M. Lobo, D.B. Tanner, J. Graybeal, D.H. Reitze, H. Tashiro, D. Arena, Y. Shen, T. Tanabe, C.-C. Kao, J.B. Murphy, X.-J. Wang, Presented at the Canadian Light Source Users Mtg and Workshops, June 06, Saskatoon, Canada

"Controlling Light with Intense Coherent THz Pulses" (INVITED) G.L. Carr, D. Arena, H. Loos, C.-C. Kao, J.B. Murphy, B. Sheehy, Y. Shen, T. Tanabe & X.-J. Wang, Presented at the New Scientific Possibilities with High Power THz Sources workshop, June 06, Daresbury/Runcorn, Cheshire, UK

"Non-linear Optical Studies using Intense Coherent THz Pulses," G.L. Carr, D. Arena, D. Liu, H. Loos, C.-C. Kao, J.B. Murphy, B. Sheehy, Y. Shen, T. Tsang, T. Watanabe, X.-J. Wang Low Energy Excitations in Solids (LEES 06), July 06, Tallinn, Estonia

LDRD FUNDING:

FY 2005	$ 50,175
FY 2006	$131,904
FY 2007 (budgeted)	$ 66,000

Nano-Imaging of Whole Cells with Hard X-Ray Microscopy

Lisa M. Miller *05-048*

PURPOSE:

The objective of this work is to develop 3-dimensional, high-resolution, hard x-ray imaging for the study of whole living (frozen) cells. This project takes advantage of the high brightness and coherence of synchrotron light and recent advances in new x-ray imaging technology (i.e. hard x-ray zone plates). To date, other imaging techniques are limited by sample thickness, e.g. soft x-ray microscopy is limited to <1 μm and electron microscopy is limited to < 100 nm. In this work, we aim to improve the sample penetration depth to 50 – 100 μm (the thickness of typical cells), and the spatial resolution to <20 nm by using hard x-rays for 3-D imaging. The NSLS has several beamlines that are well suited for developing hard x-ray microscopy, and also has an accomplished user base in the development and implementation of x-ray zone plates. This new technique will become a key element in the ongoing development of a Biomedical Imaging program at the NSLS.

APPROACH:

Currently, confocal microscopy with visible light is the most common method of imaging biological processes in living cells. However, the primary drawback to this technique is the diffraction-limited spatial resolution of ~300 nm. This resolution can be used to image large sub-cellular organelles, but cannot be used to study smaller sub-cellular structures such as cell membranes and individual protein complexes.

Other imaging techniques with higher spatial resolution, such as electron microscopy and soft x-ray microscopy, have limited sample penetration depth, so that only small cells and/or particles can be studied. We are working towards the development of an x-ray microscope that surpasses any other at the NSLS in both spatial resolution and sample penetration depth. This type of spatial resolution will enable cellular processes, such as apoptosis and mitosis, to be studied in the native cellular environment, to provide new insight into the way cells behave as "molecular machines." Moreover, the development of this nanoscale tool will not only be applicable to biological systems, but will be valuable for the study of numerous other nanoscale structures in the chemical, materials, and environmental sciences fields.

The specific aims of this proposal are: (1) to customize and test a hard x-ray zone plate to an NSLS bending magnet beamline, (2) to develop cryogenic cooling techniques, (3) to adapt current electron microscopy biochemical tags for hard x-ray microscopy, and (4) to apply the newly developed technique to image cellular processes such as mitosis or apoptosis.

TECHNICAL PROGRESS AND RESULTS:

In FY 2005, Meghan Ruppel (graduate student) developed methods for combining epifluorescence microscopy with hard x-ray microprobe in collaboration with Dr. Antonio Lanzirotti (University of Chicago). Also in FY 2005, in collaboration with Dr. Yen-Fang Song at the National Synchrotron Radiation Research Center (NSRRC) in Taiwan, we collected hard x-ray microscopy images of microdamaged bone samples in both absorption and phase contrast mode. These experiments were performed to test the technology on samples that were not

radiation-sensitive. The results demonstrated ~30 nm spatial resolution and high mineral-to-matrix contrast. Based on the results of these experiments, additional beamtime has been awarded at the NSRRC in December 2006 to continue the work on whole fibroblasts. These experiments will be performed at the NSRRC while the appropriate technology is developed at the NSLS.

In FY 2006, Ms. Ruppel set up a cell culture laboratory at the NSLS and tested methods for growing fibroblasts (human skin melanoma cells) and osteoblasts (bone cells) on x-ray transparent materials including formvar, silicon monoxide, and silicon nitride. We began to adapt immuno-fluorogold tags (standard antibody-conjugated labels) for x-ray microscopy and tested them at the NSRRC and NSLS.

In FY 2007, we will begin to examine methods for cryogenic sample cooling. In collaboration with Dr. Ken Evans-Lutterodt, we will investigate other methods of phase contrast imaging on NSLS beamline X13B.

SPECIFIC ACCOMPLISHMENTS:

Publications:

FY 2005: L.M. Miller, M.E. Ruppel, C.H. Ott, A. Lanzirotti. (2005) Development and Applications of an Epifluorescence Module for Synchrotron X-Ray Fluorescence Imaging. *Rev. Sci. Instr.*, **76**: 066107.

FY2006: M.E. Ruppel, D.B. Burr, L.M. Miller (2006). Chemical composition of microdamaged bone differs from undamaged bone in control and bisphosphonate-treated dogs. *Bone*, **39**: 318-24.

Abstracts:

FY 2005: R. Smith, Q. Wang, L.M. Miller. "Combining IR Microscopy and X-ray Fluorescence Microprobe Using a Patterned Sample Substrate." 2005 NSLS Users Meeting, May 23-25, 2005.

FY 2005: M.E. Ruppel, D.B. Burr, L.M. Miller. "Chemical Makeup of Microdamaged Bone Differs from Undamaged Bone." 2005 NSLS Users' Meeting, May 23-25, 2005.

FY 2006: M.E. Ruppel, R.J. Smith, A. Mamoon, T. Tsang, L.M. Miller. "Chemical Imaging of Skin Melanoma Cells During Photodynamic Therapy." 2006 NSLS Users' Meeting, May 15-17, 2006.

Thesis:

FY 2005: M.E. Ruppel. "Development and Applications of an Epifluorescence Module for Synchrotron X-ray Fluorescence Imaging." Master of Science, Department of Materials Science and Engineering, Stony Brook University.

LDRD FUNDING:

FY 2005	$19,496
FY 2006	$91,159
FY 2007 (budgeted)	$71,000

Study to Convert the NSLS VUV Ring to a Coherent IR Source

Boris Podobedov *05-050*

PURPOSE:

The IR user program based on the NSLS VUV/IR ring is presently the strongest in the world. As we move forward with the NSLS-II project, we would like to preserve and expand the infra-red (IR) and THz capabilities for this vibrant user community. To this end we propose to move the existing NSLS VUV/IR ring to be part of the NSLS-II complex and to operate it with top-off injection. The ring would serve the IR user community exclusively, while the present VUV and soft X-ray users would migrate to the new NSLS-II ring.

With an eye toward expanding the capabilities of our workhorse IR source, we are investigating the potential of operating the NSLS VUV/IR ring as a coherent IR facility by adding a high frequency super-conducting RF (SCRF) system. We are exploring the various coherent synchrotron radiation (CSR) emission regimes possible for both the existing and the upgraded VUV/IR ring. Broadly formulated, the definition of success will be the feasibility determination of a future VUV/IR ring upgrade with the added coherent mode of operation, as well as the choice of the optimal RF system and other accelerator hardware necessary for this upgrade.

APPROACH:

While potentially capable of providing the users within far-IR and THz spectral ranges several orders of magnitude higher photon fluxes compared to the standard incoherent mode of operation. The performance in this configuration is not easily estimated. In fact, only one ring in the world (BESSY-II, Germany) has recently achieved this mode of operation, and there is still intense debate in the accelerator community as to what exactly limits the performance. The primary factors defining the photon flux are the maximum achievable current and minimum achievable bunch length. These in turn depend on complexities of electron beam dynamics in the ring and are usually limited by various instabilities.

The RF system is one of the primary elements affecting longitudinal beam dynamics including instability thresholds, and therefore one of the primary outcomes of this LDRD would be a recommendation for the optimal RF system to provide the best performance in this new mode of operation. Generally, RF system choices are constrained due to engineering and operational issues such as the availability of cavities and power sources and injection system compatibility, as well as cost and other factors. First, however, there is still an unresolved accelerator physics question being addressed by this LDRD, as to what is the optimal RF system choice within the aforementioned constraints for the future VUV/IR ring upgrade.

Dynamics of very short and intense electron bunches in storage rings, when they are significantly interacting with emitted CSR as well as vacuum chamber components, is not entirely understood. Existing theories are fairly complex and yet they usually deal with very simplified models of the impedance. This is why in our view the experimental work as well as computer simulations must be performed to meet the above stated goals.

In particular, to probe the short bunch length regime experimentally we will do (or have already done) the following:

1) exploit the flexibility of the NSLS VUV ring magnet lattice, which allows orders of magnitude reduction in momentum compaction,
2) store small beam currents with just the 4th harmonic (211 MHz) RF cavity,
3) perform similar studies at the MIT-Bates ring which incorporates a unique 2856 MHz RF system allowing for very short bunches (few orders of magnitude shorter than what's available in the present NSLS VUV/IR ring).

Future studies will include impedance and instability studies, calculations and set up of an optimal magnetic lattice, measurement of coherent emission and the assessment of the operational impact of the proposed upgrade. We will examine the possibility of using an SCRF system identical to the NSLS-II SCRF system which could allow us to prototype the ring RF system and get an early start on coherent IR operation on the IR ring.

TECHNICAL PROGRESS AND RESULTS:

A significant fraction of the work performed was experimental in nature and took place in the MIT-Bates South Hall Ring (item 3) above.) This timeline was significantly influenced by the Bates running schedule. Specifically, as the Bates nuclear physics program was nearing completion, the accelerator operation was about to cease.

For the first time in the history of Bates, facility longitudinal beam dynamics has been extensively characterized, using the hardware and expertise from BNL. Low momentum compaction lattices, that should provide significantly shorter bunches than the nominal 18 ps rms bunch length used for nuclear physics experiments have been established. With these lattices bunches as short as a few ps rms have been measured. To observe CSR emissions from these short bunches a beam line off one of the bending magnets has been built. Subsequently, CSR emissions with their characteristic quadratic dependence on beam intensity have been measured applying several different techniques developed earlier at NSLS (see Figure).

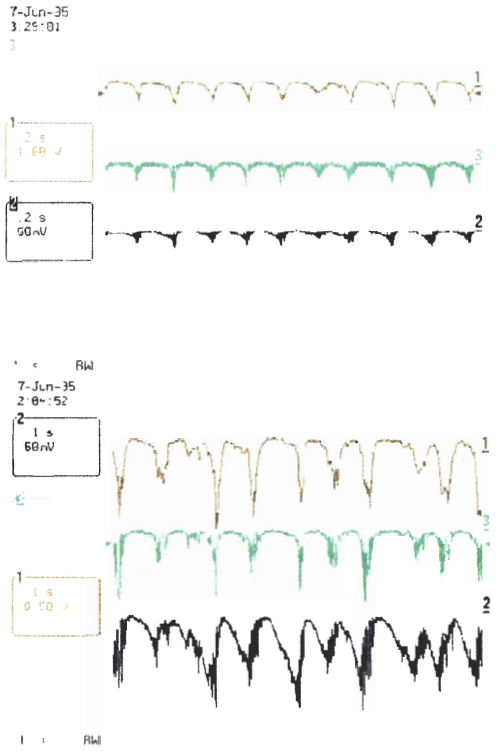

Figure: Bursts of coherent radiation (from reference below), as measured by a bolometeric detector (trace 1) and microwave detectors (traces 2 and 3). Top low current I=2 mA, bursting period is ~200 ms. Bottom I=10 mA, period is ~100 ms.

One of the most intriguing findings was that the instability threshold appears to be a factor of about 40 lower than what is predicted by the present theories using the best known model of the Bates ring impedance.

Other studies this fiscal year included R&D work for the IR ring in the context of NSLS-II project. A number of studies have been performed on the existing NSLS VUV/IR

ring or via computer simulations. Experimentally, we have succeeded in storing a few mA of current with 211 MHz RF used as the main RF system, as mentioned in item 2) of the Approach above. This work is continuing to better characterize the properties of the stored bunch. In simulations we explored a possibility of adding a coherent mode of operations to the present ring, initially in-place, and then moved to the location of the NSLS-II injector complex. We have also outlined the path for needed upgrades. These included a small number of extra magnetic elements (sextuples and octupoles) to better control the low value of the momentum compaction as well as a new powerful RF system to provide extra longitudinal focusing. For some fraction of this work we arranged a week-long visit Dr. G. Wusterfeld of BESSY, Germany, who co-discovered stable CSR in storage rings, and was the main driving force behind incorporating stable CSR mode into regular User operations for BESSY-II.

Our main conclusion is that for a modest investment we can add the CSR mode to the existing ring and then extend its life past the start of NSLS-II operations.

Unfortunately, due to the NSLS-II budget constraints a decision was made to drop the new IR ring out of the present NSLS-II scope. We are optimistic that when the NSLS-II budget outlook clears the IR ring will come back.

After the 2006 Mid-Year Review this LDRD was terminated as the Post. Doc. has not been hired and it was perceived by the LDRD committee that there was no hope of recouping.

SPECIFIC ACCOMPLISHMENTS:

Refereed publications

F. Wang, D. Cheever, M. Farkhondeh, W. Franklin, E. Ihloff, J. Van der Laan, B. Mcallister, R. Milner, C. Tschalar, D. Wang, D.F. Wang, A. Zolfaghari, T. Zwart, L. Carr, B. Podobedov, F. Sannibale, "Coherent THz Synchrotron Radiation from a Storage Ring with a High RF Frequency System," Physical Review Letters, **96**, 064801, (2006)

LDRD FUNDING:

FY 2005	$49,261
FY 2006	$16,600

Superconducting Undulator Technology Development

George Rakowsky *05-051*

PURPOSE:

Short-period superconducting undulators (SCUs) have been proposed as the ultimate X-ray sources for Protein Crystallography (PX) beamlines in NSLS-II and other high-brightness synchrotron radiation sources. Current technology of short period SCUs is limited by (a) low critical current of conventional NbTi superconductors, (b) quenching in presence of electron beams and synchrotron radiation, and (c) lack of means for "shimming" to correct field errors. In this project we seek to demonstrate technologies that may overcome these limitations and provide a basis for the design of long (up to 5 m) SCUs that will meet the demanding requirements of NSLS-II.

APPROACH:

Task (a): In-vacuum permanent-magnet undulators, pioneered at NSLS and Spring8, are the current baseline technology proposed as photon sources for PX beamlines in NSLS-II. However, the peak fields obtainable with permanent magnet technology are too low to provide the 3:1 tuning range needed for full spectral coverage by the fundamental, third and higher undulator harmonics in the multi-keV photon energy range of interest to PX.

Higher fields have been achieved in SCUs wound with conventional NbTi, but these fall short in peak field and tunability. Other National Labs (LBNL, in particular) are attempting to achieve the required high fields using Nb_3Sn to build SCU models. Nb_3Sn does operate at higher Jc, but it is very brittle, and the wind-and-react construction technique used with Nb_3Sn is more difficult.

A promising SC material with higher J_c is NbTi with artificial pinning centers (APC-NbTi). Since it is not yet available commercially, we contracted with the patent holder to develop an APC-NbTi superconductor to our specifications, with high enough J_c to achieve the required high field. A practical advantage of this material is that it is insulated and handled like ordinary NbTi, without a high-temperature react cycle or the brittleness of Nb_3Sn. We planned to demonstrate on a short model that the required higher SCU fields can be achieved using APC-NbTi.

This task included magnetic and mechanical design of the SCU model, acquisition of machining and CAD/CAM capability to fabricate the bifilar helical yoke geometry, and adapting and programming our coil winding apparatus to wind the conductors in the complex helical pattern.

Task (b): Cryogenic cooling of SCU magnets with a high beam-induced heat load presents a technical challenge. Immersion of SCU yokes in liquid helium (LHe) is not an option in an electron storage ring, since a single, thin wall between LHe and ultra-high vacuum in the beamtube is not permitted. Direct conduction-cooling of SC windings by a "cold finger" to a cryocooler, as in recent industry-built SCUs, has proven inadequate to handle the heat induced by even very low electron beam currents. Nb_3Sn models built at LBNL have somewhat higher thermal margins due to the higher critical temperature (T_c) of Nb_3Sn, but, with just conduction cooling of the superonductor, they will likely also prove incapable of handling the tens of watts/meter of beam-induced heating in modern synchrotron light sources. We planned to demonstrate a novel SCU cooling design by

co-investigator John Skaritka of NSLS. The design employs a beampipe cooled by cryogenic (10-20K) helium gas, to intercept the beam-induced heat at a higher temperature where it can be removed more efficiently than at 4K. The NbTi windings are thermally isolated from the beampipe and maintained below the critical temperature (T_c) by helium gas, sub-cooled to ~4K, circulating in embedded cooling channels under the windings. A cryocooler-based cold helium gas circulation and heat exchange system was to be designed for this purpose. Thermal isolation of the beampipe requires a slight increase of the magnetic gap. Consequently, the coils must be operated at somewhat higher current to achieve the required field, so the higher Jc of APC-NbTi is crucial. This task included cryogenic thermal analysis of the cooled beampipe and the SC windings and calculation of the helium gas flow rates needed for operation.

Task (c): Recent advances in thin- and thick-film MgB_2 high-temperature superconductors (HTS) opened the prospect of producing HTS printed conductor patterns for field error correction in SCUs. The films can be in contact with the beampipe, since MgB_2 has a T_c of 39°K. We contracted with the developer of a promising MgB_2 film deposition process to supply thin films on various substrates, as well as to print conductor patterns by photo-lithography. Laser cutting of patterns would also be explored. These test samples were to be evaluated at the Material Sciences Department's facilities.

A short prototype SCU incorporating APC-NbTi wire and our thermal intercept cooling design was to be designed, fabricated, and tested in the NSLS Vertical Test Facility located in the Superconducting Magnet Division.

TECHNICAL PROGRESS AND RESULTS:

Task (a): We have designed a SCU prototype, consisting of two low-carbon steel yokes with conductor slots cut in a bifilar, modified helical pattern to produce a planar undulator with a 15 mm period. The magnetic design has been modeled in 3D using the code Radia. In order to fabricate the yokes, we purchased and installed a 4th axis head on our CNC machine and acquired 3D CAD/CAM software to program the cutting of the complex bifilar helical conductor channels in the ferromagnetic yokes. The software translates AutoDesk Inventor 3D models into 4-axis CNC machine commands. After cutting wax and aluminum "proofs", the first of two 33 cm long low-carbon steel yokes was machined. The embedded copper cooling tube was wound into the slots. A "practice" copper wire of the same 0.5x1.0mm cross-section was test-wound in the slots on top of the cooling tube, to work out the winding procedure, especially at the conductor turn-arounds. The bifilar winding process proved out to be labor-intensive but, in the end, successful.

We did not have time to repeat the winding with the conventional NbTi wire, nor to test it in the VTF.

The first sample of APC-NbTi superconductor initially fabricated by the patent holder, L. Motowidlo, at Supra-Magnetics, Inc. turned out to be very brittle. Mr. Motowidlo modified the process and made several more attempts, which were fraught with technical and logistics problems. As of FY-06 year-end, he was attempting one final extrusion. To date we have not received the wire (and have withheld final payment.) Demonstration of APC-NbTi undulators will have to be deferred to a future project.

Task (b): To determine the effectiveness of the thermal intercept concept, a cryogenic thermal analysis of the beamtube with beam heating and helium gas cooling was subcontracted to Topsfield Engineering Services, Inc. Their analysis shows that with 100 W/m heat input to the beamtube's top and bottom inner surfaces, 99% is removed by the 20°K helium gas in the cooling channels, with only a 10° rise between the "hot spot" in the beamtube and the helium channel. Classical radiative heat transfer across the 0.1 mm gap between the beamtube and yoke is also very small. Quantum-mechanical heat transfer at 4K was estimated to contribute an additional 20%. Analysis of the SC winding with heat input from the beamtube and cooled by 4K helium in the embedded copper cooling tube shows stable SC operation.

Co-investigator J. Skaritka completed a preliminary design of the cold helium gas circulation and heat exchange system, including selection of a cryogenic gas circulation pump and a cryocoolers. A contract was let to Janis Research, Inc. for an independent review of the cryogenic design and for a detailed design and cost estimate of a cryocooler-based system for cooling short SCU models with simulated beam heating. The report confirms the validity of the design and gives detailed performance specifications for key components of such a system. Janis also demonstrated an intermediate-stage helium refrigerator with a cryocooler and a magnetically actuated cold helium gas pump. The design report and demonstration can serve as the basis for a future SCU cooling system.

Task (c): Co-investigator Cooley evaluated both YBCO and MgB_2 for field error correction in SCUs. YBCO has been shown to attain current densities as high as 500 kA/mm^2 in 1 μm thick films at 20K. However, current does not increase with film thickness above about 2.5 μm. American Superconcuctor now manufactures YBCO in copper foil in 4 cm wide ribbon that may be useful for fabricating field correctors. We visited their plant in Massachusetts, but have not yet been able to obtain samples for evaluation.

MgB_2 is a second option. Here, the reported critical current densities in the superconducting layer are much lower than those for YBCO, being about 10 kA/mm^2 at 20 K, at 1 T field for the best films. However, MgB_2 does not suffer from weak links at grain boundaries like YBCO does, which makes it possible to increase the overall current capacity by increasing the film thickness. Indeed, films as thick as 25 μm have been reported. Such a coating would provide a current of 1,000 amperes in a 4 mm by 0.25 mm wire. MgB_2 also confers the advantages of formability on a variety of substrates, in particular non-magnetic ones (in contrast to the nickel alloy used for YBCO).

Two central questions concerning MgB_2 films were addressed by this LDRD project. First, we sought to demonstrate feasibility for producing many-pole current patterns on non-magnetic substrates that could be directly attached to the beam tube. Second, we sought to demonstrate that thick films of MgB_2 could be made without reduction of the critical current density; that is, the current could be increased in direct proportion to the film thickness.

We have met both of these goals. Several 1 μm thick MgB_2 films were deposited on W, Nb, and Ti substrates by our subcontractor Brian Moeckly at Superconducting Technologies, Inc. These films were subsequently patterned into an 11-pole undulator "winding". A prototype of the films on metal substrates was produced

using 1 μm films deposited on sapphire. This wide variety of substrates demonstrates the flexibility of the MgB_2 process to different materials.

We measured the current induced by a magnetic field in films of various thickness between 0.35 and 1 μm. The current increases in proportion to the film thickness. To our knowledge, this is the first demonstration that the critical current of MgB_2 scales with the film thickness. A more straightforward demonstration, by directly applying transport current through the film, is awaiting the construction of a new test apparatus.

In summary: An ambitious multi-pronged R&D program was launched to address several key technical challenges facing SCU designers: (a) achieving the required engineering current density in superconductors, (b) managing the high beam-induced heat loads, and (c) developing means of field error correction. We tried jump-starting solutions to some of these challenges by industry leaders in these specialized fields. Significant progress was made in each area. However, to demonstrate a SCU prototype integrating all these aspects will require more time and effort, as well as funding from other sources, such as NSLS-II.

SPECIFIC ACCOMPLISHMENTS:

A provisional patent application was filed on July 7, 2006, with the US Patent Office for an invention by L.D. Cooley, G. Rakowsky, and J. Skaritka: "Small Gap High Temperature Superconducting Undulator."

Invited Presentations:
L.D. Cooley, "MgB_2 activities at BNL," Workshop on high-field MgB_2, University of Wisconsin, 10-12 August 2005

T. Tanabe, G. Rakowsky, J. Skaritka, "SC Magnet Related Activities at NSLS," at Workshop on Applications of Superconducting Technology in Synchrotron Light Sources, June 5, 2006, Taiwan.

G. Rakowsky, "Insertion Device R&D Program for NSLS-II," Workshop on New Frontiers in Insertion Devices, Nov. 20-21, 2006, Trieste, Italy.

LDRD FUNDING:

FY 2005	$189,451
FY 2006	$228,264

Characterization and Imaging of Amyloid Plaques Using Diffraction Enhanced Imaging

Zhong Zhong *05-057*

PURPOSE:

The goal of this LDRD is to explore the potential of Diffraction Enhanced Imaging (DEI) for early detection of amyloid beta peptide deposition in Alzheimer's disease (AD). Since the appearance of these plaques, a hallmark feature of AD, precedes clinical symptoms by many years, there is great interest to develop methods for their early detection.

DEI is a novel radiography method that introduces fine selectivity for the angular deviation of x rays traversing the subject. DEI's angular sensitivity allows measuring the gradient of the x-ray index of refraction in soft tissues, as well as the yield of "small angle scattering" (extinction contrast). The organized structure of amyloid plaques is expected to exhibit certain extinction contrast, thus allowing their distinction from healthy brain tissues by DEI.

APPROACH:

The technical aims of the program include improvement of the mechanical stability of the DEI system at the NSLS's X15A beamline, and the development of DEI-CT capability. Because the DEI imaging contrast from the amyloid plaques is expected to be small, these two steps are crucial to enable imaging of these plaques. DEI's effectiveness will then be tested by characterization of the extinction properties of amyloid plaques and that of healthy brain tissue, and by establishment of a correlation between the DEI images, the infrared spectroscopy images, and the histological analysis. The project was undertaken by a multi-disciplinary team consisting of the investigators A. Dilmanian, L. Miller, and Carol Muehleman, post-doctoral research associates D. Connor and C. Parham, collaborators H. Benveniste and M. Kritzer, and summer students J. Chen, T. Kao, E. Mahajna, and A. Wu.

TECHNICAL PROGRESS AND RESULTS:

The DEI system was upgraded to improve the stability, as the stability of the monochromator and analyzer is the key for DEI-CT at high spatial resolution. The system's drift after the upgrade (which included installation of a new water-cooled mount for the second crystal of the monochromator and modification of the white beam filter assembly) was reduced by a factor of 300. With the improved system, it is possible to do DEI-CT scans that last several hours.

Previous imaging of a transgenic AD-model mouse brain showed no obvious plaques, but the system was limited by the resolution of the detector. An NIH grant funded two new high-resolution (30 micron and 10 micron), low-noise CCD detectors, the second of which (10 micron) was installed in Spring, 2006. A method to integrate the detectors into the DEI system to perform robust DEI-CT imaging was subsequently established using these detectors.

Five AD brain specimens and two control specimens were acquired from Rush University Medical Center through Carol Muehleman and her collaborators. Initial DEI images obtained last year on the 30 micron detector showed microcalcifications, but did not reveal plaques. Using the new,

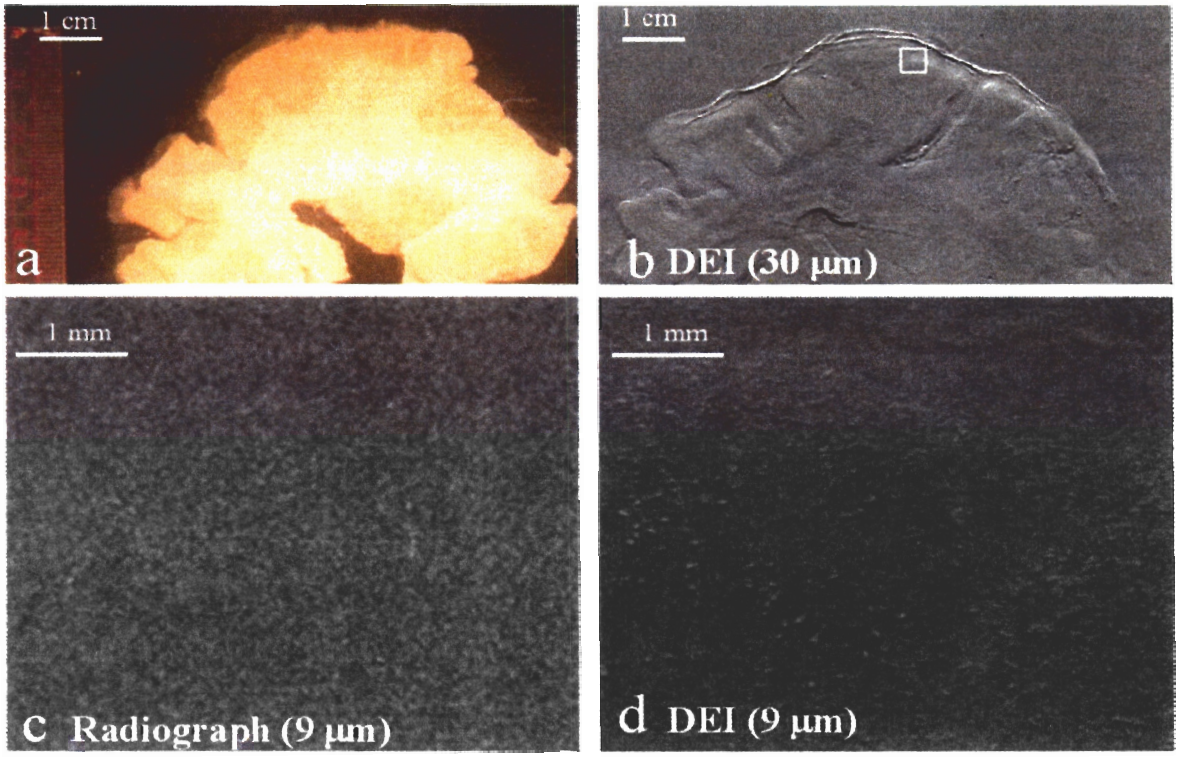

Figure 1: a) photograph Photograph of the AD brain specimen. b) DEI image. c) Radiograph of the boxed region in bB. d) DEI of the boxed region in b.

10 micron detector, the AD and control brains were re-imaged. The resulting images are shown in figure 1. Low density nodules that do not appear in the radiograph are clearly depicted in the DEI image. We believe that the discerned structures are plaques as they are the same known size as plaques (approximately 50 microns) and are distributed near the surface, in the gray matter, where plaques are expected to be found in AD brains. Therefore, the preliminary data are consistent with our hypothesis that the organized structure and higher density of amyloid plaques exhibit DEI contrast.

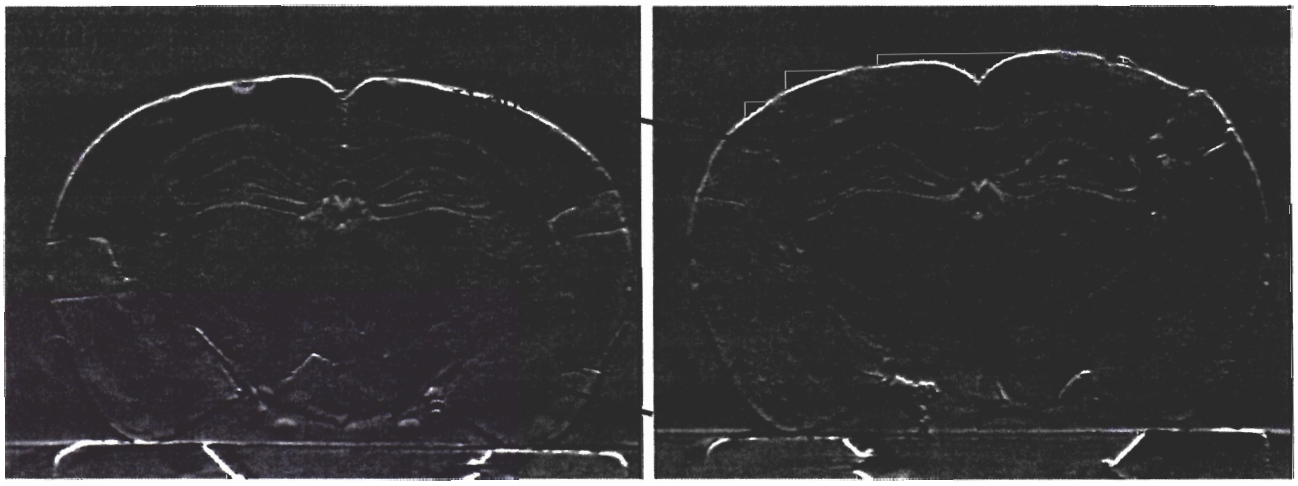

Figure 2

Brains from a commercial transgenic mouse model and age-matched wild-type mouse for control were obtained and imaged, both in planar and CT modes. An example slice is shown in figure 2. Nodules that are denser than the surrounding tissue appear in the hippocampus and cortex regions of the AD model mouse brain and are about the size that one would expect the plaques to be. Histology is currently being done to confirm that these nodules are plaques.

This project involves animal vertebrates (BNL IACUC protocol 305) and specimens from human subjects (IRB 15)

SPECIFIC ACCOMPLISHMENTS:

Patents:

1. C. Parham, E. Pisano, L.D. Chapman and Zhong Zhong, "High Energy Soft Tissue Imaging Using Diffraction Enhanced Imaging," BNL patent disclosure, 2006.

Publications :

1. A. Wagner, M. Aurich, N. Sieber, M. Stoessel, W.D. Wetzel, K. Schmuck, M. Lohmann, B. Reime, J. Metge, P. Coan, A. Bravin, F. Arfelli, L. Rigon, R. H. Menk, G. Heitner, T. Irving, Z. Zhong, C. Muehleman, and J. A. Mollenhauer, "Options and Limitations of joint cartilage imaging: DEI in comparison to MRI and sonography," *Nucl. Instrum. Methods in Phys. Res.*, **A 548** (2005) 47-53.

2. C. Muehleman, J. Li, Z. Zhong Z, J. G. Brankov, M. N. Wernick, "Multiple-image Radiography for human soft tissue" *J. Anatomy*, **208** (2006) 115-124.

3. J. G. Brankov, M. N. Wernick, Y. Yang, J. Li, C. Muehleman, Z. Zhong and M. Anastasio, "A computed tomography implementation of multiple-image radiography," *Med. Phys.*, **33** (2006) 278-289.

4. Khelashvili, G.; Brankov, J.G.; Chapman, D.; Anastasio, M.A.; Yang, Y.; Zhong, Z, and Wernick, M.N.; "A physical model of multiple image radiography," *Physics in Medicine and Biology,* **51** (2006) 221-236.

5. M. Wernick, Y. Yang, I. Mondal, D. Chapman, M. Hasnah, C. Parham, E. Pisano and Z. Zhong, "Computation of mass density images from x-ray refraction-angle images," *Phys Med Biol.* **51** (2006) 1769-1778.

6. D. Connor, D. Sayers, Z. Zhong and R. Sumner, "Diffraction Enhanced Imaging of Controlled Defects within Cortical Bone, Including Bone-Implant Interface Gaps," *Phys. Med. Bio.* **51** (2006) 3283-3300.

7. C. Muehleman, J. Li, and Z. Zhong, "Preliminary study on diffraction enhanced imaging for a canine model of cartilage damage," *Osteoarthritis and Cartilage*, **14** (2006) 882-888.

8. C. Parham, E. Pisano, C. Livasy, L. Faulconer, M. Wernick, J. Brankov, M. Kiss, D. Connor, J. Chen, A. Wu, Z. Zhong, and D. Chapman, "Application of the Multiple Image Radiography method to breast imaging," *Digital mammography, proceedings lecture notes in computer science,* 4046 (2006) 289-298.

Papers in review or in preparation:

1. C. Chou, M. Anastasio, J. Brankov, M. Wernick, E. Brey, D. Connor and Z. Zhong, "An extended diffraction-enhanced imaging method for implementing multiple-image radiography," submitted, *Phys. Med. Bio.*

2. H. Zhang, D. Chapman, Z. Zhong, C. Parham, M. Gupta, "TILT ERROR IN DIFFRACTION ENHANCED IMAGING SYSTEM," submitted, NIM A.

Presentations:

1. C. Parham, E. Pisano, C. Livasy, L. Faulconer, M. Wernick, J. Brankov, M. Kiss, D. Connor, J. Chen, A. Wu, Z. Zhong, and D. Chapman, "Application of the Multiple Image Radiography Method to Breast Imaging," p 289-298, in *Digital Mammography 8th International Workshop*, IWDM 2006, Manchester, UK, June 18-21, 2006, Springer, Vol. 4046, Astley, S.M.; Brady, M.; Rose, C.; Zwiggelaar, R. (Eds.) ISBN: 3-540-35625-8

2. F. Avraham Dilmanian, Vasilios Boronikolas, Zhong Zhong, Panayotis K. Thanos, Dean M. Connor, Michael Michaelides, Gene-Jack Wang, Lihong Li, Arun Tatiparthi, Phil Salmon, and Xuan Liu, "Single- and Dual-Energy Quantitative CT for Quantifying Adipose Tissue in Rodents Using a MicroCT System," *IEEE Medical Imaging Conference*, October 31 – November 4, 2006, San Diego.

3. D Connor, C Parham, A Dilmanian, T Kao, and Z Zhong, "Energy and dose considerations for diffraction enhanced CT in small animal studies," *SPIE Medical Imaging Conference*, February 12-17, 2007, San Diego.

LDRD FUNDING:

FY 2005	$100,793
FY 2006	$131,955

Development of Methodologies for Analyzing Transcription Factor Binding in Whole Genomes

Carl W. Anderson *05-058*

PURPOSE:

The goal of this program is to develop a robust method for identifying and characterizing protein binding sites and epigenetic markers in whole genomes of eukaryotic cells. We developed a method, Serial Analysis of Chromatin Occupancy (SACO), for profiling the functional chromatin binding sites of proteins in cells across whole genomes. A variation of this procedure, Paired-End SACO (PE-SACO) will be developed that simplifies the basic SACO procedure and makes it robust for potential automation. PE-SACO also will be extended by coupling it with a highly sensitive methylated-CpG island recovery assay, MIRA, to identify epigenetic marker in DNA that regulate chromatin function. The PE-SACO procedure will be validated through identification and analysis of the binding sites for the human tumor suppressor protein p53 in primary human epithelial cells following DNA damage (e.g. exposure to ionizing radiation) and by analyzing the methylation status of one or more characterized cell lines. The technology is relevant to developing a systems understanding of the cellular responses of human and mouse cells to low doses of ionizing radiation for DOE's Low Dose Radiation Program. This will require determining how and where radiation and other genotoxic stresses induce changes in transcription factor binding, chromosome structure and whether epigenetic changes such as methylation of cytosine residues occurs in the DNA. The methodology also is applicable to understanding the complex physiological and behavioral systems coordinated by a central nervous system.

APPROACH:

Two major principles underlie the Genome Signature Tag (GST) method that forms the basis for SACO. First, short DNA GST sequences (21 bp) are sufficient to identify unique sites within a genome; second, the concatenation of these short DNA sequences greatly increases the efficiency of identification through high throughput sequencing. SACO combines the GST methodology with a technique called **ch**romatin **i**mmuno-**p**recipitation (ChIP), in which proteins bound to DNA are reversibly crosslinked to the DNA segment to which they are bound with formaldehyde. The crosslinked chromatin is then fragmented into ~500 bp fragments by sonication, and the DNA to which any given protein is bound is recovered using antibodies that specifically recognize that protein. For a human cell, a typically transcription factor might bind to several thousand sites within the entire human genome. Thus, ChIP is expected to extract perhaps a million bp of sequence (500 bp x ~2000 binding sites), i.e. 0.3% of the total human genome, with which a given transcription factor is bound. For SACO, GSTs are then created from these fragments, concatenated, and sequenced to produce a quantitative profile of the loci to which the transcription factor was bound at the time the cells were treated with the crosslinking agent.

PE-SACO simplifies the SACO procedure and makes it more robust. For PE-SACO, the ChIP fragments will be first cloned into a specially constructed vector, pBEST (Both End Signature Tags), developed at BNL that has *Mme* I restriction sites flanking the cloning site. The Mme I restriction enzyme cleaves DNA 20 or 21 base-pairs (bp) away from its recognition site, thereby creating

~20 bp sequence tags from each end of each ChIP fragment. The cleaved vectors are then relegated to create a ~42 bp insert, a "di-tag," containing ~20 bp from each end of a ChIP fragment. The di-tags then may be amplified using the polymerase chain reaction (PCR). The PCR fragments are then digested with another restriction enzyme that cleaves sites in the PE-SACO vector flanking the Mme I sites to release each di-tag. Di-tags are then concatenated, cloned into a sequencing vector, the inserts are sequenced, and bioinformatics is then used to extract each sequence tag and determine the location in the genome from which it was derived.

An advantage of the PE-SACO methods it that for factor binding loci that are recovered many times, the factor binding site must be found with the segment that is common to all recovered DNA fragments corresponding to the locus. This feature of the method will reduce the segment that must be examined for factor binding sites from ~2000 bp to perhaps 100 bp.

The method also can be used to identify modified DNA segments in chromatin such as segments that are epigenetically marked with methylated cytosines. Chromatin segments containing methylated cytosines are recovered using a protein, such as the DNA binding segment of MeCP2, that specifically binds methylated DNA sequences in place of an antibody to a protein that recognizes DNA. G. Pfeifer, Beckman Research Institute of the City of Hope, has developed a highly sensitive protocol for isolating methylated DNA fragments. We are collaborating with Pfeifer's group to adopt his procedure for PE-SACO and to validate its use for identifying epigenetically marked DNA in human cells. We also will explore methods for the subtractive analysis of methylated DNA segments that would more readily permit identification of changes in epigenetic marks.

To validate the PE-SACO technique, we are characterizing a PE-SACO library corresponding to the binding sites of the p53 human tumor suppressor protein in human epithelial cells following treatment with ionizing radiation. p53 is a 393 amino acid, tetrameric, transcription factor that regulates the expression of genes which control cell cycle progression, the induction of apoptosis and senescence, DNA repair, and other functions involved in cellular responses to stress and maintenance of genome integrity. p53 is the most commonly mutated gene in human cancers, and loss of p53 function, either directly through mutation or indirectly through several other mechanisms, plays a central role in the development of cancer. Genomic approaches have shown that p53 induces or inhibits the expression of more than 1500 human genes. The p53 monomer binds a consensus DNA sequence, 5'-RRRC(A/T)-3', which commonly is repeated as pairs of inverted repeats separated by 0 to 14 base pairs (bp) to create a 20 bp binding site for tetrameric p53. Thus, p53 specifically recognizes the consensus sequence 5'-RRRCWWGYYY (N = 0-14) RRRCWWGYYY-3' where R stand for a purine base (A or G), Y stand for a pyrimidine base (T or C) and W stands for either A or T. For p53, as well as for most other transcription factors, the degenerate nature of the DNA binding consensus sequence makes it difficult to predict and identify authentic binding motifs in whole genomes by simply scanning the sequence (there are >65,000 unique sequences that match the p53 consensus sequence excluding the 0-14 bp spacer); in addition, not all consensus sites (p53 responsive elements, p53REs) are competent for p53 binding *in vivo*. p53 also promotes the expression of some genes through elements that are of limited similarity to the consensus

binding motif (e.g. the *PIG3* gene). Protein modifications and the presence of binding partners and their concentration, all are thought to modulate p53's ability to transcriptionally activate or conversely repress target genes. Understanding which sites in chromatin are bound by p53 after genotoxic stress is critical for understanding how p53 prevents cancer and may lead to improved cancer treatments.

TECHNICAL PROGRESS AND RESULTS:

Several technical improvements were made to the PE-SACO technique dealing mainly with vector and library construction, design of a set of *Bcl* I-based barcodes to aid in library identification and methods for employing 454 sequencing technology for sequencing the end products.

Bcl I barcoded PE-SACO libraries were prepared from presenescent IMR90 human fibroblasts that were untreated, or 4 hr after exposure to either 0.1 Gy or 8 Gy ionizing radiation. The cells were fixed with formaldehyde to crosslink p53 to chromatin, extracts were sonicated to fragment the DNA into 500-1000 bp fragments, and the p53-containing fragments were captured by immunoprecipitation with the DO-7 p53-specific monoclonal antibody using magnetic beads that interact with the antibody. Quantitative PCR analysis showed that fragments from the p21 gene promoter were enriched in the immunoprecipitates or ChIP fraction as expected compared to the input DNA. The ChIP fragments were end repaired to give blunt ended fragments and then ligated with DNA linkers to aid in cloning and PCR amplification. After PCR, the amplified fragments were cloned into the pBEST vector which places individual ChIP DNAs immediately adjacent to the oppositely oriented *Mme* I recognition sequences. These are the only *Mme* I sites in the vector. Digestion with *Mme* I cleaves bidirectionally into the ChIP inserts leaving 20-21 bp DNA fragments or "TAGs" attached to the vector. In subsequent steps the linearized vector DNAs with attached TAGS on each end are converted into circular DNA molecules while maintaining the TAG fragments spatial relationship to each other to form what we term diTAGs. During this step a synthetic DNA barcode is added to each separate sample to aid in identifying the source of the sample used to form the diTAGs during subsequent high-throughput 454 DNA sequencing.

The initial clone libraries were grown en masse for the preparation of plasmid fragment libraries. DNA from these libraries was digested with *Mme* I to create paired-end tags, DNA was isolated, and the vector fragments were ligated with *Bcl* I-containing barcoded oligonucleotides. After digestion with *Bcl* I to insure that the barcodes were monomeric and relegation, transformants were again grown en masse, collected, and the DNAs were digested and gel purified to create ~60 bp diTAG libraries. These have been sent to the DOE Joint Genome Institute for sequencing using the new Life Sciences 454 technology. Traditional concatemer libraries also were prepared for comparison purposes.

Progress was made in the biochemical and molecular analysis of the role of p53 acetylation in modulating p53-mediated transcription Cells from a transgenic mouse (created by Y. Xu, UCSD) in which the codon for lysine 317 in the endogenous p53 gene was changed to encode arginine. These were analyzed for the induction or repression of p53 regulated genes. Unexpectedly, this change to the p53 amino acid sequence, which prevents acetylation at this amino acid, significantly enhances both transcriptional activation and p53-mediated

repression in differentiated tissues but not in mouse embryo fibroblasts. Future studies will use PE-SACO to examine the binding of p53 to DNA sequences associated with these genes.

An important gene that is regulated by p53 is the phosphatase PPM1D or Wip1. The *PPM1D* gene is amplified in a significant fraction of a number of human tumors, including breast cancer. Previously we showed using a murine breast cancer model, that mice were incapable of expression of PPM1D and were partially protected from cancer. We analyzed the promoter for the PPM1D gene and identified the p53 binding site that is responsible for transcriptional activation by p53. This site is one of the targets we expect to find with PE-SACO. Cyclic peptides capable of inhibiting PPM1D activity. Advanced small molecule inhibitors, based on these cyclic peptides, may be useful anti-cancer drugs as well as important tools for the molecular analysis of PPM1D function in cell cycle control.

SPECIFIC ACCOMPLISHMENTS:

Publications:

Acetylation of mouse p53 at lysine 317 negatively regulates p53 apoptotic activities after DNA damage. Chao, C.; Wu, Z.; Mazur, S. J.; Borges, H.; Rossi, M.; Lin, T.; Wang, J. Y. J.; Anderson, C. W.; Appella, E.; and Xu, Y. Mol. Cell. Biol. 26(18), 6859-6869 (2006).

Unfolding, aggregation, and amyloid formation by the tetramerization domain from mutant p53 associated with lung cancer. Higashimoto, Y.; Asanomi, Y.; Takakusagi, S.; Lewis, M. S.; Uosaki, K.; Durell, S. R.; Anderson, C. W.; Appella, E.; and Sakaguchi, K. Biochemistry 45(6), 1608-1619 (2006).

Wip1 phosphatase modulates ATM-dependent signaling pathways. Shreeram, S.; Demidov, O. N.; Hee, W.-K.; Yamaguchi, H.; Onishi, N.; Kek, C.; Timofeev, O.N.; Dungeon,C.; Fornace, A.J.; Anderson, C. W.; Minami, Y.; Appella, E.; and Bulavin, D. V. Molec. Cell 23, 757-764 (2006).

Development of a substrate-based cyclic phosphopeptide inhibitor of protein phosphatase 2Cδ, Wip1. Yamaguchi, H.; Durell, S. R.; Feng, H.; Bai, Y.; Anderson, C.W.; and Appella, E. Biochemistry 45, 13193-13202 (2006).

Regulation of ATM/p53-dependent suppression of myc-induced lymphomas by Wip1 phosphatase. Shreeram, S.; Hee, W.-K.; Demidov, O. N.; Kek, C.; Yamaguchi, H.; Fornace, A. J.; Anderson, C. W.; Appella, E.; and Bulavin, D. V. J. Exptl. Med. (in press).

LDRD FUNDING:

FY 2005	$ 92,970
FY 2006	$143,704
FY 2007 (budgeted)	$ 71,000

Application of Endophytic Bacteria to Improve the Phytoremediation of TCE and BTEX Using Hybrid Poplar

Daniel van der Lelie *05-063*

PURPOSE:

To improve the phytoremediation of volatile organic contaminants by using endophytic bacteria to complement the metabolic properties of their host plant.

APPROACH:

Endophytic bacteria are an important tool to improve the phytoremediation of volatile organic contaminants and can be used to complement the metabolic potential of their host plant. Endophytic bacteria equipped with the appropriate degradation pathway significantly improved the *in planta* degradation of toluene in yellow lupine, resulting in its reduced phytotoxicity and release. We extended this concept to poplar, a plant species frequently used for the phytoremediation of groundwater contaminated with organic solvents. Inoculation of poplar with the endophyte *Burkholderia cepacia* VM1468 (pTOM-Bu61), which is able to constitutively degrade toluene and TCE, resulted in reduced environmental release and phytotoxicity of toluene. A major difference between the yellow lupine and poplar experiments is the use of non-sterile plants for the inoculation of the poplar. Analysis of the microbial communities associated with non-inoculated control plants and poplar inoculated with VM1468 showed that the strain had failed to establish itself within the endogenous endophytic community. However, horizontal gene transfer of the toluene degradation plasmid pTOM-Bu61 had occurred to different species of poplar's endogenous endophytic community, both in the presence and absence of toluene. This work demonstrates the potential of horizontal gene transfer to adapt an endophytic microbial community to deal with the stress imposed by an environmental insult and to improve the phytoremediation potential of its host plant.

TECHNICAL PROGRESS AND RESULTS:

Beneficial effect of inoculation. Inoculation of poplar with the *B. cepacia* strains had a positive effect on plant growth in the presence of toluene (Figure 1) and reduced the amount of toluene released via evapotranspiration (Figure 2). This effect was more dramatic for VM1468, the endophytic strain, than for Bu61. These results confirm our earlier observations with yellow lupine that endophytic bacteria, equipped with the proper degradation pathway, are able to protect their host plant against the phytotoxic effect of toluene. The results also show that degradation of toluene by the endophytic bacterium results in a reduced release of toluene in the atmosphere.

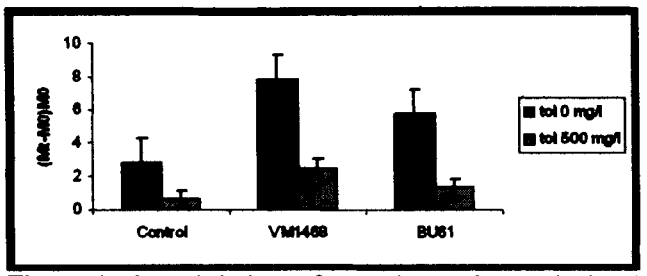

Figure 1: Growth indexes for poplar cuttings calculated after 10 weeks of growth in the presence or absence of toluene (0 or 500 mg l-1). Plants were either inoculated with *B. cepacia* VM1468 or *B. cepacia* BU61, while non-inoculated plants were used as controls. Growth indexes were calculated as [(Mt-M0)/M0]. M0: plant weight (g) before addition of toluene; Mt: plant weight (g) 10 weeks after toluene addition. Given are mean and standard error of 10 replicates. Standard deviations are indicated as bars. The statistical significance of the results was confirmed at the 5% level using a two-way ANOVA model, separately exploring treatment (bacterial inoculums) and toluene doses.

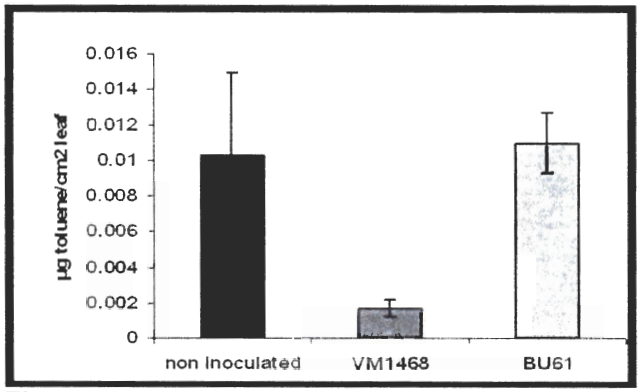

Figure 2: Total amount of toluene (µg) released from poplar into the upper cuvette compartment. Toluene was adsorbed with Chromosorb traps and its concentration was determined by GC-MS. The amount of evapotranspirated toluene was calculated per square centimeter of leaf area. Given are the mean and standard error of 3 replicates. Bars indicate standard deviations.

TCE degradation in yellow lupine. Inoculation of yellow lupine with *B. cepacia* VM1468, the endophytic bacterium that constitutively expressed the *tom* ortho-mono-oxygenase gene, had a positive effect on growth in the presence of TCE (Figure 3). On the contrary, the presence of *B. cepacia* VM1330, which requires toluene for the induction of the *tom* ortho-mono-oxygenase gene, was unable to protect its host against TCE phytotoxicity. This results is the first demonstration that endophytic bacteria can protect their host plant against TCE phytotoxicity. It also demonstrates the importance of constitutive gene expression, especially for contaminants that are normally degraded via co-metabolism. This result was confirmed by using *B. cepacia* BU61 (constitutive for TCE degradation) and comparing its phytoprotection potential for TCE with that of *B. cepacia* G4 (TCE co-metabolism via toluene degradation).

SPECIFIC ACCOMPLISHMENTS:

During the course of our experiments we noticed that the presence of endophytic bacteria had a general beneficial effect on plant growth.

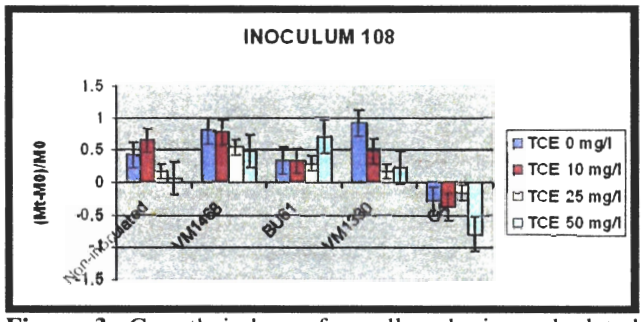

Figure 3: Growth indexes for yellow lupine calculated after 4 weeks of growth in the presence or absence of TCE (0 to 50 mg l^{-1}). Plants were either inoculated with *B. cepacia* VM1468, BU61, VM1330 or G4, while non-inoculated plants were used as controls. Growth indexes were calculated as [(Mt-M0)/M0]. M0: plant weight (g) before addition of TCE; Mt: plant weight (g) 4 weeks after TCE addition. Given are mean and standard error of 10 replicates. Standard deviations are indicated as bars. The statistical significance of the results was confirmed at the 5% level using a two-way ANOVA model, separately exploring treatment (bacterial inoculums) and TCE doses.

Publications:

Horizontal gene transfer to endogenous endophytic bacteria from poplar improves phytoremediation of toluene. Taghavi, S.; Barac, T.; Greenberg, B.; Vangronsveld, J.; and van der Lelie, D. Appl. Environ. Microbiol. 71, 8500-8505 (2005).

Endophytic bacterial diversity in poplar trees growing on a BTEX-contaminated site: The characterization of isolates with potential to enhance phytoremediation. Moore, F. P.; Barac, T.; Borremans, B.; Oeyen, L.; Vangronsveld, J.; van der Lelie, D.; Campbell, C. D.; and Moore, E. R. B. System. Appl. Microbiol. 29(7), 539-556 (2006).

Endophytic bacteria and their potential application to improve the phytoremediation of contaminated environments. Mastretta, C.; Barac, T.; Vangronsveld, J.; Newman, L.; Taghavi, S.; and van der Lelie, D. Biotech. Genetic Engin. Rev., Vol. 23 (in press).

LDRD FUNDING:

FY 2005	$212,900
FY 2006	$281,627

Design and Build Two Dimensional Protein-Lipid Thin Film: A First Step Toward Novel Biochips

Yinan Wei *05-064*

PURPOSE:

In this proposed research, we will perform structural and functional studies of metal transporter proteins and develop the technique to "polymerize" these proteins in their fully functional states into a two dimensional matrix. Subsequently phospholipids will be incorporated into the gaps of the protein matrix to form a bioactive thin film. Insight acquired during this proposed research will benefit the development of general methodologies for membrane protein expression, purification and characterization. The bioactive two-dimensional (2D) protein-lipid thin film to be constructed may bring new opportunities into the development of biotechnology.

APPROACH:

The marriage of biology and nanoscience yields the burgeoning field of biochips. Usually no larger than a fingernail, these biochips can be designed to perform reactions or detections with high quality and efficiency. The research of protein biochips starts with the attachment of protein molecules to a surface in an ordered manner. We plan to invent a structural based protein engineering approach to assemble membrane protein molecules into 2D films. In the current stage, we carried out detailed biophysical characterization of the target membrane protein, *Escherichia coli.* Zn^{2+} transporter YiiP. The YiiP is picked as the building block for the films due to its ability to transfer heavy metal ions across the membrane, which may facilitate applications such as pollution control of heavy metal ions. After necessary structural information is acquired, a docking unit will be introduced into the protein at designated positions by mutagenesis. Next biophysical properties of the modified protein molecules will be examined and active candidates with the best stability will be used in the polymerization study.

TECHNICAL PROGRESS AND RESULTS:

During FY 2006, we have made the following technical progress:

Identified a substrate binding cluster at the subunit interface of the YiiP dimer and presented a novel cooperative binding model for the protein.

Dissected the multiple Zn^{2+}/Cd^{2+} binding sites of YiiP by thermodynamic analysis coupled with site directed mutagenesis.

Identified an additional key functional site, Asp49, and established the connection between Asp49 and Asp 157.

Thus much progresses in understanding the structure and function of YiiP. This knowledge is the foundation for the potential applications of YiiP as building blocks to construct the protein-lipid film.

SPECIFIC ACCOMPLISHMENTS:

External refereed publication:

Binding and transport of metal ions at the dimer interface of the *Escherichia coli* metal transporter YiiP. Wei, Y. and Fu, D. J. Biol. Chem. 281(33), 23492-23502 (2006).

LDRD FUNDING:

FY 2005	$61,342
FY 2006	$76,898

Positron Labeled Stem Cells for Non-Invasive PET Imaging Studies of In-Vivo Trafficking and Biodistribution

Suresh Srivastava *05-068*
L. Pena

PURPOSE:

The overall goal of this project is to develop methods for radiolabeling progenitor stem cells for noninvasively tracking their behavior and fate ***in vivo*** through PET imaging. If successful, these investigations would lead in the long run to the development of a generally practical, convenient, and reliable method for following the distribution, differentiation, and survival of stem cells in a quantitative fashion. This project has the potential to significantly enhance and broaden our understanding of the mechanisms of stem cell involvement in health and disease. It involves the use of the very sensitive PET radiotracer imaging technique.

APPROACH:

Published reports identify the need for a practical, reliable, and cost-efficient way of marking progenitor stem cells to non-invasively evaluate their distribution and survival following transplantation. Our preliminary results and work from multiple laboratories suggest that radiolabeling antibodies that are specific to subpopulations of progenitor stem cells with positron emitters to allow PET imaging is perhaps the most efficient and economical way to follow stem cell trafficking, survival, and differentiation *in vivo*.

The general approach for cell labeling involves preparing a radioimmunoconjugate of the appropriate cell-specific monoclonal antibody (MAb) first with the PET radionuclide (e.g, I-124 and Co-55 proposed in this investigation), and then stably and irreversibly attaching the resulting radioimmunoconjugate to the progenitor stem cell under study. The initially selected model was the bipotential glial stem cell line, CG-4, and the monoclonal antibody A2B5, which targets an antigen present specifically on the glial cell surface. After initial experimentation it became clear that the level of A2B5 expression in these glial progentior cells (CG4) was rather low. We began looking for another cell type with high levels of A2B5 expression to use as a positive control. The best candidiate turned out to be the RIN-m5F cells. These cells are derived from a rat insulinoma model.

This work is expected to accomplish the first steps towards fulfilling the above stated unmet need for a noninvasive imaging methodology for following stem cell trafficking, survival, and differentiation *in vivo*.

In addition to the P.I.s, the other investigators involved in this project were M. Rao (NIH, Consultant), G. Meinken, Scientific Associate, N. Medvedeva, Research Associate, and D. White, Technical Assistant.

TECHNICAL PROGRESS AND RESULTS:

During FY 2006, our efforts initially involved improving the methodology for preparing milligram amounts of MAb A2B5 from an appropriate hybridoma cell line and to radioiodinate it with commercially available I-125 (as a surrogate for the positron emitter I-124) using increasing numbers of iodine atoms per MAb molecule (no-carrier-added, 0.5, 5, and 10 with carrier). The next step was to prepare a slot blot of cell lysates from test and control cell lines. The procedure for determining the binding efficiency and the retention of biological activity of the immunoconjugate included incubating the blots with the radioiodinated A2B5, and autoradiography using a Phosphor Imaging System.

We achieved the preparation of the MAb A2B5 by implementing the following steps. We grew hybridoma cells that secrete MAb A2B5 in cell culture and optimized conditions for cell growth and for harvesting the medium. We then, carried out affinity purification #1 using a T-Gel Column (that enriches thiophilic proteins including MAbs) and affinity purification #2 using a Protein L Column (to enrich immunoglobulins, particularly IgM). Following this, an ultrafiltration procedure (100K cutoff) was performed to accomplish concentration and buffer exchange in one step. Using the above optimized methodology, we were successful in scaling up the production MAb A2B5 to the required milligram quantities.

We also optimized the iodination (with I-125 and I-131) using commercially available (very expensive) as well as locally prepared A2B5 achieving good labeling efficiency (50 – 80%). The retention of biological activity of radioiodinated A2B5 was determined using positive glial cell controls. Due to the rather low expression of A2B5 MAb on the glial cell surface and in addition, possibly because of the low specific activity of I-131, our initial results were not entirely clear. However, the iodination of A2B5 with I-125 and further use of Rin-5F cells instead of CG4 cells resulted in data confirming successful radiolabeling and retention of biological activity of radioiodinated A2B5. The schematic description of these studies is shown in Figure 1.

Our plans for FY 2007 are to finish the following Specific Aims 2 - 4 and develop methods for labeling the antibody with the commercially available Co-57 (as a surrogate for positron emitter Co-55). We will optimize for the highest radioisotope loading efficiency (I-125, I-131, and Co-57) without loss of biological activity. In addition, coupling of newly purified MAb A2B5 with fluorochrome and further radiolabeling of the CG-4 and Rin-5F cells will be utilized to assure in vitro stability and biological activity of the obtained antibody. Finally, conditions will be optimized for maximum radiolabeled A2B5 loading per 10,000, and per 50,000 CG-4 cells.

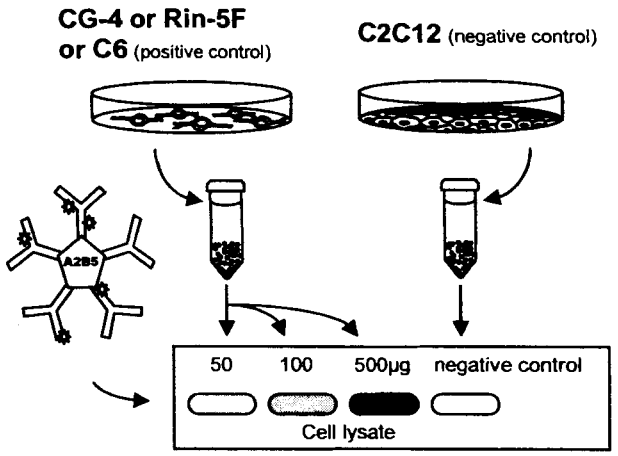

Figure 1. Schematic representation of the determination of retention of biological activity of the radioimmunoconjugates.

Future plans also include optimizing the retention of biological activity of the radioactive A2B5-labeled RIN cells, as a function of increasing A2B5 and isotope concentrations. We will use differentiation effects in vitro, and unlabeled RIN cells as controls.

The in vivo behavior (biodistribution and kinetics) in rats, following both intravenous and regional administration of the radiolabeled CG-4 cells will be studied using micro PET, tissue counting, and autoradiography. The results will be compared with those obtained with Tc-99m-RBC as a control system.

This project involves vertebrate animals.

SIGNIFICANT ACCOMPLISHMENTS:

None

LDRD FUNDING:

FY 2005	$ 63,600
FY 2006	$140,374
FY 2007 (budgeted)	$153,000

Breaking the Millimeter Resolution Barrier in fMRI

Dardo Tomasi *05-069*

PURPOSE:

The effective relaxation time of the tissue magnetization is very short (~40 ms) and limits the number of data samples in fast magnetic resonance imaging (MRI) acquisition methods. As a consequence, spatial resolution is limited in functional MRI (fMRI), preventing the study of hemodynamic /neural processes at the sub-millimeter scale in humans. To overcome this limitation we propose to speed up MRI by using parallel imaging acquisition techniques and high performance readout gradient pulses. This novel data acquisition approach will allow fMRI with increased spatial resolution and promote highly innovative and exploratory research in physiology and medicine at BNL and elsewhere.

APPROACH:

Faster sampling rates are needed to increase spatial resolution in fMRI. Partially parallel imaging (PPA) with *receiver coil arrays* use combinations of simultaneously acquired signals from multiple surface coils with different spatial sensitivities to produce images with enhanced spatial resolution. Using phased arrays with 4-8 radio frequency (RF) coils and PPA acquisition/reconstruction methods, spatial resolution can be increased by a factor that ranges from 2 to 6. High spatial resolution can be achieved in fMRI by using *high performance gradient coils* that can deliver strong and fast-switching readout gradient fields, allowing the use of higher acquisition bandwidth. Commercially available gradient coils for head imaging produce gradient pulses of 75 mT/m with a rise time of 0.2 ms. Coils with higher gradient efficiency and lower inductance can produce gradient pulses with double the amplitude and one quarter the rise time at sub magnetic stimulation threshold levels and further speed up acquisition by a factor of 4.

Therefore, we aim to develop a hybrid system composed of a high performance gradient coil, and an 8-channel RF-coil array to collect functional images of the human brain with sub-millimeter resolution. The project involves the development of 1) a gradient coil 2) RF-coils, and 3) a parallel MRI-receiver to collect multiple signals from the coils, and 4) the system integration with the MRI instrument at BNL.

TECHNICAL PROGRESS AND RESULTS:

During FY05 we developed a high performance gradient coil and an 8-channel NMR digital receiver to acquire multiple MRI signals coming from RF-coil arrays, imaging reconstruction algorithms, and stimulation paradigms for fMRI. During FY06 we developed RF coils for parallel imaging and control software for the parallel NMR receiver. We did not integrate the new head gradient coil with our gradient system during FY06 because only recently DOE approved the exemption to allow workers to enter zones of higher magnetic fields than 2Tesla. This exemption will allow us to make the required electrical interconnections in the gradient system at 4Tesla magnetic field.

SPECIFIC ACCOMPLISHMENTS:

Publication:

1. **Tomasi D.** "Optimization of biplanar gradient coils for magnetic resonance imaging." Braz J Phys **36**: 23-27, 2006.

Proceedings:

1. Solís SE, et al. "6-slot surface coil for magnetic resonance imaging at 4 Tesla" IX Mexican Symposium on Medical Physics, Guadalajara, Mexico, 2006.
2. Solís SE,et al. "Slotted Surface Coil for Magnetic Resonance Imaging at 4T" ISMRM, Fourteen Annual Meeting, Seattle, WA, 2006.

LDRD FUNDING:

FY 2005	$109,920
FY 2006	$146,891

Novel Multi-Modality MRI and Transcranial Magnetic Stimulation to Study Brain Connectivity

Elisabeth de Castro Caparelli *05-070*

PURPOSE:

I propose to develop a revolutionary methodology integrating transcranial magnetic stimulation (TMS) and interleaved acquisition of functional magnetic resonance imaging (fMRI) and diffusion tensor imaging (DTI), using BNL's 4T MR scanner, so as to provide the unique windows on brain function and connectivity. TMS can, non-invasively and painlessly, transiently disrupt activity in focal brain regions. In addition, fMRI is a well established technique used to measure changes in blood oxygenation level dependent (BOLD) signals in brain regions, which reflects changes in neuronal activity; and DTI permits the visualization of the tracts or bundles of neuronal axons that connect different parts of the brain. Thus, with this novel combination of TMS and the multi-modality of MRI techniques, in a high magnetic field we will be able to answer fundamental questions relating to brain behavior and its anatomical basis, which will promote the conduct of highly innovative and exploratory research.

APPROACH:

Background: Boning et al. (2000) applied single-pulses of TMS over the motor cortex in healthy volunteers during fMRI studies in a 1.5T MRI scanner. They verified that interleaved TMS/fMRI can be used in averaged single-pulse trials, and BOLD responses to single-pulse TMS can be detected under the TMS coil.

Guye et al. (2003) combined fMRI and DTI, to explore primary motor cortex (M1) connectivity in the human brain. The results demonstrated strong connections from M1 to the pyramidal tracts, premotor areas, parietal cortices, thalamus, and cerebellum, showing that the combination of fMRI and DTI is a promising tool to study the structural basis of functional networks in the human brain in vivo. Aim: Integrate TMS and MRI technologies for the first time in a 4-T MRI scanner. Map brain activation produced by TMS-pulses, when applied over the motor cortex area using fMRI. Map structural connectivity within the TMS-activated neural networks using DTI. Method: TMS will be applied through a nonferromagnetic double cone coil (70-mm outer wing diameter), connected to a Magstim Rapid stimulator (The Magstim Company, Wales, UK). The fixation and placement of the TMS coil will be done using a custom-made adjustable coil holder that will attach to the MRI head coil. fMRI will be performed using EPI-GRE sequences and data analysis will be performed in SPM2. DTI will be acquired using an EPI-SE sequence and data analysis will be performed using the medical imaging display and analysis group (MIDAG) package.

Collaborators: D. Tomasi, Ph.D., G-J. Wang, M.D., F. Telang, M.D., D. Anschel, M.D. and W. Backus, M.D.

References:

Bohning D.E. et al., JMRI 2000; 11: 569
Guye M. et al., NeuroImage 2003;19:1349

TECHNICAL PROGRESS AND RESULTS:

During this first year the technical implementation of TMS inside the high field MRI scanner has been initiated with the acquisition of the brain stimulator, Magstim Rapid, model 220, and the coils and an MRI

compatible and standard, both 70 mm figure of eight TMS coils. Quality tests of both TMS coils and calibration have been performed with a pickup coil. An adjustable holder was made with wood to attach the TMS coil inside of the RF-coil and tested for safety using piezoelectric to detect coil vibration. Imaging artifacts has started to be explored for the combination of TMS/MRI. DTI and the technique has been incorporated in the 4 T MRI scanner including imaging acquisition and data post-processing. A new environmental safety review (ESR) was generated and approved. The protocol, which will use 20 human, adult, healthy volunteers, was also approved.

During the second year the TMS implementation was finalized including all tests and optimization needed using a phantom. The TMS/fMRI protocol has started, showing that the initial design for coils holder is inappropriate to reach the motor cortex area. For this reason the protocol has been renewed to explore different brain regions, which have not been explored before for the TMS/fMRI combination.

Finally, the renewed protocol has already started, where we are applying the TMS over the primary visual (PV) area; and the TMS-paradigm setup has been initiated. Initial results for a block design composed with three stimulus epochs of 30s, with TMS applied each 6s, and three resting epochs did not present significant brain activation; however, changing the TMS stimulus for each 4s has shown promising results. (see figure)

For the fiscal year FY07 we plan to validate the final TMS paradigm and perform data acquisition for about 20 subjects, finalizing and co-validating the technical developmental implementation of TMS in a high field MRI.

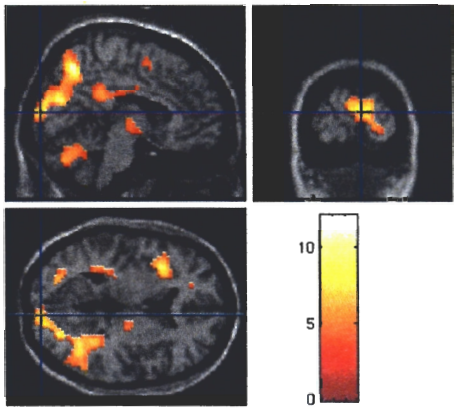

These results will, for the first time, reveal the combination of TMS and MRI techniques as a novel and effective tool to explore brain function/connectivity in other brain regions rather then the motor cortex area. The establishment of this novel/effective tool on the study of brain behavior will contribute to solving questions about brain function and anatomical connectivity changes associated with aging, disease and drug states.

SPECIFIC ACCOMPLISHMENTS:

1. **Caparelli, E.C.** "Can motion artifacts be completely removed from fMRI-activation maps?" Current Medical Imaging Review 1 (2005) 253-264
2. Foerster, B.U.; Tomasi, D.; and **Caparelli, E.C.** "Correction for Magnetic Field Shift Due To Mechanical Vibration in EPI Functional Imaging" Mag.Reson. in Medicine 54 (2005)1261–1267
3. **Caparelli, E.C.;** and Tomasi, D. "Low-pass filters can increase signal loss artifacts in EPI" Biomedical Signal processing & control (Submitted)

Grant applications

1. NIH, R21, PI: E.C. Caparelli, Pending.

LDRD FUNDING:

FY 2005	$105,571
FY 2006	$145,397
FY 2007 (budgeted)	$ 17,000

Ovarian Hormone Modulation of ICP: MRI Studies

Anat Biegon *05-071*

PURPOSE:

The objective of the work was to adopt and validate a non-invasive, MRI based technique for the measurement of intracranial pressure (ICP) and use this technique to study the possible effects of ambient hormonal environments on ICP in women. Current methods of measuring intracranial pressure are invasive and carry excessive risk, limiting their use to life-threatening situations. Therefore, development of a non-invasive technique was a prerequisite for attempting to answer a scientific question with immediate clinical implication, related to the increased vulnerability of pre-menopausal women to both idiopathic and head-injury induced intracranial hypertension. The new technique, founded on MRI technology and know-how available at BNL, may open the way to new programs centering on the role of intracranial pressure changes in a variety of diseases and conditions which could not be investigated with established technology.

APPROACH:

Increased pressure inside the brain is a dangerous and sometimes fatal phenomenon. Annually, over 1.5 million people in the United States alone suffer from neurological problems stemming from traumatic brain injuries, hydrocephalus, intracranial hemorrhages, tumors, and other disorders associated with abnormal intracranial pressure. At present, ICP measurement techniques are highly invasive, requiring insertion of a catheter tipped strain gauge or fluid filled catheter into the brain tissue or a cerebral ventricle. Insertion of these catheters damages the brain tissue and carries risks of intra cerebral bleeding and infection. The risk of infection increases with time, and there is a >27% incidence of infections associated with catheters left in place for 48 hours or more. A non invasive procedure will not only provide a substantial risk reduction and quality of life in the patient groups currently being monitored, it will also open a whole new field of research regarding the possible effect of demographic factors (age, sex, race, ethnic origin) on ICP and the correlation and possible causal relationship between transient, moderate increases in ICP and changes in normal brain function (e.g. mood and cognition) and non life threatening conditions which never the less affect quality of life, such as headache. An MRI (1.5T) based method developed by Alperin appears to have limitations which may be solved by using a higher field magnet such as the BNL 4T or SBU 3T MRI. In collaboration with MRI experts W. Rooney and M. Wagshul, we planned a series of phantom studies followed by optimization of hardware and software configurations to achieve stable and reliable MRI measurements of arterial, venous and CSF flow and calculation of ICP in human subjects.

Women are significantly more likely than men to develop idiopathic intracranial hypertension as well as head trauma induced intracranial hypertension. This is perhaps not surprising, considering that the ICP at any given time is determined by brain water content and fluid dynamics, and ovarian hormones are known to exert significant influence on water balance, including swelling and water retention, in target organs such as the uterus and breast, probably through effect of vasopressin secretion. We have also shown in the past that ovarian hormones have profound effect on brain activity of serotonin, a neurotransmitter involved in migraine, depression and cerebrovascular tone. Women are significantly more likely than men to suffer from headaches, migraine attacks, depression and exacerbations of multiple sclerosis are known to increase in frequency in the late phase of the normal menstrual cycle, when estrogen

and progesterone are declining from peak levels. We have recently found significant changes in water content in the brains of women across the normal menstrual cycle. Taken together, these observations suggest that fluctuating levels of ovarian hormones may result in ICP fluctuations, rendering women more vulnerable to developing intracranial hypertension during discrete phases of menstrual cycle.

In collaboration with Drs. M. Egnor, R. Tsabari and L. Ephraty we planned a study of the effects of ovarian hormones on ICP, involving the recruitment of pre-menopausal women at extreme phases of the menstrual cycle, as well as post menopausal women on and off hormone replacement therapy. Actual blood levels of estrogen, progesterone and LH, as well as verbal memory and mood, are measured on the same day as ICP measurement by MRI.

TECHNICAL PROGRESS AND RESULTS:

We conducted MRI flow phantom studies that simulate inflow and outflow at different flow velocities using the varian 4T magnet and coil. We were able to demonstrate a linear relationship between MRI measured phantom flow rate and calibrated linear flow rate. Optimized parameters that form the phantom studies were then examined in human subjects using a Philips Achieva 3T scanner and a volume neurovascular, head & neck coil. Prior to acquiring the flow images, MRI angiography was performed in order to select an appropriate slice, such that the carotid and vertebral arteries traverse perpendicular to the image plane. Both images were taken in approximately the same plane, at the level of C2. Subsequent to acquisition, DICOM format images were downloaded to a PC workstation to segment out the flow regions and determine net flow through the following regions: CSF subarachnoid space, two external carotid arteries, two vertebral arteries, and two jugular veins. Segmentation was based on pulsatility, which is a valid criterion for segmentation for this protocol, given that we are only interested in the pulsatile flow component for compliance and ICP measurement.

We started enrolling women into the clinical part of the study. At present, we have data from 8 (out of 10 planned) pre-menopausal women, 8/15 untreated post-menopausal women, 4/15 postmenopausal women on estrogen replacement and 3/15 women on estrogen + progesterone replacement. These women were tested for blood levels of hormones, verbal memory and affective and physiological symptoms related to ovarian hormone changes, as well as an MRI. This is the largest cohort of healthy women to undergo non-invasive measurement of ICP. Calculated ICP values for this population all fall within the normal range (3-15 mmHg) as determined by invasive means, suggesting that hormone effects, if present in healthy women, are not large enough to shift baseline ICP values in women to values higher than those recorded in healthy men. Continued enrollment (with continued GCRC support) is anticipated until the planned group size (enabling the assessment of hormonal environment) is achieved.

This project uses human subjects

SPECIFIC ACCOMPLISHMENTS:

None

LDRD FUNDING:

FY 2005	$107,120
FY 2006	$144,973

Feasibility of CZT for Next-Generation PET Performance

Paul Vaska *05-072*

PURPOSE:

We aim to demonstrate the feasibility of using cadmium zinc telluride (CZT) as a gamma-ray detector for medical imaging with positron emission tomography (PET). In particular, CZT provides the opportunity to achieve extremely high spatial resolution, a very important goal in PET because it will allow meaningful imaging of the mouse brain, which opens up access to all the powerful transgenic models available in this species. CZT has been discussed in this context for years and the quality and availability of CZT detectors has steadily improved, but a diverse team of detector and imaging scientists is required to overcome a number of technical obstacles. We have assembled such a team that is uniquely qualified to tackle these problems.

APPROACH:

CZT has great potential for PET because of its potentially high spatial resolution (1 mm or less, including in depth which is important to minimize parallax problems), high energy resolution (to reject scattered radiation), favorable geometry (no photosensor, compact), and insensitivity to magnetic fields (to permit simultaneous imaging with PET and MRI, currently a very hot topic in nuclear medicine). The main hurdles are poor timing (required to reject random coincidences) and relatively low stopping power at 511 keV. The high risk element of the project is how well we can mitigate these shortcomings.

Collaborators include for CZT detectors: Aleksey Bolotnikov, Giuseppe Camarda, Gabriela Carini, and Ralph James, for low-noise electronics: J.-F. Pratte and Paul O'Connor, and for imaging: Avraham Dilmanian, Sang-June Park, and Paul Vaska.

The general approach is to first develop methods to overcome the timing and sensitivity drawbacks of CZT using actual CZT devices, incorporate the optimized methods and measured detector performance into a realistic Monte Carlo simulation of a full PET system to estimate the ultimate performance of CZT for PET, and develop a prototype system for PET imaging.

TECHNICAL PROGRESS AND RESULTS:

After verifying that timing sufficient for PET can be achieved using relatively thick (1 cm) pixel detectors in FY05, we have proceeded to:

1) develop a Monte Carlo simulation of a full PET system to analyze CZT performance on a system level
2) conceive a novel approach for ultra-high resolution PET with CZT, and
3) complete the design and acquire enough detectors and electronics to build a full mouse brain imager

The first goal was to develop a Monte Carlo model of a full PET system. The GATE software package, based on GEANT4, was installed and used to simulate a CZT-based version of the popular Siemens microPET Focus 120 scanner which currently uses LSO scintillator crystals. The 2 systems were compared in simulation and some results are shown in Fig. 1. As expected, the spatial resolution was improved at the edges of the field-of-view where the LSO scanner suffers from the parallax effect, but the CZT system does not due to its depth-of-interaction (DOI) measurement capability. While this was meant to be a "fair"

comparison and so used equal-sized detector elements for the 2 systems, higher spatial resolution is far easier to achieve with CZT compared to LSO.

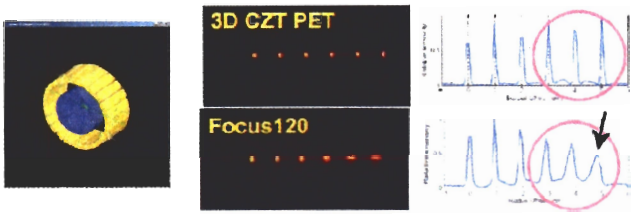

Figure 1. Scanner geometry (left), point-source images across FOV (middle), and profiles through images (right).

However, also as expected, overall sensitivity of the CZT system is much lower, although this can be compensated for by using a smaller system diameter (which increases solid angle and is made possible by its DOI capabilities), by using multiple layers of CZT, and by using Compton kinematic techniques to reject randoms and scatter backgrounds (which increases signal-to-noise and is enabled by the excellent energy resolution of CZT). Refinements of the model to account for these effects are underway.

The second goal is to design a full prototype PET system with ultra-high spatial resolution for mouse brain imaging. Recent work by Stickel & Cherry has shown that 0.5 mm PET resolution is possible based on general principles, but how to achieve it in a practical way has been elusive. We have conceived of a novel CZT detector geometry which can achieve this resolution in what is likely the most practical approach possible with CZT, minimizing the amount of detector processing and the number of electronic channels required.

We have proceeded to develop the appropriate detectors with eV Products and to acquire enough of them to build a full-ring prototype. The readout electronics is under development, and will be based on either the Instrumentation Division's MIOS system, or Nova R & D's RENA-3 ASIC. We have initiated and shepherded through a Non-Disclosure Agreement with Nova to facilitate our access to their technology.

In FY07, our ambitious goal is to complete the first full-ring prototype with our novel CZT PET architecture, and acquire preliminary PET images, which would demonstrate the extremely strong feasibility for this concept.

SPECIFIC ACCOMPLISHMENTS:

Proceedings:

1. Vaska, P.; Bolotnikov, A.E.; Carini, G.; Camarda, G.S.; Pratte, J.-F.; Dilmanian, F.A.; and James, R.B.: Studies of CZT for PET Applications. IEEE Nuclear Science Symposium and Medical Imaging Conference, Puerto Rico, Oct. 24-29, 2005 (poster presentation and proceeding).

2. Park, S.-J.; Bolotnikov, A.; Carini, G.; Camarda, G.; Pratte, J.-F.; James, R.; Dilmanian, F.; and Vaska, P: Investigation of a small animal PET using 3D position-sensitive CZT detectors with GATE simulation. 53rd Annual Meeting of the Society of Nuclear Medicine, San Diego, CA, June 3-7, 2006 (oral presentation and abstract).

3. Bolotnikov, A.E.; Camarda, G.S.; Carinic G.A.; Fiederle, M.; Li, L.; Wright, G.W.; and James, R.B.: Performance studies of CdZnTe detector by using a pulse shape analysis. SPIE Hard X-Ray and Gamma-Ray Detector Physics VII San Diego, CA, July 31 - August 4, 2005 (oral presentation and proceeding).

An Invention Disclosure has been filed on our unique detection approach.

LDRD FUNDING:

FY 2005	$111,425
FY 2006	$135,784
FY 2007 (budgeted)	$136,000

Biology on Massively Parallel Computers

James W. Davenport *05-074*
J. Glimm
D. Keyes
Y. Deng

PURPOSE:

Propose to develop new algorithmic approaches for computational biology on massively parallel computers. The aim is to make effective use of machines such as the 12,000 processor Quntumchromodynamics on a Chip (QCDOC) and the 131,000 processor BlueGene/L (BG/L) requiring a combination of algorithms and applications.

The algorithmic research includes the development of efficient molecular dynamics (MD) codes which take account of data non-locality and apply explicit routing protocols suitable for both QCDOC and BG/L.

The applications involve molecular dynamics simulations of several small proteins including the adenovirus protease studied structurally by Mangel and co-workers and Botulinum neurotoxin studied by Swaminathan and co-workers both at the NSLS.

APPROACH:

Molecular dynamics simulations require large amounts of computer time in addition to efficient algorithms. To deal with these a new MD code specifically adapted to QCDOC is being developed. The time limitations are usually due to the long range nature of the forces between atoms. These are evaluated by fast Fourier transforms (FFTs), which are known to be slow on massively parallel machines. Hence, an important component of this research is the development of communication routines for FFTs which is being carried out by Y. Deng and students at Stony Brook. Application to the proteins mentioned above uses the AMBER suite of codes. The adenovirus work is being performed at BNL, the Botulinum at Stony Brook.

TECHNICAL PROGRESS AND RESULTS:

A large number of simulations of the adenovirus proteinase have been completed and are being analyzed. All have used the AMBER code on both Linux clusters and the IBM p series at BNL. Different protonation states as well as explicit and implicit water simulations have been performed. A total of more than 50 nanoseconds of simulated time has been completed. In all these, large increases in the size of the catalytically active site have been observed which are consistent with the hypothesized activation process. Further comparisons with experimental data are underway.

The FFT code has been written and shows excellent scaling in tests on QCDOC up to 4096 processors. The new MD code has been written and is undergoing tests. More than 50 nanoseconds of simulated time have been completed for the botulinum. Changes in the structure of Botulinum have been studied as a function of pH. In these, simulations are being further analyzed and compared with experiments.

SPECIFIC ACCOMPLISHMENTS:

Publications:

X. Chen and Y. Deng, *Botulinum structures at various temperatures and pH values*, J. Mol. Modeling (Submitted).

G. Han, Y. Deng, and J. Glimm, and G. Martyna, *Error and timing analysis of symplectic multiple timestep integration methods for molecular dynamics.* J. Comp. Phys. 2006 (under review).

P. Rissland and Y. Deng, *Structure and performance of molecular dynamics package MDoC on QCDOC*, Parallel Computing, (Submitted)

Presentations:

J. W. Davenport, Computational Biology, Stony Brook – BNL Workshop, June 2006. J. W. Davenport, Y. Deng, L. Slatest, Computational Biology at BNL, SuperComputer 2005, Seattle, 2006, Tampa. (Poster)

P. Rissland and Y. Deng, *Electrostatic force computation on supercomputers with torus networks.* International Conference on Computational Science, Istanbul Turkey, June 2005.

LDRD FUNDING:

FY 2005	$168,787
FY 2006	$222,345
FY 2007 (budgeted)	$ 40,000

Ionic Liquids in Biocatalysis and Environmental Persistence

Arakiosamy J. Francis *05-078*
S.V. Malhotra
C. Zhang
H. Wang
C.J. Dodge

PURPOSE:

The overall goal of this project is to determine the application of ionic liquids (ILs) to industrial, agricultural and environmental remediation processes (i.e., to separate and remediate actinides in DOE wastes) leading to improved new green chemistry based methodologies as well as determine the persistence of ILs in the environment.

APPROACH:

We investigated (i) the interaction of uranium with N-ethylpyridinium tetrafluoroborate ($EtPyBF_4$), ethylpyridinium trifluoroacetate ($EtPyCF_3COO$), and 1-butyl-3-methylimidazolium hexafluorophosphate ($BMIMPF_6$); (ii) bioreduction of U in the presence of ILs, and (iii) biodegradation of the ILs.

TECHNICAL PROGRESS AND RESULTS:

Interactions of uranium with ionic liquids. The interaction of U with $[BMIM]^+[PF_6]^-$, $[EtPy]^+[CF_3COO]^-$ and $[EtPy]^+[BF_4]^-$ was investigated by UV-vis absorption spectrophotometry, potentiometric titration, electrospray ionization-mass spectrometry (ESI-MS), and x-ray absorption spectroscopy (XAS). Potentiometric titration and UV-vis absorbance of U with $[EtPy][BF_4]$, $[BMIM][PF_6]$, and $[EtPy][CF_3COO]$ showed complexation of U with $[EtPy][CF_3COO]$. ESI-MS (in both the positive and negative modes), and EXAFS analyses showed that $[EtPy][BF_4]$ and $[BMIM][PF_6]$ formed a monodentate complex with U, while a bidentate complex was formed with $[EtPy][CF_3COO]$. These results show the potential application of $[EtPy][BF_4]$, and $[EtPy][CF_3COO]$ to separate and recover uranium from waste stream.

Effect of ionic liquids on uranium biosorption by bacteria. The effects of $[EtPy][BF_4]$, $[EtPy][CF_3COO]$, and $[BMIM][PF_6]$, on uranium biosorption by *Clostridium* sp. were determined by batch experiments followed by transmission electron microscopy (TEM) and energy dispersive x-ray spectroscopy (EDS). In presence of ILs, most of U accumulated extracellularly. The amount of biosorbed U decreased in the presence of three ILs due to formation of U-BF_4, U-PF_6 and U-CF_3COO complexes having different affinities to cell surfaces. Stronger complexes showed less absorption. Biosorption of uranium decreased in the order of U > U+$[BMIMPF_6]$ (weak monodentate complex) > U+$[EtPy][BF_4]$ (strong monodentate complex) and U+$[EtPy][CF_3COO]$ (strong bidentate complex). Damages to cell membranes were also observed.

Biodegradation of ionic liquids. We investigated the biodegradation of $[BMIM]^+[PF_6]^-$, $[EtPy]^+[CF_3COO]^-$, and

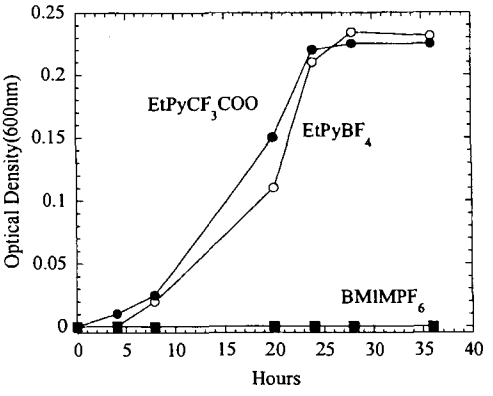

Figure 1. Growth of bacteria in ILs.

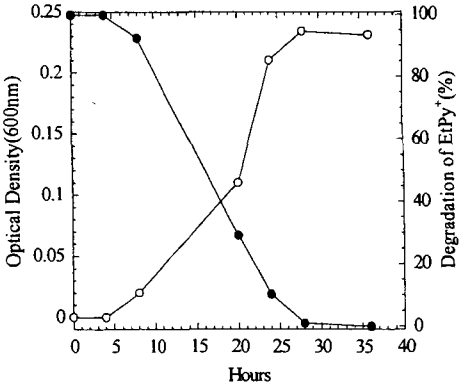

Figure 2. Biodegradation of N-ETPy ILs.

$[EtPy]^+[BF_4]^-$ by soil enrichment culture technique. Biodegradation of N-ethyl pyridinium-based ionic liquids $[EtPy]^+[CF_3COO]^-$ and $[EtPy]^+[BF_4]^-$ but not $[BMIM]^+[PF_6]^-$ as a sole carbon source by a bacterial culture was observed (Figures 1 and 2). Identification of the degradation products by ESI/MS revealed pyridine ring cleavage between C2-C3. The intermediate products identified were N-ethyl-(4-(carboxyamino) but-3-enoicacid semi-aldehyde and (4-(carboxyamino) but-3-enoic acid. The final products (acetic acid and glyoxylate) were confirmed by MS (Figure 3). This is the first report showing complete biodegradation of a N-substituted pyridinium compound, and thus provides fundamental information concerning the assessment of the environmental risks posed by those environmental friendly ionic liquids.

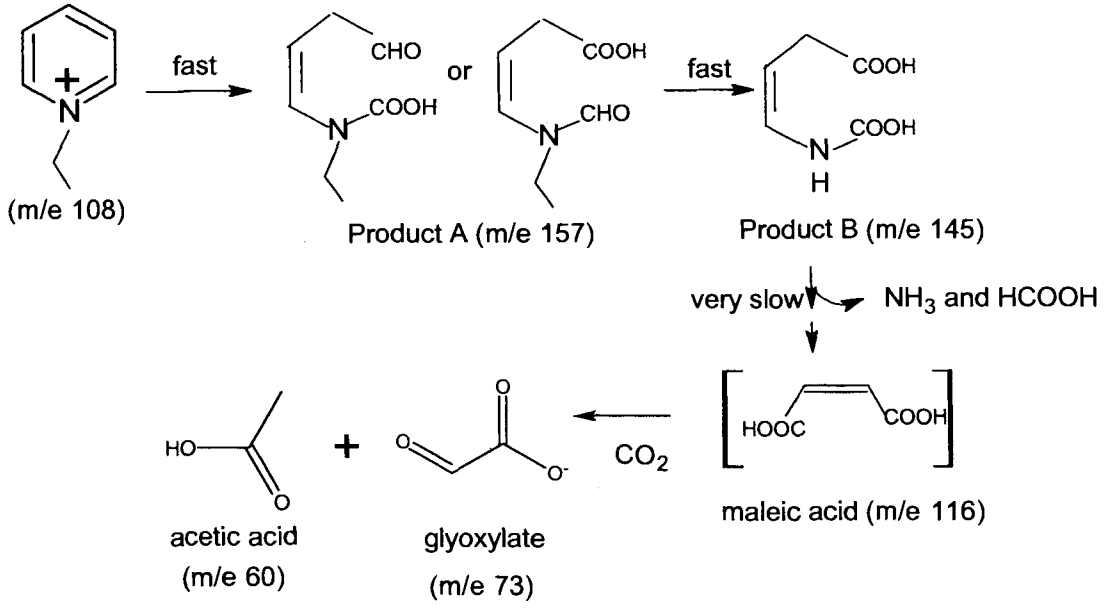

Figure 3. Proposed degradation pathway of N-Ethylpyridinium based ionic liquids.

Bioreduction of uranium by *Clostridium* sp in the presence of ionic liquids.

Bioreduction of U(VI) to U(IV) by an anaerobic bacterium *Clostridium* sp. was affected by the presence of ILs. The rate of reduction of U(VI) to U(IV) in the presence of $BMIMPF_6$ and $EtPyBF_4$ was similar to the reduction of uranyl nitrate (Figures 4 to 6). However, there were differences in the

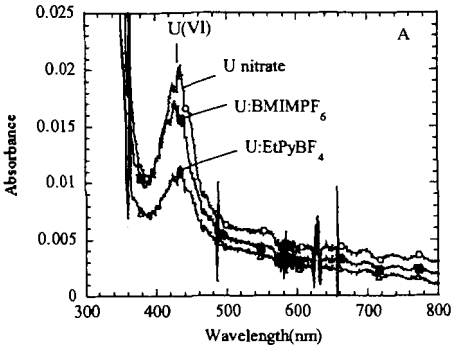

Figure 4. UV-vis spectra of U(VI) before bioreduction.

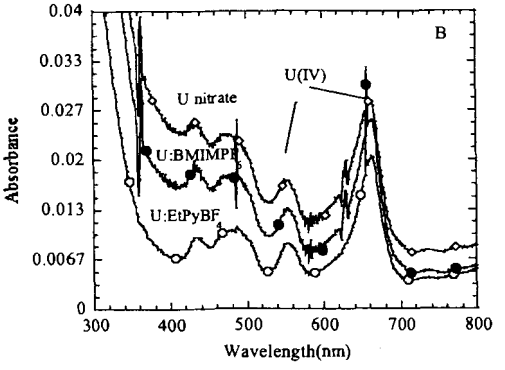

Figure 5. UV-vis spectra of U(IV) after bioreduction.

rate of precipitation of reduced uranium from solution: without ILs > $BMIMPF_6$ >$EtPyBF_4$. The extent of precipitation of bioreduced U(IV) from solution appears to be related to the nature of the complex formation with the IL. In contrast, the U(VI) complexed with $EtPyCF3COO^-$ was not reduced by the bacterium. These results suggest the potential application of ILs in conjunction with microbiological action to

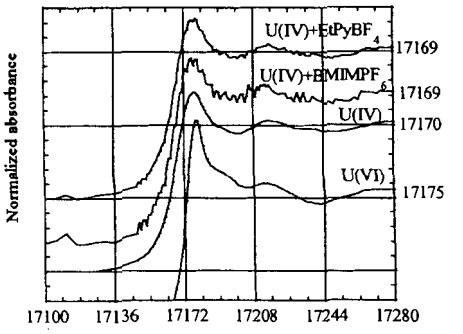

Figure 6. XANES spectra of U(VI) and U(IV) before and after bioreduction.

separate and recover redox sensitive actinides from solution.

SPECIFIC ACCOMPLISHMENTS:

Presentations

1. Malhotra, S.V.; A.J. Francis, C. Zhang. Biocatalysis in ionic liquids for environmental application. Paper presented at 24th Rare Earth Research Conference, Colorado, June, 2005.
2. Zhang, C.; S.V. Malhotra, A.J. Francis. Interaction of ionic liquids with uranium and its implication on bioreduction. Paper presented at 230th ACS national meeting, Washington D.C., August 2005.
3. Zhang, C.; S.V. Malhotra, A.J. Francis. Effects of ionic liquids on uranium bioreduction. Paper presented at Pacifichem 2005 International Chemical Congress of Pacific Basin Societies, Honolulu, Hawaii, December 15-20, 2005.
4. Malhotra, S.V.; C. Zhang, Francis, A.J. Biocatalysis of uranium in presence of ionic liquids. 10th Annual Green Chemistry and Engineering Conference June 26-30, 2006, Washington DC.

LDRD FUNDING:

FY 2005	$ 99,464
FY 2006	$120,049

Single Particle Laser Ablation Time-of-Flight Mass Spectrometer (SPLAT-MS) Enhancements: Aerosol Optical Properties and Increased Particle Detectivity

Gunnar Senum *05-082*

PURPOSE:

SPLAT-MS is an aerosol mass spectrometer designed and assembled by BNL. This was loaned to PNNL for about two years and has been returned to BNL. The purpose of this program is to reassemble SPLAT at BNL and examine several enhancements that could be applied to SPLAT to improve its value as a laboratory and field instrument in the DOE Atmospheric Science Program (ASP). These include measuring the aerosol Mie scattering pattern with increased spatial resolution to possibly determine aerosol refractive index, absorbivity and asphericity.

The second enhancement is the improvement in the laser timing algorithms which controls the firing of the ablation laser. This would extend the aerosol particle sampling diameter range.

APPROACH:

Before SPLAT-MS was loaned to PNNL, I worked with the designers of SPLAT on this instrument. I participated in both laboratory and a field experiment with SPLAT during which SPLAT was disassembled and reassembled several times. During this period, I performed many aerosol characterization experiments on SPLAT, allowing me to become quite familiar with its operation and the theory behind the instrument. Similarly, I noticed some of the deficiencies in the present design of SPLAT, which has led to this LDRD, which will either improve or explore the feasibility of enhancements to remove the timing deficiency and to explore the feasibility of enhanced spatial resolution of the Mie scattering patterns from the first timing laser. The approach will be to use my expertise in previous reassemblies to reassemble SPLAT, and to use my expertise in electronics, computer programming, and instrumentation to examine the feasibility of these enhancements. I am also making use of the expertise in the Atmospheric Science Division, particularly, Art Sedlacek.

TECHNICAL PROGRESS AND RESULTS:

SPLAT was received in late FY2005 (May 2005) from PNNL in a highly disassembled form, that is, completely broken down into component parts. Work started in September 2005. In that month, essentially only the inventory of SPLAT was performed along with recovery of software from the SPLAT computer.

Progress in FY2006:

- SPLAT was required to meet the newer laser safety rules, consequently a new support with laser safety curtains were installed around SPLAT.
- Three of the four Varian Scroll roughing vacuum pumps were rebuilt.
- The electrical connections to the Time-of–flight mass spectrometer were rebuilt.
- The aerodynamic lenses, which transports aerosol particles from the ambient into the vacuum system and focused them into a tight beam were also rebuilt.
- The vacuum integrity of SPLAT was restored by repairing 3 leaks and the instrument was able to pump down

below 5 x 10^{-8} torr meeting its vacuum requirement.

- The aerosol and laser optical paths were aligned.
- The SPLAT computer program, which analyzes the scattered light from the timing lasers was recovered, however only as Visual C code. The executables could not run. It was discovered that certain WinDriver drivers had to be installed. The SPLAT data acquisition program was then operational. With the timing lasers, I was able to detect aerosol particles on the first timing lasers at about 10 percent of the counts that I had previously measured using the electronic counters. Alignment of the second laser, unfortunately, has required the reopening of SPLAT to manually adjust the laser alignment position; nonetheless, it is expected that SPLAT will be operational.

The feasibility of deriving additional aerosol particles properties, such as refractive index, absortivity and asphericity has been examined with the Mie scattering code. The back scattering is most sensitive to refractive index, whereas, absorptivity tends to smooth the Mie resonances. The three additional variables, beside particles size, add a complexity to the scattering that could not be viably determined on a 4 x 4 PMT array as originally proposed with the requirement of fast ns response. Nonetheless, optical technology is rapidly developing and if 16 X 16 arrays with fast response become available, then this is viable.

The improved timing algorithm is totally viable and will be implemented, especially now that the C code is available and I am able to reprogram this to include any nonlinear corrections which will be uncovered.

SPECIFIC ACCOMPLISHMENTS:

None

LDRD FUNDING:

FY 2005	$ 97,705
FY 2006	$132,696

Transition Metals in Oil and Gas Exploration

Appathurai Vairavamurthy *05-088*

PURPOSE:

The overall purpose was to conduct exploratory research in petroleum geochemistry, focused on improving our knowledge of the science and technology for recovering and utilizing petroleum (natural gas and oil), primarily based on analytical capabilities at BNL's National Synchrotron Light Source. The specific objectives were to enhance fundamental understanding of the science of gas and oil exploration and exploitation, building on our expertise on x-ray absorption spectroscopy,

APPROACH:

The primary goal was to better understand the significance of transition-metal catalysis in generating natural gas in sediments. Conventionally, the generation of gas from oil was thought to be thermally induced. But, some giant gas deposits occur in shallow low-temperature reservoirs suggesting catalysis could be involved. Based on laboratory experiments, it was proposed that zero-valent-transition metals, particularly nickel, catalyze this conversion. Thus, our goals were (1) verify the occurrence of Ni(0) in late diagenetic sediments using x-ray spectroscopy, and (2) examine the potential mechanisms of Ni(0) formation under conditions appertaining to deep sediments.

A second research area focused on improving the science of heavy oils and tar sands. The presence of macromolecular polar compounds containing sulfur and nitrogen is a major hindrance to economically recovering heavy oils. The geochemistry of this polar fraction is poorly known because of problems in analyzing complex molecules. Thus, an important aim of this research was to use the non-destructive XANES spectroscopy to shed new light on the composition of sulfur compounds in heavy oils and tar sands.

Ni Speciation in Sediments

To explore the significance of Ni(0) in gas generation, we examined the speciation of nickel in two well-known petroleum source/reservoir rocks where catalytic conditions for natural gas formation could prevail: (1) the Miocene Monterey Formation, California, U.S.A., and (2) the Kimmeridge Clay Formation, Dorset, England (main source rocks of the North Sea oil). Using synchrotron -radiation based x-ray absorption spectroscopy, we probed the chemical state of nickel non-destructively. The shale samples were obtained through collaboration from the United States Geological Survey (USGS).

The K-edge x-ray absorption spectra of nickel were collected in the fluorescence mode at the X-18B beamline, NSLS, using a Si(111) channel-cut monochromator. The EXAFS were analyzed using the IFEFFIT software package involving standard procedures. To establish the spectroscopic behavior of different types of nickel-containing bonds and molecules, we also collected spectra from several model compounds.

Mechanistic Studies on Ni Transformation

These experiments tested the hypothesis that zero-valent nickel could have been formed from the reduction of Ni(II) by reduced organic sulfur compounds in the sediments.

Our approach was to react Ni(II) with various reduced organic sulfur compounds at temperatures relevant to sediments (closed system, 150-250 ^{0}C), and to monitor changes in the chemical speciation of the metal and sulfur using XANES and EXAFS spectroscopies.

TECHNICAL PROGRESS AND RESULTS:

EXAFS Analysis of Nickel Speciation in Shales

X-ray absorption spectroscopy did not reveal any elemental nickel in the sediment samples, but rather, showed it existed predominantly as Ni(II). Oxygen appeared to be the main ligand in the first coordination shell, although sulfur also constituted a significant fraction in the organic-rich sediments from the Monterey Formation, probably as nickel sulfide. While our results did not directly support the hypothesis that zero-valent nickel was the active catalyst for generating natural gas in sediments, they did not entirely rule out the possibility that it could be involved. Indeed, a different form of nickel, or a different transition-metal species, other than zero-valent nickel, might catalyze the generation of natural gas in sediments.

Mechanistic Studies

Heating a mixture of a reduced sulfur compound, for example, cysteine, and Ni(II) (nickel chloride) in the presence of water around 225C in a closed reactor led to the copious production of gas as evidenced by the buildup of intense pressure. XANES analysis of the residue revealed that Ni(II) was converted to nickel sulfide (NiS). The gas was shown to be mainly hydrogen and carbon dioxide (>90%), along with small amounts of low-molecular-weight hydro-carbons. Our inference is that the reaction of reduced sulfur with Ni(II) generated a catalytically active form of NiS that transformed the organic molecule into hydrogen, carbon dioxide and pyrobitumen.

Speciation of sulfur in heavy oils

We studied sulfur XANES spectra from several heavy oils and tar sands from the Western Canada Sedimentary Basin. The dominant sulfur forms were thiophenes and sulfides that accounted for more than 70% of the total sulfur in most oils.

An important factor affecting the ratio of thiophene-to-sulfide is the thermal history of non-biodegraded oils. However, most heavy oils are biodegraded. In laboratory studies using model compounds, sulfides were found to be degraded more easily than thiophenes. Thus, biodegradation is expected to alter sulfur composition post-thermally. However, surprisingly, our results based on a series of biodegraded and non-biodegraded oils, revealed that the thiophene-to-sulfide ratio was unaffected by degradation. These results implied that the thiohene-to-sulfide ratio could be used as an important tool for studying the thermal history of heavy oils.

SPECIFIC ACCOMPLISHMENTS:

Submitted a proposal titled "Speciation of Sulfur and Nitrogen in Heavy Oils" to the Office of Fossil Energy, U.S. Department of Energy in March 2005. The Program could not consider this proposal for funding at that time.

LDRD FUNDING:

FY 2005	$128,489
FY 2006	$163,631

An Innovative Infiltrated Kernel Nuclear Fuel for High-Efficiency Hydrogen Production with Nuclear Power Plants

Jacopo Saccheri *05-092*
B. Bowerman

PURPOSE:

This project aimed at demonstrating the feasibility of a new manufacturing process for an innovative nuclear fuel, the Infiltrated Kernel Nuclear Fuel (IKNF), for thermo-chemical hydrogen production with nuclear plants at superior efficiencies. Within this project, IKNF samples have been fabricated and characterized at the Brookhaven National Laboratory (BNL).

It is believed that the IKNF process will be less expensive, more robust, and more suitable for on-line quality monitoring than the current sol-gel fabrication technique (graphite infiltration involves a few, easily measurable and controllable variables, it is reproducible and predictable).

APPROACH:

The technology on which IKNF is based upon was developed in the late '80s at BNL for the Space Nuclear Thermal Propulsion program (SNTP). Based on those experiments, the IKNF production process has been designed. A specific laboratory has been set up at BNL and several IKNF samples have been fabricated. Finally, the samples have been characterized through experiments at the BNL NSLS.

The fabrication process consisted of four steps:

1. *Uranyl Nitrate Infiltration.* Uranyl nitrate, $UO_2(NO_3)_2$, is dissolved in methyl alcohol and infiltrated into nuclear grade graphite. After infiltration, the alcohol is removed by vacuum drying.
2. *Uranyl Nitrate Conversion to Uranium Oxide.* The infiltrated graphite is heated to about 300°C for 30 minutes to convert $UO_2(NO_3)_2$ to UO_2.
3. *Uranium Oxide Conversion to Uranium Carbide.* The infiltrated graphite is further heated to convert the uranium oxide (UO_X) molecules into uranium carbide (UC_2). During this chemical conversion, CO_X gases (mainly CO) are also released, which further increases the porosity of the graphite matrix. The conversion is believed to start at approximately 900°C and be promoted by a continuous increase in temperature.
4. *Uranium Carbide Melting and Kernel Formation.* The graphite is further heated to above the melting temperature of UC_2 (2800°C). At this step, any remaining uranium oxide will also be converted into uranium carbide. The molten UC_2 is drawn inside the graphite by capillary action to form the inner fuel kernel. The outer surface of the graphite is relatively clean for subsequent coating processes.

The IKNF samples have been fabricated at BNL using surrogate material (natural uranium). The fabrication process would not have been possible without the collaboration of Jay Adams and Laurence Milian, from the Environmental Sciences Department at BNL. Lynne Ecker, from the Energy Sciences & Technology Department at BNL, has also been part of the team and a key contributor to the development of this project since its inception. Likewise, Hans Ludewig, from the Energy Sciences & Technology Department at BNL, provided support and considerable contribution during the whole project. Last but not least, the work benefited from the valuable

contribution of James Ablett, from the NSLS at BNL, whose help was essential in order to characterize the IKNF samples.

TECHNICAL PROGRESS AND RESULTS:

Overall, results were not exactly as expected and characterization of the material was more difficult than anticipated. However, we believe that designing the IKNF process, implementing it and successfully fabricating nuclear fuel at BNL was a major accomplishment.

Technical Progress:

In the previous fiscal year, FY 2005, the experimental apparatuses necessary for step 1 of the fabrications process (uranyl nitrate infiltration), step 2 (Uranyl Nitrate Conversion to Uranium Oxide), and step 3 (Uranium Oxide Conversion to Uranium Carbide) were set up. Some preliminary fuel samples were fabricated (steps 1 through 3 only). In FY 2006, the following accomplishments were achieved:

- The high temperature induction furnace needed to perform step 4 of the fabrication process was assembled and set up.
- The entire fabrication process (steps 1 through 4) was tested and several IKNF samples were fabricated (see below for a discussion of unexpected issues encountered with the high temperature furnace).
- A number of experiments were performed at the NSLS using the X-ray Absorption Near Edge Spectroscopy (XANES) technique to characterize (1) the distribution of uranium within the samples, and (2) the oxidation state of uranium to determine which uranium compounds were present.
- More experiments were also conducted at the NSLS using a different technique (Infrared Microspectroscopy) to distinguish between the uranium compounds present within the samples (UC_X and UO_2). Unfortunately, this technique did not provide better results than those obtained with XANES.

Results:

Figure 1 and Figure 2 show two representative results from the measurements performed at the NSLS with the XANES technique. They are for samples that underwent the high temperature treatment for about 30 minutes. Initially, the samples were supposed to be kept in the high temperature furnace for a couple of hours, but after 30 minutes they began cracking and breaking on the surface, compromising the integrity of the surface; thus they had to be removed after ½ hour. Sample 2-M (in Figure 1) had a lower initial concentration of uranium than sample 2-T (Figure 2) however; both figures show that the highest concentration of uranium is not at the center. Therefore, uranium did not wick inside as expected and did not create the uranium kernel surrounded by a relatively pure graphite structure. After in-depth analysis of the fabrication process, the following two reasons seem to be the most relevant for the unexpected results:

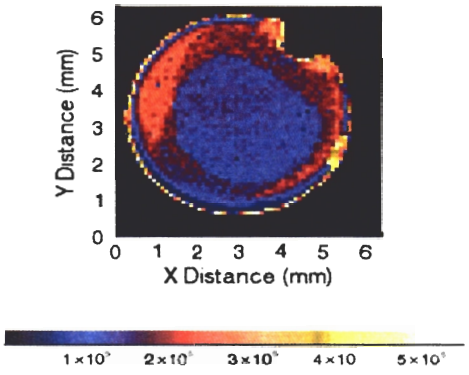

Figure 1 –Uranium map of a cross section of a IKNF rod after 30 minutes of high temperature treatment (IKNF sample 2-M).

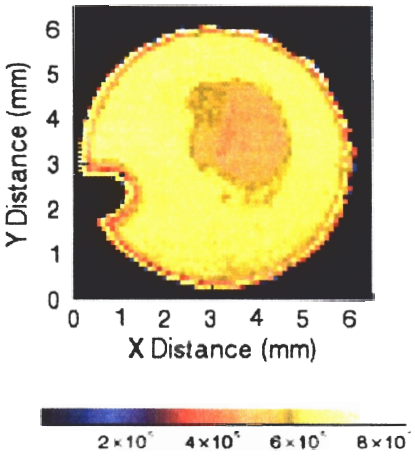

Figure 2 – Uranium map of a cross section of a IKNF rod after 30 minutes of high temperature treatment (IKNF sample 2-T).

1. The high temperature treatment is really key in the process since uranium must liquefy (i.e. go beyond its melting temperature of about 2800°C) in order to wick into the sample. Due to limitations in our high temperature furnace, we could not go beyond ~2900°C (reached on the external surface) and due to the unexpected embrittlement of the samples, we could not hold them inside the furnace for more than ½ hour. Both these effects might have prevented the uranium from totally liquefying and moving towards the center of the samples.
2. Our samples had a diameter (~ ¼ of an inch) more than ten times larger than that of the samples used in the previous experiments for the SNTP program (~ 450 micron). Therefore, an even longer time in the high temperature furnace or a slightly different approach applied to foster the wicking of uranium inside the sample, might be required.

Efforts to distinguish between UC_X and UO_2 with the XANES technique showed that more work is needed and a finer resolution must be achieved through the use of standards (i.e. reference UC_X and UO_2 samples) specifically created and calibrated to our samples (e.g. such to match our samples' form, size, density etc.). More extensive numerical analysis of the collected data from the NSLS will also be needed in order to pin point the beginning of the absorption edge of UC_X vs. the one of UO_2.

As an example, Figure 3 shows the XANES of 27 measurements throughout one sample combined together in one plot. Some of the uranium is expected to be in carbide form and some in oxide form, but the absorption edge position (at the middle of the rising portion of the curve) seems to be the same for all. More detailed analysis of normalized peaks and energy levels beyond 17200 eV might provide more useful information in discerning between the two forms, but it would require a very lengthy and specific analysis of all the data, from all the samples (which of course are not the same, do not have exactly the same heat treatment and initial concentrations of uranium and will display a statistical distribution of uranium distributions and uranium conversions).

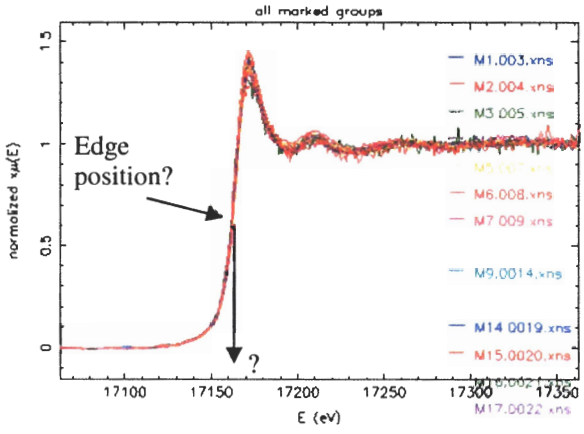

Figure 3 – 27 XANES scans from one sample, plotted together.

SPECIFIC ACCOMPLISHMENTS:

Presentations

- L. Blake, L. Ecker, J. Saccheri, B. Bowerman, and H Ludewig; "Weight Gain Predictions for Infiltrated Kernel Nuclear Fuel." Murdock Conference, Nampa, Id. Nov 11, 2005.

Proposals

- L. Ecker et al., BNL White Paper to DOE – "An Infiltration Manufacturing Process for Nuclear Fuels," 2006
- L. Ecker et al., Letter of Intent with Columbia University "Graphite Infiltration Techniques for Nuclear Fuel Fabrication and Long-Term Storage of Fission Products Following Aqueous Separation of Spent Nuclear Fuel." (submitted for NERI) 2006.

LDRD FUNDING:

FY 2005	$130,393
FY 2006	$172,648

Development of Green Processes: Catalytic Hydrogenation in Water Utilizing *In Situ* Biologically Produced Hydrogen

Devinder Mahajan *05-094*
D. van der Lelie

PURPOSE:

Hydrogenation reactions, vital to the manufacture of numerous products, require fossil fuel-derived H_2, an organic solvent, high pressures, high temperatures, and stirring for efficient gas/liquid/solid mixing to attain fast reaction rates. Green Chemistry is a sensible approach to develop the next generation processes to achieve sustainable development. A challenge is to develop hydrogenation reactions that operate in an aqueous phase using H_2 produced from a renewable source.

APPROACH:

Our integrated approach (BIO/CHEM) combines biological H_2 production with hydrogenation process using a homogeneous transition metal catalyst in an aqueous phase. For proof-of-concept, a renewable H_2 production source and a water-soluble catalyst/olefin system is selected. *Thermotoga neapolitana*, a thermophilic bacterium of the order *Thermotogales* that is able to produce clean (CO-free) H_2 gas from a variety of carbon sources under a broad range of physiological conditions is selected. H_2 produced *in situ* is readily available for subsequent hydrogenation of an olefin with a catalyst dissolved in the same aqueous solution.

TECHNICAL PROGRESS AND RESULTS:

Previous work involved a set of baseline H_2 production runs with *Thermotoga neapolitana* extremophile. The cultures were grown in a 1977 ATC medium, of which 1 mL was transferred to a 160 mL glass bottle (110 mL medium, 50 mL head space) that was incubated at 70°C and ambient atmosphere and H_2 evolution was monitored as a function of time. In parallel, in order to develop a catalytic system that was effective for olefin hydrogenation in an aqueous phase, various rhodium-based catalysts (rhodium is known to be an efficient hydrogenation catalyst) were evaluated for hydrogenation of itaconic acid. Since $RhCl_3.3H_2O$/TPPTS yielded the fastest reaction rate, this system was selected for further evaluation.

In FY 2006, the work concentrated on understanding the role of O_2 in the bio H_2 production cycle. The cloning and expression of *T. neapolitana* hydrogenase genes in *E. coli* was carried out. All 3 subunits were successfully identified, cloned and expressed in *E. coli*. The major catalytic subunit that produces H_2- the Hyd A subunit- showed low activity when expressed in *E. coli* using maturation proteins from *Clostridium*. Therefore, heterogeneous co-expression of TN HydEFG maturation proteins in *E. coli* was started. For a functional hydrogenase complex, 6 proteins have to be expressed simultaneously. In another set of experiments, the O_2 exposure of the *T. neapolitana* hydrogenase versus H_2 activity was monitored. In the cell-free extract preparations, the cells lost their integrity but the hydrogenase remained relatively insensitive to O_2, indicating that the observed O_2 tolerance is an intrinsic property of the hydrogenase and not the

result of a local shielding against O_2 in the cells. After a semi-purification via gel filtration under strong reducing conditions it was found that the native enzyme complex became more active but at the same time more sensitive to O_2. It was concluded that the enzyme can exist in two redox stages, and the procedure (purification, reduction) made the active center more accessible for hydrogenation but also made it more O_2 sensitive.

Experiments to demonstrate a catalytic cycle that involved utilization of bio produced H_2 were conducted. First, a baseline run in which *T. neapolitana* was grown under high pressure without an olefin substrate showed H_2 production but the yield was lower by a factor of 8 compared to that at ambient pressure, likely due to contamination of the stainless steel reaction vessel used. The ultimate task to catalytically hydrogenate substrates using bio H_2 in aqueous solutions involved itaconic acid hydrogenation with the Rh-TPPTS catalyst (Table 1). The maximum concentration of IA used was 77 mM at which the substarte was not toxic to bacteria. The H_2 produced by bacteria after 60h in the pressure vessel was 4.8% that reduced to 2.2% indicating hydrogenation reaction. The hydrogenation in the BIO/ CHEM coupled system was demonstrated.

Solvent	Initial H_2, %	Initial [IA]mM	P kPa	Final H_2, %
H_2O	20.6	500	5500	3.6
H_2O	5.0	500	5500	0.3
Media (No T.Nea)	6.7	500	5500	2.2
Media + T.Nea	0*	77 **	2300	2.2

(Catalyst- $RhCl_3.3H_2O$: 3mM; Ligand: TPPTS = 10 mM; Solvent: 100 mL; Substrate: IA (Itaconic Acid); Gas: H_2 in N_2; T: 70°C; Reactor vol: 300 mL).
*No inital H_2 was added.

**Maximum IA added (see text)

The data shown are consistent with our objective of developing a BIO/CHEM coupled system (Green Process) consisting of aqueous phase/extremophiles/ catalyst/ media.

SPECIFIC ACCOMPLISHMENTS:

Presentations

D. Mahajan, K. Ro, and B. Anton. Opening Remarks. Symposium on Clean Fuels from Biomass and Wastes. 232nd ACS National Meeting, San Francisco, CA, September 10-14, 2006.

D. Van-der Lelie, M. Anjom, S. Taghavi and D. Mahajan. Microorganisms Mediated Hydrogen from Biomass: Scale-up Issues for Farm-based Economical Production. Symposium on Clean Fuels from Biomass and Wastes. 232nd ACS National Meeting, San Francisco, CA, September 10-14, 2006.

D. Mahajan. Role of Fuels R&D in Sustainable Development. Technical Approach to Sustainable Development. Sponsor: ACS Committee on Environmental Improvement, ACS Committee on Energy Policy Issues, Fall 2006 American Chemical Society Meeting, San Francisco, CA, September 9, 2006.

D. Mahajan. Developing Decarb Energy Carriers: A Transition to Hydrogen Economy. Sponsor: School of Chemical and Biomedical Engineering. Cornell University, New York, August 10, 2006.

D. Mahajan. Livestock Waste for Energy Production Symposium: Advances and Potential. Soil and Water Conservation Society, 2006 Annual Conference, Keystone, Colorado. July 25, 2006.

D. Mahajan. Developing Decarb Energy Carriers: A Transition to Hydrogen Economy. Sponsors: Earth & Environmental Engineering and Chemical Engineering Departments, Columbia University Colloquium, New York, February 27, 2006.

D. Mahajan. Advanced Fuels and the Role of Catalysis. Queens College (CUNY) Colloquium, New York. February 6, 2006.

D. Mahajan. "Processing Biomass and Farm Waste in Clean Fuel Factories: The BioCat/ChemCat Approach," U.S. Dept. of Agriculture Annual Workshop, Florence, South Carolina. November 16, 2005. [Keynote Lecture].

S. Taghavi, M. Anjom, C. Garafola, B. Greenberg, P. King, D. Mahajan, D. van der Lelie. Oxygen tolerance of hydrogen production by Thermotoga neapolitana. Presented at the 106th General Meeting of the American Society for Microbiology, May 21-25, 2006, Orlando, Florida.

LDRD FUNDING:

FY 2005	$274,561
FY 2006	$358,800

Fast Neutron Imaging Detector

Charles Finfrock *05-098*

PURPOSE:

The project will demonstrate feasibility of a directionally sensitive detector for fast neutrons that has practical detection sensitivity at ranges sufficient to search large areas for improvised nuclear explosive devices (IND) or nuclear materials that could be used to manufacture INDs. The neutron sensitive medium is a polymer emulsion containing microscopic drops of superheated Freon. Neutrons striking the medium release the stored chemical energy to form a macroscopic bubble in the polymeric medium of the detector plane. Since fast neutrons cannot be easily focused, the coded-aperture technique will be used to encode the directionality to the source as a spatially varying pattern in the planar bubble medium. The coded-aperture is a redundant array of open areas and blocks made of neutron thermalizing and absorbing materials that cast a pattern on the detector plane. The bubble pattern in the detector plane will be recorded for analysis by illumination with visible light and photographing with a digital camera or if necessary by other means. The pattern of varying optical intensity due to the bubbles will be digitized and deconvolved to recreate the image of the neutron source and the direction to its location. To spatially modulate a flux of fast neutrons, the coded aperture must be rather thick, compared to coded apertures for thermal neutrons made of cadmium metal. The pixel size and corresponding image will be somewhat coarse. Nevertheless, the directional information about source location should be superior to that provided by currently available neutron detectors consisting of large slabs of polyethylene with imbedded ^{3}He tubes. Pressurizing the bubble medium to collapse the bubbles and re-liquefy the Freon regenerates the bubble medium for reuse. Design of sufficiently thin mask elements to efficiently attenuate fast neutrons is a key element of the project. When produced in large quantities, the Superheated-emulsion (SHE) medium is expected to be significantly less expensive than electronic detectors for fast neutrons. When feasibility of this novel application of SHE technology has been demonstrated, the project should be of interest to DOE, DHS, and collaborating international partners who would support development of a full-scale prototype and its commercialization.

APPROACH:

SHE technology is available commercially, most commonly as pencil-shaped personal neutron dosimeters and is used in various configurations and combinations for neutron spectroscopy. In a previous LDRD project E. Kaplan, J. Lemley, and T. Tsang developed electronic readout technology that would enable neutron bubble dosimeters to be deployed in counterterrorism applications such as instrumentation of multi-mode shipping containers for detection of neutron-emitting materials during transit.

In other work at BNL, P. Vanier, et al., developed a coded-aperture imaging detector for thermal neutrons. The fission neutron spectrum of weapons-usable materials (e.g., plutonium) contains more fast neutrons than thermal neutrons. Since fast neutrons are more penetrating than thermal neutrons, they can potentially be detected at greater distances. Since SHE are sensitive only to fast neutrons and can be manufactured in a planar array, development of an imaging detector for fast neutrons seemed feasible.

Materials to attenuate fast neutrons are being investigated both experimentally and through Monte Carlo calculations. Superheated emulsions in the form of disks have been acquired from BTI.

TECHNICAL PROGRESS AND RESULTS:

The FY 2006 effort was focused on demonstrating experimentally that fast neutrons can generate a useful pattern of coded-aperture components in a detector plane consisting of the bubble medium. Image recording by simple photographic techniques was employed. Manipulation and performance of the SHE detector material required considerable effort to resolve. The form of the sensor elements used in this investigation was a gelatinous material in which the superheated Freon was dispersed. The material was contained in Petri dishes with a diameter of 9 cm. A series of neutron exposures was conducted to characterize the SHE material. These exposures demonstrated that the material exhibited significant variations in neutron sensitivity. Variations in sensitivity as determined by bubbles formed for a given neutron flux varied between disks by as much as a factor of two. Variation in bubble uniformity within a disk was also observed, with some disks having definite areas in which there was little or no neutron sensitivity. Handling requirements for the gels dictate that they be kept immersed in mineral oil and maintained under pressure except when being actively used. The method used to achieve this was to stack the dishes in a pressure vessel filled with oil and apply a cover pressure with nitrogen gas. There was concern that the Freon component in the gels was migrating out of the gels as they aged and accumulated time out of the pressure vessel. This would manifest itself as a reduction in sensitivity over time. Neutron exposures of the SHE gels were made with portions of the gels masked by various thicknesses of polyethylene moderator to verify Monte Carlo calculations performed to predict the appropriate moderator thickness to use in the coded aperture mask. These measurements confirmed the ability of 5cm of polyethylene to reduce the fast-neutron-induced bubble formation by a factor of two, as predicted by the Monte Carol calculations. Ultimately, it was found that for our method of visualization, 10cm of polyethylene provided better images. A primitive coded aperture mask was constructed, and an array of gel disks was used to form an image plane. A series of point-source neutron irradiations were performed on the assembly with various source-to-detector orientations. For every test, a unique visual signal was observed and could be geometrically projected back to the point of origin of the neutron source.

SPECIFIC ACCOMPLISHMENTS:

A Record of Invention for the fast-neutron imaging detector based on SHE technology was filed with the BNL Intellectual Property Office in September 2004 when LDRD funding for FY 2005 was received.

LDRD FUNDING:

FY 2005	$124,052
FY 2006	$190,989

Giant Proximity Effect in High-Temperature Superconductors

Ivan Bozovic *05-104*

PURPOSE:

We are investigating systematically the Giant Proximity Effect (GPE) in high-temperature superconductors (HTS) using the atomic-layer-by-layer molecular beam epitaxy (ALL-MBE) system newly acquired by BNL. The atomic-layer engineering capability allows us to synthesize atomically perfect HTS films and fabricate precise multilayers and superlattices. We proved that GPE is real and intrinsic to HTS, and this imposed a new experimental constraint on the theory of HTS. We are tightening this further by determining quantitative dependence of the proximity-induced superconductivity on a number of parameters.

APPROACH:

Our strategy is to synthesize a series of SN' bilayers and SN'S junctions; here, S denotes an optimally doped HTS compound and N' an underdoped or overdoped HTS material with a reduced T_c. [GPE is observed at temperature $T_c < T < T_c$.] We can systematically vary the doping level x, the temperature T, the external magnetic field $\boldsymbol{H}$, the power P of microwave radiation, etc. Combinatorial synthesis and parallel testing greatly increase the density of data points; this is a novelty in physics experiments. G. Logvenov, V. Butko, A. Gozar and A. Bollinger are also participating in this project.

TECHNICAL PROGRESS AND RESULTS:

In FY 2006, we performed about 200 thin film synthesis experiments. Every film was characterized by Reflection high-energy electron diffraction (RHEED), transport measurements (resistivity and susceptibility as a function of temperature down to 4.2 K), and atomic force microscopy. Selected ones were also characterized by Rutherford Back-scattering. We have greatly improved the MBE system calibration and film synthesis protocols, and have achieved essentially 100 % yield of atomically smooth films. This surpassed what used to be the state-of-the art anywhere in the world in this field.

SPECIFIC ACCOMPLISHMENTS:

Publications:

G. Logvenov, I. Sveklo, and I. Bozovic, "Combinatorial Molecular Beam Epitaxy of $La_{2-x}Sr_xCuO_{4+\delta}$," Physica C (2006) in press

J. He, R. F. Klie, G. Logvenov, I. Bozovic, and Y. Zhu "Microstructure of strained $La_2CuO_{4+\delta}$ thin films on varied substrates," Journal of Applied Physics (2006) in press

V. Y. Butko, H. Wang and D. Reagor, "A Metallic State in a Crystalline Insulator due to the Normal Electron Proximity Effect," submitted to Physical Review Letters

Proceedings:

G. Logvenov and I. Bozovic, "Molecular Beam Epitaxy of Complex Oxides," Proc. 2nd International Conference on "Fundamental problems of HTS," Zvenigorod, Russia, 9-13 Oct. 2006

A. Bollinger, G. Logvenov and I. Bozovic, "Atomic-Scale Engineering of Thin Films of Complex Oxides Using ALL-MBE," Proc. ICCE-14, Boulder, CO, 2006

Invited talks:

I. Bozovic, "Giant proximity effect," 18th ISS, October 24-26, 2005, Tsukuba, Japan

I. Bozovic, "Strong electron-phonon coupling in high-temperature superconductors," International Workshop on Electron State and Lattice Effects in Cuprate High Temperature Superconductors, October 27-28, 2005, Tsukuba, Japan

I. Bozovic, Conference Summary, International Workshop on Electron State and Lattice Effects in Cuprate High Temperature Superconductors, October 27-28, 2005, Tsukuba, Japan

I. Bozovic, "Atomic-layer engineering of high-T_c heterostructures," Workshop on Nanoscale Correlations in Heterostructures, 2006 NSLS & CFN Joint Users' Meeting, May 16, BNL

I. Bozovic, "(Giant) Proximity Effects in high-Tc superlattices," APS Meeting, March 13-17, Baltimore, Maryland.

G. Logvenov, "MBE Growth of Complex Oxides," Winter Seminar, Finkenberg, Austria, March 18-25, 2006.

I. Bozovic, "Atomic-layer engineering of cuprate superconductors: what have we learned in the two decades," International Symposium on 20 Years of High-T_c Superconductivity in Zurich, Switzerland.

I. Bozovic, "Designed Josephson barriers," International Workshop on Lattice Effects in Superconductors, April 15-22, Santa Fe, New Mexico

I. Bozovic, "Superconducting Materials: the status of the field," DOE BES Workshop on Basic Research Needs for Superconductivity, May 8-11, 2006, Washington, DC

I. Bozovic, "Atomic-layer engineering of high-T_c superconductors," DOE BES Workshop on Basic Research Needs for Superconductivity, May 8-11, 2006, Washington, DC

I. Bozovic, "Superconducting Materials: the Workshop survey," DOE BES Workshop on Basic Research Needs for Superconductivity, May 8-11, 2006, Washington, DC

I. Bozovic, "Atomic-layer tailoring of high-temperature superconductors," International Conference "From Solid State to BioPhysics III, June 25-July 1, Cavtat, Croatia

A. Gozar, "Antiferromagnetic resonances and magnetic field induced ordering in undoped and lightly doped cuprates," International Conference on Low Energy Electrodynamics in Solids, July 1-6, 2006, Tallinn, Estonia.

A. Bollinger "Atomic-Scale Engineering of Thin Films of Complex Oxides Using ALL-MBE," ICCE-14, The Fourteenth International Conference on Composites/Nano Engineering (ICCE-14), July 2-8, 2006, Boulder, CO

G. Logvenov, "Atomic-layer engineering of cuprates superconductors," 8th International Conference on Materials and Mechanisms of Superconductivity and High Temperature Superconductors, Dresden, Germany, July 14-23, 2006

I. Bozovic, "Atomic-layer tailoring of high-temperature superconductors," International Workshop "Twenty years from the discovery of High T_c Superconductivity," July 20-26, 2006 Erice, Sicily, Italy.

I. Bozovic, "Nano-structuring cuprate superconductors," Int. Workshop on Mott's Physics in Nanowires and Quantum Dots, July 29-Aug 2, 2006 Cambridge, United Kingdom

A. Bollinger, "Superconductor-Insulator Transition in Quasi-One-Dimensional Nanowires," The Second International Workshop on Quantum Transport and Noise, September 3-15, 2006, Corfu, GreeceI. Bozovic, "Casting high-temperature superconductors atomic layer-by-layer," (plenary talk) YUCOMAT 8, Sept. 4-8, 2006, Herceg Novi, Montenegro

LDRD FUNDING:

FY 2005	$267,837
FY 2006	$366,753
FY 2007 (budgeted)	$255,000

Development of an Observation Based Photochemical-Aerosol Modeling System

Douglas Wright *05-105*

PURPOSE:

The objective of this project was to develop a modeling system for evaluation of the chemical and aerosol components of chemical transport and climate models by extensively incorporating field observations and observation-derived model constraints. The modeling system was conceived as a unique integration of datasets collected in major field campaigns and their subsequent incorporation into state-of-the-art chemical transport models, and should provide a unique tool tailored to upcoming field experiments such as those involving the DOE Atmospheric Science Program. Implicit in this objective was an examination of current possibilities and limitations in the use of such datasets to evaluate aerosol models, and how data collection and associated modeling might better coordinate with each other in future campaigns.

APPROACH:

Recent advances in data collection and instrumentation, as well as the appearance of more sophisticated models make possible a new degree of integration of observations with models. We approached this integration in an innovative way in that the models are constrained by one subset of the observations and evaluated by another, rather than proceeding entirely from first principles and a handful of poorly known initial conditions with the hope that model results will, in some respects, resemble the observations. Given that the detailed models used in this study require a large amount of input and evaluation data, a serious concern and risk in this undertaking is that the observations will still prove to be inadequate for model evaluation beyond what can already be done more readily by other means. Further, until the observations are studied in detail, it is not known what opportunities for model evaluation the collected datasets will present: i.e., if the formation of new particles or organic aerosol in the atmosphere was not observed, model representation of these important but poorly understood processes cannot be evaluated with these datasets.

To investigate this approach to model-observation integration, the present study examined the extent to which the datasets obtained onboard the DOE G-1 aircraft during the NorthEast Aerosol eXperment (NEAX) in the summer of 2004, which included chemical, aerosol, and meteorological quantities, could be used to evaluate detailed models of aerosol evolution, focusing on processes that shape the particle size distribution.

A modeling system was designed and tailored to the flight plans and datasets of NEAX, and introduced model constraints forcing the model to match the observations for most all processes except those governing aerosol microphysical evolution. These constraints permitted model examination to focus on the aerosol microphysical processes governing the particle size distribution.

Development of the modeling system was greatly aided by the several scientists in the Atmospheric Sciences Division responsible for data collection, processing, and the building of instruments deployed during NEAX (S.R. Springston, J. Wang, Y.-N. Lee). In this connection, Larry Kleinman

was a close collaborator in the strategy and design of this project.

TECHNICAL PROGRESS AND RESULTS:

The principal task originally planned for FY 2006 was the creation of new model components for secondary particle formation from gas-phase precursors. A new particle formation module was completed and has been implemented in a regional scale model run at BNL, the Community Multiscale Air Quality (CMAQ) modeling system, and was evaluated using data from the 2004 International Consortium for Atmospheric Research on Transport and Transformation (ICARTT) field campaign.

Most of the effort in the second half of FY 2006 was directed toward a modeling project, with the promise of follow-on funding and successful aerosol model evaluation. This project resulted in a collaboration with researchers at GISS. In the course of this work, the new particle formation module already developed was incorporated in the new Multiconfiguration Aerosol TRacker of mIXing state (MATRIX), an aerosol module under development at BNL. An early version of MATRIX is now a part of the climate model of the Goddard Institute for Space Studies (GISS), where the module and the aerosol model components it consists of will be extensively evaluated against observational data, fulfilling the original scientific intent of this proposal.

SPECIFIC ACCOMPLISHMENTS:

Proposal to the NASA Atmospheric Chemistry Program in collaboration with GISS

LDRD FUNDING:

FY 2005	$109,033
FY 2006	$106,242

Computational Science

James W. Davenport *05-110*
J. Glimm
Y. Deng
K. Kang
D. Keyes

PURPOSE:

Propose to develop new basic parallel algorithms for the efficient solution of large linear systems, both sparse and dense and to apply them to the electronic structure of nanoscale clusters of atoms. An additional application concerns the optimization of complex metabolic networks within bacterial cells. The nanoscale quantum mechanics codes use density functional theory (DFT) and require the solution of coupled Schrodinger and Poisson equations which is performed using localized basis sets. Thus, they naturally lead to large linear systems. We use techniques developed through our DOE SciDAC project TOPS (Terascale Optimal Partial Differential Equation Simulation, www.tops-scidac.org). Application is to palladium clusters, with potential use in hydrogen storage, and to gold clusters which are important catalysts. In the second problem, the possible use of large linear system optimization was investigated as an aid to defining the metabolic pathways in bacterial cells related to energy production.

APPROACH:

Most DFT calculations apply to small molecules or to crystals. The approach here provides a new capability for finite clusters. A localized basis set made up linear augmented Slater type orbitals (LASTO) is utilized. These consist of exponentially declining functions (STOs) outside atom centered spheres and numerical solutions of the radial Schrodinger equation inside. Solutions of the Poisson equation in the region between spheres is done numerically on an overset grid. Inside the spheres it is given in a spherical harmonic expansion, which is also extremely rapidly varying near the nuclei. A key step here is the incorporation of modern grid based techniques including multigrid and sparse matrix solvers into a usable, massively parallel, code.

TECHNICAL PROGRESS AND RESULTS:

The parallel LASTO code has been written and undergone extensive testing. Currently it appears to be working correctly and computations on a series of palladium clusters are nearing completion. Preliminary tests on transition metal clusters containing cobalt and nickel have been completed and the gradient corrected exchange-correlation energy has been implemented. Calculations will be started soon on the interaction of hydrogen with the finite palladium clusters. An additional result using LASTO for studying defects and optical properties of large cadmium selenide and cadmium telluride.

The studies of the application of high end computing to metabolic processes have not led to new results.

SPECIFIC ACCOMPLISHMENTS:

The rigorous mathematical analysis carried out here has clarified a number of problems and the results were incorporated into a DOE proposal.

Publications:

Y.-C. Chang, J. W. Davenport, and R. B. James, *Symmetrized-basis LASTO calculations of defects in CdTe and ZnTe*. Physical Review B **73,** 035211, 2006.

B. Fang and Y. Deng, *Parallel FFT on QCDOC supercomputer*, SIAM J. Sci. Comp. (Submitted).

P. Rissland and Y. Deng, *All-gather on QCDOC,* Parallel Computing, (Submitted).

K.-S. Kang, J. W. Davenport, J. Glimm, and D. Keyes, *Full Potential Linear Augmented Slater type Orbital Method for Free Standing Clusters.* (in preparation).

Presentations:

K.-S. Kang, J. Davenport, D. Keyes, and J. Glimm, *Scalable Linear Electronic Structure Method for Free Standing Clusters*, APS March Meeting, Baltimore, Md, March, 2006.

J. W. Davenport, *Computational Studies of Magnetic Materials,* Rochester Computational Science and Education Conference, Rochester, NY August, 2006.

LDRD FUNDING:

FY 2005	$109,776
FY 2006	$ 87,284

Study of High-T_c Nanostructures

Ivan Bozovic *05-114*

PURPOSE:

We are investigating systematically the effects of reduced dimensionality and confined geometries on high-temperature superconductors (HTS). This allows us to attack some of the most basic questions in HTS physics such as what are the spin and the charge of free carriers, what is the nature of superconducting transition – do Cooper pairs form and condense at T_c or else the pairs formed at some higher temperature T^* undergo Bose-Einstein condensation at T_c - and is the presence of dynamic stripes a necessary condition for HTS to occur. If we demonstrate that HTS can be sustained in mesoscopic samples (such as nanowires or nanodots), this would rule out a large class of theoretical models currently under active investigation and narrow down the playing field; this could be an important step towards elucidation of the mechanism of HTS.

APPROACH:

We use the state-of-the art atomic-layer-by-layer molecular beam epitaxy (ALL-MBE) system to synthesize atomically smooth HTS films, multilayers, and superlattices. Electron-beam nanolithography allows fabrication from such films of a variety of mesoscopic (nanoscale) devices such as nanowires, nanorings, and nanodots. Measurements of transport properties of these nanostructures reveal their critical temperature T_c, the critical current density j_c, etc. It is important to make as perfect samples as possible, in order to discriminate between extrinsic and intrinsic causes of T_c reduction. Apart from the PI, other participants in this project are G. Logvenov, V. Butko, A. Gozar and A. Bollinger.

TECHNICAL PROGRESS AND RESULTS:

In FY 2006, we performed about 200 thin film synthesis experiments. Every film was characterized by Reflection high-energy electron diffraction (RHEED), transport measurements (resistivity and susceptibility as a function of temperature down to 4.2 K), and atomic force microscopy. Selected ones were also characterized by Rutherford Backscattering. We have greatly improved the MBE system calibration and film synthesis protocols, and have achieved essentially 100 % yield of atomically smooth films. This surpassed what used to be the state-of-the art anywhere in the world in this field. We have also achieved the 20 nm nanowires width using electron-beam nano-lithography.

SPECIFIC ACCOMPLISHMENTS:

Publications:

1. M. Quazilbash, A. Koitzsch, B. Dennis, A. Gozar, H. Balci, C. Kendziora, R. Green aand G. Blumberg, "Evolution of superconductivity in electron-doped cuprates: Magneto-Raman spectroscopy," Phys. Rev. B 72, 214510 (2005)
2. M. Reehuis, C. Ulrich, K. Prokes, A. Gozar, G. Blumberg, S. Komiya, Y. Ando, P. Pattison and B. Keimer, "Crystal structure and high field magnetism in $La2CuO_4$," Phys. Rev. B 73, 144513 (2006)
3. L. Benfatto, M. Silva-Neto, A. Gozar, B. Dennis, G. Blumberg, L. Miller, S. Komiya and Y. Ando, "Field dependence of the magnetic spectrum in anisotropic and Dzyaloshinskii-Moriya antiferromagnets. II. Raman spectroscopy," Phys. Rev. B 74, 024416 (2006)
4. A. Rogachev, T. -C. Wei, D. Pekker, A. T. Bollinger, P. M. Goldbart and A. Bez-

ryadin, "Magnetic-Field Enhancement of Superconductivity in Ultranarrow Wires," Phys. Rev. Lett. 97, 137001 (2006).
5. A. T. Bollinger, A. Rogachev, and A. Bezryadin, "Dichotomy in short superconducting nanowires: Thermal phase slippage vs. Coulomb blockade," Europhys. Lett., published online September 27, 2006.
6. G. Logvenov, I. Sveklo and I. Bozovic, "Combinatorial Molecular Beam Epitaxy of $La_{2-x}Sr_xCuO_{4+\delta}$," Physica C (2006) in press
7. I. Bozovic "About physics, myself, and Ginzburgs," Journal of Superconductivity (2006), in press
8. N. Gedik, D-S. Yang, G. Logvenov, I. Bozovic and A. H. Zewail, "Direct observation of structural non-equilibrium phase transition in a cuprate superconductor," submitted to Nature
9. A. Gozar, G. Logvenov, V. Y. Butko and I. Bozovic, "Surface Structure Analysis of Atomically Smooth $BaBiO_3$ films," submitted to Physical Review Letters
10. J. He, R. F. Klie, G. Logvenov, I. Bozovic and Y. Zhu, "Microstructure of strained $La_2CuO_{4+\delta}$ thin films on varied substrates," submitted to Journal of Materials Science
11. V. Y. Butko, H. Wang and D. Reagor, "A Metallic State in a Crystalline Insulator due to the Normal Electron Proximity Effect," submitted to Physical Review Letters
12. W. Y. So, D. V. Lang, V. Y. Butko, X. Chi, J. C. Lashley and A. P. Ramirez, "Relationship between Mobility and Localized Gap States in Single-Crystal Organic Field-Effect-Transistors," submitted to Physical Review Letters
13. G. Logvenov and I. Bozovic, "Molecular Beam Epitaxy of Complex Oxides," Proc. 2nd International Conference on "Fundamental problems of HTS," Zvenigorod, Russia, 9-13 Oct. 2006
14. A. Bollinger, G. Logvenov and I. Bozovic, "Atomic-Scale Engineering of Thin Films of Complex Oxides Using ALL-MBE," Proc. ICCE-14, Boulder, CO, 2006
15. G. Logvenov and I. Bozovic, "Artificial superlattices grown by MBE: could we design novel superconductors?" Proc. Workshop on Room Temperature Superconductivity, Notre-Dame University, ed. B. Janko (2006)

Proceedings:

1. I. Bozovic, "Giant proximity effect," 18th ISS, October 24-26, 2005, Tsukuba, Japan
2. I. Bozovic, "Strong electron-phonon coupling in high-temperature superconductors," International Workshop on Electron State and Lattice Effects in Cuprate High Temperature Superconductors, October 27-28, 2005, Tsukuba, Japan
3. I. Bozovic, Conference Summary, International Workshop on Electron State and Lattice Effects in Cuprate High Temperature Superconductors, October 27-28, 2005, Tsukuba, Japan
4. I. Bozovic, "Atomic-layer engineering of high-T_c heterostructures" Workshop on Nanoscale Correlations in Heterostructures, 2006 NSLS & CFN Joint Users' Meeting, May 16, BNL
5. I. Bozovic, "(Giant) Proximity Effects in high-Tc superlattices," APS Meeting, March 13-17, Baltimore, Maryland.
6. G. Logvenov, "MBE Growth of Complex Oxides," Winter Seminar, Finkenberg, Austria, March 18-25, 2006.
7. I. Bozovic, "Atomic-layer engineering of cuprate superconductors: what have we learned in the two decades," International Symposium on 20 Years of High-T_c Superconductivity in Zurich, Switzerland.
8. I. Bozovic, "Designed Josephson barriers," International Workshop on Lattice Effects in Superconductors, April 15-22, Santa Fe, New Mexico
9. I. Bozovic, "Superconducting Materials: the status of the field," DOE BES Workshop on Basic Research Needs for Superconductivity, May 8-11, 2006, Washington, DC

10. I. Bozovic, "Atomic-layer engineering of high-T_c superconductors," DOE BES Workshop on Basic Research Needs for Superconductivity, May 8-11, 2006, Washington, DC
11. I. Bozovic, "Superconducting Materials: the Workshop survey," DOE BES Workshop on Basic Research Needs for Superconductivity, May 8-11, 2006, Washington, DC
12. I. Bozovic, "Atomic-layer tailoring of high-temperature superconductors," International Conference "From Solid State to Bio-Physics III," June 25-July 1, Cavtat, Croatia
13. A. Gozar, "Antiferromagnetic resonances and magnetic field induced ordering in undoped and lightly doped cuprates," International Conference on Low Energy Electrodynamics in Solids, July 1-6, 2006, Tallinn, Estonia.
14. A. Bollinger "Atomic-Scale Engineering of Thin Films of Complex Oxides Using ALL-MBE," ICCE-14, The Fourteenth International Conference on Composites/Nano Engineering (ICCE-14), July 2-8, 2006, Boulder, CO
15. G. Logvenov, "Atomic-layer engineering of cuprates superconductors," 8th International Conference on Materials and Mechanisms of Superconductivity and High Temperature Superconductors, Dresden, Germany, July 14-23, 2006
16. I. Bozovic, "Atomic-layer tailoring of high-temperature superconductors," International Workshop "Twenty years from the discovery of High T_c Superconductivity", July 20-26, 2006 Erice, Sicily, Italy.
17. I. Bozovic, "Nano-structuring cuprate superconductors," Int. Workshop on Mott's Physics in Nanowires and Quantum Dots, July 29-Aug 2, 2006 Cambridge, United Kingdom
18. A. Bollinger, "Superconductor-Insulator Transition in Quasi-One-Dimensional Nanowires," The Second International Workshop on Quantum Transport and Noise, September 3-15, 2006, Corfu, Greece
19. I. Bozovic, "Casting high-temperature superconductors atomic layer-by-layer," (plenary talk) YUCOMAT 8, Sept. 4-8, 2006, Herceg Novi, Montenegro

LDRD FUNDING:

FY 2005	$265,787
FY 2006	$367,080
FY 2007 (budgeted)	$255,000

Lattice Studies of QCD Thermodynamics on the ACDOC

Frithjof Karsch *06-001*

PURPOSE:

The objective of the project is to reach a better understanding of the thermodynamics of strongly interacting matter through large-scale numerical simulations on the new supercomputers, Quantumchromodynamics on a Chip (QCDOC) operated at BNL. The main goals are a determination of the QCD equation of state and the critical parameters controlling the transition as well as the study of in-medium properties of hadrons. These calculations shall be extended to QCD at a non-zero baryon chemical potential.

APPROACH:

Numerical studies of the phase structure of QCD have in the past had to rely on approximations (unphysically large quark masses, crude discretization of the continuous space-time) in order to become feasible at all. New supercomputers like the QCDOC machines at BNL now allow calculations with a realistic quark mass spectrum to be performed on lattices with strongly reduced discretization errors. Furthermore, newly developed simulation algorithms now also allow the performance of simulations without intrinsic step-size errors inherent in previous discretization schemes for the molecular dynamics evolution of the QCD Hamiltonian.

In this project we perform a large scale simulation of QCD with light up and down quark masses close to their physical value and a strange quark mass value fixed to its physical value. For this purpose we use a lattice discretization scheme (improved staggered fermions) that has been optimized by us for thermodynamic calculations.
The numerical calculations are performed at BNL as well as on a supercomputer, apeNEXT, at Bielefeld University, Germany. The collaboration involves about 15 members from Bielefeld University (Prof. E. Laermann et al.), Columbia University (Prof. N.H. Christ, Prof. R.D. Mahinney et al.) and our BNL based Lattice Group (P. Petreczky, C. Schmidt, S. Datta, T. Umeda and myself).

TECHNICAL PROGRESS AND RESULTS:

During most of FY 2005 the basic computer programs needed for calculations on the QCDOC and apeNEXT computers have been developed and first test simulations have been performed. During FY 2006 we performed large scale simulations on the QCDOC and apeNEXT computers that aimed at a determination of the transition temperature in QCD with light quarks. This part of the project has been completed. We then continued to perform studies of the QCD equation of state, developed programs for studies of QCD thermodynamics at non-vanishing quark chemical potentials and started the analysis of various physical observables that give information about the structure of the high temperature phase of QCD.

A major result of these studies is an improved estimate for the transition temperature to the high temperature phase of strongly interacting matter, which has been determined by us to be about 190 MeV.

SPECIFIC ACCOMPLISHMENTS:

Publications:

S. Ejiri, F. Karsch, E. Laermann and C. Schmidt, The isentropic equation of state of

2-flavor QCD, Phys. Rev. D 73, 054506 (2006)

M. Cheng, N.H. Christ, S. Datta, J. van der Heide, C. Jung, F. Karsch, O. Kaczmarek, E. Laermann, R.D. Mawhinney, C. Miao, P. Petreczky, K. Petrov, C. Schmidt, and T. Umeda, Phys. Rev. D 74, 054507 (2006)

Presentations:

T. Umeda, QCD thermodynamics with $N_f=2+1$ near the continuum limit at realistic quark masses, PoS(LAT2006)15

C. Schmidt and T. Umeda, Thermodynamics of (2+1)-flavor QCD, International Conference on Strong & Electroweak Matter 2006, May 10-13 2006, BNL, NY, USA, hep-lat/0609032

F. Karsch, Lattice simulations of the thermodynamics of strongly interacting elementary particles and the exploration of new phases of matter in relativistic heavy ion collisions, Journal of Physics: Conference Series 46 (2006) 122

C. Schmidt, QCD Thermodynamics with Almost Realistic Quark Masses, 41st Rencontres de Moriond: Workshop on Cosmology, Mar. 18-25 2006, La Thuile, Italy, hep-lat/0606020

C. Schmidt, Lattice QCD at Finite Density, Lattice 2006, 23-28 Jul 2006, Tucson, Arizona, hep-lat/0610116

T. Umdea, QCD thermodynamics with Nf=2+1 near the continuum limit with realistic quark masses, Lattice 2006, 23-28 Jul 2006, Tucson, Arizona, hep-lat/0610019

LDRD FUNDING:

FY 2006	$158,792
FY 2007 (budgeted)	$161,000

Detector Development for Very Long Baseline Neutrino Experiments

Milind V. Diwan *06-004*

PURPOSE:

We are developing new concepts, originated by BNL researchers, for the design of a very large (500 kT) multipurpose Water Cherenkov detector with a broad band accelerator neutrino beam. A large mega-ton scale detector, with high electron-neutrino detection efficiency, good energy resolution and background rejection is needed to reach the physics sensitivities of the next generation of very long baseline neutrino and proton decay experiments. We envision placing such a detector deep underground in the proposed Deep Underground Science and Engineering Laboratory (DUSEL) facility currently under consideration by NSF.

This research is also carried out partly in response to the charge from DOE and NSF to the Neutrino Scientific Assessment Group (NUSAG) dated on March 3, 2006 to "address the American Physical Society's recommendation for a next-generation neutrino beam and detector configurations." To that end, NuSAG has initiated the US Long Baseline Neutrino Experiment Study which is led jointly by BNL and Fermi National Lab (FNAL). The co-leaders of the Advisory Committee are Milind V. Diwan from BNL and Gina Ramieka from FNAL. Part of the charge is to address the detector options for a very long baseline neutrino experiment. The NuSAG group has charged the US Long Baseline Neutrino Study group to address the following questions pertaining to the detector design:

"What are the associated detector options which might be needed to fully realize the envisioned physics potentials? What are the rough cost ranges for these detector options? What would be the optimal construction and operation timeline for each accelerator-detector configuration? What would be additional important physics questions that can be addressed in the same detector(s)?"

APPROACH:

Our current study focuses on addressing the NuSAGs charge as it pertains to the design and costing of a large underground 500 kT Water Cherenkov detector. We chose Water Cherenkov as the initial detector technology to consider due to the proven track record of such detectors in neutrino and proton decay physics. Currently, the largest such detector built is the SuperKamiokande detector which is 50 kT. Ultimately, we will need a detailed design of a large detector with mass greater than 100 kT. Our approach is in three parts:

1) Developing detailed simulations of a large Water Cherenkov detector to determine the feasibility of using this technology to achieve the required signal sensitivity and background rejection capabilities for the next generation of long baseline neutrino experiments. To that end, Brett Viren from BNL has worked with colleagues from Stony Brook University (SBU) to create a simulation program while Chiaki Yanagisawa, collaborator from SBU, has used existing simulations of water Cherenkov detectors to understand the performance of such a detector.
2) An engineering study to determine the design requirements and cost estimate of building a 500 kT Water Cherenkov detector deep under-ground in the proposed DUSEL site at the Homestake mine in South Dakota. We are assembling a BNL and University based engineering team to study the mechanical design of 100kT Water Cherenkov detector modules with the goal of constructing at least 5 such modules in the Homestake Mine.
3) Research into new photodetection technology and the characterization of the response of different photomultiplier tube

(PMT) technologies to assess their feasibility for use to instrument 100kT Water Cherenkov detector modules. To that end we have instrumented a laboratory space for use in the automated measurement of photodetector response. This effort also includes pressure testing of PMTs. We have obtained 32 large 10.5" PMTs from Hamamatsu for destructive testing. This PMT research and development work shares testing facilities and effort with the proposed Daya Bay Reactor Neutrino Experiment of which the BNL Electronic Detector Group is a leading collaborator.

TECHNICAL PROGRESS AND RESULTS:

The most important accomplishment this year was further confirmation by simulation that the background to electron events could be controlled in a Water Cherenkov detector.

This work was carried out in collaboration with Stony Brook and Colorado State Universities (part of the UNO Underground Nucleon Decay and Neutrino Observatory Collaboration). The main contribution came from our collaborators Chiaki Yanagisawa and his student, Le Phoc Trung. They performed the background calculationusing a large sample of Super-Kamiokande atmospheric neutrino Monte Carlo events re-weighted to the flux from a BNL neutrino source. The current simulation is based on the existing Super-Kamiokande detector. We anticipate the continuation of our simulation effort with the goal of simulating the performance of a 100kT Water Cherenkov detector.

Our engineering effort on the mechanical design, timeline and costing of several 100 kT scale Water Cherenkov modules has been very successful, and we now have a preliminary cost estimate of $308.9 M, including a 30% contingency for 3 modules (a total of 300 kT fiducial volume) and the timeline for the construction of the photomultiplier tubes. We anticipate further engineering work is needed to refine the cost estimate as well as continuing the PMT R&D effort.

SPECIFIC ACCOMPLISHMENTS:

The performance of a large Water Cherenkov detector and the cost estimate and timeline have been incoporated into the Homestake DUSEL conceptual design report submitted to NSF. In addition, we note the following selected reports:

"Proposal for an Experimental Program in Neutrino Physics and Proton Decay in the Homestake Laboratory." M. Diwan et. al. hep-ex/0608023, July 12, 2007. Report presented to the Physics Advisory Committee (PAC) of the proposed Underground Science and Engineering Laboratory.

"Background Rejection Study in a Water Cherenkov Detector," C. Yanagisawa, C. K. Jung, P.T. Le, B. Viren. Report prepared as part of the US Study on Long Baseline Neutrino Experiments. July 18, 2006.

"DEEP SCIENCE. A Deep Underground Science and Engineering Initiative." October 12, 2006. Interdisciplinary report presented to NSF in response to the first solicitation (S1) from the NSF for site-independent proposals for the Deep Underground Science and Engineering Program Planning and Technical Requirements.

"The Homestake Underground Laboratory: Conceptual Design Report," K.T. Lesko, W.M. Roggenthen (coPI), In fulfillment of NSF Solicitation 05-506 Cooperative Agreement with the University of California, Berkeley. (Milind V. Diwan is one of the senior personnel as defined by NSF)

LDRD FUNDING:

FY 2006	$ 66,230
FY 2007 (budgeted)	$126,000
FY 2008 (budgeted)	$ 76,000

Detector for High Quality Imagers of Electron Microscopy

Pavel Rehak *06-012*

PURPOSE:

The technical objective of this LDRD project is to develop an Active Pixel Imager (API) based detector for electron microscopy. The image produced by the sensor under development is the most complete information of the picture formed by electrons of the microscope allowed by laws of physics. The detector will be capable of providing these high quality pictures at frame rates high enough allow dynamic studies of biological objects and structures in nano-science. A successful development of this kind of detector would facilitate the biological research beyond BNL biology department and will benefit the new growing field of nano-science. A different implementation of the same idea may find application in trackers for the International Linear Collider (ILC), a proposed electron-positron Collider under consideration.

APPROACH:

Detectors are a critical part of any electron microscope, since all the image, diffraction and spectroscopy information must pass through them prior to analysis. A wide range of topics, both in materials science and biology, are currently beyond reach due to limitations in detector technology.

Constant progress in semiconductor (silicon) technology is responsible for the recent devices in digital imaging technology called Active Pixel Sensors, APS (imagers). These sensors were already designed, produced, and tested as detectors of charged particles crossing the plane of sensors. The information being read-out is the total charge released in the active layer of silicon during the whole integration time of the sensor. The number of charged particles crossing the sensor and producing the charge is obtained from the total charge accumulated in individual pixels. These numbers of crossing particles are different from the true numbers due to imperfections of the charge measurement and because of intrinsic fluctuations of the charge produced by the passage of a single particle. Moreover, the dynamic range of the charge measurement limits the dynamic range of the particle count. The proposed detector improves all shortcomings of the present APS.

BNL is the right place to undertake this project due to the availability of experts in field of electron microscopy in biological sciences such as Joseph Wall, experts in microscopy in material sciences and nano-technology such as Yimei Zhu, and experts in silicon technology and electronics in the Instrumentation Division of the Laboratory.

TECHNICAL PROGRESS AND RESULTS:

This year was dedicated to modeling the device. The modeling can be divided into two main parts: i) Modeling of the process of the ionization and of the collection of the signal charge within the epitaxial part of the silicon pixel, and ii) amplification of the charge and the signal processing. The process of the ionization produced by the electron beam of the microscope and the collection of the signal charge is not part of any commercially available software. The software to simulate this part of the detection process was developed and used for the optimization of the geometry of the n- and p- wells in the pixels and for the values of voltages to be applied at individual

wells. The linear part of the read-out electronics chain was designed with the help of commercial programs for the design of Integrated Circuits (IC). A first iteration of the design of the digital part of the electronics was finished.

The submission of the first prototype of the electronic parts of the design will be done by January 22, 2007, in fulfillment of the first milestone of the original plan. The timing of the second milestone is summer 2007 when a substantially scaled down version of the detector will be submitted for production.

The funding for a full size detector will come from the Transmission Electron Aberration-corrected Microscopes (TEAM) project. Brookhaven National Laboratory is one of the principal participants in this DOE project.

SPECIFIC ACCOMPLISHMENTS:

Publication:

G. De Geronimo, G. Deptuch, V. Radeka, P. Rehak, A. Castoldi, A. Fazzi, E. Gatti, C. Guazzoni, M. Rijssenbeck, W. Dulinski, A. Besson, M. Deveaux, and M. Winter; "A Novel Position and Time Sensing APSs with Field Assisted Electron Collection for Tracking of Charged Particles and Imaging Detectors for Electron Microscopy," Nucl. Instrum. & Meth. A 568 (2006) 167-175.)

LDRD FUNDING:

FY 2006	$ 70,180
FY 2007 (budgeted)	$141,000
FY 2008 (budgeted)	$ 71,000

Transparent Photocathode Development

John Smedley *06-017*

PURPOSE:

The aim of this project is to develop a photocathode which will provide a significant average current while being illuminated in a transmission mode. Such a cathode is needed for applications where it is difficult or impossible to illuminate the cathode in a reflection mode. One such application of particular importance to BNL is the diamond amplified photocathode project, which would cover the electron-emitting side of the photocathode with a thin diamond layer, forming a capsule (figure 1). This cathode is intended as the electron source for the C-AD Energy Recovery Linac project and the e-cooler upgrade that is part of RHIC II.

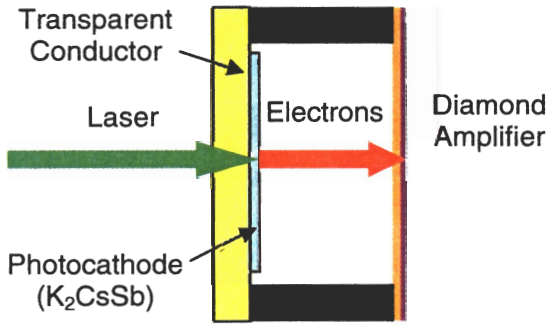

Figure 1: Schematic of capsule photocathode with a diamond amplifier, including a transparent photocathode.

As shown in the figure, in the transmission mode, the laser light passes through the transparent substrate and a thin conducting layer to irradiate the photocathode at the conductor-cathode interface. The electrons generated by the laser then travel through the cathode material to be emitted from the opposite surface.

APPROACH:

This project will build on an existing collaborative program between the Instrumentation Division and CAD aimed at establishing the fabrication specifications of K_2CsSb photocathodes on metallic substrates. This project will require modification of the existing deposition system to allow the cathode to be illuminated by the laser in both transmission and reflection modes. The system must also be modified to allow the substrate to be cooled to -170 C and to accommodate average currents up to 10 mA.

Several factors will impact the performance of a transmission photocathode. The substrate must be optically transparent and a good thermal conductor. It must be coated with a layer of sufficient conductivity to provide electron re-supply to the photocathode. This layer must also be optically nearly transparent and must be compatible with the photocathode material. The cathode layer should be thick enough to absorb a significant fraction of the laser photons and yet thin enough to transmit a significant fraction of the electrons generated. The resulting photocathode should be able to produce significant average current, and the lifetime at high current will need to be characterized.

The first cathode material to be investigated will be K_2CsSb. This cathode is used in photomultiplier tubes in transmission mode, and has a high quantum efficiency (QE) for visible light. The deposition recipe will be optimized for high QE in both reflection and transmission modes, by adjusting the thickness of cesium, potassium and antimony used, as well as the substrate temperature during deposition. Once a recipe is determined, a cathode will be tested for performance at high current and the lifetime will be measured.

The initial choice for a transparent conductor will be a thin metal layer on a glass slide. Commercially available transparent conductors, such as Indium-Tin Oxide (ITO) will also be tested. The substrate may be replaced with sapphire if necessary to improve the thermal conductivity.

TECHNICAL PROGRESS AND RESULTS:

The deposition system has been modified to allow illumination of the cathode in both reflection and transmission modes. Figure 2 shows the deposition system after modification, and Figure 3 shows the new sample mount to allow illumination in both reflection and transmission modes.

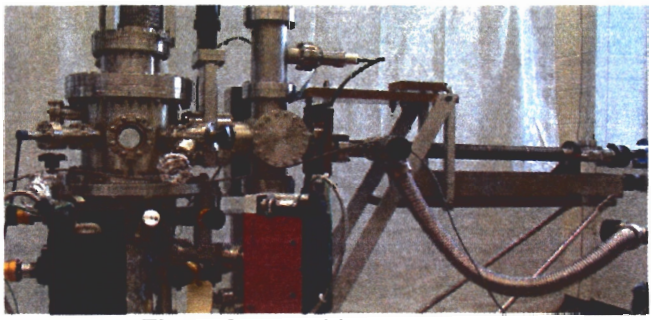

Figure 2: Deposition system

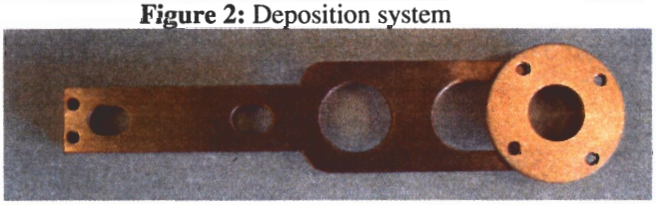

Figure 3: Mount to allow illumination in reflection and transmission mode

This system used a shorter source-to-substrate distance compared to the old design. The uniformity of the deposition was established for the desired cathode diameter of one cm (Figure 4). A glass slide sputtered on one side with 5 nm of titanium and 5 nm of platinum was used as a substrate. This metal coating was sufficiently thin to allow transmission of light, so the QE could be measured in transmission mode and reflection mode. The cathode QE was measured after 2 months in sub nTorr vacuum, and found to decrease slightly. Although the QE from this first cathode is poor, the deposition is uniform.

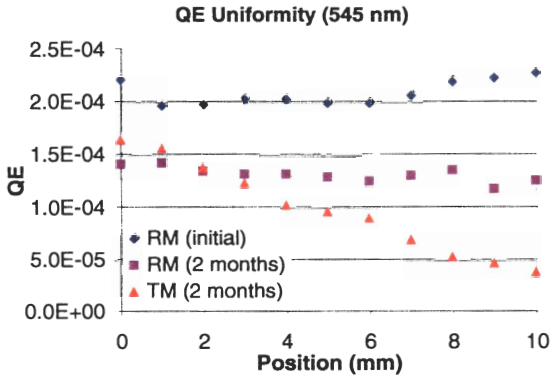

Figure 4: Quantum efficiency of first photocathode, in reflection mode (RM) and transmission mode (TM).

SPECIFIC ACCOMPLISHMENTS:

Presentation

J. Smedley, I. Ben-Zvi, A. Burrill, X. Chang, J. Grimes, T. Rao, Z. Segelov, Q. Wu; Diamond Amplified Photocathodes - Preparation and Capsule Formation; Workshop on High Quantum Efficiency Photocathodes, Milan, Italy, October 3-7, 2006

LDRD FUNDING:

FY 2006	$ 67,470
FY 2007 (budgeted)	$135,000
FY 2008 (budgeted)	$ 67,000

Synthesis and Characterization of Band-Gap-Narrowed TiO_2 Thin Films and Nanoparticles for Solar Energy Conversion

Eli Sutter *06-021*
P. Sutter
E. Fujita
J. Muckerman

PURPOSE:

TiO_2 is considered to be the most promising semiconductor material for solar energy conversion into chemical energy (H_2) via photo-decomposition of water because of its high stability, availability, low cost and non-toxicity. Its only disadvantage is being photoactive under ultraviolet (UV) light irradiation [wavelength (λ) < 387 nm] rather than from the main part of the solar spectrum. For optimum utilization of solar energy it would be desirable to shift TiO_2 absorption towards the visible part (λ > 400 nm) of the spectrum by reducing its large band gap. One promising approach to making TiO_2 highly reactive under visible light is to modify it via substitutional doping with nitrogen, carbon, and boron that can lower the energy gap and shift absorption towards longer wavelengths. Under this LDRD project we are developing synthetic routes for the reliable in-situ doping of TiO_2 single crystalline thin films and nanoparticles with N, C, and B. We will use the synthesized material for basic research in solar water photoelectrolysis, important aspects of which are understanding of the mechanism of doping and the interaction of H_2O with doped TiO_2.

APPROACH:

In previous studies doping of TiO_2 surfaces was achieved by exposure to ammonia (NH_3) or methane (CH_4), or by ion-implantation of N. However, these approaches are very limited since impurity incorporation in the bulk likely occurs at different sites than "doping" of the surface layer. Further, ion implantation requires expensive facilities and subsequent high temperature treatment to anneal defects that inevitably leads to the redistribution of the dopant atoms. In this project we focus on bulk N-doped TiO_2 single crystals that we propose to synthesize and use in our studies. They are clearly preferred as they offer material stability associated with the bulk substitutional doping and do not require additional high temperature annealing steps that lead to uncontrolled redistribution of dopants. We are uniquely equipped to perform homoepitaxy and doping in our ultrahigh vacuum (UHV) magnetron sputtering deposition system combined with a scanning tunneling microscope (STM). This combination allows us to study the synthesized doped material in-situ, without any further surface cleaning or annealing, using tunneling microscopy and spectroscopy to determine the surface electronic structure and the interaction of H_2O with doped TiO_2. We use state-of-the-art analytical techniques in transmission electron microscopy (TEM) to determine dopant densities and distribution and to evaluate the stability of the doped material.

TECHNICAL PROGRESS AND RESULTS:

In the first six months of this LDRD project we made progress in both major areas: *(A)* Epitaxial deposition and in-situ doping of TiO_2 thin films and *(B)* N-doping of TiO_2 nanoparticles.

(A) TiO_2 homoepitaxy. We made a big step forward by establishing the epitaxial growth of TiO_2 in our system. This required (i) finding suitable conditions for the surface preparation of single crystal substrates prior to deposition, (ii) setting up the epitaxy and (iii) developing a state-of-the-art high temperature/O_2 atmosphere heating stage. The conditions for surface preparation of bulk rutile (110) TiO_2 crystals suitable for consequently producing good quality films were found to consist of 10-12 sputtering cycles (Ar gas, 500 eV, 260°C, 25 min) with annealing steps (640°C, 4 min) in between. This preparation yields surfaces with large flat, clean terraces (Figure 1).

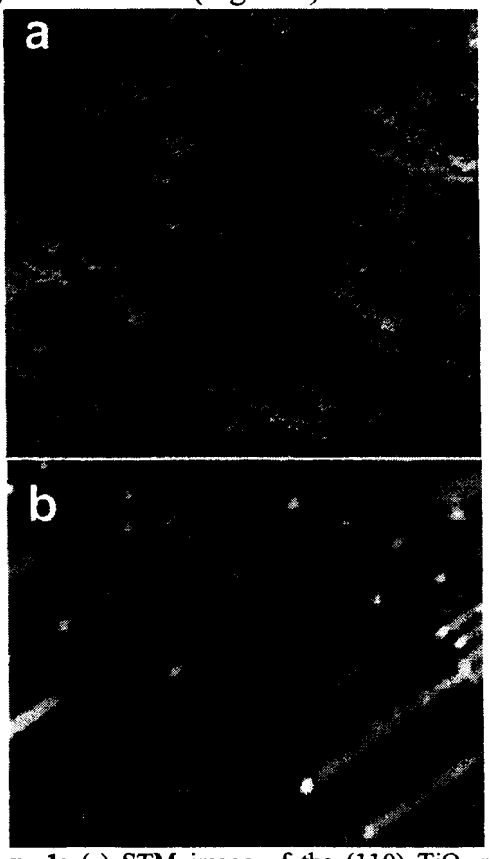

Figure 1: (a) STM image of the (110) TiO_2 rutile substrate after surface preparation (FOV: 4000Å). (b) Close-up, showing the bulk terminated (1x1) surface structure (FOV: 300 Å).

Homoepitaxy of TiO_2 was then carried out on these starting surfaces via reactive dc magnetron sputtering. The deposition was carried out from Ti targets in Ar/O_2 ($10^{-3}/10^{-4}$ torr) atmosphere at 600°C. The deposition was originally hindered by the incompatibility of our regular heating stage with a high-temperature deposition in oxygen. A special state-of-the-art heater stage was developed and implemented that allows us to carry out depositions at temperatures as high as 650°C. Typical STM images of the surface after TiO_2 deposition (Figure 2) show that the growth is in the step-flow regime proceeding via attachment of diffusing adatoms at existing atomic surface steps.

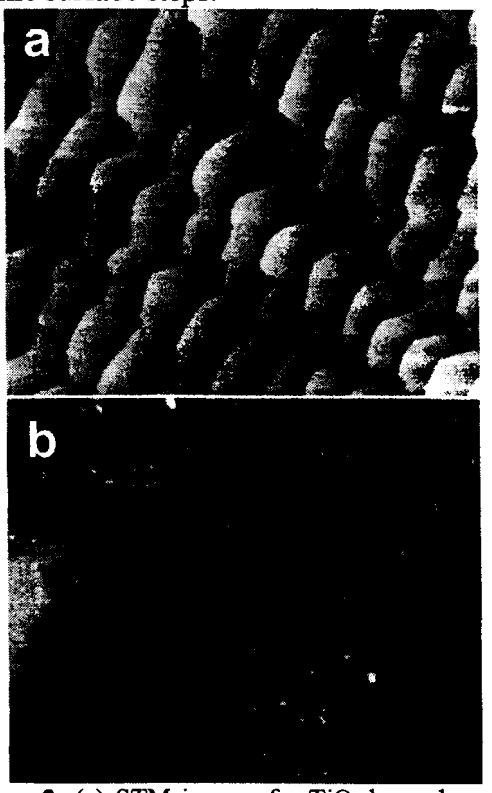

Figure 2: (a) STM image of a TiO_2 layer deposited by magnetron sputtering (FOV: 4000 Å). (b) Close-up, showing large flat terraces (FOV: 1000 Å x 800 Å).

The quality of the surface is excellent with large atomically flat terraces (Figure 2b). This is a major achievement, prerequisite for the N doping experiments that we are currently preparing by attaching a nitrogen dioxide (NO_2) source to our system.

(B) N-doping of TiO_2 nanoparticles. The doping and stability of TiO_2 nanoparticles was studied using commercial TiO_2 powders (Degussa P25). The particles were N-doped via exposure to (i) triethylamine (Et_3N) (80°C, 96 hrs.) and (ii) NH_3 (600°C, 1-3 hrs.). The doping levels determined using electron energy loss spectrometry (EELS) in the TEM were below the detection limit in (ii) but were rather high (8±1%) in (i). The undoped TiO_2 nanoparticles appeared structurally well–defined with atomically sharp facets (Fig. 3a) and were found to be very stable under electron beam irradiation even at elevated temperatures (room temperature to 450°C) for several hours. In contrast, the N-doped TiO_2 particles showed apparent structural changes and pronounced surface roughening (Fig. 3b) under the same observation conditions. Moreover, under the electron irradiation they underwent structural changes over a few minutes. Using TEM these were observed to propagate from the surface inward over some "near-surface" area but leaving an unaffected TiO_2 core that remained stable during prolonged irradiation (Fig. 3c). These observations confirmed that doping after the formation of the TiO_2 nanoparticles affects only the near-surface region and leads to an N-induced structural destabilization. They also confirm that our approach is correct, and substitutional bulk doping during materials synthesis is the viable way to producing stable material.

Our original achievements are the development of TiO_2 epitaxial growth as a route to single crystal material. We are currently implementing the in-situ N-doping of TiO_2 thin films from N_2 and NO_2. We will investigate the dopant distribution, film structure and interfaces using TEM, and in our unique deposition system combined with an in-situ STM we will determine the near surface electronic structure of the doped films and elucidate the atomistic doping mechanism under controlled UHV conditions, i.e. without breaking vacuum and without any damaging procedures or high temperature steps that can lead to the redistribution of dopant atoms. We will simultaneously establish the synthesis of N- doped TiO_2 nanoparticles and we will use TEM and EELS to characterize them and evaluate their stability.

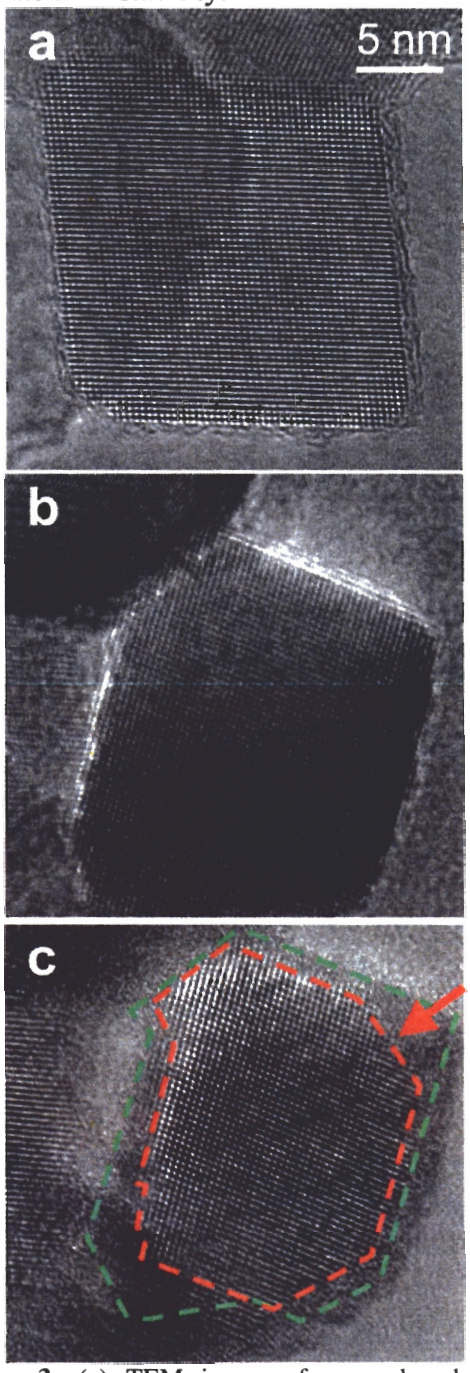

Figure 3: (a) TEM image of an undoped TiO_2 nanoparticle with atomically sharp facets. (b) The same particle after N-doping, showing surface roughness. (c) Structural transformation of a TiO_2 nanoparticle over 7 minutes of electron beam irradiation in the TEM. The green line identifies the

initial shape of the particle; the red outlines, at the end of the "near-surface" transformation, the undoped TiO_2 core that remains unaffected under further irradiation.

SPECIFIC ACCOMPLISHMENTS:

Presentation:

"Exploration of Controlled Nitrogen Doping of TiO_2 Single Crystalline Thin Films and Nanoparticles," E. Sutter, P. Sutter, E. Fujita and J. Muckerman, European Materials Research Society Meeting, Symp. M: Materials, Devices and Prospects for Sustainable Energies, Nice (France), June 2006.

LDRD FUNDING:

FY 2006	$ 69,484
FY 2007 (budgeted)	$207,000
FY 2008 (budgeted)	$138,000

Multiscale Analysis of *in vivo* Nanoparticle Exposure

Wynne K. Schiffer *06-026*

PURPOSE:

By virtue of their unusual size, nanoparticles have greater potential to travel through a living organism than other materials or larger particles. However, there are few ways to test where these new materials deposit in living systems and whether they will be tolerated by the host. In the service of this goal, we developed a unique imaging approach to investigate nanoparticle distribution in living rodents. At the heart of this in vivo approach is a new family of nanoparticle probes that can be imaged using PET. By conjugating existing classes of nanoparticle materials with a positron emitting isotope such as carbon-11 or fluorine-18, we will be able to quantitatively address current questions regarding the in vivo distribution, clearance, metabolism and toxicity of a broad range of nanoscale materials.

APPROACH:

For many pharmaceutical drug agents, quantitative pharmacokinetic studies in animals are the first step to determine drug dosing and toxicity, and these are followed by closer analysis using in vitro cell and tissue cultures. Without a method to quantitatively describe nanoparticle pharmacokinetics in living systems, studies of nanoparticle dosing and toxicity have been limited to in vitro cell and tissue cultures. Although some approaches have capitalized on the fluorescent properties of semiconducting quantum dots for in vivo, fluorescent imaging, insufficient signal strength and limited imaging depth remain problematic and preclude quantitative analyses. We, therefore, developed a general strategy to incorporate nanomaterials into our existing armamentarium of biomedical imaging tools.

We developed a strategy to synthesize positron-emitting nanoparticles for use with PET. This radiolabeling strategy is general and not limited to a particular type of manufactured nanoparticle, allowing us to develop models of exposure to predict the dispersion of a broad range of nanomaterials in living systems. Systematic variations in physio-chemical parameters such as elemental composition, particle number, size distribution and surface conjugation will allow us to determine how these properties influence the in vivo dissemination of nanoparticles.

Since nanoparticles have not been labeled with short lived isotopes such as carbon-11, several approaches are used to validate the PET measurements and to track nanoparticle accumulation at a cellular and ultrastructural level. Because the physico-chemical properties of nanoparticles may change during preparation, administration or over time in the living system, the physical and chemical properties of nanoparticle preparations are evaluated at multiple points in the process, from acquisition to labeling to imaging. These evaluations are done in collaboration with Drs. Mathew Maye and Oleg Gang of the Center for Functional Nanomaterials and include Dynamic Light Scattering (DLS) and Uv-vis for concentration estimates, Transmission Electron Microscopy (TEM) to measure particle size and X-ray photoelectron spectroscopy (XPS) to assess the integrity of surface chemistry composition after radiolabeling. Dr. Barbara Panessa-Warren determines elemental composition with energy dispersive X-ray analysis (EDX) and scanning electron microscopy (SEM). Evaporative loss experiments ensure that the

carbon-11 remains with the nanoparticle in systemic circulation. PET experiments are validated using fluorescent light microscopy where appropriate (i.e. with semiconducting quantum dots) and EDX is used to quantify metals (i.e. cadmium) in tissue.

TECHNICAL PROGRESS AND RESULTS:

We have successfully radiolabeled cadmium-selenide/zinc sulfur (CdSe/ZnS) semiconducting quantum dots (QDs) and tracked their distribution in living mice. DLS and UV-vis were both used to verify nanoparticle concentrations, and it was found that the concentrations quoted by the nanoparticle vendor were overestimated by a factor of three. The integrity of radiolabeled suspensions were examined at an electron microscopic level with TEM and particles were found to be intact and unaffected by the carbon-11. Evaporative loss experiments in rodent plasma demonstrated that the isotope-nanoparticle complex is stable and that measured carbon-11 is not in the form of [^{11}C]-CO2 or [^{11}C]-MeOH. Preliminary radiolabeling experiments with gold nano-particles indicated that the radiosynthesis can be applied to particles of different core material.

In the same animals studied with PET and [^{11}C]-CdSe/ZnS, EDX was used to confirm the presence of trace cadmium in organs such as the liver and kidney. Future experiments will focus on reducing background noise and enhancing the metallic signal from tissue using this approach.

Results from preliminary PET experiments indicate that the in vivo distribution of radiolabeled CdSe/ZnS quantum dots is significantly impacted by core size and surface coating. Smaller particles (3 nm core size) readily penetrated protected organs such as the brain where larger particles (10 nm) did not. Coating particles with surfactant (polysorbate-80, Tween) also significantly impacted the in vivo distribution, increasing blood circulation time and brain penetration of 3 nm particles.

Future studies will include other core nanomaterials such as gold. Based on PET measurements, we can see that CdSe/ZnS nanoparticles accumulate in the liver, spleen and kidneys. Future studies will use light and electron microscopic approaches to both validate these PET measurements and to establish the precise location of nanoparticles within tissues and ultimately, within cells.

SPECIFIC ACCOMPLISHMENTS:

Meetings, Proceedings and Abstracts:

1. Schiffer, W.K.; Ferrieri, R.; Shea, C.; Gang, O.; Panessa-Warren, B.; and Fowler, J.S. Positron-emitting nanoparticles to explore in vivo pharmacokinetics and pharmacodynamics with PET. Society for Nuclear Medicine (SNM), San Diego,CA, June 02 – 06, 2006

2. Schiffer, W.K.; Carrion, J.; Panessa-Warren, B.; Shea, C.; Gang, O.; Ferrieri, R.; and Fowler, J.S. In vivo PET imaging with labeled nanoparticles. IDEA League, Ascona, Switzerland. September 2006

Grant Submissions:

Grant Submissions: National Institute of Environmental Health Sciences (NIEHS) (returned unscored)
National Institute of Biomedical Imaging and Bioengineering (NIBIB) (under review)

LDRD FUNDING:

FY 2006	$192,178
FY 2007 (budgeted)	$192,000

Development of Gadolinium-Loaded Liquid-Scintillators with Long-Term Chemical Stability for a New High-Precision Measurement of the Neutrino Mixing Angle, Theta-13

Richard L. Hahn *06-030*

PURPOSE:

Our previous LDRD grant in FY-02/03 (related to the LENS project) led to our development of chemical methods to prepare ~10% In-loaded Liquid Scintillator (LS). We now are applying this expertise to the development of new antineutrino detectors that would be used in experiments at nuclear-reactor power stations, where the reactor outputs are on the order of GW (Giga Watts). For this application, we would need only 0.1-0.2% of a Gd-loaded LS to detect the neutrons that are produced by the antineutrinos.

The purpose of such experiments is the measurement, with unprecedented precision to ~1%, of the remaining unknown neutrino-oscillation mixing-angle, theta-13 (which determines the flavor mixing between the first and third neutrino mass-eigenstates).

DOE has accepted the recommendations of different scientific review committees that it is important to construct at least one high-precision theta-13 experiment. The Office of High Energy Physics has narrowed its theta-13 focus to an experiment that is planned to be done at the Daya Bay nuclear power station in southeastern China. BNL scientists from the Chemistry and Physics Departments are active members of the U.S.-China Daya Bay Collaboration, which began to make headway in 2006.

APPROACH:

We are been developing chemical methods to synthesize Gd-organo complexes that are soluble and stable in different organic LS. One major LS we are studying is pseudocumene, PC. However, PC has some shortcomings, especially a very low flashpoint, 44 °C, that makes it hazardous, especially in the underground laboratories where we would perform the neutrino experiment. So we are doing R&D with a new LS candidate, Linear Alkyl Benzene, LAB. It has a high flashpoint and is relatively innocuous chemically, being a starting material in the commercial production of synthetic detergents.

The goals of this LDRD project are research oriented: (1) To apply our expertise in nuclear chemistry to develop methods to assay, reduce, and/or eliminate radioactive contaminants in the materials that we work with. (2) To study chemical speciation of (trivalent) Lanthanide-organo complexes, to gain understanding of their chemical composition and structure and the factors that determine their stability. (3) To perfect a 2-meter baseline optical system, to improve the way that we measure long attenuation lengths (at present we use 10-cm cells and extrapolate the result to >1000 cm).

TECHNICAL PROGRESS AND RESULTS:

We have successfully prepared many Gd-LS samples, and have begun a Quality Control program to monitor the characteristics of these samples over time, to make sure that they do not deteriorate. We have prepared hundreds of Gd-complexes, mainly in PC and in LAB. The results are very encouraging; to date, the optical properties of our Gd-LS samples have been stable for >600 days.

This work does not involve animal vertebrates and/or human subjects.

SPECIFIC ACCOMPLISHMENTS:

Publications:

1. Minfang Yeh, A.Y. Garnov and R.L. Hahn, Gadolinium-Loaded Liquid Scintillator for High-Precision Measurements of Antineutrino Oscillations and the Mixing Angle, θ_{13}, Submitted to Nuclear Instruments & Methods A, 2006.
2. Amanda Storm, Tigisti Kesete, Suzanne Seleem (FAST undergraduate team from BNL Office of Educational Programs), Minfang Yeh and Richard L. Hahn, Solvent Purification and Fluor Selection for Gadolinium-loaded Liquid Scintillator, accepted for publication in Department of Energy Journal of Undergraduate Research, V7, 2007

Meetings:

1. Minfang Yeh and Richard Hahn, Gadolinium-loaded Liquid Scintillator for New Reactor Antineutrino Experiments, talk at the Seaborg Award Symposium, 231st ACS Meeting, Atlanta, March 26 –30, 2006.
2. Minfang Yeh and Richard L. Hahn, Overview of Gd-loaded and Unloaded Liquid Scintillator for Reactor Antineutrino Experiments, talk at the Workshop on Future PRC-US Cooperation in High Energy Physics, Beijing, China, June 11- 18, 2006.
3. Minfang Yeh, A. Y. Garnov, and Richard L. Hahn, Metal-loaded Liquid Scintillators for New Neutrino Experiments, poster at Neutrino-2006, the XXII International Conference on Neutrino Physics and Astrophysics, Santa Fe, NM, June 13-19, 2006.
4. Minfang Yeh and Richard L. Hahn, Metal-loaded Liquid Scintillator for Neutrino Physics, talk at the LONU-LENS, Workshop on Low-Energy Solar Neutrinos & LENS, Blacksburg, Virginia, October 14-15, 2006.
5. Richard L. Hahn, Minfang Yeh and A. Y. Garnov, Development of Gadolinium-Loaded Liquid Scintillators for 1%-Precision Measurement at the Daya Bay Nuclear Reactors of the Neutrino Mixing Angle, θ_{13}, talk at the Division of Nuclear Physics Annual Meeting, American Physical Society, Nashville TN, October 25-28, 2006.

Report:

A draft of the Conceptual Design Report, "The Daya Bay Project", has undergone several revisions by members of the Daya Bay collaboration. BNL and LBNL are the lead Laboratories that are preparing this CDR., and Hahn and Yeh are authors of sections of the CDR. It is still undergoing changes, even though the latest version has been sent to OHEP/DOE.

Reviews:

1. DOE Review of national LDRD programs, held at BNL in May 2006. Hahn was one of six invited BNL scientists who gave presentations to the visitors from other National Laboratories and DOE.
2. BNL Director's Review at BNL of the Physics of the Daya Bay Theta-13 Proposal, September 28-29, 2006. Data from this LDRD project were presented as part of the overview of the proposal.
3. DOE/OHEP Review at LBNL of the Physics of the Daya Bay Theta-13 Proposal, October 16-17, 2006. Hahn presented a talk on Gd-loaded liquid scintillator at this Review.

In FY-2006, the U.S. members of the Daya Bay Collaboration received initial funding from OHEP for R&D activities. The goals of the OHEP work are oriented towards development of the construction project: (1)

To perfect the development of stable (~years) Gd-LS with high light yield and long attenuation length ~15m. (2) To evaluate chemical compatibility of Gd-LS with acrylic and other construction components (e.g., the acrylic detector vessel). (3) To develop mass-production techniques to go from current bench-top scale of tens of kg (tens of Liters) to tons (thousands of Liters). (4) By 2007, to complete a prototype ~1-ton detector.

This LDRD and the OHEP project we are working on are separate and complementary programs.

LDRD FUNDING:

FY 2006	$199,946
FY 2007 (budgeted)	$191,000

Electronic Properties of Carbon Nanotubes and Novel Multicomponent Nanomaterials

John Hill *06-037*

PURPOSE:

The purpose of this LDRD is to develop an interdisciplinary tool set to understand the electronic properties of organic nanomaterials. These materials are important from both a fundamental and applied perspective, with promising applications in fields such as optoelectronics and photovoltaics. Central to their application in these fields, however, will be a complete understanding of their electronic behavior – the subject of this program.

APPROACH:

The approach taken is a multidisciplinary one, bringing to bear a range of experimental and theoretical tools with a goal of understanding, and ultimately manipulating, the electronic properties of organic nanomaterials. Initial work is centered on carbon nanotubes, which are the prototypical example of organic nanomaterials, and which have a wide range of potential applications, particularly photovoltaic uses. A unique challenge in this work will be producing single phase samples (that is to control the band gap of the molecules).

Experimentally, inelastic x-ray scattering will be used to probe the electronic response of these systems, and these data will be combined with electron energy loss, optical conductivity and Raman scattering measurements of the same system. Taken together, these data will provide a complete picture of the electronic excitation spectrum. Calculations will then be used to gain an intuitive understanding of the physics of these materials. In particular, we will follow a novel theoretical approach involving a real-space formalism that will allow a detailed understanding of the all-important excitons.

Collaborators include D. Casa and T. Gog (ANL), G. Eres and D. Lowndes (ORNL) and R. F. Klie, Y. Zhu and A. Stein (BNL).

TECHNICAL PROGRESS AND RESULTS:

In FY 2006 we began investigating the carbon nanotube system, probing the low energy Coulomb screening by measuring the $\pi+\sigma$ plasmon energies of a series of nanotube arrays with different physical parameters using inelastic x-ray scattering and electron energy loss spectroscopy. The physical properties of the carbon nanotube samples were further characterized by TEM and Raman scattering to allow a direct connection to be made between the physical structure and the electronic properties.

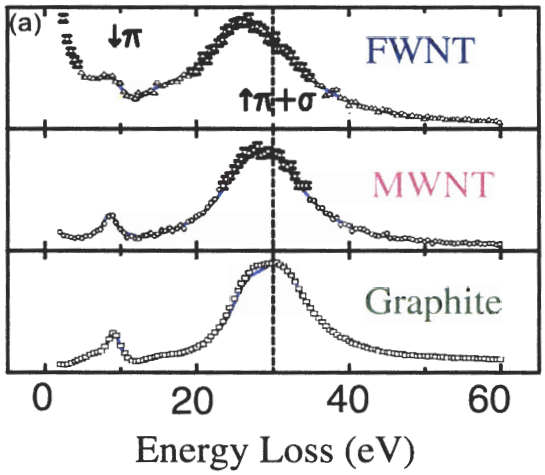

Figure 1: Inelastic x-ray scattering spectra showing a systematic shift in the plasmon peak position as the number of walls is varied. Samples shown are "few-walled nanotubes" with ~3 walls on average (FWNT), "multi-walled nanotubes" with ~14 walls (MWNT), and bulk graphite.

As shown in Figure 1, this work demonstrated, for the first time, that the low-energy screening of carbon nanotubes depends on the number of walls of the nanotube and not on the radius or chiral vector of the nanotube.

Unfortunately, because of sample issues, we have not been able to observe the exciton to date. It is now clear that this will require samples that are purely semi-conducting and of small diameter. We have begun a program to attempt to prepare such samples by reducing the average diameter of the nanotubes in an array through resistive heating methods. This is the single most challenging aspect of this project, and the highest risk. It is one of the goals for FY07. Success here would have wide reaching consequences. To date, we have successfully passed current through an array and are trying to improve our understanding of this process and our ability to control it.

In addition to the nanotube work, initial inelastic x-ray scattering measurements of the excitations of LiC_6 have been performed. This organic electronic material is interesting because it is the anode material for lithium ion batteries, and because it is an example of a graphite intercalate compound – these have recently been shown to be amongst the highest temperature organic superconductors known. Preliminary results have revealed an interesting excitation with a very large momentum width in the direction of momentum transfer perpendicular to the planes. One of the other goals for FY 2007 is to understand the origin of this feature.

Finally, beam-time proposals to the have been submitted to measure the dispersion of phonons of the related intercalate CaC_6. Such measurements will help distinguish between the competing models of superconductivity in this system and will also allow us to determine the feasibility of similar measurements in the carbon nanotube system.

SPECIFIC ACCOMPLISHMENTS:

- "Effect of Number of Walls on Plasmon Behavior in Carbon Nanotubes." M. H. Upton, R. F. Klie, J. P. Hill, T. Gog, D. Casa, W. Ku, Y, Zhu, M. Y. Sfeir, J. Misewich, G. Eres and D. Lowndes. Submitted paper to Phys. Rev. Lett:
- Advanced Photon Source Users' meeting, May 1- May 5, ANL. Poster: "Inelastic X-ray study of Plasmons in oriented single and mulitwall carbon nanotubes" D. Casa, presenter
- SRMS-5 (August, 2006): Synchrotron Radiation in Materials Science, Chicago, July 30th – Aug 2nd. Poster: "Inelastic X-ray study of Plasmons in oriented single and mulitwall carbon nanotubes" D. Casa, presenter
- ESRF seminar (November, 2006), European Synchrotron Radiation Facility, Grenoble, France. Talk: "Inelastic X-ray study of Plasmons in oriented single and mulitwall carbon nanotubes" D. Casa, presenter.
- NSLS Lunchtime seminar, May 12th, 2006, "Inelastic X-ray Scattering Studies of Plasmons in Carbon Nanotubes," M. Upton, presenter

LDRD FUNDING:

FY 2006	$ 45,590
FY 2007 (budgeted)	$180,000
FY 2008 (budgeted)	$ 90,000

Growth and Characterization of CdZnTe Crystals for Improved Nuclear Radiation Detectors

Genda Gu *06-038*
A. Bolotnikov

PURPOSE:

CdZnTe (CZT) is recognized as the best choice of material for room-temperature gamma-ray detectors. It is quite challenging to grow crystals of CZT because of the high vapor pressures of the constituent elements. So far, no one has managed to grow adequate large and high quality single crystals for commercial detectors. This project is to develop and demonstrate the ability to grow CZT crystals and fabricate detectors with high energy resolution, <1% FWHM at 662 keV.

APPROACH:

Previous crystal growth methods are not able to produce large and high quality single crystals. A new approach to grow single crystals with infrared image furnaces and a related facility were developed. It includes a number of optimized processes for crystal growth.

We will characterize the grown crystals and fabricate and test the radiation detectors. These include measurements of the electrical and carrier transport properties, structural defects, and tellurium inclusion in as-grown crystals. In addition, we will fabricate and test the crystals configured as planar and Frisch-ring detectors.

TECHNICAL PROGRESS AND RESULTS:

We have obtained all the crystal growth equipment and all raw materials which are used to grow the single crystals and are now doing the crystal growth.

We want to grow the new high quality and large single crystals of CZT materials and study their physical property.

We have upgraded the equipment used for material characterization and device testing: I-V measurements stations, IR transmission microscope, x-ray mapping system. To test and evaluate the equipment, some baseline measurements have been carried out with currently available CZT material.

SPECIFIC ACCOMPLISHMENTS:

Presentations:

A. E. Bolotnikov, M. Black, G. S. Camarda, G. A. Carini, Y. Cui, K. T. Kohman, L. Li, M. B. Salomon, and R. B. James, "The effect of Te precipitates on characteristics of CdZnTe detectors," Proceedings of SPIE Hard X-Ray and Gamma-Ray Detector Physics and Penetrating Radiation Systems VIII, edited by L. A. Franks, A. Burger, R. B. James, H. Bradford Barber, F. Patrick Doty, and Hands Roehrig (SPIE, Bellingham, WA, 2006), Vol. 6319, 631903-1.

G. S. Camarda, A. E. Bolotnikov, G. A. Carini, Y. Cui, K. T. Kohman, L. Li, and R. B. James, "High spatial resolution imaging of Te Precipitates in CZT material," Proceedings of SPIE Hard X-Ray and Gamma-Ray Detector Physics and Penetrating Radiation Systems VIII, edited by L. A. Franks, A. Burger, R. B. James, H. Bradford Barber, F. Patrick Doty, and Hands

Roehrig (SPIE, Bellingham, WA, 2006), Vol. 6319, 63190Z-1.

LDRD FUNDING:

FY 2006	$ 62,932
FY 2007 (budgeted)	$185,000
FY 2008 (budgeted)	$131,000

Design, Synthesis and Characterization of a New Class of Hydrocarbon Polymers Containing Zwitter Ions and Nano-structured Composites for High Temperature Membrane in PEM Fuel Cells

Xiao-Qing Yang *06-039*

PURPOSE:

Membranes are a critical component of the fuel cell stack. Novel membranes with higher ionic conductivity, better mechanical strength, lower cost, and longer life are critical to the success of fuel cell technologies and other technologies that depend on ionic transport. Polymeric membranes that conduct protons and remain hydrated up to high temperatures are needed. Unfortunately, no breakthrough has been accomplished in designing and synthesizing these new polymeric membranes with satisfactory proton conductivity and mechanical strength at high temperature. Therefore, the innovative approach of synthesizing a new Zwitterion containing polymer membranes with aromatic backbones could be highly rewarding.

APPROACH:

The Key is to balance the water uptake and mechanical properties of the membrane.

The approach is a:
1) molecular design of Zwitterion containing polymers to enhance the water uptake and water holding function
2) molecular design of a balanced aromatic backbone and sulfonic acid containing side chains
3) radiation induced cross-linking to improve the mechanical strength
4) composite the polymer with inorganic nano-particles or nano-tubes to improve the overall performance.

TECHNICAL PROGRESS AND RESULTS:

Sulfonated polybenzimidazole (PBI) can be considered as a good example of using a Zwitterion for the proton conducting membranes. This material has received much attention, both as a proton exchange membrane candidate and also as a host for phosphoric acid. Unfortunately, the sulfonated PBIs are insoluble and brittle, which make them unusable for polymer electrolyte membrane (PEM) fuel cells.

Our innovative approach is to use various aromatic groups as co-polymer backbones to balance the mechanical strength and the proton conductivity and using a Zwitterion with an alkyl chain for water uptake.

The enormous challenge we encountered in 2006 was the difficulty in finding a proper procedure to synthesize the polymer with a sulfonic group containing Zwitterions. The polymerization was prohibited by the Zwitterion groups which had been attached to the monomers we synthesized. If we polymerize the monomer without the Zwitterion, then the Zwitterion grafting after polymerization failed.

Our great progress in 2006 was the development of a new synthesis procedure combining a functionalized aromatic co-polymer backbone with a post-polymerization Zwitterion attachment using sulton as described in Fig. 1. Using this new procedure, several new polymer membranes were synthesized and more are to follow.

Future studies and milestones for 2007:
Design and synthesize more sulfonic acid and Zwitterion containing polymers for both the fundamental understanding of the performance-structure relationship and the practical application to obtain polymer membranes.
Radiation induced cross-linking to improve the mechanical strength.
Water uptake, ionic conductivity, gas permeability mechanical properties and other physical property tests in collaboration with University of Massachusetts at Boston.

SPECIFIC ACCOMPLISHMENTS:

"Design, Synthesis, Processing, and Characterization of a New Class of Zwitter Ion Containing Polymers and Nano-structured Composites for High Temperature, Low Relative Humidity Membranes in PEM Fuel Cells."

LDRD FUNDING:

FY 2006	$133,331
FY 2007 (budgeted)	$131,000

Figure 1. A schematic scheme of the successfully synthesized Zwitterion containing co-polymer

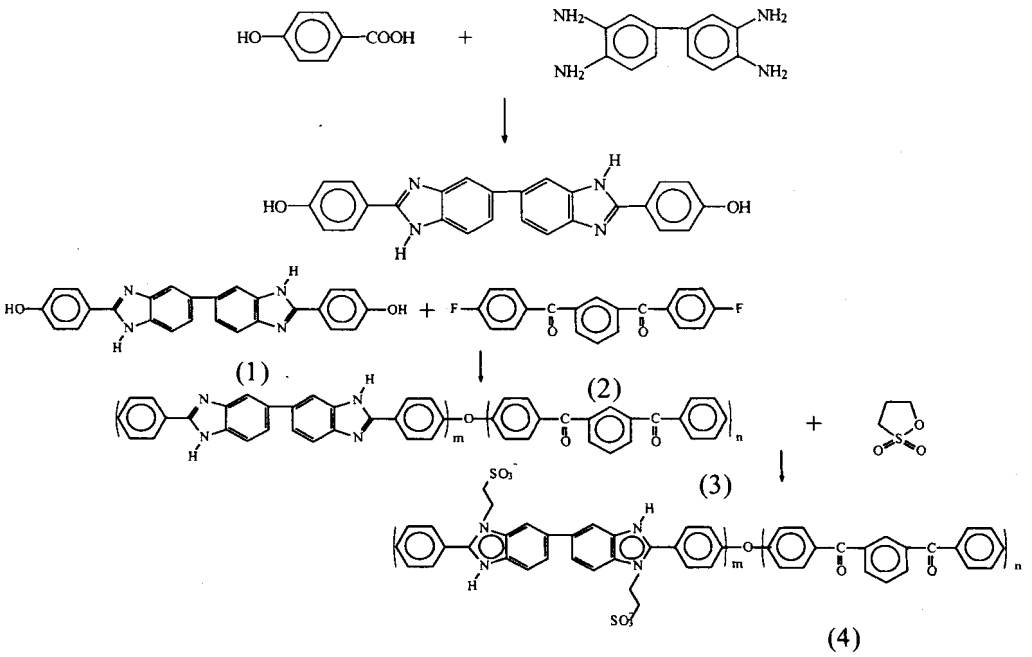

New High Resolution X-ray Monochromators for Condensed-matter Science Experiments

Wolfgang A. Caliebe *06-044*

PURPOSE:

Recently, some new concepts for the implementation of high-resolution x-ray monochromators have been proposed [1] which promise the possibility of sub-milli-eV resolution at photon energies of a few keV. Previous methods based on conventional Bragg diffraction have only been able to achieve this performance at higher photon energies, 25keV and higher, because of the intrinsic properties of Bragg diffraction in the dynamical limit. This opens up the possibility of new instruments, previously impossible. This project is intended to provide manpower for a detailed study of the limits of applicability of these new ideas, and to implement some of them in the context of solving a previously intractable problem. In the longer term, such optical systems will be crucial to the realization of the potential gains provided by third- and fourth-generation light sources.

APPROACH:

In the first year we planned to hire a Research Associate to perform most of the laboratory work which includes calculating the performance of candidate systems and estimate available flux and cross-sections for the various physical processes to be studied (photoemmission, inelastic scattering) and then construct the chosen monochromator configuration.

TECHNICAL PROGRESS AND RESULTS:

After a lengthy search an outstanding candidate was identified and recruited for this project. However, the candidate was also recruited and subsequently hired by another National Laboratory. With no viable candidate available this project was canceled. The only cost incurred was related to the search process for a Research Associate.

SIGNIFICANT ACCOMPLISHMENTS:

None

LDRD FUNDING

FY 2006	$ 1,871

Novel Materials for Hard X-Ray Optics

Kenneth Evans-Lutterodt *06-046*

PURPOSE:

In order to take full advantage of existing and future medium energy synchrotron high brightness x-ray sources, we will need high quality hard x-ray optics with sub-10nm resolution and with high efficiency to enable the full range of hard x-ray microscopy and spectroscopy techniques that will benefit nano-science. In this project we plan to fabricate high quality kinoform lenses out of silicon and diamond.

APPROACH:

The limiting resolution for an optic is proportional to the $\lambda/(N.A.)$, where N.A. is the numerical aperture of the optic, which is the angular range subtended by the optic as viewed from the focal point. For refractive optics, the numerical aperture of a single lens is limited by the small value of the real part of the refractive index δ, leading to resolutions of order $\lambda/\sqrt{(2\delta)}$. In this project we plan to get around this limit by fabricating compound lenses, i.e. an array of single lenses. A further obstacle for high resolution hard x-ray optics is that conventional diffractive optics need to be fabricated with feature sizes that are of the order of the desired optic resolution. In this project we plan to take advantage of one of the features of the kinoform type of optic, which allows one to fabricate optics with feature sizes that can be many multiples of the desired optic resolution, i.e. using a kinoform in higher order.

TECHNICAL PROGRESS AND RESULTS:

During this year we have fabricated 2 lenses, one a compound lens array of 4 lenses, and a single lens with features 8 times the minimum feature size. We have measured both lenses at NSLS beamline X13B, and additionally we have measured the single lens at beamline 8-IDI at Advanced Photon Source (APS). We have demonstrated for the first time experimentally that one can exceed the critical angle by using compound lenses, and have obtained deflection of 1.1+-0.05 times the critical angle, while yet retaining the focusing property of the lens. This is shown in Figure 1. At APS we used the brighter source and more stable beamline to show that the idea of using a kinoform in higher order works, and we obtained a spot size of between 100nm and 200nm.

We have hired a Post-doctoral fellow, Abdel Isakovic who will develop improved etching processes for silicon and will begin to investigate diamond etching.

SPECIFIC ACCOMPLISHMENTS:

The results for the compound optics were included in the hard X-ray optics section of the NSLS-II CD-1 proposal which will undergo Lehman review Dec 16th.

LDRD FUNDING:

FY 2006	$ 24,809
FY 2007 (budgeted)	$147,000

Using multiple kinoform lenses to go beyond the critical angle limit

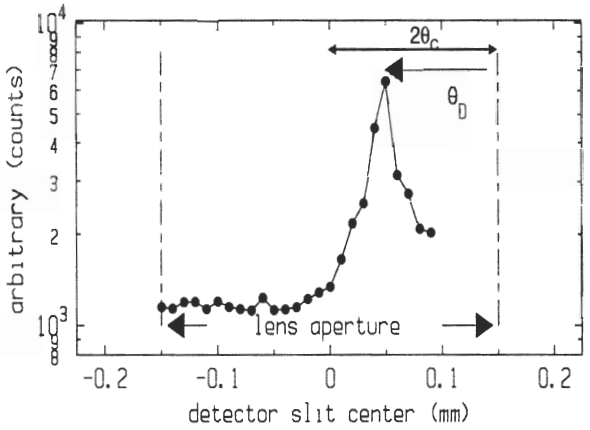

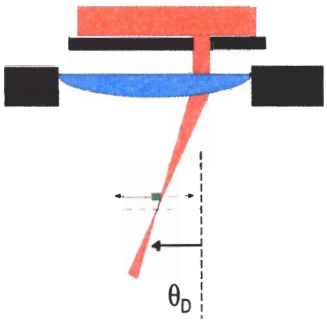

Figure 1. Single refractive lens has a deflection angle $\theta_D = \theta_c$ and hence resolution limit is λ/θ_c . Using an array of 4 lenses we design a lens with f =25mm, total aperture =0.3mm, $\theta_D = 2\theta_C$

Nano-Crystallography of Individual Nanotubes and Nanoparticles

Christie Nelson *06-047*

PURPOSE:

The goal of this project is to develop both theoretical and experimental techniques for carrying out nano-crystallography on individual nanotubes and nanoparticles. The motivation for this work is that x-ray scattering can provide extremely high resolution — on the sub-Angstrom level — for precise structural characterization. Since in many nanomaterials the functional properties are determined by the structural properties, such characterization is extremely important. This work is also motivated by the new capabilities that the NSLS-II will provide, with focusing down to the nanometer scale. In order to fully take advantage of some of the anticipated NSLS-II capabilities, exploratory work on the feasibility and potential of nano-crystallography is called for.

APPROACH:

On the theoretical side, numerical simulations are carried out by co-investigator Natasha Bozovic using the 256-processor, Galaxy cluster, at the Computational Science Center at BNL. Using the anticipated NSLS-II flux and expected focusing capabilities, simulated images for exposures of a "reasonable" duration (~1 hour) of individual nanotubes or nanoparticles are obtained. The important questions to address from these simulations are: is the anticipated NSLS-II performance sufficient for the study of individual nanotubes and nanoparticles in a reasonable amount of time; and, can detailed information about the structure — including diameter, chirality, and the presence of adatoms, in the case of carbon nanotubes — be extracted from the images.

On the experimental side, in the absence of an existing synchrotron radiation source with the anticipated NSLS-II brightness, the focus of the project has been on radiation damage to nanotubes and nanoparticles. Specifically, the goal is to answer the question of whether or not individual nanotubes and nanoparticles will be able to survive the radiation dose required to result in useful images. To pursue this, the experimental team that includes co-investigators Chi-Chang Kao, Ivan Bozovic, and James Misewich, and collaborators Aaron Stein and Matt Sfeir, have studied the radiation damage of carbon nanotubes at the Advanced Photon Source (APS). Beam time for these studies has been provided through the General User Program on microdiffraction beamline 34-ID-E.

TECHNICAL PROGRESS AND RESULTS:

Simulations to date were carried out for carbon nanotubes, and examples are displayed in Figure 1, below. The top row shows the effects of nanotube diameter for an armchair nanotube, where the spots get closer together as the diameter increased. In the first column, the manifestation of chirality can be seen: for armchair, zigzag, and chiral structures, completely different images were obtained. And finally, in the last row, the effects of an adatom, such as can be due to catalyst residue, are shown. In fact the exact position of the adatom affected the simulated scattering, which can be seen by comparing the two images for adatoms on the side versus the top of the nanotube. The take home messages of these simulations were that the expected NSLS-II performance is sufficient for the study of individual carbon nanotubes in a reasonable

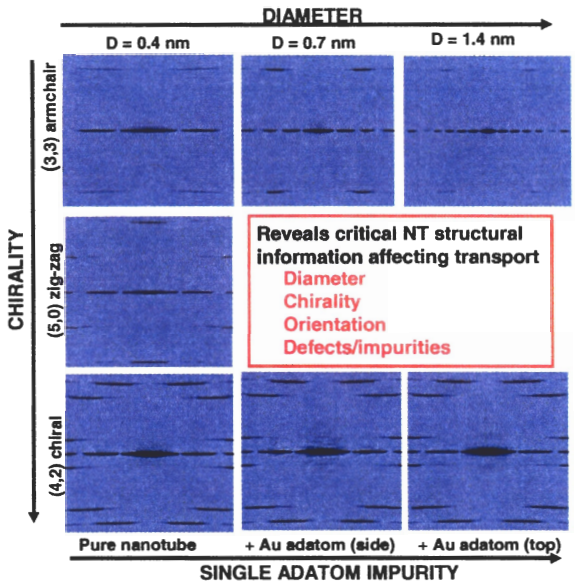

Figure 1: Simulated images of scattering in transmission mode from individual carbon nanotubes (Natasha Bozovic, Ivan Bozovic, and James Misewich).

amount of time; and second, that detailed information about the structure can be obtained.

At the APS, carbon nanotubes deposited on x-ray transparent, silicon nitride windows were exposed to a microfocused x-ray beam from an undulator source. Copper fiducials allowed the position of the ~1 μm^2 samples of interest to be monitored, and the samples were exposed for a variable amount of time in order to investigate the damage as a function of accumulated dose. As an example, "before" and "after" Scanning Electron Microscope (SEM) images for a sample that was **not** exposed to direct, focused beam, is shown in Figure 2. Note that the carbon nanotubes (string-like items) in the central part of the "before" image are essentially absent in the "after" image. These results indicated that the nanotubes did not survive even a short exposure, and also that the sample environment may be important to control.

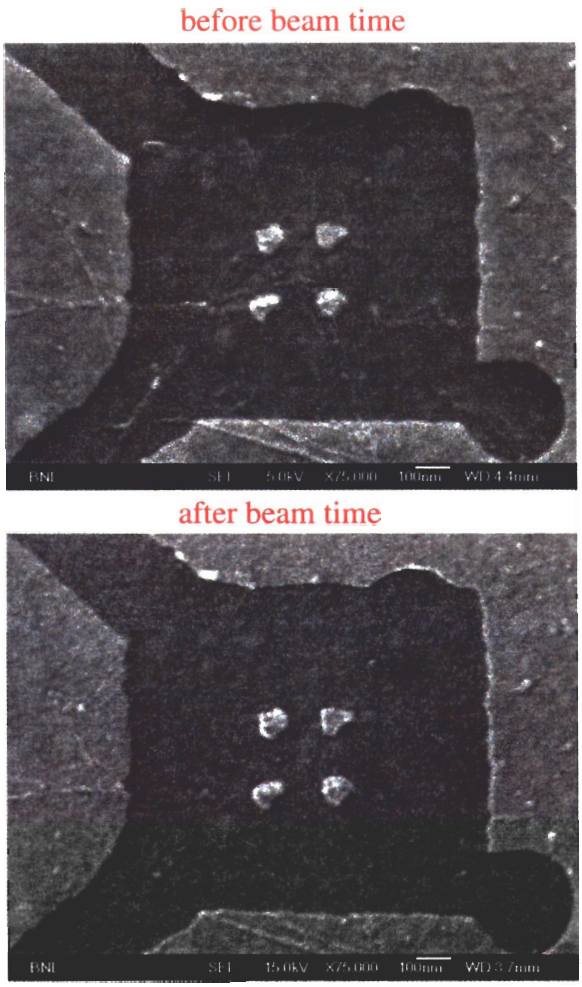

Figure 2: before and after SEM images of carbon nanotubes on a silicon nitride window.

In the next fiscal year, the theoretical work will broaden to include the contributions of Compton scattering, thermal effects, diffuse scattering, etc., to the simulations. Additionally, simulations of scattering from other nanoparticles of interest will be carried out.

Experimentally, the need for real-time monitoring of sample integrity is clear from our initial studies of carbon nanotubes. Therefore $SrRuO_3$ nanowires are currently under preparation for beam time to be carried out at the APS in December 2006. This material was chosen because it is

extremely robust and not expected to require significant control of its environment. Single nanowires — as well as arrays of nanowires — will be exposed to a focused x-ray beam while a current passing through them is monitored. These studies are anticipated to provide real-time information about any deleterious effects of the radiation on the nanowires.

SPECIFIC ACCOMPLISHMENTS:

Publications:

"Nano-crystallography of individual carbon nanotubes," N. Bozovic, I. Bozovic, and J. Misewich, in preparation.

LDRD FUNDING:

FY 2006	$ 62,673
FY 2007 (budgeted)	$132,000
FY 2008 (budgeted)	$ 66,000

High-Temperature Superconducting Magnet Development

Toshiya Tanabe *06-052*

PURPOSE:

High-Temperature Superconducting (HTS) accelerator magnets that could replace conventional synchrotron light source lattice magnets have been proposed. They are expected to reduce operating costs and to facilitate upgrades in machine performance. Present accelerator systems employ one of two magnet technologies: (a) conventional, employing room-temperature iron yokes with water-cooled copper coils; (b) low-temperature superconducting (LTS), using NbTi or Nb_3Sn superconductors cooled to around 4K by liquid helium. HTS magnet technology now offers a third option for synchrotron light sources and accelerators with moderate magnetic field requirements. In this project we seek to demonstrate technologies that are viable and provide a basis for design of future light source lattice magnets.

APPROACH:

1. We will develop cost-effective designs for form/fit/functional HTS coil/cryostat ("cryopack") replacements for copper coils in conventional sextupole magnets. We plan to use commercial first-generation HTS (BISSCO) conductor initially, but we may try 2nd generation (YBCO) or even MgB_2 conductor if these become available in practical lengths. As a case study, we will address replacing the coils in an existing NSLS sextupole magnet with HTS coil/cryostat packages. The sextupole is inherently more complex than a dipole or quadrupole, so design concepts developed here could be applicable to the other types of lattice magnets such as dipole and quadrupole.

2. We will develop integrated HTS magnet, yoke and cryostat designs, without the restriction of retrofitting existing iron yokes if possible, but maintaining a footprint and envelope comparable to the conventional magnet it is to replace. We will strive to attain higher fields than in the original magnet, to provide operating headroom and perhaps allow future performance upgrades. Several optional cooling methods will be explored, including cold gas systems and cryocoolers.

3. We will then construct and test HTS coils and "cryo-coilpacks" individually, and finally on a one-pole, magnetic equivalent to a sextupole magnet.

4. We will connect it to the cold He gas refrigerator and characterize the field quality.

5. We will generate preliminary life-cycle cost estimates for an HTS-based magnet system for a facility such as the NSLS, for example.

TECHNICAL PROGRESS AND RESULTS:

Task 1: We have conducted preliminary 3D magnetic simulations using Radia to estimate the effect of smaller coil dimensions to the resulting multipole fields. They showed little change in terms of the field quality. More elaborate simulations with Opera3d/TOSCA are in progress. An engineering design has been made and 3D CAD models have been created by Inventor®. Thermal transfer simulations using ANSYS and have been carried out to ensure that there is sufficiently uniform temperature distribution on the coils.

In order to fabricate proto type coils, we purchased BISCCO tape from American

Superconductor. However, the company discontinued the production of all BISCCO tape after our first purchase. Therefore, an alternative source (SUMITOMO Electric) has been sought and identified. We plan to purchase their tape in the coming FY. So far we have refrained from purchasing YBCO tape due to its high price at this moment. When it becomes economical, YBCO coils can replace BISCCO coils in our design with little modification.

Task 2: Our first cryostat design is based on the cold gas circulation system. Co-investigator, J. Skaritka, has completed a preliminary design of the dual helium gas circulation and heat exchange system, including selection of a cryogenic gas circulation pump and a cryocooler. Cryocooler-based HTS dipole design studies have been conducted in conjunction with the NSLS-II related project.

Task 3: We are in the middle of the fabrication process of the coils and cryostats. A new winding machine was made by modifying an existing one utilized for another NSLS project. BNL central shop has fabricated parts for the cryostat. They are being assembled at NSLS. Once coils are wound, they will be connected and the lead will be attached with the help of SMD technicians.

SPECIFIC ACCOMPLISHMENTS:

Presentations:

Tanabe, T.; Chouhan, S.; Harder, D.; Lehecka, M.; Skaritka, J.; and Rakowsky, G. "SC Magnet-Related Activities at the NSLS," Applications and Superconducting Technology in Synchrotron Light Sources, June 5-6, 2006, Hsinchu, Taiwan

LDRD FUNDING:

FY 2006	$236,846
FY 2007 (budgeted)	$214,000

Epigenetics: Methamphetamine (MAP)-Induced Brain Dysfunction and Methylation of DNA

John J. Dunn *06-056*
P. K. Thanos

PURPOSE:

Cytosine methylation is an important epigenetic DNA modification regulating mammalian gene expression. One immediate goal of this project is to develop methods for high-throughput, unbiased genome–wide identification of genic sites that show changes in DNA methylation. These data, coupled with complementary gene expression data, will be used to establish whether correlations exist in the brains of experimental animals between the position and level of DNA methylation near and within genes and levels of gene expression following administration of MAP. We anticipate that differences in methylation patterns among genes will be tissue-specific and that these changes will be associated with physiological responses to MAP and other addictive compounds; thereby providing clinically important clues to understanding the effects of addictive drugs on brain biochemistry and networks of changes that may lead or contribute to drug addiction.

One of the main challenges of this project is to optimize and standardize procedures for separating methylated and unmethylated regions of the genome that use only small quantities of starting tissue, such as those obtained following brain dissection. Another is to be able to identify the methyl-cytosine positive genic regions using the ultra high-throughput sequencing approach developed by 454 Life Sciences which utilizes a solid state, real-time method to sequence several hundred thousand single-DNA molecules in a single pass.

APPROACH:

We initially attempted to utilize a modified version of a new methyl-cytosine DNA fractionation technique developed in G. Pfeifer's group at the City of Hope, CA. In this assay a recombinant form of a mammalian methyl-cytosine binding protein (MBD2b) fused to an N-terminal glutathione-S-transferase polypeptide tag to aid in purification is used in combination with one of its cellular binding partners to form a protein-protein complex with very high affinity and specificity for DNA fragments containing methylated cytosines. The samples are then passed through a matrix which binds proteins with the glutathione-S-transferase tag. DNA fragments with methyl-cytosines are thereby retained on the matrix while unmethylated fragments pass through. A high ionic strength salt solution is used to elute the methylated fragments which are cloned into a special recombinant DNA vector, pBEST (Both End Signature Tags), which is based on the pSCANS vector developed at BNL. The original vector was modified for efficient cloning of DNA fragments in a manner that places them immediately adjacent to oppositely oriented *Mme* I recognition sequences. These are the only *Mme* I sites in the vector. Digestion with *Mme* I cleaves bidirectionally into the inserts leaving 20-21 bp DNA fragments or TAGs attached to the vector. In subsequent steps the linearized vector DNAs with attached TAGS on each end are converted into circular DNA molecules while maintaining the TAG fragments spatial relationship to each other to form what we term diTAGs. During this step a synthetic DNA barcode is added to each separate sample

to aid in identifying the source of the sample used to form the diTAGs during subsequent high-throughput DNA sequencing.

TECHNICAL PROGRESS AND RESULTS:

Initial attempts to produce the recombinant MBD2b and MBD3L1 proteins in the expression vectors provided by Pfeifer's lab were unsatisfactory: i.e. poor solubility after expression in *E. coli*, difficulty in downstream purification, especially of the glutathione-S-transferase tagged MBD2b protein, and lack of reproducibility in their use for affinity purification of DNA fragments with methylated cytosines. Since most of these problems seemed to be caused by the glutathione-S-transferase tagged MBD2b protein, we recloned the MBD2b portion into a double affinity tag expression vector we constructed specifically to overcome the problems inherent with the use of a glutathione-S-transferase fusion tag. In this vector the MBD2b coding sequence is now fused to an amino-terminal poly-histidine amino acid tag followed by a polypeptide sequence that allows the recombinant protein to interact with streptavidin. Our preliminary studies with this new system look very encouraging, i.e. the double tagged MBD2b protein is expressed at very high levels when placed behind a bacteriophage T7 promoter and most of the protein is solubil. Furthermore, it can easily be purified via affinity chromatography on Ni-NTA (nickel-nitrilotriacetic acid) resin and eluted with immidazole or by chromatography on immobilized streptavidin followed by elution with biotin. Experiments are now in progress to separately purify our form of MBD2b and the Pfiefer's lab version of MBD3L1 since it also has an amino-terminal poly-histidine amino acid affinity tag by Ni-NTA affinity chromatography. We will then mix the two purified proteins and apply the mixture to a streptavidin column and elute the bound material with biotin. Since MBD3LI lacks a streptavidin binding sequence it will not bind to immobilized streptavidin unless it forms a protein-protein complex with MBD2b; therefore, retention of both proteins on the streptavidin matrix followed by their elution with biotin would demonstrate that they had successfully formed a protein-protein complex and by inference are presumably biologically active. The purified complexes will then be used to separate unmethylated from methylated DNA fragments in DNA samples obtained from brain segments of rodents administered MAP or matched controls. The methylated fractions from the experimental and control animals will then be cloned into our pBEST diTAG vector to begin sequence analysis aimed at obtaining genome-wide high-resolution maps of the methylated genic loci in both samples.

This project involves animal vertebrates (approval on file).

SPECIFIC ACCOMPLISHMENTS:

Brain region morphological and volumetric quantitative assessment using the 17.6T MRI in rats chronically exposed to methylphenidate (MP). V. Boronikolas, M. Michaelides, G. Wang, S. Blackband, S. C. Grant, D. N. Metaxas, J. Zhou, N.D. Volkow, and P. K. Thanos.
Poster presentation at Neuroscience 2006 Annual Meeting, Society for Neuroscience, October 14-18, 2006, Atlanta, GA.

LDRD FUNDING:

FY 2006	$ 76,620
FY 2007 (budgeted)	$181,000
FY 2008 (budgeted)	$ 87,000

Molecular Mechanism of Chromosomal Replication Initiation in Eukaryotic System

Huilin Li *06-060*

PURPOSE:

The yeast Original Recognition Complex (ORC) is a six-protein molecular machine that constitutively labels the chromosome replication origin and helps to initiate replication process. Our goal is to determine the molecular architecture of ORC by electron microscopy (EM) and image processing. Structures of ORC and ORC in complexation with initiation factor Cdc6 at medium resolution will provide insight into the mechanism of DNA replication initiation.

APPROACH:

Eukaryotic chromosomal replication is an intricate process that requires the coordinated and tightly regulated action of numerous molecular machines. Failure to ensure once only replication initiation per cell cycle can result in uncontrolled proliferation and genomic instability, two hallmarks of tumorigenesis. The yeast ORC constitutively binds to and marks the replication origin throughout the cell cycle. Licensing of the DNA replication origin starts when the critical cell division cycle protein Cdc6p binds to ORC. Cdc6p binding activates an ATPase switch in ORC. This activation causes an extended pre-replication complex (pre-RC)-like nuclease protection footprint on origin DNA. Our preliminary EM work reveals a ring-like structural feature in the ORC-Cdc6p complex that is similar in size to the replicative hexameric MCM helicase. This result supports the emerging concept that the helicase is loaded by replication initiators in a mechanism similar to the loading of the DNA polymerase clamp PCNA by the RF-C clamp loader complex. The formation of the extended pre-RC-like footprint by ORC and Cdc6p, a crucial event in replication origin licensing, is ATP-binding and -hydrolysis dependent.

Our goals are to (1) define the molecular organization of the ORC, and (2) investigate the conformational changes of ORC-Cdc6 upon ATP binding and hydrolysis events that underlie the DNA melting and helicase loading process.

This work is in collaboration with Dr. Bruce Stillman at Cold Spring Harbor Laboratory. The Stillman lab performs molecular biology and biochemical portion of the work, and BNL carries out the cryo-EM and image processing and structural reconstruction.

TECHNICAL PROGRESS AND RESULTS:

We focused on and have completed our first goal of defining the ORC organization. We utilized a maltose binding protein (MBP) fusion approach and designed a unique EM image classification procedure for this purpose. The MBP fusion approach eliminated the uncertain occupancy and unspecific binding problems associated with the traditional immuno-labeling and the functionalized nanogold-labeling methods. The MBP fusion constructs were found to be active in origin DNA binding and competent for Cdc6 interaction. The unique image classification procedure we developed anticipated and dealt with the flexibility problem of the fusion protein. With this approach, we successfully mapped all six subunits of the ORC complex, thus providing unambiguous determination of the overall organization of the ORC. The detailed ORC architecture suggested

potential modes of interaction with DNA origins.

To complement our structural studies, the Stillman lab conducted the molecular biology and biochemical studies to verify the binary protein interactions identified in our EM work. Their *in vivo* studies so far met with difficulty because the individually expressed component proteins were sticky and aggregated in cell. To overcome the problem the *in vitro* translation approach has been initiated, and the work is in progress.

Our research plan for FY 2007 is to investigate the conformational changes of ORC-Cdc6 protein complex during the ATP cycle.

SPECIFIC ACCOMPLISHMENTS:

Publications:

Dimeric organization of the yeast oligosaccharyl transferase complex. Chavan, M.; Chen, Z.; Li, G.; Schindelin, H.; Lennarz, W. J.; and Li, H. Proc. Natl. Acad. Sci. USA 103(24), 8947-8952 (2006).

Electron microscopic structure of purified, active gamma-secretase reveals an aqueous intramembrane chamber and two pores. Lazarov, V. K.; Fraering, P. C.; Ye, W.; Wolfe, M. S.; Selkoe, D. J.; and Li, H. Proc. Natl. Acad. Sci. USA 103(18), 6889-6894 (2006).

Inhibitors of amyloid toxicity based on beta-sheet packing of Aβ40 and Aβ42. Sato, T.; Kienlen-Campard, P.; Ahmed, M.; Liu, W.; Li, H.; Elliott, J. I.; Aimoto, S.; Constantinescu, S. N.; Octave, J. N.; and Smith, S. O. Biochemistry 45(17), 5503-5516 (2006).

LDRD FUNDING:

FY 2006	$101,859
FY 2007 (budgeted)	$208,000
FY 2008 (budgeted)	$106,000

Diversification of Isoflavonoid Biosynthesis

Chang-Jun Liu *06-061*

PURPOSE:

Plant phenolics play vital roles in plant structure construction and plant defense responses. Isoflavonoids, as a large family of polyphenolics, are the major anti-microbial phytoalexins in plant-pathogen interactions, and the signaling molecules mediating plant-microbial symbioses for N2 fixation or Pi absorption. In addition, isoflavonoids constitute the most potent group of phytoestrogens with potential dietary utility in the prevention of several lines of human diseases and disorder. Diverse biological activities of isoflavonoids lie on their characteristic chemical structures. The biosynthesis leading to a variety of isoflavonoids remains to be further elucidated as the catalytic mechanisms of the key enzymes that govern the formation of the characteristic chemicals are elusive. In addition, the structurally diversified isoflavonoid chemical libraries are required for exploring their biological values. The goal of this project is to characterize the key biosynthetic enzymes responsible for isoflavonoid formation; to explore the structure and function of the key enzymes; and to apply the means of structure-based protein evolution to diversify isoflavonoid biosynthesis.

APPROACH:

We are applying biochemical genomics, X-ray crystallographic structural biology and protein mutagenesis/engineering approaches to functionally characterize isoflavonoid biosynthetic enzymes responsible for O-methyl- and O-acylation; to determine the structures of those methyl- and acyltransferases; and to systemically engineer isoflavonoid hydroxylase functionalities. Part of the work is in collaboration with R. A. Dixon at the Noble Foundation and J. P. Noel at the Salk Institute.

TECHNICAL PROGRESS AND RESULTS:

We conducted several lines of studies on the structure and function characterization of (iso)flavonoid methyltransferases and acyltransferases, and the protein engineering for hydroxylases.

- We did comprehensive data mining on the EST database of model legume plant *Medicago truncatula* and identified 77 putative genes encoding (iso)flavonoid acyltransferases.
- We developed a rapid analytical procedure for genome wide functional identification of plant acyltransferases. Applying this procedure, we characterized 5 acyl (acetyl and malonyl)transferases responsible for (iso)flavonoid modification. Subsequently, we initiated X-ray crystallographic studies on those enzymes.
- Working with our collaborators, we characterized a group of isoflavonoid *O*-methyltransferases. Subsequently, we determined several sets of crystal structures of *O*-methyltransferases in complex with different substrates and created sets of enzyme variants in order to probe their regio- specific methylation.
- Attempting to engineer P450 enzymes to diversify isoflavonoid chemical structures, we performed homology modeling and molecular docking analyses on isoflavone hydroxylases, identified the key amino acids that potentially control the specific hydroxylation. We designed a combinatorial rational mutagenesis strategy and created 18 combinatorial mutants by SCOPE. Meanwhile, we screened and expressed the mutant variants in yeast and determined their *in vivo* functions by Liquid Chromotography Mass Spectrometry and by colorimetric assay.

The knowledge gained from these studies will lead to a more complete understanding of the molecular basis that underlies the complexity of (iso)flavonoid biosynthesis and will eventually benefit for creating healthier biomass production plants.

In FY 2007, we will continue the structure-function studies on several sets of acyltransferases and methyltransferases, and will adopt additional biochemical and biophysical techniques to further probe the enzyme catalytic properties and mechanisms. We will also purify the created isoflavonoid hydroxylase mutant enzymes (yeast microsome) and conduct cell free *in vitro* assays. Subsequently, we will identify and structurally elucidate the hydroxylated products.

SPECIFIC ACCOMPLISHMENTS:

Publications:

Methylation of sulfhydryl groups: a new function in a family of plant *O*-methyltransferases. Coiner, H.; Schröder, G.; Wehinger, E.; Liu, C.-J.; Noel, J. P.; Schwab, W.; and Schröder, J. Plant J. 46, 193-205 (2006).

Functional analysis of members of the isoflavone and isoflavanone *O*-methyltransferase enzyme families from the model legume *Medicago truncatula.* Deavours, B. E.; Liu, C.-J.; Naoumkina, M.; Tang, Y.; Farag, M. A.; Sumner, L. W.; Noel, J. P.; and Dixon, R. A. Plant Mol. Biol. 62, 715-733 (2006).

Flavonoids: Recent advances in molecular biology, biochemistry, pharmaceutical applications and metabolic engineering. Liu, C.-J. and Noel, J. P. *Plant Genetic Engineering*, Vol. 7: Metabolic Engineering and Molecular Farming-1, P. K. Jaiwal, ed., pp. 225-259, Studium Press, LLC, Houston, TX (2006).

Development of an analytical method for genome-wide functional identification of plant acyl-CoA dependent acyltransferases. Yu, X.-H. and Liu, C.-J. Anal. Biochem. 358, 146-148 (2006).

Structural basis for dual functionality of isoflavonoid *O*-methyltransferases in the evolution of plant defense responses. Liu, C.-J.; Deavours, B. E.; Richard, S. B.; Ferrer, J.-L.; Blount, J. B.; Dixon, R. A.; and Noel, J. P. Plant Cell (in press).

Biochemical and structural bases for (iso)flavonoid biosynthetic diversity. Liu, C.-J.; Wang, C.; Noel, J. P.; and Dixon, R. A. Congress Proceedings of the 11th International Association for Plant Tissue Culture and Biotechnology (IAPTC&B) Congress, August 13-18, 2006 in Beijing, P.R. China, Kluwer Academic Publishers, China (in press).

Investigating allelochemical biosynthesis in *Sorghum* root hairs by EST mining: Characterization of a 5-*n*-alk(en)ylresorcinol *O*-methyltransferase proposed for the biosynthesis of the allelopathic benzoquinone sorgoleone. Baerson, S. R.; Dayan, F. E.; Rimando, A. M.; Dhammika Nanayakkara, N. P.; Liu, C.-J.; Schröder, J.; Fishbein, M.; Pan, Z.; Kagan, I. A.; Pratt, L. H.; Cordonnier-Pratt, M.-M.; and Duke, S. O. Plant Cell (in revision).

Different genetic and cellular mechanisms underly isoflavonoid phytoalexin accumulation in response to pathogen- or wound-signals in the model legume *Medicago truncatula.* Naoumkina, M.; Farag, M.; Sumner, L. W.; Tang, Y.; Liu, C.-J.; and Dixon, R. A. Proc. Natl. Acad. Sci. USA (submitted).

LDRD FUNDING:

FY 2006	$437,328
FY 2007 (budgeted)	$481,000

Metabolic Flux Analysis in *Arabidopsis thaliana*

Jorg Schwender *06-065*

PURPOSE:

The objective of this LDRD project is to study the formation of different seed storage products in *Arabidopsis thaliana*, a well characterized plant model organism. This will lead to an understanding of how plants allocate carbon into different storage and biomass compounds. Methods of *in-vivo* ^{13}C-steady state metabolic flux analysis will be applied to developing seeds of *Arabidopsis thaliana*. A large number of mutant lines and other genomic resources are available in *A. thaliana* that can be used to study the impact of genetic modifications in central metabolism by means of detailed flux maps. In addition, ^{13}C-tracer methods will be adapted to enable medium throughput fluxome profiling, allowing fingerprinting of metabolic phenotypes prior to detailed, more time consuming flux analysis studies.

APPROACH:

Systems biology approaches employing genomics, metabolomics and similar techniques provide plentiful information that identifies and describes parts of cellular infrastructure like genes, enzymes and metabolites. So far the *in vivo* function of the cellular metabolic infrastructure cannot be predicted from this kind of information. Metabolic Flux Analysis (MFA) allows measuring cellular biochemical conversions *in-vivo*, i.e. to quantify the interaction of enzymes and metabolites within the living cell. By use of stable isotope tracers, MFA can help to lead to an understanding of the complex effects of changes in genotype on the metabolic phenotype.

Two principal types of insights can be expected from this research. First, for transgenics which have a severe phenotype of altered seed composition, flux maps may identify metabolic branchpoints where carbon flux is redirected to other end products. Second, for transgenics altered in the functionality of the central metabolism but without metabolic phenotype, the flux maps may reveal how redundant metabolic functions (like bypass routes) compensate for the loss of a metabolic connection.

TECHNICAL PROGRESS AND RESULTS:

- Microscopic dissection and culture of growing embryos from *Arabidopsis thaliana* was established.
- In order to analyze labeled biomass of the very small embryos of *A. thaliana*, the existing extraction and derivatization procedures were scaled down, allowing GC/MS analysis by maintaining the quality of the resulting data.
- Appropriate ^{13}C-labeled precursors have been identified.
- Different *Arabidopsis* wild types were compared to each other using [U-^{13}C]glucose as a tracer. The labeling profiles were highly correlated. We conclude that different transgenics with different genetic background (wild type) can be compared to each other to reveal differences caused by the transgenic event.
- Different mutants were compared based on a flux fingerprinting approach, which allows discerning quickly if in a given mutant any change in metabolic flux can be detected by the applied ^{13}C-tracer technique.

In FY 2007 the detailed characterization of several mutants with severely changed seed

composition will be explored. In addition, in order to allow medium throughput analysis, the quantification of embryo biomass components has to be improved in order to obtain accurate measurements in very small sample sizes. For this purpose it is planned to quantify oil, protein, and carbohydrate content by using FTIR microscopy. In addition, after recent reports on successful use of antisense oligo-deoxynucleotide inhibition in plant tissues, we will try to inhibit gene expression in cultured *A. thaliana* embryos by addition of anti-sense oligo's targeted against specific genes of interest into the growth medium.

SPECIFIC ACCOMPLISHMENTS:

Publication:

Mitochondrial metabolism in developing embryos of *Brassica napus*. Schwender, J.; Shachar-Hill, Y.; Ohlrogge, J. J.; Biol. Chem. 281(45), 34040–34047 (2006).

LDRD FUNDING:

FY 2006	$425,511
FY 2007 (budgeted)	$481,000

Transformation and Fate of Nanoparticles in the Environment

Jeffrey Fitts *06-066*
O. Gang

PURPOSE:

The objective of this work is to determine how the molecular-level chemical characteristics of the organic shell and inorganic core components of water-soluble nanoparticles govern their transformation and fate in the natural environment. Our results will demonstrate that ongoing studies of this type are required in order to produce accurate toxicity and environmental risk assessments of nanoparticles.

APPROACH:

This work focuses on the behavior of water-soluble nanoparticles because they pose the greatest risk to the environment and humans. This type of particle is typically composed of an inorganic, often crystalline core, and an organic outer shell, which is necessary to prevent particle aggregation and modify the nanoparticle surface charge. Based on our knowledge of contaminant behavior, once these nanoparticles are released into the environment they will interact with microbiota, which are ubiquitous in soils and water resources, and this will result in 1) modification of the molecular chemical nature of the particle, specifically the crystalline core and/or 2) profound changes in the surface chemistry of a particle's organic shell.

This work seeks to develop an understanding of the interactions between naturally-occurring soil and groundwater microorganisms with functionalized nanoparticles, specifically, organic-coated cadmium selenide (CdSe) and gold (Au) nanoparticles. This work is done in collaboration with Post Doc Garry Crosson. In order to study processes specific to the inorganic core, we use commercially available CdSe quantum dots, given that the oxidized breakdown products are known toxins and both the nanocrystalline core and reaction products are ideally suited to synchrotron-based studies at the NSLS. In contrast, Oleg Gang and Matthew Maye (Center for Functional Nanomaterials) synthesize Au nanoparticles with a variety of organic functionalizations. By contrasting different functionalities we investigate mechanisms of nanoparticle reactivity and transport that depend on the organic coating.

We study nanoparticle chemistry in pure cultures and cultures containing important soil minerals. In addition, advective-flow soil-column experiments are in the planning stages. The pure cultures of bacteria used include an aerobic (O_2-respiring) strain *Pseudomonas fluorescens* and an anaerobic (fermentative) strain *Clostridium* sp. and soil minerals including quartz sand, clays and iron oxides. Abiotic and biotic processes are examined to understand the role of microbiota and soil minerals in modifying transport behavior.

The fate of the nanoparticles in the soil matrix of the batch studies, soil columns and column effluent is characterized on a macroscopic scale by determining a distribution coefficient (Kd) for each type of nanoparticle and on the molecular scale in terms of their physical chemical state (e.g., dispersed in solution, mineral or cell-surface embedded in an extracellular matrix, or localized intracellularly). A suite of methods are used to determine the molecular scale interactions including transmission electron microscopy (TEM) at the CFN with Dr. Eli Sutter, scanning electron microscopy (SEM) at Stony Brook University (SBU)

with Dr. James Quinn, and scanning transmission x-ray microscopy (STXM) at the NSLS with Prof. Chris Jacobson (SBU). The chemical modification of the nanoparticle crystal core and organic surface will be interrogated by spectroscopic methods at the NSLS with Dr. James Ablett.

The molecular scale studies are used to identify the predominant mechanisms of biotransformation in order to understand how such transformations affect nanoparticle fate and transport. Ultimately this information is included in risk assessment models of nanoparticles by collaborating with Dr. Vasilis Fthenakis (BNL).

TECHNICAL PROGRESS AND RESULTS:

We have studied citrate-capped Au nanoparticles over a range of particle diameter in pure bacterial cultures and mineral batches. SEM and TEM studies suggest that the Au nanoparticles interact with aerobic bacteria (*Pseudomonas fluorescens*) but do not penetrate the cell wall. Most significantly this type of nanoparticle preferentially interacts with and aggregates in the extracellular organic matrix of an anaerobic bacterium versus the bacterial cell wall. This organic matrix is only produced by certain bacterial species. In addition, studies of these same nanoparticles in batches containing bacteria and quartz sand indicate that nanoparticle attenuation only occurs when soil bacteria are present. These results provide a powerful example of the importance of understanding the charge, reactivity and stability of the organic shell of water soluble nanoparticles when predicting their fate and transport.

In FY 2007 it will be important to synthesize Au nanoparticles with functional organic shells that possess different charge characteristics and then repeat the pure culture and batch experiments in order to contrast the effect on bacterial interactions. In addition, studies of Au and CdSe nanoparticles in soil columns will be conducted to quantify their transport behavior. We plan to conduct the CdSe soil column experiments in collaboration with Dr. V. Fthenakis and Prof. Kartik Chandran (Columbia University).

SPECIFIC ACCOMPLISHMENTS:

"*Natural Attenuation of Vinyl Chloride Compared to Enhanced In Situ Degradation by Particulate Zero Valent Iron*" PI of proposal submitted to Strategic Environmental Research And Development Program (SERDP) along with Co-PIs Jeff Gillow (EE), Dev Chidambaram (EE), Rich Ferreri (Chem) and Dave Schlyer (Chem); (submitted March 8, 2006; requested $300K/yr for three years; rejected August 2006).

"*Life Cycle Analysis of nanomaterials*" proposal submitted to EPA through Columbia University; Jeffrey Fitts is listed as a collaborator; (submitted April 2006, pending; funding level for this activity has yet to be determined)

Presentation

"Biotransformations of Engineered Nano-particles in the Environment" Jeffrey P. Fitts, Jeffrey B. Gillow, Garry Crosson, Mathew Maye, and Oleg Gang oral presentation at the Geological Society of America National meeting Philadelphia, PA October 22, 2006.

LDRD FUNDING:

FY 2006	$140,086
FY 2007 (budgeted)	$148,000

Development of a Cloud Condensation Nucleus Separator

Jian Wang *06-071*

PURPOSE:

The technical objective of this project is to develop a novel Cloud Condensation Nucleus Separator (CCN separator) that is capable of separating CCN and non-CCN at climatically important supersaturations. Once the CCN and non-CCN are separated, their microphysical, chemical, and optical properties can be further analyzed using a variety of aerosol instruments. Detailed studies can be carried out on what type of aerosols and how those aerosols affect the properties of clouds, which will lead to an improved understanding of the aerosol indirect effect on global climate. The development of the CCN separator supports the laboratory strategic research initiative of Aerosol Research, and is closely related to the Atmospheric Science Program of DOE. Given its unique capability, the CCN separator would likely be deployed in field studies with aerosol instruments from other research institutions.

APPROACH:

Atmospheric aerosols could strongly influence the climate by scattering and absorbing sunlight (direct effect) and by changing the microphysical structure, lifetime, and amount of clouds (indirect effect). Among the effects of aerosol on climate, the indirect effects of aerosol are the most uncertain components in climate systems. Successful prediction of aerosol effects on climate requires a detailed understanding of the aerosol indirect effects, i.e. what type of aerosols and how those aerosols affect cloud properties. Among aerosol particles, only those that can grow into cloud droplets at certain supersaturations, which are also called cloud condensation nucleus (CCN), affect the cloud properties. Whether a particle can serve as a CCN under particular supersaturations depends on its physical size, chemical composition, water solubility, and surface property, etc. Detailed understanding of aerosol indirect effects necessities characterizing the physical and chemical properties of CCN in different air masses and under a variety of meteorological conditions. Such studies are very rare, mainly due to the lack of a method for separating the CCN from the rest of aerosol particles (non-CCN).

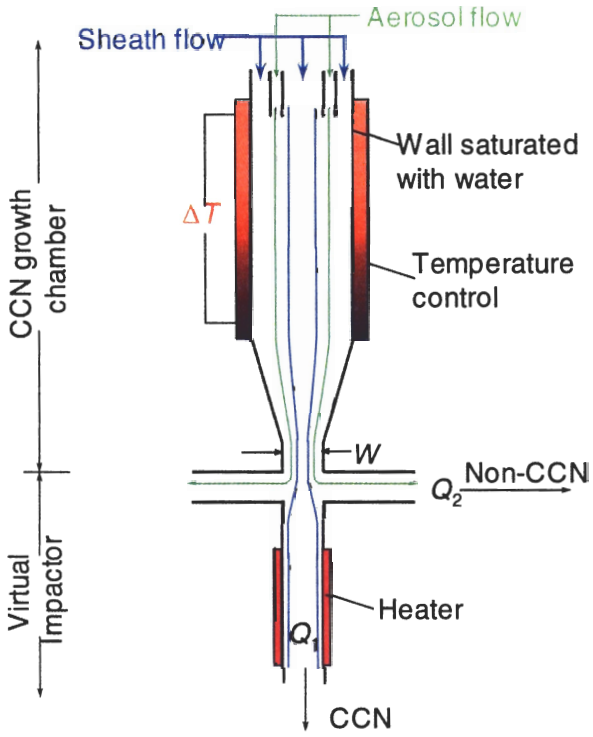

Figure 1. Schematic of the CCN separator.

The proposed CCN separator is capable of separating CCN and non-CCN under climatically important supersaturations. The schematic of the CCN separator is given in Figure 1. The CCN separator consists of two major components. The first

component is a CCN growth chamber that grows CCN into supermicron droplets under a prescribed supersaturation. The growth chamber is a cylindrical column, and its inner wall is made of porous ceramic that is maintained wet with water. Precise temperature controls are applied to generate a linear temperature gradient along the axial direction of the column. Due to the differences in water vapor diffusivity and air thermal diffusivity, a constant supersaturation is achieved near the centerline of the column. A wide range of supersaturations can be achieved by varying the flow rate, and the temperature gradient. The aerosol sample is introduced from the top of the column, and is confined in an annulus region sandwiched by particle-free sheath flows. Exposed to the supersaturation environment, CCN will grow into supermicron droplets at the end of the growth chamber. The grown droplets, along with non-CCN that remain unactivated, are then accelerated out of the chamber in a jet flow through a focusing nozzle. The second component, a Virtual Impactor (VI), separates the grown droplets and non-CCN by taking advantage of the substantial differences in their inertia. Non-CCNs, which are small and have little inertia, follows the gas flow streamline and exit from the sides (Q_2 Fig. 1). In contrast, supermicron droplets that are activated from CCN have enough inertia to cross the flow streamlines and be collected by the flow Q_1 (Fig.1). After separation, the CCN and non-CCN can be subsequently characterized using a suite of aerosol instruments.

TECHNICAL PROGRESS AND RESULTS:

We have carried out detailed simulations of the CCN separator and finalized its design. Detailed simulations revealed that the original proposed design, which employs a Counter-Flow Virtual Impactor, is not capable of separating grown CCN from non-CCN at low but climatically important supersaturations. The current design uses a Virtual Impactor, which significantly improves the performance of separation. Simulation showed the current design is capable of separating grown CCN from non-CCN at supersaturations as low as 0.1%. The physical dimensions and operation parameters have been determined. The operating flow rate of the CCN separator will increase accordingly with increasing supersaturation. At lower supersaturations, a lower flow rate will be used to increase the residence time of the particles within the growth chamber, which allows CCNs to grow into sufficiently large sizes and be separated. At high supersaturations, droplets grow faster, and operating at a higher flow rate increases the sample rate and statistics of further characterizations. The mechanical design of the instrument is underway.

In FY 2007, we will complete the mechanical design and the construction of the CCN separator. The performance of the CCN separator will be tested using particles of known CCN activities.

LDRD FUNDING:

FY 2006	$ 69,661
FY 2007 (budgeted)	$140,000
FY 2008 (budgeted)	$ 70,000

Aluminum Hydride – An Ideal Hydrogen Source for Small Fuel Cells

Jason Graetz *06-074*

PURPOSE:

The purpose of this project is to synthesize and characterize three crystalline polymorphs of AlH_3: α, β and γ. The crystallographic structures and the thermodynamic properties of each of the phases will be determined. This data will be used to establish the relative stabilities of the different AlH_3 polymorph structures. In addition, the thermodynamic data will allow us to adjudicate a discrepancy reported for α-AlH_3 that has been unresolved for the past 20 years. Finally, the development of a more convenient synthesis route and the possibility of using AlH_3 as a hydrogen source for small fuel cells will also be explored.

APPROACH:

The renewed interest in the "concept of a hydrogen economy" provides the motivation for this study. The approach is to prepare different polymorphs of AlH_3 (α, β and γ) using an organometallic synthesis route. Low temperature H_2 evolution rates will be measured by isothermal decomposition in a Sievert's type apparatus for all three polymorphs. Structural characterizations of γ and β AlH_3 and AlD_3 will be performed using synchrotron x-ray powder diffraction at the NSLS and neutron powder diffraction at IFE (Norway), respectively. Thermodynamic values will be measured using differential scanning calorimetry. The possibility of hydrogenating Al metal (to form AlH_3) under high pressure will also be investigated.

TECHNICAL PROGRESS AND RESULTS:

Technical progress was realized for the AlH_3 polymorphs in three areas; 1) low temperature decomposition rates were measured; 2) the crystallographic structure of β-AlH_3 was determined; 3) the thermodynamic properties were measured at ambient pressure.

The potential of using aluminum hydride as a hydrogen storage medium has been explored. We found that the H_2 evolution rates for freshly prepared of α, β, and γ-AlH_3 (undoped) meet the DOE full flow target for a 50 kW fuel cell (1 gH_2/s) at 114°C (based on 100 kg AlH_3). At low temperatures (<60 °C) the β and γ phases decompose more rapidly than the α phase. The most significant low temperature decomposition was observed in γ-AlH_3, which decomposed at a steady rate of 6.0 gH_2/h at 28 °C.

Structural characterization using x-ray and neutron powder diffraction revealed that β-AlH_3 (and β-AlD_3) crystallize in the *Fd-3m* space group. Similar to α-AlH3 (R-3c), the structure is composed of corner connected AlH_6 octahedra with each H atom forming a bridging bond between octahedra.

The decomposition thermodynamics were measured using differential scanning calorimetry and ex situ x-ray diffraction. The decomposition of the less stable polymorphs, β and γ-AlH_3, occurs by an exothermic transformation to the α phase (~100° C) followed by the decomposition of α-AlH_3. Preliminary high-pressure studies of α-AlH_3 suggest that a H_2 gas pressure of ~7 kbar is required to hydrogenate Al metal to form α-AlH_3.

SPECIFIC ACCOMPLISHMENTS:

Publications:

H.W. Brinks, W. Langley, C.M. Jensen, J. Graetz, J.J. Reilly, B.C. Hauback, "Synthesis and crystal structure of β-AlD_3" *J. Alloys Compd.*, in press (2006).

S. Chaudhuri, J. Graetz A. Ignatov, J. J. Reilly and J. T. Muckerman, "Understanding the role of Ti in reversible hydrogen storage as sodium alanate: A combined experimental and first-principles theoretical approach" *J. Amer. Chem. Soc.* **128** 11404 (2006).

J. Graetz and J. J. Reilly, "Thermodynamics of the α, β and γ polymorphs of AlH_3" *J. Alloys Comp.*, **424** 262 (2006)

G. Sandrock, J. Reilly, J. Graetz, W.-M. Zhou, J. Johnson and J. Wegrzyn, "Alkali metal hydride doping of α-AlH_3 for enhanced H_2 desorption kinetics" *J. Alloys Comp.*, **421** 185 (2006).

Meetings, Proceedings, and Abstracts:

"Bonding and Local Atomic Structure of Ti in Complex Metal Hydrides", *Spring Meeting of the Materials Research Society*, 2006.

"Thermodynamics and Kinetics of the aluminum hydride polymorphs", *Spring Meeting of the Materials Research Society*, 2006.

"Aluminum Hydride (AlH_3) as a Hydrogen Storage Compound" (invited), *TMS Annual Meeting*, 2006.

"Kinetics and Thermodynamics of the Aluminum Hydride Polymorphs" (invited), International Symposium on Metal-Hydrogen Systems, 2006.

Jason Graetz received the Ewald Wicke Award for research on metal hydrides originating in part from this LDRD.

LDRD FUNDING:

FY 2006	$132,601
FY 2007 (budgeted)	$134,000

Gamma Ray Imager for National Security Applications

Peter Vanier *06-087*
P. Vaska

PURPOSE:

Our goal is to develop a compact and robust, room-temperature gamma-ray imager which can be used to detect, localize, and identify illicit nuclear materials. We are examining the performance of a scintillator-based coded aperture prototype for this application, which is readily expandable to larger areas and hence larger sensitivities. This will potentially culminate in a practical system that fulfills a critical need in the nation's security infrastructure.

APPROACH:

Our approach is to combine BNL's expertise in homeland security (NNSD), medical imaging (Medical Department), and electronics (Instrumentation Division) to deliver a unique and practical device for this application. We have chosen the coded aperture approach because it is the most efficient to image the localized radiation sources expected in this application.

Proven scintillator/photosensor technology provides very high counting efficiency with some ability for isotope identification. Specifically, the bright and efficient scintillator, gadolinium oxyorthosilicate (GSO), was selected and coupled to solid-state avalanche photodiode (APD) photosensors. This combination is fully compatible with a highly integrated, low-power readout microchip in development by the Instrumentation Division. This chip was designed for detectors based on a similar scintillator containing lutetium (LSO), but LSO has a high intrinsic background radioactivity from lutetium. GSO is similar in many respects, such as the required shaping time, but has essentially no activity.

The microchip couples directly to a data acquisition system which has been developed and validated for the RatCAP project, providing a very compact, robust and practical data acquisition backbone. An overview of the system is shown in Figure 1.

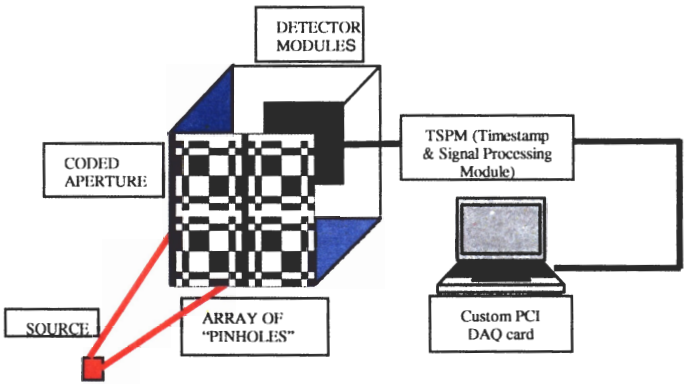

Figure 1. System overview.

TECHNICAL PROGRESS AND RESULTS:

We studied the various options available and completed the design of the first prototype imager, which includes a detector area of 10 cm x 10 cm and a coded aperture mask of twice that dimension. While the finished GSO crystals are more or less readily available directly from the manufacturer (Hitachi) in custom sizes, the APDs have required more negotiations with the manufacturer to achieve an optimum geometry with minimal gaps between individual APDs. Fortunately, Hamamatsu, which manufactures the highest quality APDs on the market, has been willing negotiate with us, partly based on the understanding that this might ultimately be a high-volume market for them. We have settled on 5 mm x 5 mm APDs on a 6.4 mm pitch, which covers the 10 cm x 10 cm area with a 15 x 15 array of APDs. An individual

GSO crystal size of 5 x 5 x 20 mm has already been quoted by Hitachi. We are awaiting a final quotation from Hamamatsu on the APDs.

Meanwhile tests were carried out on the energy resolution of a GSO crystal on a Hamamatsu 5 x 5 mm APD. Figure 2 shows that although the light output is significantly lower than LSO, the energy resolution degrades only slightly, from 16% FWHM at 511 keV for LSO, to 19% for GSO.

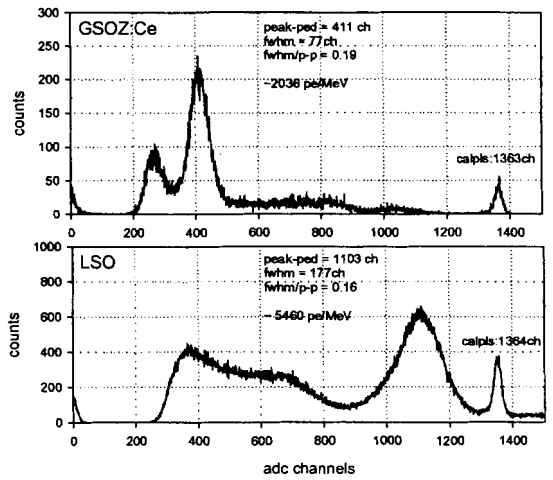

Figure 2. Energy spectra for LSO and GSO on Hamamatsu 5 x 5 mm APD for 511 keV gamma-rays.

The 225 detector channels can be read out and processed with 8 of the 32-channel ASIC microchips developed originally for the RatCAP PET imager. This is fewer than the 12 chips accommodated by the RatCAP data acquisition system, so all of the RatCAP data acquisition components can be used without modification. A new microchip was developed and manufactured in the past year which has many additional capabilities, including variable gain for each channel and an upper level discriminator, which allows true energy windowing (a feature that was added specifically for this project).

A supply of machinable tungsten was obtained in the form of sintered plates approximately 1 cm thick. The shield box for the imager and the coded aperture were designed. A simple mask pattern was chosen to locate a point source and provide data on signal-to-background ratio as well as spatial resolution.

In FY07, we will complete the procurement of GSO crystals and APDs, fabricate a PC board to accommodate the APDs and the improved version of the ASIC microchips, complete the shield box and mask, and assemble and test the whole system.

In parallel, we will evaluate the potential of different scintillators, photosensors, and electronics for the imager. Specifically, we will evaluate higher resolution scintillators such as $LaBr_3$ and $CeBr_3$, higher gain photosensors such as silicon photomultipliers (prototypes of which are now available from multiple vendors), and a data acquisition system which records gamma energies for isotope identification.

Note also that the medical imaging physics group within the Brookhaven PET group plans to hire a new postdoc and the lead candidate (from Glen Knoll's group at U. Michigan) at present happens to have significant experience and interest in coded aperture imaging for homeland security applications.

SPECIFIC ACCOMPLISHMENTS:

None.

LDRD FUNDING:

FY 2006	$110,380
FY 2007 (budgeted)	$134,000

Neurogenomics:
Collaboration between the Biology Department and the Brookhaven Center for Translational Neuroimaging to Investigate Complex Disease States

Nelly Alia-Klein *06-088*

PURPOSE:

This proposal represents a joint effort by the Biology Department and the *Brookhaven Center for Translational Neuroimaging* (*BCTN*) to establish vital tools that combine genetics and neuroimaging to find causes for human disease. Following the recent completion of the human genome project, the ability to define genetic differences at the DNA-sequence level is facilitating a vast realm of possibilities in the exploration of gene-brain pathways contributing to human health and disease. However, very little is currently known about the relationship between variations in a given gene and the **specific** expression of the gene product (a specific protein such as receptor or transporter) in the brain. Specifically, we will target genotypes that encode different levels of the major neurotransporters of Dopamine (DAT) and serotonin (5-HTT), that are known to regulate brain functioning and may confer vulnerability to certain disease. The *BCTN* is an international leader in radiotracer development and implementation capable to capture DAT/5-HTT activity in the human brain using PET technology. DNA variations that affect gene function are found not only within the coding regions, but also in regulatory regions, the variation in the promoter region of the monoamine oxidase A (*MAOA*) will be analyzed based on the published data implicating this polymorphism in the degradation of dopamine and serotonine.

The Biology Department has the equipment and the expertise for DNA analysis. These combined resources within BNL to conduct the proposed neurogenomic research is currently limited to only a small number of laboratories worldwide and it thus presents an opportunity for BNL to pioneer the frontier of this exciting neurogenomic era. By pursuing this goal we will combine and enrich BNL's existing capabilities to promote the *genome to life* initiative with unique application to the living human brain.

APPROACH:

Next to nothing is known about how the distributions of neurotransmitters in the brain vary as a function of polymorphisms that encode the activity of those same neurotransmitters. The reason for this is that there are very few laboratories in the world that have mastered the integration of molecular genetics and neuroimaging, which represents a fledgling field called *neurogenomics*. The thinking behind neurogenomics is that differences in polymorphisms, accounting for transcript abundance, reflect a mechanistic link between genes and behavior. In fact, basic studies show that genetic transcription is not always predictive of protein expression and it has been noted that some differences in gene expression are a consequence, not a cause, of a behavioral change. By having the blood sample of each subject enrolled in neuroimaging studies at BNL, we will be in a position to link the genomic data with the neuroimaging findings and behavioral analysis. Together, this provides a unique opportunity to develop a modern integrative science of neurogenomics in BNL.

TECHNICAL PROGRESS AND RESULTS:

Our first goal was to establish a working laboratory that will create a registry of DNA information from every human subject enrolled in neuroimaging studies. Toward this goal we have recruited Dr. Shumay, who is a seasoned cell biologist. She was sent to The University of California in Irvine (UCI), wherein there is expertise in DRD4-genotyping. At the UCI Laboratory; Dr. Shumay received special training in performing this type of genetic analysis. She has established the procedure of obtaining blood samples from the subjects taking part in brain imaging studies and has initiated creation of a blood bank (currently, we store the blood samples in freezer by -80°C). Dr. Shumay successfully carried out the assay of DNA extraction from blood samples and analyzed 10 samples for genomic variation on MAOA gene and DAT1 gene. We anticipate performing genotyping for several additional projects and combining genotyping with sequencing.

We will use a portion of the blood for the immortalization of the cells. This procedure will allow us to have a renewable source of the material for future projects and studies of linkage with neurotransmitter activity research.

We currently are using 3 protocols for DNA collection, storage and analysis from human subjects that are CORIHS approved. A separate protocol specifically designed for the genomic studies has been submitted for IRB approval. In this new protocol, we specified definitive methods for analysis of brain function-relevant genetic polymorphisms in human subjects: genomic variations in *MAOA, 5-HTT, DRD4, DAT, COMT, BDNF* and *CHT1* genes will be analyzed by genotyping with set of specific primers. To analyze the specific single nucleotide variation in several genes (*COMT*), we will apply sequencing (SNP Genotyping). As a novel approach to study gene-brain-behavior correlations, we plan to implement epigenetic analysis. When this protocol is approved we will be able to collect blood from each human subject that is recruited for neuroimaging at BNL, making the DNA and cell bank more comprehensive. In parallel, we focus on the monoamine oxidase A genotype.

This project uses human subjects.

ACCOMPLISHMENTS:

None

LDRD FUNDING:

FY 2006	$149,971
FY 2007 (budgeted)	$157,000

Nanoparticle Labeled Neural Stem Cell Tracking in Vivo by Magnetic Resonance Microscopy

Helene Benveniste 06-092
E. Caparelli
M. Maletic-Savatic
T. Vogt
L. Managanos

PURPOSE:

The objective of this proposal is to develop and implement new *in vitro* and *in vivo* technologies using (a) neuroprogenitor stem cells (NSC), (b) commercial and new nano-particles coated with organic moieties and, (c) high-resolution magnetic resonance microscopy to track the fate of neuronal stem cells on a bio-systems level *in vivo*. Several researchers have labeled blood borne cells such as macrophages and hepatocytes with nanometer-sized particles *in vitro* referred to as Super-Paramagnetic Iron-Oxide nanoparticles (SPIO). To our knowledge no group has yet labeled neural precursor cells *in vitro* using nano-particles and/or looked at the differentiation of the neuronal precursor cells after the nano-partical loading. Only one group has recently attempted to label neuroprogenitor cells *in vivo* using micro-sized iron oxide particles MION.

APPROACH:

Our initial approach has been to study the uptake of two different nano-particles - 1) Mixed Manganese-Iron (MnFe) Nano-particles and 2) Commercially available SPIO particles (Feridex I.V. – ferumoxides which is a sterile aqueous colloid of SPIO associated with dextran) – into neuronal stem cells *in vitro* and our studies have not yet involved direct use of living animals. Neuronal stem cells were derived from mouse embryo brains which are subsequently cultured for 2-4 weeks before they are used for the experiments. We first added the MnFe nanoparticles at different concentrations to neuronal stem-cells cultured for 14 days to test uptake and survival of the neuronal stem cells. Subsequently, we have also tested the effect of different nano-particle concentrations on the survivability of the stem cells.

TECHNICAL PROGRESS AND RESULTS:

Figure 1 shows NSC survival (%) following incubation (for 48 hrs) with different concentrations of MnFe. As can be seen most concentrations are affecting survival of the stem cells and concentrations >2 μg/ml are definitely toxic.

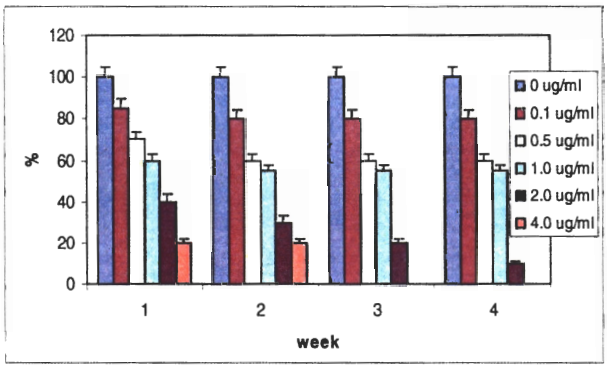

Figure 2 shows spin echo MR images of phantoms of different concentrations of MnFe (in 1 μg/ml) acquired on the 9.4T microMRI scanner:

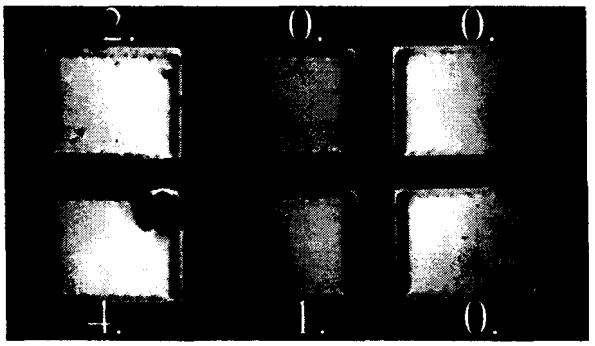

As can be seen concentrations of <1 μg/ml of MnFe are not always visible in the MRI images.

One of the major problems with the initial MnFe nanoparticle design was their size (30nm) and difficulty in regards to dispersing them into solution as is necessary for coating with poly-lysine prior to incubation which could have affected the toxicity profile of the particles as individual cells might have been exposed to larger than expected concentrations...

We also observed that the MnFe nanoparticles weere toxic to neuronal stem cells at concentrations necessary for detection with MRI. Because no other study has looked at the effect of nanoparticles on the growth, survivability and differentiation pattern of neuronal stem cells we decided to first examine the 'gold-standard' commercial nanoparticle (SPIO (feridex)) which is know to be non-toxic to many cell types in vivo and in vitro. We are in the process of examining the uptake of Feridex coupled to Poly-lysine on neural stem cells but in this new series of experiments we have decided to vary the following parameters: 1) age of neuronal culture at the time of incubation; 2) the feridex concentration. Further, we will be assessing viability of the cells daily. The final step of this protocol will look at how the nanoparticles affect differentiation of the neural stem cells; this latter part of the experiment will be done by staining with astrocyte, neuron and oligodentrocyte markers. Dr. L. Managanos, a cell biologist in Dr. Maletic-Savatic Laboratory, will finalize these experiments. We expect these data to be available by mid-December. Specific findings include:

1) MnFe particles are toxic to neuronal stem cells and cannot be used for MRI labeling
2)MnFe particles at a concentration of 0.1μl/ml is detectable by MRI at 9.4T

SPECIFIC ACCOMPLISHMENTS:

None

LDRD FUNDING:

FY 2006	$109,022
FY 2007 (budgeted)	$117,000

MicroCT Methods of Quantitative Adipose Imaging: Development of a Long-Term Assessment Technique for Studying Obesity in a Rodent Model

Gene-Jack Wang *06-094*

PURPOSE:

Obesity research needs an accurate and reproducible method of quantifying regional and total body fat in rodents at high spatial resolution. To address this, we use a microCT system (a SkyScan Model 1076), to develop methods of single-energy and dual energy quantitative CT (SEQCT and DEQCT, respectively). The work is becoming an integral part of Obesity Research Program of Drs. Gene-Jack Wang and Peter Thanos in the Medical Department. Partial results show that, when used at the right beam energies, SEQCT provides highly precise total and regional measures of body fat useful for cross-sectional and longitudinal studies. Because the system's beam energy can be easily tailored to specific needs (by changing the kVp setting and beam filtration), the method can help development beam tailoring protocols of clinical CT for a variety of applications.

APPROACH:

CT is among the most suitable imaging modalities for fat quantification. This is because a) x-ray attenuation coefficients for fat (mean atomic number(Z) of 6.46) and lean tissue (mean Z of 7.64) are very different, especially at the low energies of 20-30 keV (the lower the beam energy the larger the contrast between these two tissue types), and b) the method's high spatial resolution, especially in microCT, reduces "partial-volume" inaccuracies and allows obtaining fine regional body composition information (the pixel sizes options for SkyScan 1076 are 9, 18, and 35 μm). As for the former effect, the wide range of the kVp settings in SkyScan 1076, namely 20-100 kVp, allows the use of very low beam energies. Our use of 41 kVp with 0.5 mm Al beam filtration provides a 24.5-keV mean energy. At this energy, the contrast ratio between fat and muscle is large (0.58:1.0).

The higher spatial resolution of the microCT compared to other imaging modalities is also of a high importance. It minimizes the "partial volume' effect, which is important when the tissue includes regions of different compositions intertwined in fine dimensions.

Our low energy images served both the SEQCT and the DEQCT methods, while our high-energy images, 100 kVp with a 0.25 mm Cu filter, were used in DEQCT only.

SEQCT was used to measure regional and total body fat. Counting on the great separation at low energy of the voxel values in the CT reconstructed image slices in these two tissue types, we set a boundary value on the voxels in the reconstructed images, separating fat and lean tissue. We then counted the fat voxels in the entire mouse body. The count was converted to fat grams using a mouse fat phantom. Because low-energy lung and fat voxels have similar contrasts, the chest was also imaged at 100 kVp (with 0.25 mm Cu). The lung voxels were then counted and deducted from the fat ones, providing the net fat voxel count.

DEQCT subtracts the low- and high-energy images with the appropriate coefficients to produce a "pure" fat image. Here, the gray scale represents the fat density, as opposed

to the x-ray linear attenuation coefficient represented in single-energy images.

TECHNICAL PROGRESS AND RESULTS:

The radiation dose was ~0.3 Gy for the low-energy image, and ~0.05 Gy for the high energy one.

A histogram method provided regional attenuation coefficient profiles of fat at high signal to noise ratio. The result for one mouse is presented in Fig. 1. The method is rich in information on the quality of the fat, and can be applied to small body regions with adequate signal-to-noise ratio.

The precision of the total body fat measurement was ±0.4% (σ/mean). It was obtained from three daily measurements in a live mouse. The tentative accuracy of total body fat was about 10% reached by studying 3 mice comparatively with quantitative magnetic resonance spectroscopy.

In a cross-sectional study of two small mice groups, percent body fat was 6.3 ± 0.7% for a diet-restricted group of mice (n = 3; 28.1 ± 0.7 g weight), and 25.1 ± 2.3% for diet-unrestricted (n=3; 38.6 ± 0.6 g weight).

Figure 2 shows the abdomen of a live mouse at both energies, together with the DEQCT images of the pure fat and lean ("muscle") tissues, and discuss their attributes and significances. The problem of excessive noise in the DEQCT images was addressed by subjecting them to an image-processing routine that reduces the noise with minimal effect on spatial resolution. Although, in principle, DEQCT is a more powerful method that SEQCT, at the present stage of our work, its image noise can be too large for successful image quantification.

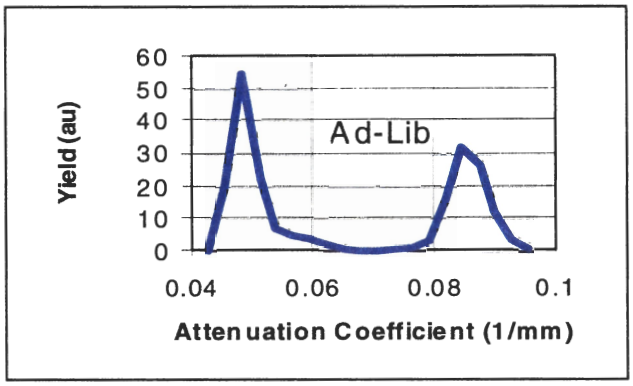

Figure 1. SEQCT histogram of attenuation coefficients in a mouse, whole body, showing the fat left peak) and lean tissue.

A longitudinal study of two groups of mice using SEQCT is underway. We will apply our SEQCT method to animal experiments that may resolve problems with certain clinical CT applications. As an example, clinical CT scanners cannot detect liver fibrosis without the use of contrast agents, and even then the detection is difficult. If we show in a rat model of liver fibrosis that tailoring the beam energy can improve the outcome, we may be able to encourage the radiology community to develop new models of CT scanners in which the beam energy is tailored for specific applications. The project involves animal vertebrates.

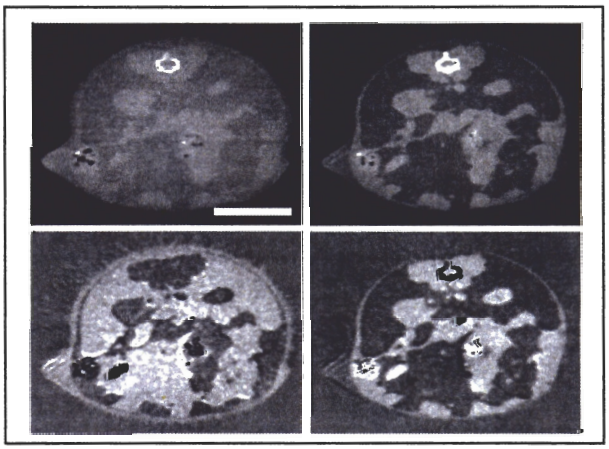

Figure 2. DEQCT image of a mouse abdomen, showing (counterclockwise from top right) low energy, high energy, fat, and lean tissue. The low-energy's contrast advantage over high energy is clear.

SPECIFIC ACCOMPLISHMENTS:

Presentations:

Dilmanian, F.A. Fat quantification in rodents using a MicroCT system. Seminar presented in the Body Composition Group of St. Luke's/Roosevelt Medical Center, New York, in December 2005.

Dilmanian, F.A. MicroCT as an imaging modality: technical aspects and research applications. Seminar presented on October 30, 2006 in the Department of Biomedical Engineering, Ben Gurion University, Be'er-Sheva, Israel.

Dilmanian, F.A.; Boronikolas, B.; Zhong, Z.; Thanos, P.K.; Connor, D.M.; Michaelides, M.; Wang, G.-J.; Li, L.; Tatiparthi, A.; Salmon, P.; and Liu, X. Single- and dual-energy quantitative CT for quantifying adipose tissue in rodents using a microCT system. Poster presented at the 2006 IEEE Medical Imaging Conference, November 1-4, 2006, San Diego, CA.

Dilmanian, F.A. The MicroCT system of the Medical Department and its application. To be presented in the November 22, 2006 session of the Imaging Group Meetings, BNL Medical Department (Wynne Schiffer, Organizer).

LDRD FUNDING:

FY 2006	$ 77,143
FY 2007 (budgeted)	$197,000
FY 2008 (budgeted)	$ 82,000

Study of Overdoped High-T_c Materials

Ivan Bozovic *06-095*

PURPOSE:

We are investigating systematically overdoped high-temperature superconductors (HTS) using the atomic-layer-by-layer molecular beam epitaxy (ALL-MBE) system recently acquired by BNL. The atomic-layer engineering capability allows us to synthesize atomically perfect HTS films and fabricate precise multilayers and superlattices. We are determining the quantitative dependence of key physical properties in normal and superconducting states on the chemical doping level.

APPROACH:

We use the ALL-MBE system to synthesize atomically smooth HTS films, multilayers and superlattices. Measurements of transport properties of these films reveal their critical temperature T_c and other important physical properties (resistivity, magnetic susceptibility, etc. It is important to make as perfect samples as possible, in order to discriminate between extrinsic and intrinsic causes of T_c reduction. Other participants in this project are G. Logvenov, V. Butko, A. Gozar and A. Bollinger.

TECHNICAL PROGRESS:

In FY 2006, we performed about 200 thin film synthesis experiments. Every film was characterized by Reflection high-energy electron diffraction, transport measurements (resistivity and susceptibility as a function of temperature down to 4.2 K), and atomic force microscopy. Selected ones were also characterized by Rutherford Back-scattering. We have greatly improved the MBE system calibration and film synthesis protocols, and have achieved essentially 100 % yield of atomically smooth films. This surpassed what used to be the state-of-the art anywhere in the world in this field. We have discovered an unusual variation of the critical temperature on the doping level.

SPECIFIC ACCOMPLISHMENTS:

Publications:

1. M. Quazilbash, A. Koitzsch, B. Dennis, A. Gozar, H. Balci, C. Kendziora, R. Green, and G. Blumberg, "Evolution of superconductivity in electron-doped cuprates: Magneto-Raman spectroscopy," Phys. Rev. B 72, 214510 (2005)
2. M. Reehuis, C. Ulrich, K. Prokes, A. Gozar, G. Blumberg, S. Komiya, Y. Ando, P. Pattison and B. Keimer, "Crystal structure and high field magnetism in La_2CuO_4," Phys. Rev. B 73, 144513 (2006)
3. L. Benfatto, M. Silva-Neto, A. Gozar, B. Dennis, G. Blumberg, L. Miller, S. Komiya and Y. Ando, "Field dependence of the magnetic spectrum in anisotropic and Dzyaloshinskii-Moriya antiferromagnets. II. Raman spectroscopy," Phys. Rev. B 74, 024416 (2006)
4. N. Gedik, D-S. Yang, G. Logvenov, I. Bozovic and A. H. Zewail, "Direct observation of structural non-equilibrium phase transition in a cuprate superconductor," submitted to Nature

Proceedings:

1. G. Logvenov and I. Bozovic, "Molecular Beam Epitaxy of Complex Oxides," Proc. 2nd International Conference on "Fundamental problems of HTS", Zvenigorod, Russia, 9-13 Oct. 2006
2. A. Bollinger, G. Logvenov and I. Bozovic, "Atomic-Scale Engineering of Thin Films of Complex Oxides Using ALL-MBE," Proc. ICCE-14, Boulder, CO, 2006
3. G. Logvenov and I. Bozovic, "Artificial superlattices grown by MBE: could we design novel superconductors?" Proc. Workshop on Room Temperature Superconductivity, Notre-Dame University, ed. B. Janko (2006)

Invited talks:

1. I. Bozovic, "Giant proximity effect," 18th ISS, October 24-26, 2005, Tsukuba, Japan

2. I. Bozovic, "Strong electron-phonon coupling in high-temperature superconductors," International Workshop on Electron State and Lattice Effects in Cuprate High Temperature Superconductors, October 27-28, 2005, Tsukuba, Japan

3. I. Bozovic, Conference Summary, International Workshop on Electron State and Lattice Effects in Cuprate High Temperature Superconductors, October 27-28, 2005, Tsukuba, Japan

4. I. Bozovic, "Atomic-layer engineering of high-T_c heterostructures" Workshop on Nanoscale Correlations in Heterostructures, 2006 NSLS & CFN Joint Users' Meeting, May 16, BNL

5. I. Bozovic, "(Giant) Proximity Effects in high-Tc superlattices," APS Meeting, March 13-17, Baltimore, Maryland.

6. G. Logvenov, "MBE Growth of Complex Oxides," Winter Seminar, Finkenberg, Austria, March 18-25, 2006.

7. I. Bozovic, "Atomic-layer engineering of cuprate superconductors: what have we learned in the two decades," International Symposium on 20 Years of High-T_c Superconductivity in Zurich, Switzerland.

8. I. Bozovic, "Designed Josephson barriers," International Workshop on Lattice Effects in Superconductors, April 15-22, Santa Fe, New Mexico

9. I. Bozovic, "Superconducting Materials: the status of the field," DOE BES Workshop on Basic Research Needs for Superconductivity, May 8-11, 2006, Washington, DC

10. I. Bozovic, "Atomic-layer engineering of high-T_c superconductors," DOE BES Workshop on Basic Research Needs for Superconductivity, May 8-11, 2006, Washington, DC

11. I. Bozovic, "Superconducting Materials: the Workshop survey," DOE BES Workshop on Basic Research Needs for Superconductivity, May 8-11, 2006, Washington, DC

12. I. Bozovic, "Atomic-layer tailoring of high-temperature superconductors," International Conference From Solid State to Bio-Physics III, June 25-July 1, Cavtat, Croatia

13. A. Gozar, "Antiferromagnetic resonances and magnetic field induced ordering in undoped and lightly doped cuprates," International Conference on Low Energy Electrodynamics in Solids, July 1-6, 2006, Tallinn, Estonia.

14. A. Bollinger "Atomic-Scale Engineering of Thin Films of Complex Oxides Using ALL-MBE," ICCE-14, The Fourteenth International Conference on Composites/Nano Engineering (ICCE-14), July 2-8, 2006, Boulder, CO

15. G. Logvenov, "Atomic-layer engineering of cuprates superconductors," 8th International Conference on Materials and Mechanisms of Superconductivity and High Temperature Superconductors, Dresden, Germany, July 14-23, 2006

16. I. Bozovic, "Atomic-layer tailoring of high-temperature superconductors," International Workshop "Twenty years from the discovery of High T_c Superconductivity," July 20-26, 2006 Erice, Sicily, Italy.

17. I. Bozovic, "Nano-structuring cuprate superconductors," Int. Workshop on Mott's Physics in Nanowires and Quantum Dots, July 29-Aug 2, 2006 Cambridge, United Kingdom

18. A. Bollinger, "Superconductor-Insulator Transition in Quasi-One-Dimensional Nanowires," The Second International Workshop on Quantum Transport and Noise, September 3-15, 2006, Corfu, Greece

19. I. Bozovic, "Casting high-temperature superconductors atomic layer-by-layer," (plenary talk) YUCOMAT 8, Sept. 4-8, 2006, Herceg Novi, Montenegro

LDRD FUNDING:

FY 2006	$181,219

HTS Trilayer Josephson Junctions

Ivan Bozovic *06-096*

PURPOSE:

We are trying to attack the most basic questions in the high temperature superconductor (HTS) physics such as what is the nature of superconducting transition – do Cooper pairs form and condense at T_c or else the pairs formed at some higher temperature T^* undergo Bose-Einstein condensation at T_c – and what is the nature of the 'glue' (exchange of boson excitations) that pairs electrons at such high temperature.

APPROACH:

We use the state-of-the art atomic-layer-by-layer molecular beam epitaxy (ALL-MBE) system to synthesize atomically smooth HTS films, multilayers and superlattices. Trilayer films, with HTS top and bottom electrodes and a normal metal or insulating barrier, can be fabricated using lithography into Josephson junctions. Measurements of transport properties of these junctions reveal the physics we are after. It is important to make as perfect samples as possible, in order to discriminate between extrinsic and intrinsic causes of T_c reduction.

Other participants in this project are G. Logvenov, V. Butko, A. Gozar and A. Bollinger.

TECHNICAL PROGRESS:

In FY 2006, we performed about 200 thin film synthesis experiments. Every film was characterized by Reflection high-energy electron diffraction (RHEED), transport measurements (resistivity and susceptibility as a function of temperature down to 4.2 K), and atomic force microscopy. Selected ones were also characterized by Rutherford Backscattering. We have greatly improved the MBE system calibration and film synthesis protocols and have achieved essentially 100% yield of atomically smooth films. This surpassed what used to be the state-of-the-art anywhere in the world in this field.

SPECIFIC ACCOMPLISHMENTS:

Publications:

1. I. Bozovic "About physics, myself, and Ginzburgs," Journal of Superconductivity (2006), in press
2. N. Gedik, D-S. Yang, G. Logvenov, I. Bozovic and A. H. Zewail, "Direct observation of structural non-equilibrium phase transition in a cuprate superconductor," submitted to Nature
3. A. Gozar, G. Logvenov, V. Y. Butko and I. Bozovic, "Surface Structure Analysis of Atomically Smooth $BaBiO_3$ films," submitted to Physical Review Letters

Proceedings:

1. G. Logvenov and I. Bozovic, "Artificial superlattices grown by MBE: could we design novel superconductors?" Proc. Workshop on Room Temperature Superconductivity, Notre-Dame University, ed. B. Janko (2006).

Invited talks:

1. I. Bozovic, "Giant proximity effect," 18th ISS, October 24-26, 2005, Tsukuba, Japan
2. I. Bozovic, "Strong electron-phonon coupling in high-temperature superconductors," International Workshop on Electron State and Lattice Effects in Cuprate High Temperature Superconductors, October 27-28, 2005, Tsukuba, Japan
3. I. Bozovic, Conference Summary, International Workshop on Electron State and Lattice Effects in Cuprate High Temperature

Superconductors, October 27-28, 2005, Tsukuba, Japan

4. I. Bozovic, "Atomic-layer engineering of high-T_c heterostructures" Workshop on Nanoscale Correlations in Heterostructures, 2006 NSLS & CFN Joint Users' Meeting, May 16, BNL

5. I. Bozovic, "(Giant) Proximity Effects in high-Tc superlattices," APS Meeting, March 13-17, Baltimore, Maryland.

6. G. Logvenov, "MBE Growth of Complex Oxides," Winter Seminar, Finkenberg, Austria, March 18-25, 2006.

7. I. Bozovic, "Atomic-layer engineering of cuprate superconductors: what have we learned in the two decades," International Symposium on 20 Years of High-T_c Superconductivity in Zurich, Switzerland.

8. I. Bozovic, "Designed Josephson barriers" International Workshop on Lattice Effects in Superconductors, April 15-22, Santa Fe, New Mexico

9. I. Bozovic, "Superconducting Materials: the status of the field," DOE BES Workshop on Basic Research Needs for Superconductivity, May 8-11, 2006, Washington, DC

10. I. Bozovic, "Atomic-layer engineering of high-T_c superconductors," DOE BES Workshop on Basic Research Needs for Superconductivity, May 8-11, 2006, Washington, DC

11. I. Bozovic, "Superconducting Materials: the Workshop survey," DOE BES Workshop on Basic Research Needs for Superconductivity, May 8-11, 2006, Washington, DC

12. I. Bozovic, "Atomic-layer tailoring of high-temperature superconductors," International Conference "From Solid State to Bio-Physics III, June 25-July 1, Cavtat, Croatia

13. A. Gozar, "Antiferromagnetic resonances and magnetic field induced ordering in undoped and lightly doped cuprates," International Conference on Low Energy Electrodynamics in Solids, July 1-6, 2006, Tallinn, Estonia.

14. A. Bollinger "Atomic-Scale Engineering of Thin Films of Complex Oxides Using ALL-MBE," ICCE-14, The Fourteenth International Conference on Composites/Nano Engineering (ICCE-14), July 2-8, 2006, Boulder, CO

15. G. Logvenov, "Atomic-layer engineering of cuprates superconductors," 8th International Conference on Materials and Mechanisms of Superconductivity and High Temperature Superconductors, Dresden, Germany, July 14-23, 2006

16. I. Bozovic, "Atomic-layer tailoring of high-temperature superconductors," International Workshop "Twenty years from the discovery of High T_c Superconductivity," July 20-26, 2006 Erice, Sicily, Italy.

17. I. Bozovic, "Nano-structuring cuprate superconductors," Int. Workshop on Mott's Physics in Nanowires and Quantum Dots, July 29-Aug 2, 2006 Cambridge, United Kingdom

18. A. Bollinger, "Superconductor-Insulator Transition in Quasi-One-Dimensional Nanowires," The Second International Workshop on Quantum Transport and Noise, September 3-15, 2006, Corfu, Greece

19. I. Bozovic, "Casting high-temperature superconductors atomic layer-by-layer," (plenary talk) YUCOMAT 8, Sept. 4-8, 2006, Herceg Novi, Montenegro

LDRD FUNDING:

FY 2006	$212,075

Photocatalytic Reduction of CO_2 in Supercritical CO_2

David C. Grills *06-097*

PURPOSE:

The purpose of this project is to investigate the use of supercritical CO_2 ($scCO_2$) as a medium for the photocatalytic reduction of CO_2 into useful chemical forms. Such an approach is innovative since the solvent is now being used as a primary reactant, leading to many potential advantages, such as significantly higher reaction rates and catalyst turnover frequencies. There is an urgent need for new photocatalytic processes that can efficiently use solar energy to generate clean fuels from the abundant molecule, CO_2. This project seeks to explore one such novel approach to this problem, with an ultimate aim of developing new, efficient photocatalysts designed specifically for use in $scCO_2$.

APPROACH:

The photoreduction of CO_2 into useful chemicals (with the ultimate goal of generating methanol as a clean fuel), using metal-based catalysts, has been the subject of intense investigation for many years, since it offers the possibility of a clean source of energy that would also mitigate the Greenhouse Effect. A variety of transition-metal complexes have been investigated as potential photocatalysts for these processes due to their long lived charged separated photoexcited states. A major setback however, has been that solvent molecules tend to coordinate to a vacant site at the metal center in the active catalytic species, thus competing with CO_2 reactant molecules and substantially reducing the catalytic activity.

A promising alternative to the use of conventional solvents is to replace such solvents with $scCO_2$ (CO_2 at pressures and temperatures exceeding those at the critical point). Indeed, $scCO_2$ has been used as a replacement solvent in many different homogeneous catalysis processes. However, its combined use as a solvent/reactant has received much less attention. The tunable physical properties of $scCO_2$ (*e.g.* density, viscosity *etc.*) and the fact that extremely high concentrations of CO_2 can be achieved (~20 M @ 3000 psi/35 °C), offers the possibility of dramatic enhancements in catalyst efficiency for the photoreduction of CO_2. Furthermore, competition with conventional solvent molecules is now eliminated.

Polar molecules, such as transition metal complexes, are often insoluble in $scCO_2$. Thus, our approach is to synthetically modify previously studied CO_2 photoreduction catalysts in order to render them soluble in $scCO_2$. This involves the modification of ligands by the addition of long alkyl or perfluoroalkyl chains and the use of CO_2-soluble anions, such as $[BAr^F{}_4]^-$ (Ar^F = 3,5-bis(trifluoromethyl)phenyl) for charged complexes. The photochemical and photophysical properties of these new catalysts are then studied in conventional solvents and subsequently in $scCO_2$. This involves the use of fast time-resolved spectroscopic techniques (UV-vis and IR) on the nanosecond timescale to probe and characterize the intermediate species generated during photocatalysis. Catalyst efficiencies are determined by steady-state irradiation studies. A collaboration in these studies has been initiated with Prof. Michael W. George (University of Nottingham, UK), a leading expert in the combination of supercritical fluids with transient spectroscopy.

TECHNICAL PROGRESS AND RESULTS:

We successfully synthesized a new CO_2 photoreduction catalyst, $[Re(CO)_3(dnb)]_2$ (dnb = 4,4'-dinonyl-2,2'-bipyridyl) that bears long alkyl chains (see below). The alkyl chains rendered the catalyst soluble in *n*-hexane (and thus it is expected to also be soluble in $scCO_2$).

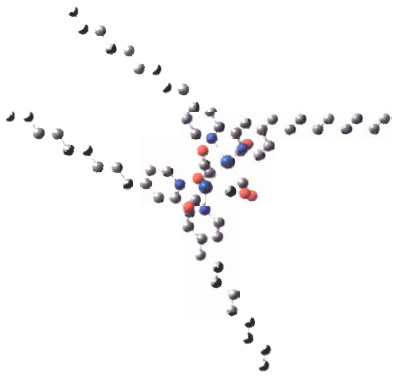

Unlike similar catalysts without long alkyl chains, this new catalyst was found to exhibit unusual solvato- and thermochromic behavior. Thus, in hexane it is pink at room temperature and green at low temperature, whereas it is green in polar solvents, such as acetonitrile. This behavior was investigated in detail by variable temperature IR and NMR spectroscopy and theoretically with DFT calculations. It was found that these properties are due to interconversion between different conformations of the catalyst, with the skewed-*trans* conformer being the most stable in room temperature hexane solution.

Flash photolysis and transient IR investigations (see Figure below) of $[Re(CO)_3(dnb)]_2$ were carried out in *n*-hexane solution in an effort to determine the rate of dimerization of the photolytically generated active catalytic radical species, $(dnb)Re(CO)_3$ in this virtually non-coordinating solvent. The dimerization rate constant in *n*-hexane was found to be ~10^9 M^{-1} s^{-1}. In contrast, in the coordinating solvent, THF the dimerization rate constant was significantly slower (100 M^{-1} s^{-1}). This supports our original hypothesis that in non-coordinating solvents (and thus presumably in $scCO_2$ also), the active catalytic species is considerably more reactive.

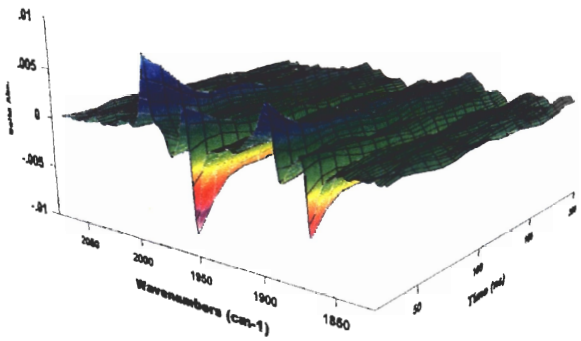

Construction of the high-pressure spectroscopic apparatus necessary for studies in $scCO_2$ solution has begun and is now almost complete. In the next Fiscal year, transient spectroscopic studies on $[Re(CO)_3(dnb)]_2$ will be conducted in $scCO_2$ solution as a detailed function of pressure and temperature. Continuous photolysis under catalytic conditions will also be performed to determine catalytic efficiency in $scCO_2$. New $scCO_2$-soluble metal-based catalysts will also be synthesized and their CO_2 photoreduction capabilities determined in $scCO_2$.

SPECIFIC ACCOMPLISHMENTS:

"Photochemical CO_2 Reduction in Non-Coordinating Solvents and Supercritical CO_2" Poster presentation at 28th DOE Solar Photochemistry Research Conference, Warrenton, VA, June 2006.

LDRD FUNDING:

FY 2006	$ 80,098
FY 2007 (budgeted)	$155,000
FY 2008 (budgeted)	$ 71,000